Revised

ERATA	p 19, l 5	whilst ...
ERTA	p 26, l 6	tendon with ...
	p 95, l 13	greater reliance ... rapidly for which saving elastic..
	p 232, l 13	muscle strength by suggesting ...

THE STORAGE OF ELASTIC ENERGY BY THE MUSCLE TENDON COMPLEX: THE EFFECTS OF TENDON COMPLIANCE AND MUSCLE STRENGTH AND THE IMPLICATIONS FOR LOCOMOTION.

KAREN M. ROOK

A thesis submitted for the degree of
Doctor of Philosophy in the
University of London

Department of Physiology
University College London
March 1995

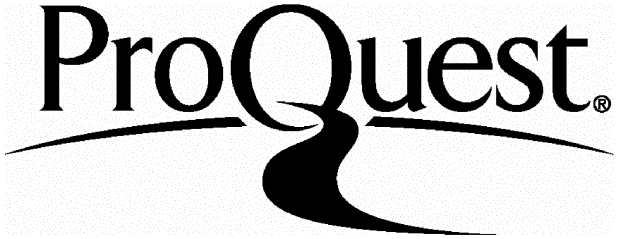

Abstract

1) A computer model of a hopping "beast" (a muscle tendon complex) was developed to show how the energetics of hopping maybe affected by changes in the compliance of the tendon and changes in muscle strength. The model shows firstly for a given spring stiffness there is a sharp optimum for the amount of muscle. Secondly for a given mass of "beast", there is an optimum spring stiffness, but it is not a sharp optimum.

2) In men it was found that a 29% reduction in maximum voluntary force per cross sectional area (MVF/CSA) of the adductor pollicis muscle, happens gradually with age. The decline in men begins at about 60 years of age. The time course of the decline is similar to the time course of the decline in free testosterone levels, which is known to decline also at about 60 years of age (McKinlay, 1989). This suggests that in men, reduced testosterone levels might be responsible for the reduced MVF/CSA associated with old age.

3) Quick length release experiments were conducted on mouse soleus muscle to determine its compliance. The compliance of the three components in series add up: the tendon, the aponeurosis and the crossbridges. In order to determine what proportion of the total compliance is due to each component, the timing of the T_1 to T_2 transition needs to be known. The T_1 to T_2 transition was found to be faster in mouse soleus muscle than that found by Huxley and Simmons (1971) in frog muscle. It is concluded that 41% of the compliance of mouse soleus muscle is due to the crossbridges and 59% due to aponeurosis compliance.

4) In ovariectomized and castrated mice it was found that the extensor digitorum longus tendons were approximately 15% more compliant than in aged matched control mice. Indicating that in the absence of oestrogen and testosterone the increase in stiffness of the tendon with age is inhibited.

CONTENTS

LIST OF FIGURES

CHAPTER 1

CHAPTER 2

CHAPTER 3

CHAPTER 4

LIST OF TABLES

CHAPTER 1

CHAPTER 2

CHAPTER 3

INTRODUCTION

The Muscle Tendon Complex

Muscles and tendons are usually studied separately. The tendon is usually regarded as a nuisance by muscle physiologists, however muscle and tendon work as one unit in vivo. Tendons do not stop abruptly at the muscle belly, but continue as tendinous sheets (aponeurosis), to which bundles of muscle fibres attach (generally via short collagenous straps) (van Leeuwen, 1991). In the cat hindlimb (Loeb *et al.*, 1987) and in the sartorius muscle in humans (Barrett, 1962) the muscle fibres do not run continuously throughout the muscle belly. The muscle fibres are found to be connected to each other in series with short straps of connective tissue, thus the aponeurosis can form a large proportion of the muscle belly. Power output by the muscle-tendon complex (MTC) is the sum of the power output by the muscle tissue, the parallel elastic element in the muscle belly, the aponeurosis, and the tendon (van Leeuwen, 1991). It is known that power output is modified by age, this thesis is investigating how the changes in the muscle, aponeurosis, and the tendon effect the power output.

Elastic Behaviour of The MTC Consists of Two Major Components

The elastic behaviour of the MTC has been described as consisting of two major components; the parallel elastic component (PEC) and the series elastic component (SEC). When muscle is stretched, the contractile component (CC), PEC, and SEC all contribute to the development of tension (Schottelius & Senay, 1956).

i) The PEC provides resistive tension when a muscle is passively stretched, and is responsible for resting tension. The PEC lies parallel to the contractile mechanism, and is thought to consist of the sarcolemma, sarcoplasm, and elastic fibres of the epimysium, perimysium, and endomysium (Schottelius & Senay, 1956). Another possible contributor to the PEC, is Titin, an extremely long "elastic" protein (about 1μm) that links the myosin filament to the Z line. Titin is also found at the A-I junction and in other parts of the A- and I-bands (Squire, 1986). The crossbridges pull together the two thick filaments. When the crossbridges pull the load is taken off titin. The contrary situation occurs when titin pulls, i.e. the load is taken off the crossbridges. Thus titin also lies in parallel to the contractile elements, when there are no crossbridges attached titin can

exert force.

ii) The SEC acts as a spring to store elastic energy when an active muscle is stretched. The series elastic component is considered to consist of all those structures within a MTC, which are connected in series with the contractile element. SEC is considered to consist of two main elements: tendinous structures (extracellular) and elasticity located within the fibres (intracellular), which have different elastic characteristics. The extracellular series elastic elements can be further divided into free tendon and aponeurosis (intramuscular tendon plate), whereas within intracellular SEC elastic myofilaments and elastic behaviour of the crossbridges can be distinguished (Schottelius & Senay, 1956). Active muscle fibres are capable of only slight "elastic" stretching and recoil. The myosin crossbridges are known to be compliant structures which may be stretched to some degree before detachment of crossbridges occurs. Some of this compliance is thought to be due to the rotation of the heads of the myosin crossbridges and some is due to elongation of the arm. This latter part is believed to have a helical configuration and for this reason one would expect it to be extensible. The tension sustained in each crossbridge depends on the extent to which the compliant S2 portion of the myosin is stretched (Huxley & Simmons, 1971). Recent experiments by Huxley *et al.*, (1994), have shown that there is also a significant degree of extensibility in the myosin filament backbone.

Small Elastic Length Changes Occur In The Muscle Fibres

As stated above muscle fibres are capable of only slight elastic stretching and recoil. Large length changes are not elastic, but are due to protein filaments sliding past each other. Small elastic length changes can occur, without detachment of crossbridges. This has been shown by experiments in which a single fibre from a frog muscle was held at constant length while being stimulated electrically to exert tension (Huxley & Simmons, 1971). Suddenly the clamps holding the fibre are moved slightly closer together. The tension falls, just as the tension in a stretched rubber band falls when it is allowed to shorten, but the fibre (unlike the rubber band) re-developed tension during the first few milliseconds at its new length. It did this by moving crossbridges to take up the slack. The tension fell briefly to zero whenever the active fibre was allowed to shorten by 1.3% or more. This showed that the tension in the active fibre stretched it by 1.3%

(Huxley & Simmons, 1971). These points are explained in more detail in chapter 3.

Muscle and Tendon Interactions

Locomotion such as running and jumping are dependent on the dynamic interaction of the muscle and tendon forming the MTC. In both running and jumping the MTC involved are seen to be first forcibly stretched whist active (eccentric contraction) and then shorten (concentric contraction) (Alexander & Bennet-Clark, 1977). Thus the MTC undergoes a stretch-shortening cycle (SSC). Heglund and Cavagna (1987) showed that stretching an active muscle before allowing it to shorten increases the force exerted during the shortening. The positive work done in shortening was found to be increased by a larger percentage than the increase in the oxygen consumption. It has been suggested that this increase in efficiency could be due to the storage and release of elastic strain energy in tendons. Thus enabling the muscles to contract isometrically instead of lengthening then shortening (Alexander, 1989), this would thus save the animal a great deal of metabolic energy.

Storage Of Elastic Energy In Muscle

Some of this elastic energy will also be stored in the tendon / aponeurosis and some in the crossbridges. This has been shown in experiments by Cavagna *et al.*, (1994), on isolated frog muscle fibres where the tendon / aponeurosis compliance is eliminated. These experiments suggest that previous stretching of an active muscle fibre increases the ability of the individual crossbridges to do work. They found that the crossbridges obtained a level of potential energy, greater than that obtained in isometric contraction. In addition this increase in potential energy was retained for an appreciable time interval after stretching (Cavagna *et al.*, 1994). The storage of elastic energy by the contracted muscle, however, is not a static characteristic such as that of rubber or a spring. In fact it is linked to the contraction state, which is a dynamic molecular phenomenon requiring energy expenditure. Storage of elastic energy by the muscle, is therefore a costly process; obviously the energy expenditure will be greater the longer the contraction time is. Therefore, if the stretch-elastic recoil cycle takes place in a very short time, the elastic work can be done with a small energy expenditure; if the contraction is long lasting the energy expenditure is correspondingly larger and the whole process may become inefficient (Cavagna *et al.*, 1964). This is because the stored energy in the

crossbridges has been dissipated, the energy is therefore replaced by the splitting of ATP in the crossbridges.

Resting muscle cannot store elastic strain energy as it has a low stiffness in the physiological range of movements. Active muscle however has a high degree of stiffness within the same range. Thus it is proposed that storage of elastic energy occurs in the undamped elastic elements of a muscle (i.e. the crossbridges), when it is active whilst being stretched (eccentric contraction). It has been calculated that the quantity of elastic strain energy which can be stored in unit mass of material is 5J/Kg or less for muscle but is 2000 - 9000J/Kg for tendon collagen (at 10% strain) (Alexander & Bennet-Clarke, 1977). Thus as a mechanical energy store, muscle is orders of magnitude less effective than tendon.

Energy Storage Versus Energy Utilization Features of The Muscle

As stated above the crossbridges can store elastic energy, but they are also a machine that splits ATP in crossbridge cycling to provide mechanical energy. ATP is bound to myosin molecule, the hydrolysis of it to its products ADP and Pi which remain bound to myosin, is thought to activate the S1 head making it ready to bind to actin again. The release of phosphate from the actomyosin complex is thought to initiate the rotation of the S1 head, which results in force generation due to the stretching of the S2 portion. ADP is released towards the end of the rotation phase, which results in ATP binding to the actomyosin complex, followed by actin and myosin dissociating with the ATP bound to myosin (Cook & Pate, 1985)

Storage of Elastic Energy in Tendon

Evidence that the energy storage occurs in the tendons is presented by Alexander (1974), from experiments of dogs jumping on force plates. Graphs of force against muscle length were plotted for the gastrocnemius muscle, which acts to decelerate the dog on landing from a jump. This muscle is found to be forcibly stretched as the foot hits the platform and shortens again as the dog takes off. The force in the muscle increases as it is stretched and declines as it shortens. Thus work is done on the MTC in stretching it, and it returns about the same amount of work when it is released (Alexander, 1974).

It appears that the gastrocnemius is stretched about 3cm, and then recoils, however this muscle is pennate consisting of fibres that are only 2.5cm long in the resting state. It is thus impossible for a muscle fibre of this length to be stretched by 3cm, and still exert large forces as obtained from the force plate measurements (Alexander, 1974). Since the overlap between the actin filament and myosin crossbridge would be very small at this stretched length. According to the Huxley 1957 model, force is proportional to the degree of interaction between actin and myosin. This suggests that the muscle fibres remain almost constant in length while tendons stretch (Alexander, 1974). Energy can be stored in a tendon by stretching it, but only if the muscle fibres in series with it are stiff enough to resist most of the length change, i.e. the muscles must be active whilst the tendon is being stretched (Morgan *et al.*, 1978).

It has been calculated using Young's modulus for tendon that the forces involved when the dogs jumped is sufficient to stretch the tendons by about 2.5cm, indicating that it is possible that most of the stretching does occur in the tendon (Alexander, 1974). The ability of the crossbridges to function elastically, operates over small strains. Hence it can only store a small part of the work done by a muscle which shortens by a large fraction of its length. Also it can only be responsible for a small part of the total energy store of elastic strain energy if the muscle is in series with a long compliant tendon. For these reasons it is relatively unimportant in mammalian running (Alexander & Bennet-Clark, 1977).

A Delay In The SSC Reduces The Pre-stretch Effect

Cook (1993) showed in the first dorsal interosseus muscle (FDI) of the human hand, that if a delay occurs between the stretching and shortening of the MTC (i.e. if the muscle is held at the stretched length), the effect of the pre-stretch on increasing the force exerted in the shortening phase is reduced. This is a consequence of the fact that the force in the muscle declines rapidly, which therefore will lead to a shortening of the tendon by elastic recoil. However, since the length of the MTC is constant during this delay, the shortening of the tendon cannot produce any useful work. Instead the shortening of the tendon must result in the extension of the muscle fibres, which results in the stored energy from the tendon being dissipated as heat (Cook, 1993). In order to maximise shortening performance the delay time should be minimised. Cook (1993)

found with a delay of 80ms, similar to that observed in natural movements, the amount of extra force due to the pre-stretch, in shortening was reduced by half. Thus the initial fast recoil of the tendon can only be useful in natural movements if the delay between stretching and shortening is very brief or non-existent (Cook, 1993).

In animal locomotion a delay often occurs between the stretching and shortening phases. For example on landing in running the triceps surae muscle group is forcibly stretched by gravitational forces as the foot hits the ground. The muscle is acting as a brake and has to resist the external force of gravity. The MTC shortens when the force the muscle exerts, overcomes the external force. Thus in natural movements this switching of the muscle from stretching to shortening is not instantaneous and can take many milliseconds (Cook, 1993). In re-jumping from a drop jump of 40cm, Cook (1993) found a delay of 50-80ms between dorsiflexion and plantar flexion.

Muscle Fibres Shorten During A MTC Stretch

The sequence of events in the contraction of ankle extensor muscles during locomotion involves a primary excitation of the muscle just prior to the foot being placed on the ground (Griffiths, 1989), this is followed by stretch of the MTC as the foot starts to bear the weight of the animal. Followed by the shortening of the MTC just before take-off (Griffiths, 1991). Griffiths (1991) measured the lengths of muscle fibres in the medial gastrocnemius (MG) muscle of anaesthetized cats using ultrasound technique. Slow to medium speed stretches were applied shortly after the onset of contraction, simulating the situation that occurs in cat MG during walking and trotting. It was found that the stretch was entirely taken up in the tendon and the muscle fibres actually shortened throughout the imposed MTC stretch (Griffiths, 1991).

As the speed of the muscle stretch increases, the rate of rise of force also increased, but the degree of muscle fibre shortening was found to be decreased. If the stretch was still taking place when force was approaching the peak "isometric" level, then the muscle fibres were also stretched at this stage. This is a consequence of the fact that tendon compliance is high at low tensions and diminishes as the applied tension increases. Muscle stretches at a speed of 100mm s^{-1}, applied after the onset of force, resulted in muscle fibre stretch but of a lower speed and extent than was imposed on the muscle

(Griffiths, 1991). Thus it was concluded that muscle fibres do not stretch except at high speeds of locomotion, when the stretch rate is also high. Thus the tendon was found to act as a mechanical buffer to protect the muscle fibres from damage during eccentric contractions, since when the muscle is being stretched at high speeds the muscle fibres remain at constant length or stretch only slowly and by a moderate amount (Griffiths, 1991).

Cook (1993) showed in the first dorsal interosseus muscle (FDI) of the human hand, that the force during the subsequent shortening was largely unaffected by the velocity of the pre-stretch. The small amplitude of stretch of the muscle fibres is not a disadvantage because the crossbridges do not exceed the short-range stiffness (SRS). When the crossbridges exceed the SRS (a stretch of greater than 1-2% of the fibre length) they lose the elastic energy stored in them, whereas below the SRS they may be able to recoil and contribute to the shortening. Cook (1993) showed that small and slow stretches returned the most energy during the shortening. Cook (1993) concluded that the MTC cannot be treated as a simple spring, but must be considered as a CC and a SEC acting together in a feedback loop.

Ratio of Tendon To Muscle

Optimal Tendon Length

Tendon to muscle fibre length ratios as high as 10 have been found in many of the MTC involved in locomotion (Ker *et al.*, 1988). If the length of the tendon is much greater than the length of the muscle then the compliance of the SEC will be dominated to a much larger extent by the tendon. In animals such as advanced ungulates, the extensor muscles of the wrist, ankle and digits have evolved extremely short muscle fibres and correspondingly long tendons. It is thought these tendons serve as springs in running, enabling the storage of elastic strain energy to be stored from step to step (Alexander, 1989). Force is not sacrificed in this trade in of muscle for tendons, since force is proportional only to CSA, not to muscle length. Short muscle fibres can exert as much force as an equal number of long ones, but presumably need less energy to activate them, since less volume of muscle is activated in each step, less metabolic energy is therefore used (Alexander, 1989). Shorter muscle fibres, however, will result in a decrease in the maximal speed of shortening of the muscle, since this is proportional to

muscle length (Alexander, 1989). It is possible this will be of no consequence, since only a small distance has to be shortened by a muscle possessing a long compliant tendon.

A disadvantage of such an arrangement, however is a loss of flexibility of movement. Thus such tendons are only found in specialized running mammals (Alexander, 1989). The muscles that have short fibres in ungulates have much longer ones in monkeys, which have to be able to position their legs in a wide variety of angles and exert large forces whilst climbing trees (Alexander, 1989). Some large muscles with long fibres will be needed to do the positive and negative work needed for rapid acceleration and deceleration, and for jumping, but there maybe an advantage in shortening the fibres of the distal leg muscles, whose tendons serve as springs in running.

Optimal Tendon Thickness

In a muscle-tendon system, the extension of the tendon may be disadvantageous, as when the muscle is supplying energy to the external system, or it may be advantageous, as when the tendon acts as a spring. These circumstances lead to very different predictions for the optimal tendon thickness (Ker *et al.*, 1988). Ker *et al.*, (1988) state that the tendon should be as thin as possible for negative work or acting as a spring. For this function, the optimum tendon thickness is expected to be determined by the strength of the tendon, with a safety factor that can be quite small (Ker *et al.*, 1988). The thinner the tendon is the more compliant it is. If it is too thick, the muscle is not able to exert enough force to stretch it sufficiently.

The other function the muscle with its tendon has to perform is as a combined system which delivers mechanical energy to achieve joint displacement. Muscles contract under load, thus acting as a source of energy. A tendon extends under load and therefore some of the contraction of the muscle fibres serves only to take up the extension of its tendon without contributing to the displacement of the joint (Ker *et al.*, 1988). A thinner tendon extends more and so impairs the ability of the MTC to displace the joint. To take up this stretch, the muscle would require longer muscle fibres. Increasing the fibre length increases the mass of the muscle, since the CSA of the muscle fibres is fixed, being determined by the force the muscle is required to develop (Ker *et al.*, 1988). Thus

for positive work, a much thicker tendon is optimal in minimizing the combined mass of the muscle and the tendon. Both these extremes are observed among the leg tendons of mammals and also everything in between, which reflects the range of muscle functions (Ker *et al.*, 1988).

Force and Position Control: Interaction of Muscle And Tendon

When muscles are required to exert a constant force, such as when holding a pen in writing, the presence of a compliant tendon helps this function, by ironing out minor fluctuations. We use our fingers and thumb as the two components of a pincer for gripping and handling, and on many occasions it is probably more important to maintain an accurately controlled force than to have precise control of actual position (Rack, 1985). However when the muscles are required to keep position constant, the presence of a compliant tendon hinders this task. It is the function of the muscle spindles to keep position constant (Rack, 1985). A compliant tendon thus reduces the precision with which the nervous system can control the position of the digits (Rack, 1985). This springiness provided by the tendon can be eliminated by putting everything under tension. Since tendons are compliant when they are under low tension, but stiffer when forces are high; hence, when the gripping pressure is small the fingers and thumb will meet displacing movements with only a small increase in force, but a more forcible grip will be correspondingly more resistant to any disturbance (Rack, 1985).

Changes In The MTC With Age

i) Muscles Become Weaker With Age

Muscle weakness associated with ageing has two components. There is a weakness due to muscle atrophy (Essen-Gustavsson & Borges, 1986: Kallman *et al.*, 1990: Vandervoort & McComas, 1986). In addition it has also been found in both mice (Brooks and Faulkner, 1988) and humans (Bruce *et al.*, 1989a) that there is a reduction in the maximum voluntary force (MVF) per CSA of the muscle with age. The present study, in chapter 2, set out to investigate the age-related changes in MVF/CSA of the thumb adductor muscle (adductor pollicis) in men between the ages of 17 and 85 years, to help to further the understanding of the mechanism of this reduction in MVF/CSA.

ii) Tendon Stiffness Increases With Age

Tendon stiffness increases with age. The tangent modulus in the linear region of the stress-strain curve has been shown to increase with age in rat tail tendon, indicating the stiffness of the collagen fibre is increased (Torp *et al.*, 1975b). The amount of cross-links derived from the process of non-enzymic glycosylation has been found to increase with age (Naresh & Brodsky 1992). Cross-linking appears to: (a) increase the resistance of the collagen to degenerative enzymes and urea degradation (Davison, 1982); (b) increase its tensile strength; (c) decrease its elasticity and decrease its solubility (Verzar, 1963). In addition to this collagen content is known to increase with maturation and aging of the tissue (Everitt & Delbridge, 1976). These points are discussed in more detail in chapter 4.

Consequences Of Changes In The MTC With Age For Locomotion

If the tendon stiffness increases with age and if the force (F) per cross sectional area of the muscle decreases with age, what will the effect be on locomotory performance? Assuming that the same jump height / task has to be achieved, as before the increase in tendon stiffness, then the animal can do either of two things to increase the muscle force. A higher muscle force is needed because the muscle now has a reduced F/CSA and secondly a higher muscle force is now required to stretch the stiffer tendon, to enable the same degree of elastic storage of energy to occur. The animal cannot do anything to alter the tendon stiffness, but the animal could choose to do either of the following:

1) Increase the time the muscle is on for.

or

2) Increase the amount of muscle used.

The question that is being asked is: Is more muscle on for less time, more efficient than less muscle on for more time? To answer this question a model of a MTC has been developed and is described in chapter 1. The model will be used to determine whether there is an optimum muscle amount, for a given spring stiffness. If an amount of muscle is used that is smaller than the optimum, it would mean that the muscle would be on for longer (to achieve the same jump height). If this was found to be less efficient, then it would seem sensible for the animal to choose to re-optimize its muscle amount. So that

not much efficiency may be lost in all but maximum contractions.

Hypothesis

The hypothesis this thesis is investigating is: Are the changes that occur with age in muscle and tendon related and do they suffice to maintain relatively efficient locomotion, when combined with the appropriate change in motor control strategy?

The changes in muscle and tendon are with ageing are investigated in chapters 2 and 4 respectively. It is also necessary to consider the aponeurosis, as well as the tendon, since it is also a component of the MTC (see chapter 3). The model will then be used to see if these two changes do fit together functionally and whether a change in motor control strategy is needed to conserve efficiency (see chapter 1).

Limitations In The Current Understanding

The limitations in the current understanding are:

1) It is not known how muscle strength is matched to tendon compliance (this is investigated in chapter 1). A model of a MTC was developed to determine how tendon compliance, muscle mass and Vmax are optimized, to produce the highest efficiency for the MTC. The elucidation of this will help in the understanding of the role muscle strength and tendon compliance play in locomotion.

2) The time course of the reduction in muscle F/CSA with age in men, is not known (this is investigated in chapter 2). This is important to further the understanding of the mechanism of the reduction in F/CSA with age.

3) The compliance of the aponeurosis is not known (this is investigated in chapter 3). It is important to determine the compliance of the aponeurosis since it is one of the components of the MTC.

4) It is not known if the hormones oestrogen and testosterone affect the compliance of tendons (this is investigated in chapter 4). It is known the levels of these hormones in women and men respectively, decline with age. Reduced oestrogen levels are known to affect bone and muscle strength, therefore it is possible these hormones could also affect

tendon compliance.

The elucidation of each of the above points will help in the understanding of the role muscle strength, and the compliance of the tendon and aponeurosis play in locomotion.

Chapter 1. THE MUSCLE TENDON MODEL

1.1. Introduction

It has been stated that much of the energy involved in running is stored from step to step, as elastic strain energy in the tendons. If this were the case it would perhaps save the animal a great deal of metabolic energy. At first sight this point might seem obvious, however it is a subject of great debate and has at present not been conclusively proved.

All animal locomotion depends upon certain basic principles that are incorporated in Newton's three Laws of Motion. According to the first of these, a body that is at rest can be set in motion only by the application of an external force. In order to elicit such a force from the environment, an animal must actively move part or all of its body. According to the second law, the velocity imparted to the body is directly proportional to the magnitude of the force and the duration of time in which it acts, and inversely proportional to the mass of the body. Newton's third Law of Motion states that for every action there must be an equal and opposite reaction. When a force is applied to an object, the object will push back with an equal amount of force. The magnitude of the reaction force will be the same but it will act in the opposite direction (see figure 1.1). These two forces are called an action-reaction pair. Thus in standing and walking the supporting surface pushes up against the feet with the same amount of force and along the same action line as the downward thrust of the feet. This is called the ground reaction. In other words, to subject its body to a propulsive force an animal must exert an equal force against the environment, but in the opposite direction.

The mechanical energy of an animal's body is the sum of its kinetic energy, gravitational potential energy and elastic strain energy. These components of mechanical energy often interconvertible, energy is converted back and forth between the kinetic, potential and elastic forms. The total mechanical energy of the body increases and decreases in the course of a stride. Whenever it increases, the increase must be provided by muscles doing positive work. A decrease must be brought about by air resistance or

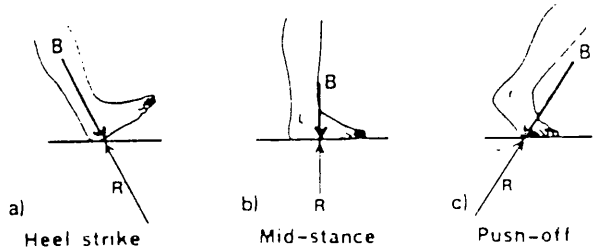

Figure 1.1. Ground reaction force, R, during stance phase of gait at, (a) heel strike, (b) mid-stance and (c) push off. B is the force exerted by the foot.
From Galley & Forster (1990).

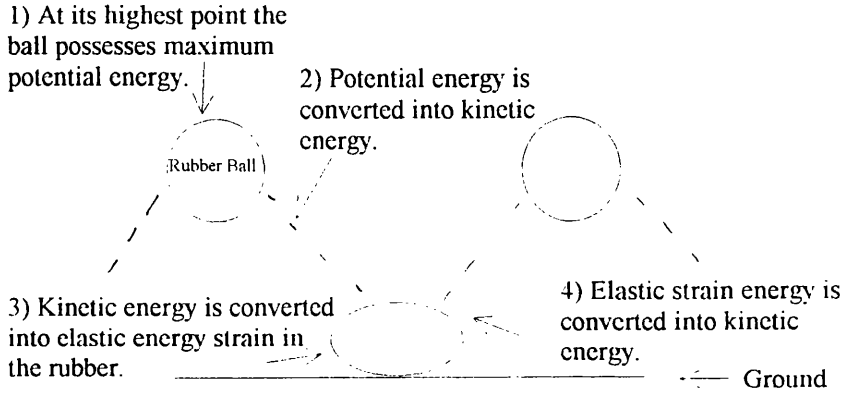

Figure 1.2. A schematic diagram of a bouncing rubber ball.

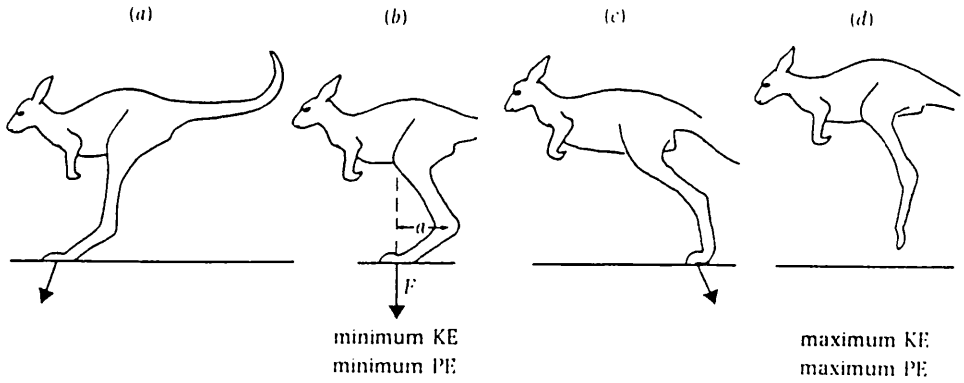

Figure 1.3. Outlines traced from a film of kangaroo hopping. The arrows represent forces exerted by the feet on the ground.
KE = Kinetic Energy, PE = Potential Energy
From Alexander (1990).

by frictional or viscous losses in the body. The decrease which occurs in the course of a walking stride are largely achieved by muscles doing negative work.

A bouncing ball utilizes the mechanism of stored elastic energy. A ball thrown upwards loses kinetic energy as it gains potential energy. When the ball is in the air it possesses potential energy, as it begins to fall back to earth under the influence of gravity it gains kinetic energy. On hitting the ground the mechanical energy is stored in the ball as distortion (stretch) of its rubber material. Possessing elastic properties the rubber returns to its original size releasing the stored energy with an elastic recoil, sending the ball into the air once again (see figure 1.2). A bouncing ball on a rigid surface will make many bounces without any fresh input of energy. The ball would keep bouncing on a rigid surface for eternity if it were not for air resistance and viscous processes in the rubber leading to frictional loss of energy, a perfect rubber does not exists, thus the molecules rub against each other and heat is dissipated. The difference in the bouncing of a ball and animal locomotion is that animals have legs and can therefore push against the ground at an angle and therefore move forward, whereas a ball can just go up and down.

1.1.1. Kangaroo Hopping

The animal which has been used most to investigate stored energy has been the kangaroo, since it uses only two legs both of which are doing the same thing at the same time. The principles however also apply to other mammal gaits including the bipedal running of humans and the quadruped running of most other large mammals. The function of an energy store, is to store energy in one stage of a locomotory cycle and release some of it at some other stage. A kangaroo travels in a series of bounds so that it rises and falls, consequently its kinetic and potential energy also rise and fall (Alexander, 1990).

At stage (d) (see figure 1.3) the kangaroo has maximal (kinetic plus potential) energy. At stage (a) the kangaroo decelerates itself by pushing forward on the ground, indicating that the leg act as brakes here to halt the movement, thus absorbing the mechanical energy (potential and kinetic). The knees are bent, and the leg muscles are active (quadriceps and calf muscles) and therefore their tendons are stretched and thus elastic

strain energy is stored in the tendons. If however this mechanical energy could not be stored in the tendons it would be degraded to heat in the muscle. In stage (c) the stored elastic energy in the tendon is returned to the muscle as an elastic recoil thus saving the muscles having to do work to provide the necessary energy for acceleration (Alexander, 1990).

The gastrocnemius and plantaris muscles of the kangaroo and other running mammals have long tendons. Tests have shown that these tendons are composed of an excellent elastic material, returning in its elastic recoil about 93% of the work done in stretching it (Alexander, 1988). The kangaroo's feet collide with the ground at a force of up to six times body weight for kangaroos hopping fast (Alexander, 1990). The forces involved in kangaroo hopping are thought to stretch the tendons by about 3%. This is thought to reduce the amount of work done by the muscles by approximately 1/3. Presumably this saves metabolic energy by enabling its muscle to remain in relatively isometric contraction while exerting force, rather than lengthening and then shortening. Relatively isometric is stressed since not all the energy is saved, therefore the muscles have to shorten to do work to make up the loss (Alexander, 1988).

1.2. The Model

A computer model of a hopping "beast" (a muscle tendon complex) was developed using a dynamic modelling program called Professional Dynamo. The model is intended to be used to investigate the effect of tendon compliance and the amount of muscle mass on the energetics and mechanics of hopping. In the body there is a maximum distance over which the limbs can be moved and a maximum force that can be exerted by the muscles. Therefore there is an optimum spring stiffness in the body. Since in order to store a large amount of elastic energy a substance must have the right degree of elastic stiffness (change in length / change in force). If it is too stiff it cannot store elastic energy as it does not get stretched enough by the maximum force the muscles can exert. If it is too flexible it cannot store energy as it can not be stretched to a sufficient distance.

1.2.1. The Model A Brief Description

The language of Professional Dynamo requires that there are certain types of equations;

levels (l), auxiliaries (a) and rates (r) (see appendix 1). Levels are obtained by integration over time, for example the position of the body is obtained by integrating the velocity of the body over time. Auxiliaries are simple algebraic functions of levels, rates and other auxiliary variables at the current time. The input to the level equations are called rate equations.

The model is one dimensional in order to be as simple as possible. The model consists of three mechanical elements in series; a mass, a leg of variable length and a spring (see figure 1.4). The "beast" had to be given a certain mass, or else it would not be able to jump. However in order to keep the model as simple as possible all the mass was located in one place (the body). A dashpot has been included to prevent the unstimulated muscle lengthening fast. The model has a flat length tension curve, i.e. the model muscle has potentially infinite length, however the length of the muscle has been controlled by giving the leg length limits. This is of course not like real muscles. What the muscle experiences can be defined by the length changes it undergoes. In the model and as in real life, the leg was made to get longer and the muscle to get shorter when the muscle is activated. Therefore in the model the changes in leg length were made to be the same as those in the muscle, but of the opposite sign.

The tendon is represented in the model by a spring. This compliance has been placed in series with the muscle to test whether it would improve the energetics of repetitive jumps. It has not been specified whether the spring is attached to the body or attached to the foot, since mathematically, it will not make any difference. For mathematical convenience the spring is treated as if it were a compression spring, i.e. it stores energy when it is compressed and releases energy when it lengthens towards its initial length. However for presentation purposes it is plotted as an extension spring (see figure 1.9). The model spring is linear, however in life the tendons spring characteristics at high and low strain are not linear (see section 4.2.3.). Therefore the model spring is operating in the linear portion of the stress-strain curve. A non-linear spring is simulated in section 1.6.

Real tendons have a slight hysteresis, however the energy dissipation has been shown to be a small proportion (approximately 0.07) of the total energy stored (Alexander,

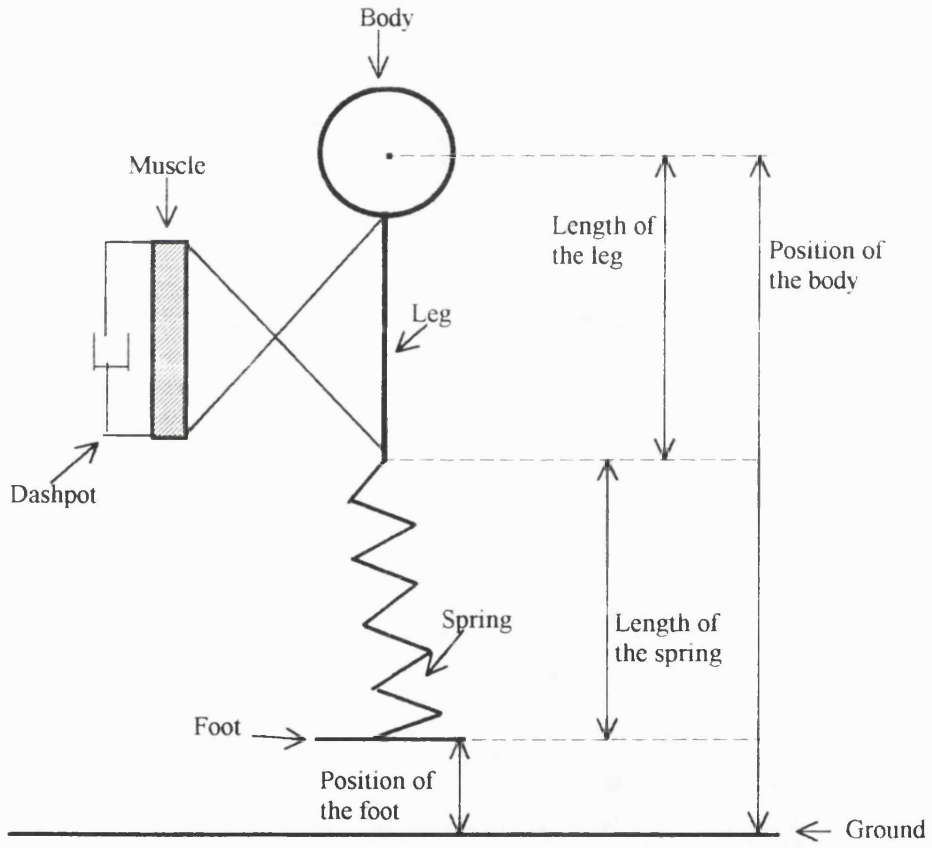

Figure 1.4. Diagram of the muscle tendon complex.

Position of the body = position of the foot + spring length + leg length.

Muscle shortening increases the leg length.

For mathematical convenience the spring is treated as if it were a compression spring, i.e. it stores energy when it is compressed and releases energy when it lengthens towards its initial length. However for presentation purposes it is plotted as an extension spring (see figure 1.9).

1988) (see Figure 4.5). Although the spring in the model does not possess in itself energy absorbing properties, the model does contain a property of energy absorbtion. Small amounts of energy are absorbed in the viscosity. This arrangement is not identical to the energy absorbing properties of real tendons, but is very similar. The tendon in real life is in series with the muscle, whereas the viscosity feature of the model is in parallel with it. However since the energy absorbing properties of real tendons are known to be very small, this arrangement in the model is considered to be accurate enough to represent the properties of real tendons. There is only one force in the model muscle spring complex, since all the forces are in series, i.e. the muscle plus the dashpot (treated as one component) and the spring. The stiffness of the crossbridges was not stated in the model (i.e. they were considered infinitely stiff).

The model is bound by the first law of thermodynamics that is, it has to conserve energy. The energy that comes out of the muscle as work and heat is constant: a) Gravitational energy (this is the product of jump height and the mass of the beast), b) Kinetic energy, c) Heat in viscosity, d) Heat in the muscle (see figure 1.19). The energy is constant, but energy can be added by the muscle splitting ATP, and energy can be removed by being dissipated as heat. The model uses the approach of attaining the total energetic cost (the amount of ATP split) by integrating the rate of ATP use. The rate at which ATP is split (Katp) has been specified in the model to be 5 ATP split/second/site in isometric contraction (which is descriptive of muscle of small mammals e.g. a mouse). In the model it is assumed the relationship between the rate of ATP splitting and velocity follows the relationship shown on figure 1.5. This is similar to what has been observed in isolated muscle studies (Woledge *et al.*, 1985). The rate of ATP consumption is assumed to be a monotonic function of the rate of shortening (i.e. a particular ATPase has only one velocity on the graph). However this might not be true with the real life situation, it might in fact depend on what has happened to the muscle before.

Hill's force velocity curve (Hill, 1938) has been incorporated into the model. The model simulates a muscle-dashpot system, the velocity of the muscle and dashpot (viscosity) are the same since they are in parallel (see figure 1.4). The energy dissipated in the viscosity is small. Viscosity was put into the model, to stop huge velocities being

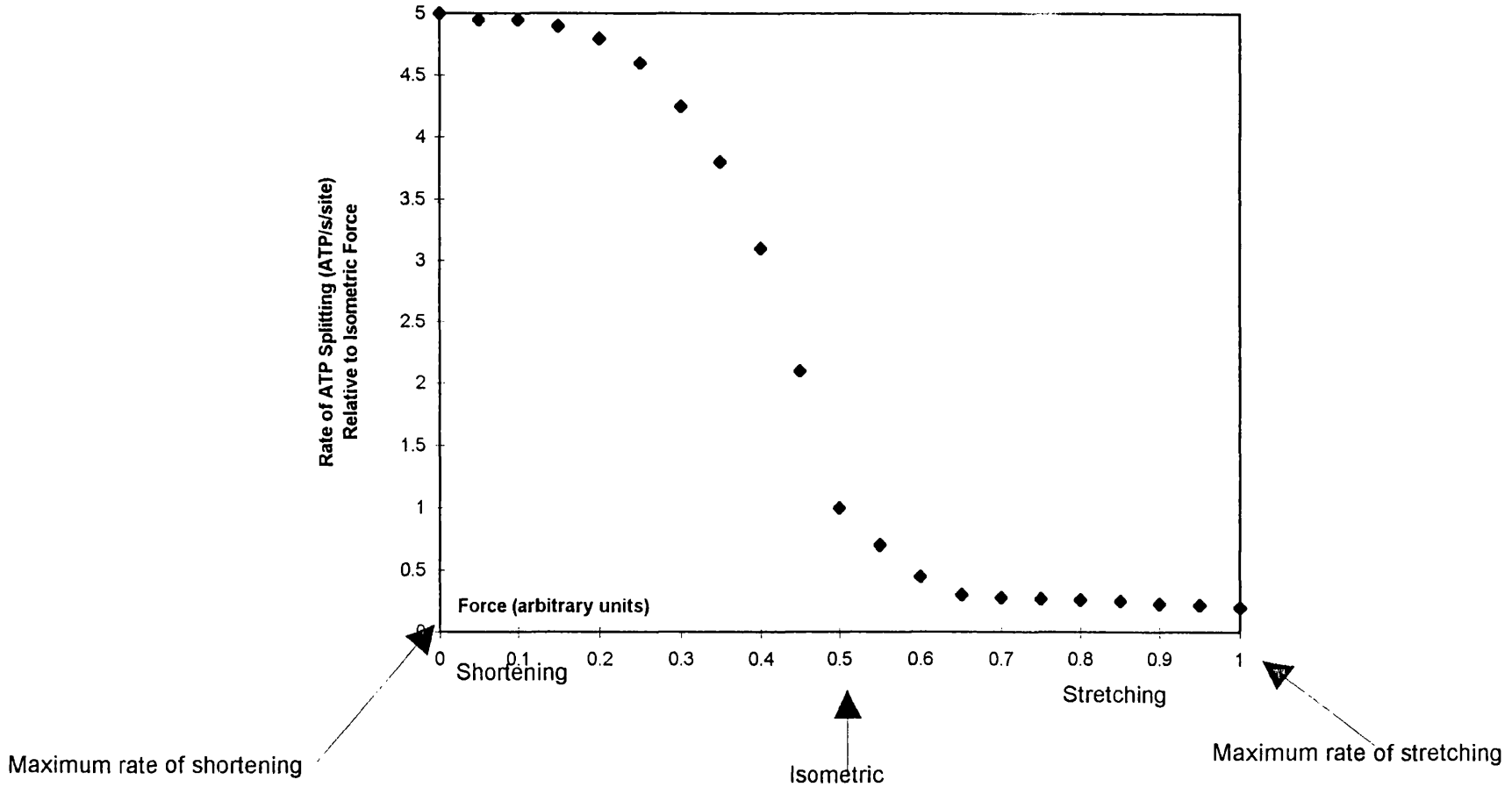

Figure 1.5. The rate of ATP splitting as a function of shortening velocity. The values on this graph are called aptab values in the model.

reached when the muscle is not switched on. Thus it prevents the muscle being stretched at very high speeds, this upsets the model and is not realistic. Viscosity is associated with limbs which have not been included in the model. Since viscosity is a small value (see figure 1.16B) it is not important an important feature of the model. The important features of the model are the two equations in the model that deal with the properties of the muscle to dissipate energy compared to its property to produce energy. Equation 9 (see appendix 1) shows the muscle dissipates energy when it is stretched. Equation 18 (see appendix 1) shows the muscle transduces energy.

The viscosity has been given a value that gives an appropriate shape to the force velocity curve. Only the overall force (F_e) is known (i.e. neither the force in the muscle (F_m) nor the force in the dashpot (F_d) are known). Therefore simultaneous equations were used to find the velocity of a muscle and dashpot in parallel (see figure 1.6).

Vyrep and vyren in the model instructions are solutions to simultaneous equations. Vyrep refers to the positive velocity (muscle shortening) and Vyren to the negative velocity (muscle stretching). Plotted as a function of the relative force in the muscle, they approximate the shape of Hill's force velocity curve (see figure 1.6). The viscosity is in parallel with the muscle therefore the force in each adds up. When the muscle is shortening F_m is greater than F_e, since some of the muscle force is being used to make the dashpot move. However when the muscle is being stretched F_m is less than F_e because some of the external force is used to make the dashpot move.

In real life how long the muscle is turned on for is controlled by two methods: 1) Ballistics; this happens in forceful movements, e.g. jumping. 2) Feedback control; this happens in delicate movements, e.g. picking up a pencil. In the model the muscle is controlled by a ballistic method of controlling the muscle. The term "go", the degree of activation, can either be 0 or 1. "Go" becomes 1 for a single time interval when the muscle is switched on, it can be thought of as the decision to go. "Go" is only true if all of the 3 muscle switch on conditions are true.

To turn the muscle on:

1) The foot must be on the ground (i.e. the foot position must be less than 0.01).

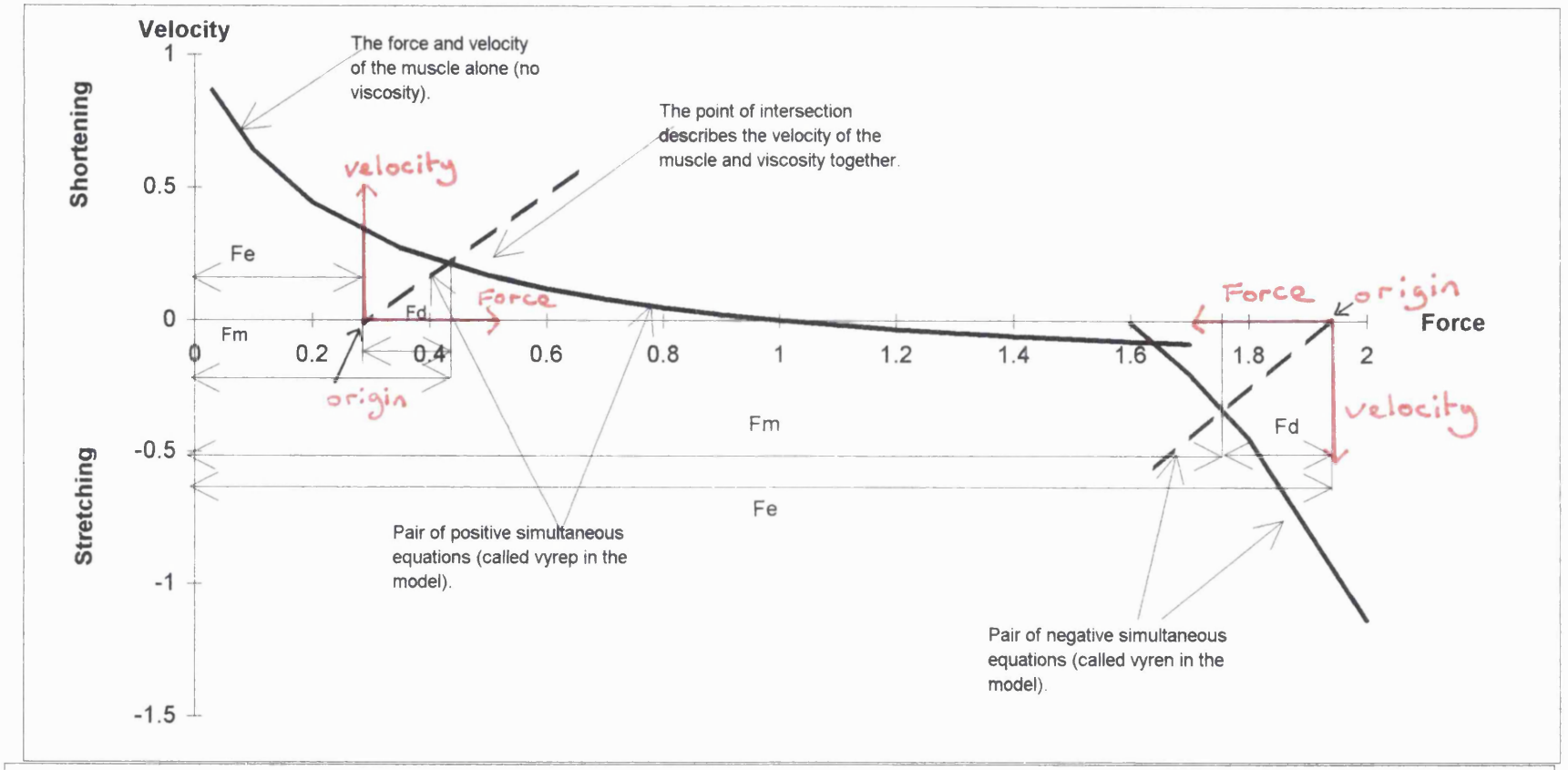

Figure 1.6. Simultaneous equations are plotted as a function of the relative force in the muscle. Two examples are shown; the first when the muscle is shortening (vyrep) and the second when the muscle is stretching (vyren). Force is expressed relative to the isometric force. Since the dissipating system is in parallel, the forces add up. Thus the viscosity and muscle experience different forces, and are plotted here with different origins for their co-ordinate systems. The origins of the viscous line are shown in red.

Fe = external force (overall force), Fm = force in the muscle, Fd = force exerted by the dashpot.
Fe = Fm + Fd

Ve = overall velocity, Vm = velocity of the muscle, Vd = velocity of the dashpot.
Ve = Vm = Vd

2) The muscle should not be already active (i.e. act must be less than 0.01).
3) The leg length must be less than the on length.

There is no active turning off of the muscle, only a passive decay. The "charge" (chconst) that is put into the muscle decays passively with a relaxation rate of 1/15 second.

1.2.2. A Series Of Steady State Jumps Were Obtained

(see figures 1.7 to 1.11)

Position of the body (Pnbdy)

The initial position of the body starts at position 19.9mm. It rises after the beast takes off and falls as the beast proceeds to land. Initially the muscle is unstimulated, the mass of the body falls towards the ground (see figure 1.7), thus the position of the body falls slightly. This stretches the muscle, thus the length of the leg shortens and the spring is compressed. When the length of the leg is shorter than the "on length" (onlng = 9.5) the muscle is switched on, since it is not already active. On landing the beast's legs shorten and the muscle lengthens absorbing work, therefore the position of the body falls to below 19.9mm. Jump height for the steady state is defined as the difference between the maximum and the minimum body position. The height of the jump is equal to the position of the body, not the position of the foot, because the mass of the "beast" is all situated in the body, therefore it requires no effort to raise the foot. A person can jump its own body height. Therefore a feasible large jump in the model should be considered to be 20mm (the "beast's" body height).

Position of the foot (Pnfot)

The position of the foot follows the same pattern as the position of the body.

Length of the leg (Lgleg)

The length of the leg increases during take-off, is constant whilst the muscle is in the air and shortens on landing. The changes in muscle length were made to be the same as those in the leg, but of the opposite sign. Thus the length of the muscle is shortening on take-off, constant whilst in the air and lengthening on landing.

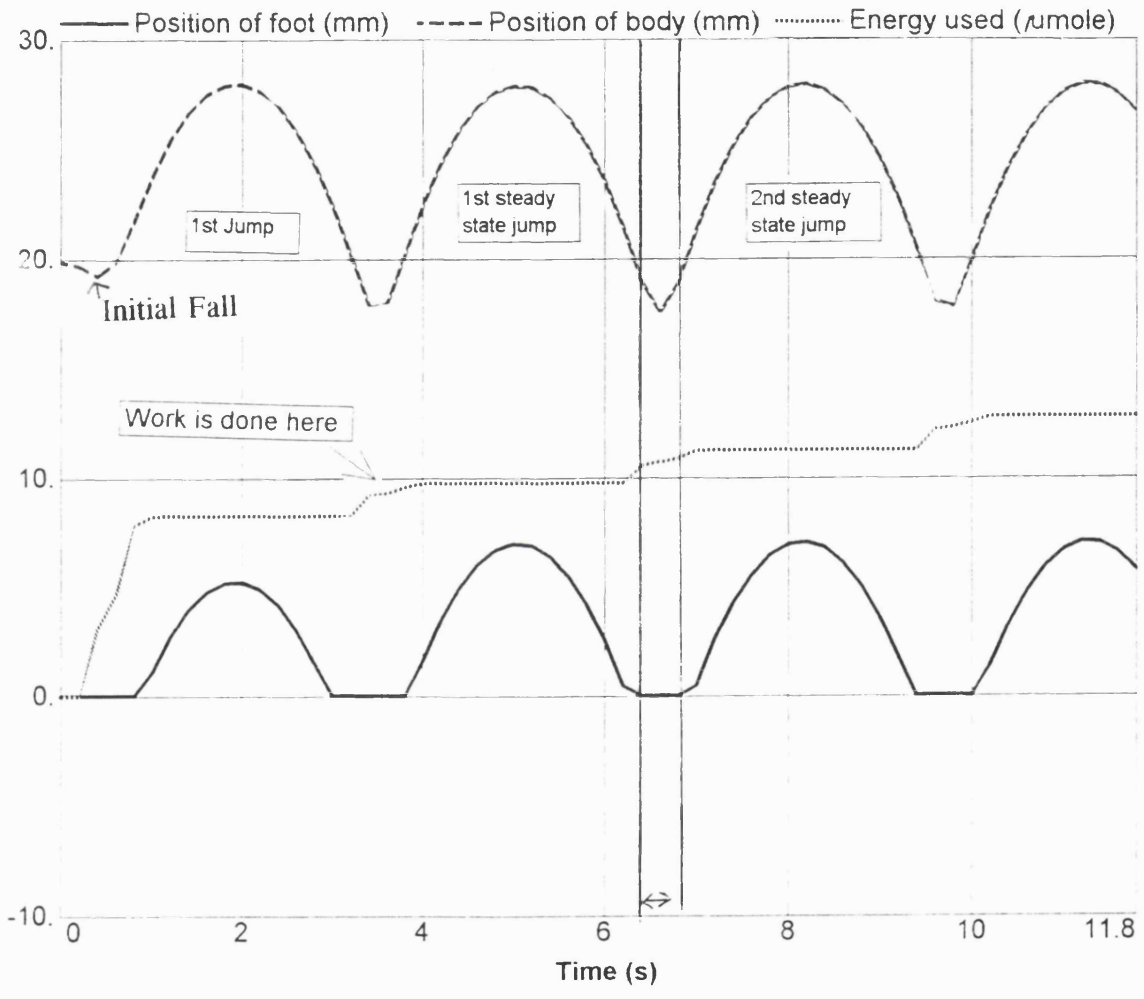

Figure 1.7. Print out from the Dynamo modelling program of a series of jumps reaching a steady state. The time 6.2 to 7.0 s is shown in more detail in figures 1.17 to 1.19.

Pmaxi = 100N, pmaxf = 70N, spring stiffness = 40N/mm.
Pmaxi and pmaxf are defined on page 45 and 47.

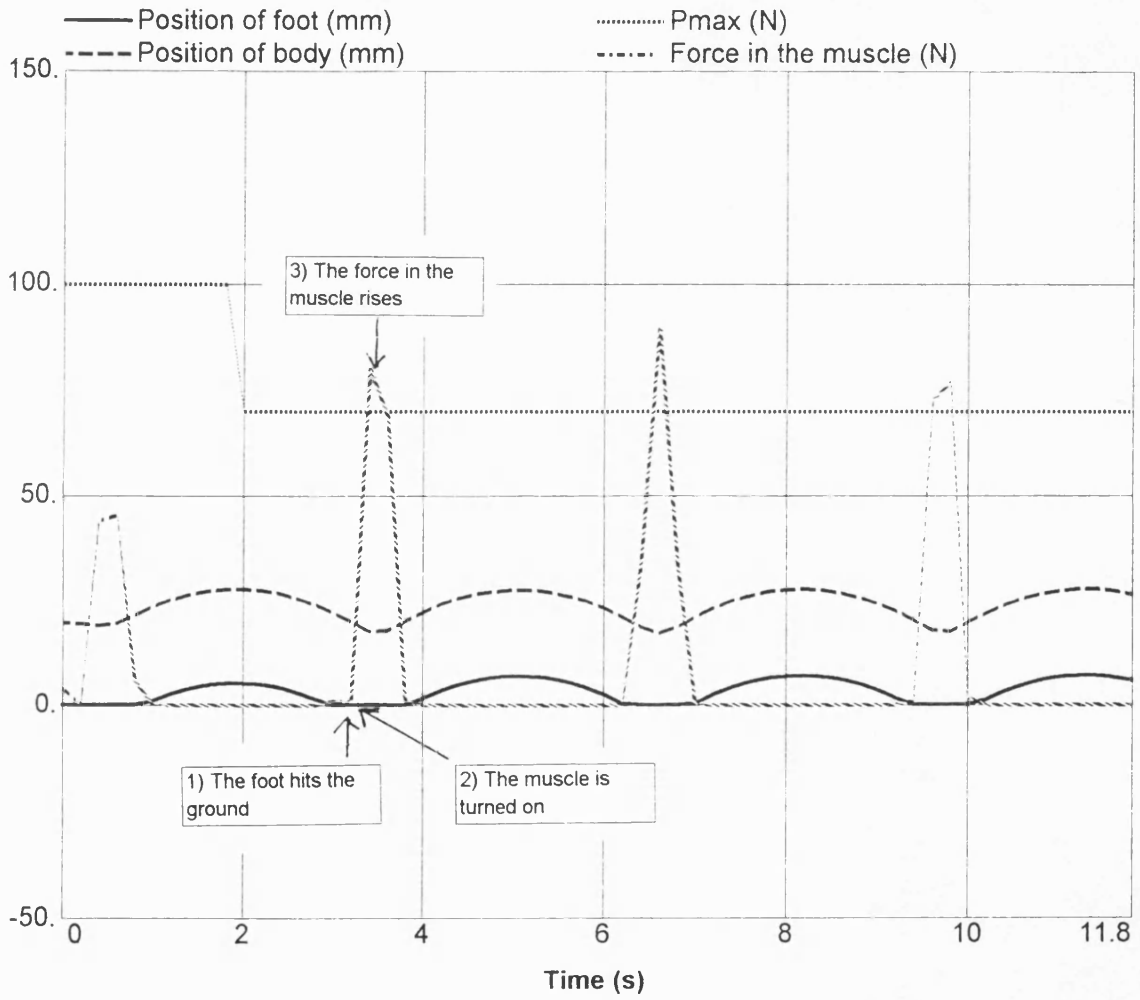

Figure 1.8. Print out from the Dynamo modelling program of a series of jumps reaching a steady state.

Pmaxi = 100N, pmaxf = 70 N, spring stiffness = 40N/mm.

Pmaxi and pmaxf are defined on page 45 and 47.

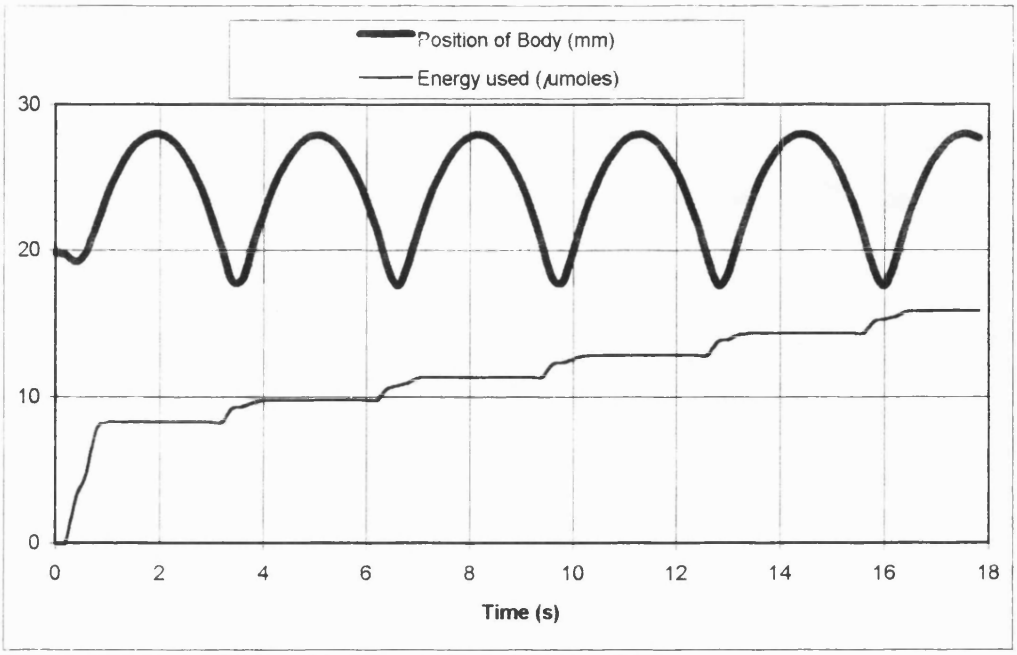

Figure 1.8a
Pmaxi = 100N
Pmaxf = 70 N
Spring stiffness = 40 N/mm
Jump height (jump no. 3) = 10.16mm, Energy used = 1.51 μmoles.

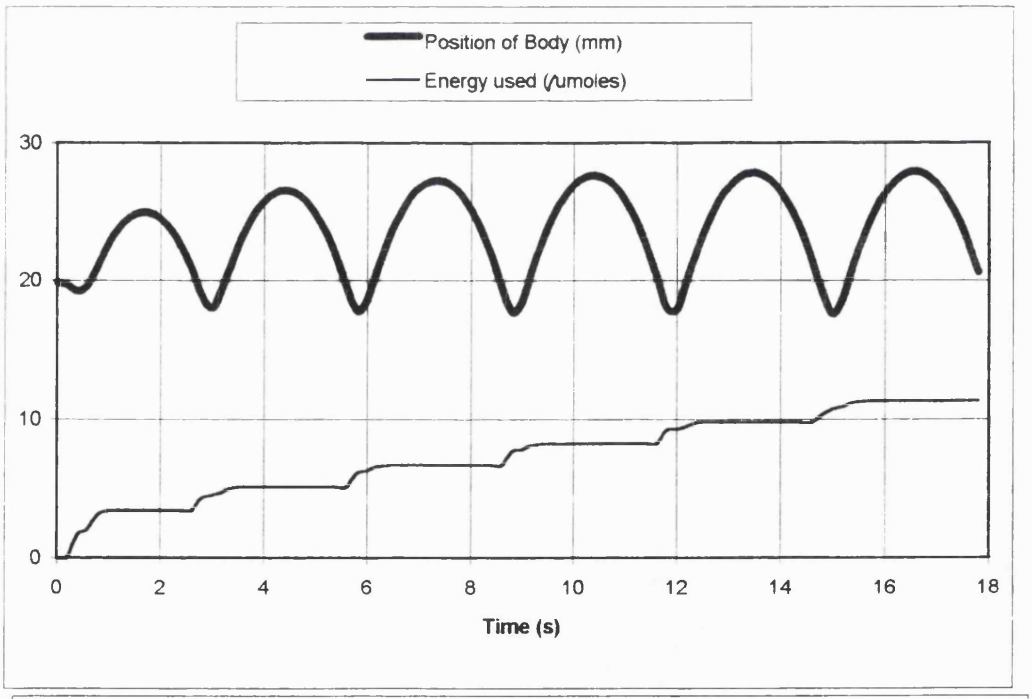

Figure 1.8b

Pmaxi = 70N
Pmaxf = 70 N
Spring stiffness = 40 N/mm
Jump height (jump no. 6) = 10.37mm, Energy used = 1.52 μmoles.

In figure 1.8a, Pmaxi is set at 100N and in figure 1.8b it is set to 70N. Increasing Pmaxi is a convenient way of achieving steady state jumps quickly (Pmaxi and Pmaxf are defined on page 45 and 47).

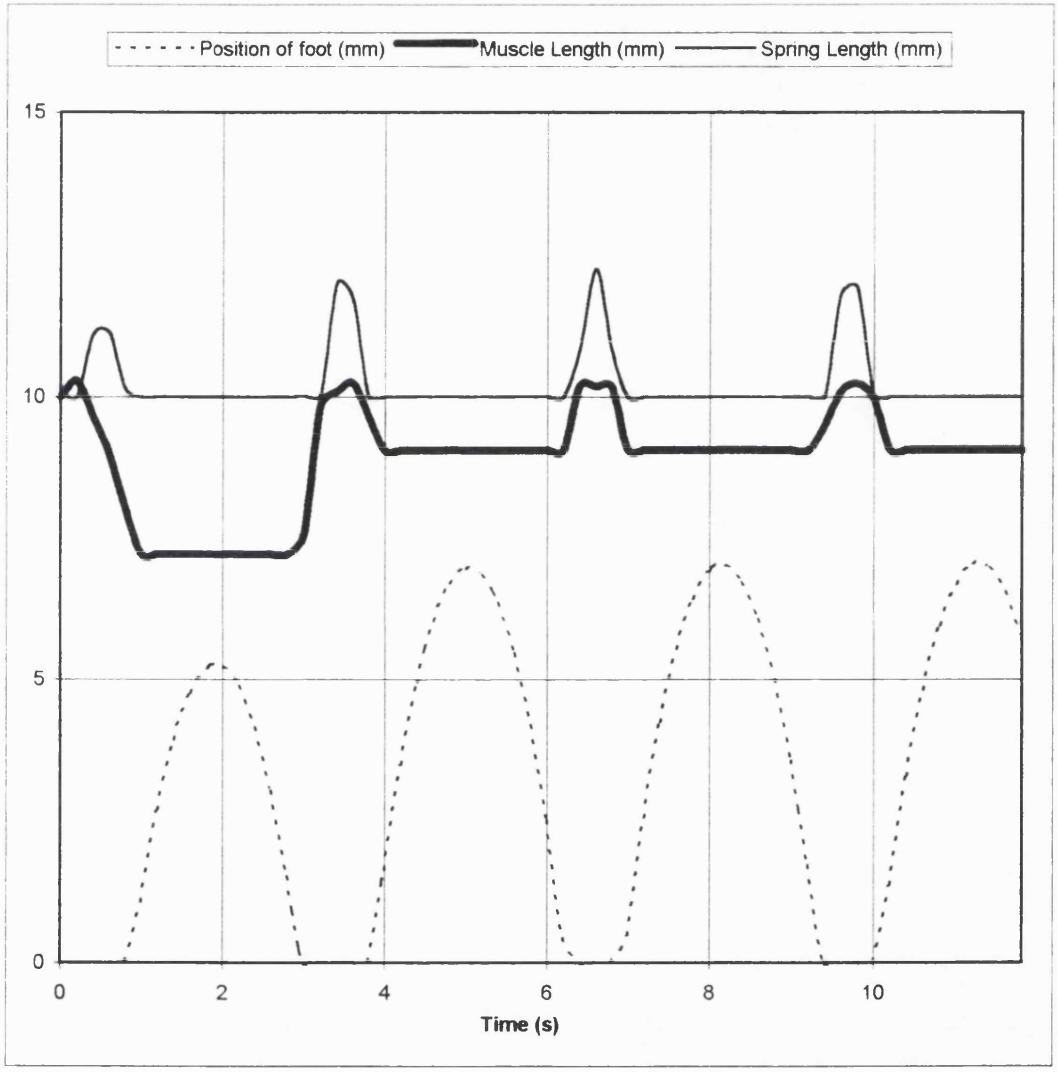

Figure 1.9. Print out from the Dynamo modelling program of a series of jumps reaching a steady state.

Pmaxi = 100N, pmaxf = 70 N, spring stiffness = 40N/mm.

Pmaxi and pmaxf are defined on page 45 and 47.

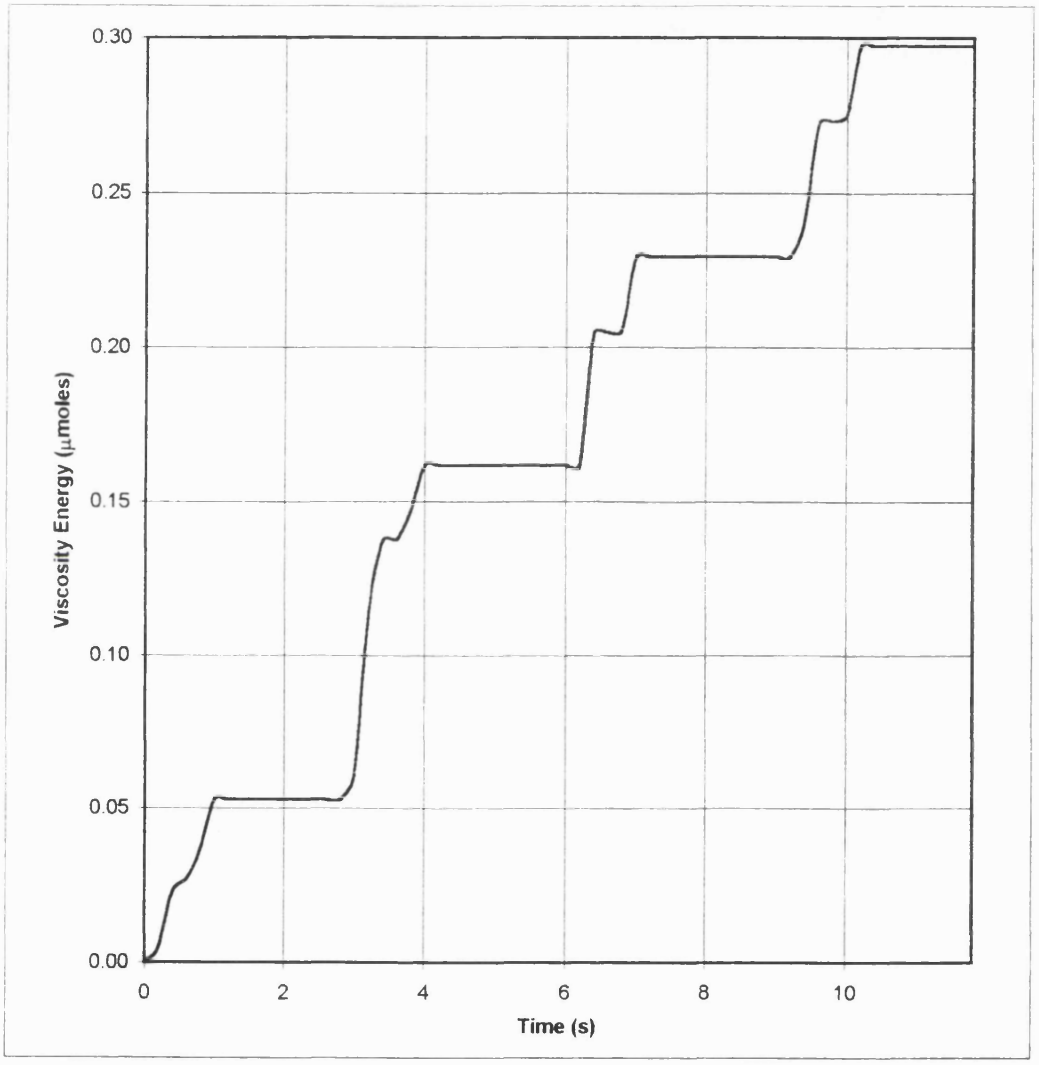

Figure 1.10. Print out from the Dynamo modelling program of a series of jumps reaching a steady state.

Pmaxi = 100N, pmaxf = 70 N, spring stiffness = 40N/mm.

Pmaxi and pmaxf are defined on page 45 and 47.

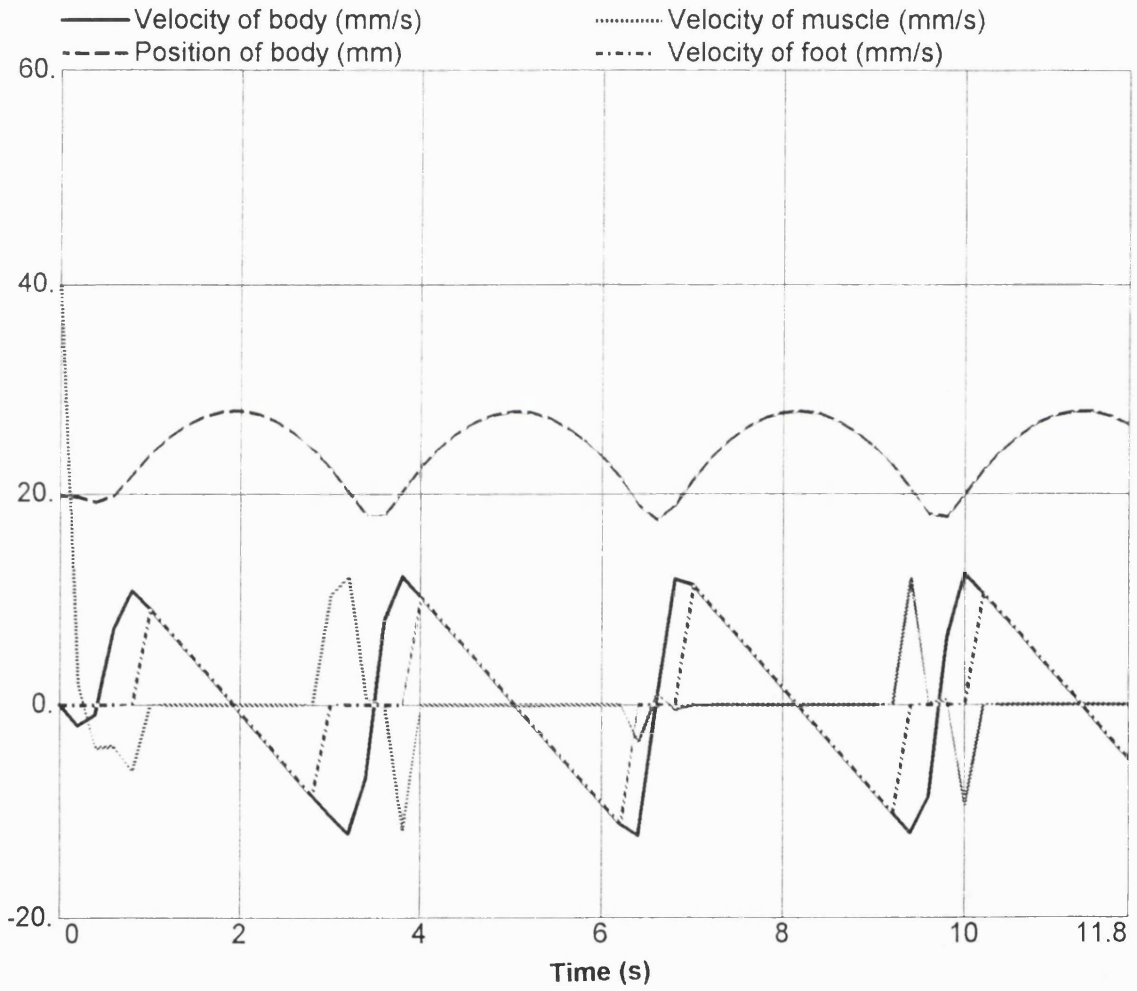

Figure 1.11. Print out from the Dynamo modelling program of a series of jumps reaching a steady state.

Pmaxi = 100N, pmaxf = 70 N, spring stiffness = 40N/mm.

Pmaxi and pmaxf are defined on page 45 and 47.

The length of the spring (Lgsel)

The length of the spring gets longer when the "beast" takes off and shortens on landing. Whilst in the air it is of a constant length.

The energetic cost (Enmus)

The energetic cost of the first hop is much greater than the subsequent hops. This is because the first hop requires a large amount of muscle to be activated to start the hopping (Pmax 100N), compared to subsequent hops (Pmax 70N). This is because there is no energy stored from previous hops. In the model ATP is used in isometric, shortening and stretching conditions.

The force in the muscle (Fcmus)

As the force in the muscle rises the spring length decreases because it is depressed. There should only be any significant force in the muscle when the "beast" lands and takes off. The force in the muscle drops to zero when the foot is off the ground, since the foot cannot exert force if it is not pushing against anything. In accordance with Newton's third Law of Motion, which says that for every reaction there is an equal and opposite reaction. Thus the muscle switches off after take-off and then does not generate force as it has nothing to push against.

Velocity

The velocity of the foot and body follow the same pattern. A negative velocity of the muscle is muscle shortening (take-off) and a positive velocity is muscle lengthening (landing) (see figure 1.11).

1.2.3. Different Sized Steady State Jumps

A series of different sizes of steady state jumps were obtained for Pmaxf (Pmax final) value 60N and spring stiffness value 40N/mm. The first jump has nothing to do with energy storage, as no landing is involved. Therefore the only role compliance plays is as a nuisance. For the first jump, as expected, as jump height is increased so does the amount of energy used (see figure 1.12). This is also the case for the steady state jumps (see figure 1.13). In taking off for the first time the muscle is doing work accelerating the body. Therefore if more muscle is present the body is accelerated higher, (i.e. the

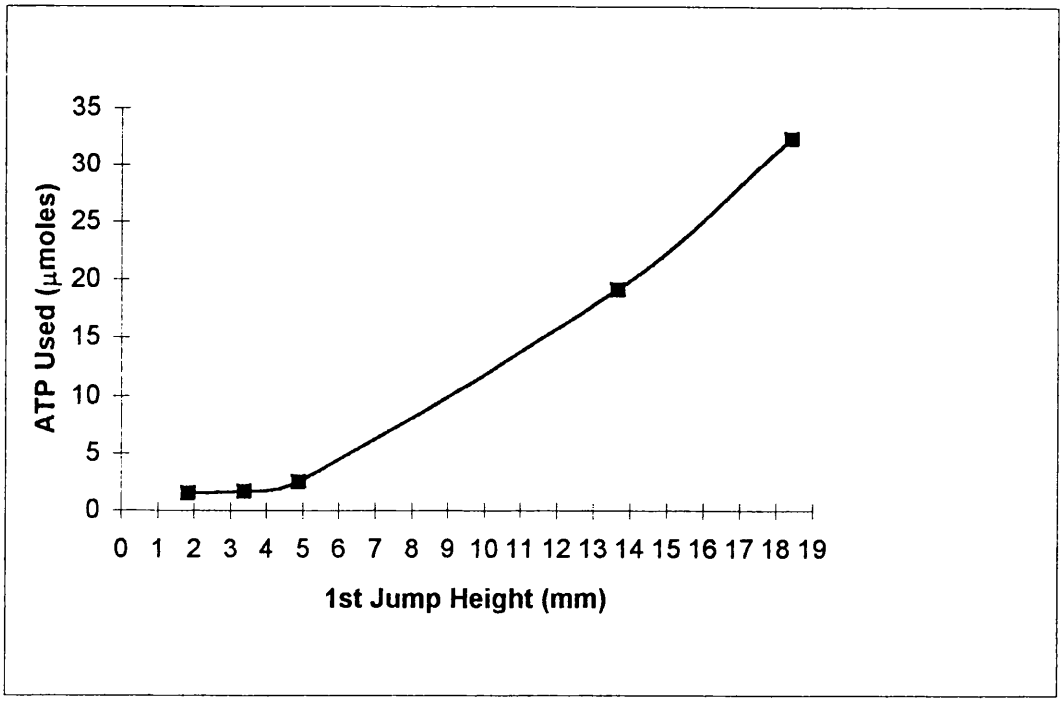

Figure 1.12. The amount of ATP used in the first jump plotted as a function of the first jump height.

Pmaxf = 60 N, Spring stiffness = 40 N/mm.

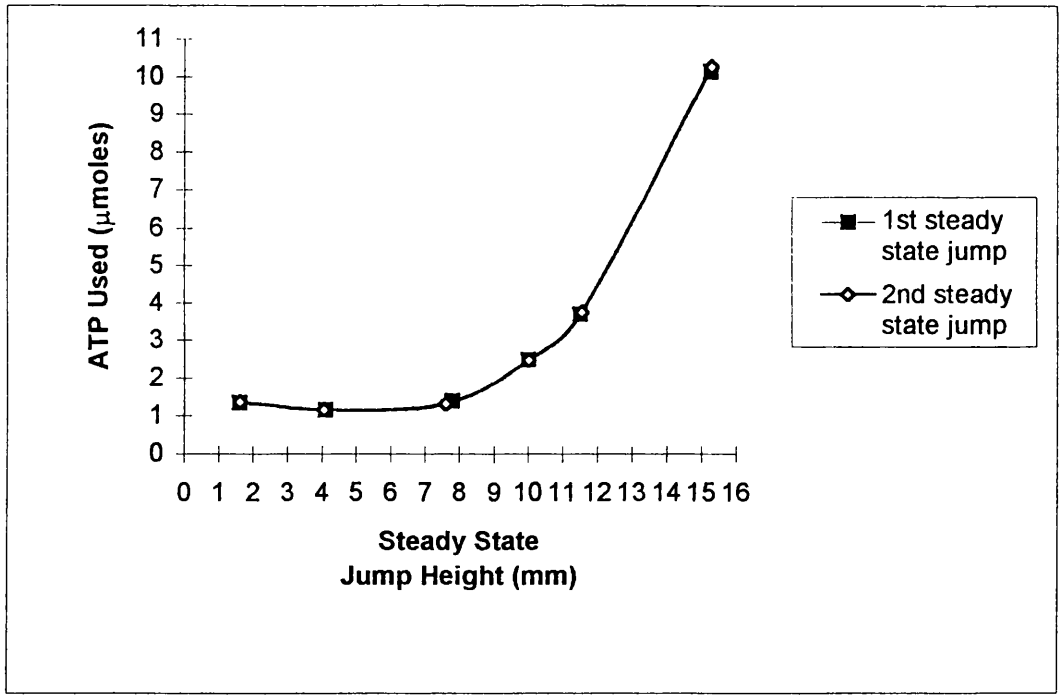

Figure 1.13. The amount of ATP used in one steady state jump plotted as a function of the jump height. The amount of ATP used in the next jump is also shown.

Pmaxf = 60 N, Spring stiffness = 40 N/mm.

jump is higher) and the energetic cost is greater. When looking at the steady state jumping two consecutive jumps are compared of a similar size, to determine where the energy has come from to jump to that height for the second jump. The variable chconst controls the jump size, it is a logarithmic variable, i.e. if it is doubled, it adds a constant to the time the muscle is activated. If the stimulation is stopped the activation decays exponentially (see figure 1.14).

A series of steady state jumps, for a given Pmaxf, was obtained by varying the value of Pmaxi (Pmax initial). Two values for Pmax were necessary because the first hop requires much more muscle to be activated to set the "beast" hopping, than the subsequent hops in which the "beast" can make use of the elastic energy stored in the spring. The first hop is therefore more energetically costly than the subsequent jumps (see figure 1.7). Pmaxi and Pmaxf values switch at 2 seconds in the model (see figure 1.8). Thus Pmaxi has no direct effect on the second jump, only Pmaxf influences it. In figure 1.8, Pmaxi is 100N and Pmaxf is 70N, this was done to enable steady state jumps to be reached quicker. Figure 1.8b is the same run as figure 1.8, except that Pmaxi has been set to 70N. It can been seen that the jumps are increasing slightly. Taking jump number six to be a steady state jump (jump height = 10.37mm, energy used = 1.52 μmoles), the values compare very similarly with the steady state jumps of figure 1.8 (jump height = 10.16mm, energy used = 1.51 μmoles). Therefore the fact that Pmaxi was varied in not really important, it is just a convenient way of achieving steady state jumps quickly. Looking at figure 1.8a and b, it can be seen that to achieve the steady state the "beast" can either start with a big initial jump or a small initial jump in which case the steady state will be reached after a larger amount of time. However when a large initial jump is used the energy cost of the initial jump is greater.

There are three variables that can be varied in the model.

1) Viscosity (this is negligible and therefore was not varied) (see figure 1.16b).
2) Muscle Amount and time the muscle is on for.
3) Spring stiffness.

1.2.4. Optimum Muscle Amount Simulations

A series of different sized steady state jumps were obtained for Pmaxf values from 35

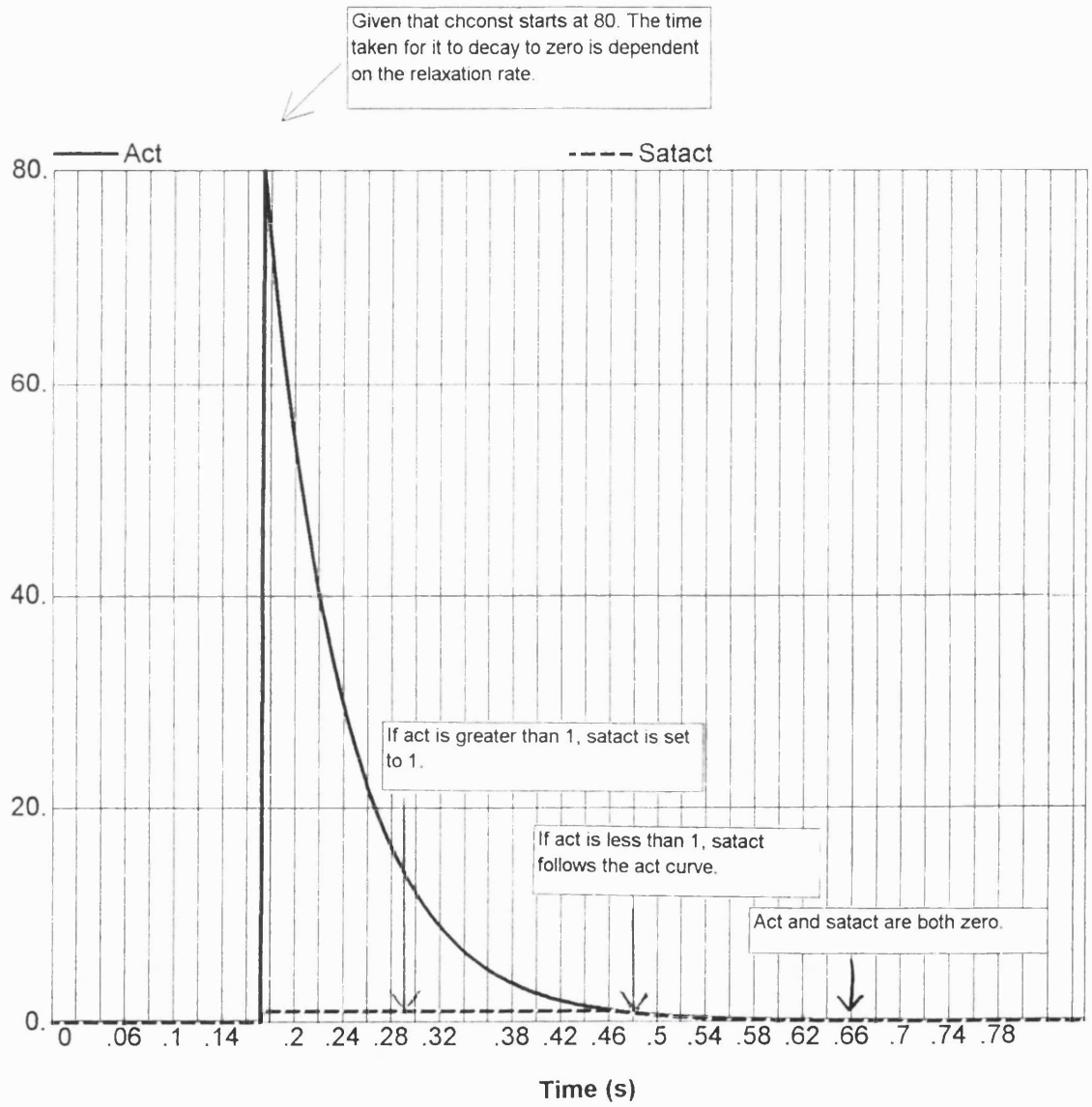

Figure 1.14. The stimulation "charge" put into the muscle decays exponentially. Chconst is the name of the variable which determines how much "charge" the muscle receives. Act is the name of the variable which gives a running account of the decay of the stimulation charge. Satact is a variable that varies from 0 (no activation) to 1 (full activation). Satact determines what percentage of the total amount of muscle available is being used.

to 100N. The stiffness value was set to 40N/mm (see figure 1.15). It can be seen that for a given sized jump (for example 10mm) that the energetic cost (μmoles of ATP used) decreases as the amount of muscle mass increases, from Pmaxf 50 to 60 to 70N. Thereafter as the muscle mass is increased the energetic cost increases. Thus for a spring stiffness of 40N/mm, pmaxf 70N is the muscle mass, which gives the lowest energetic cost for a 10mm jump. From figure 1.16a, it can be seen that the Pmaxf value that gives the lowest energetic cost, increases as the jump height increases from 5 to 15mm. It can be seen that the viscosity energy is very small and decreases as Pmaxf is increased.

There are two places in the model where energy can be lost, since as an animal jumps both the viscosity (dashpot) and the muscle accumulate energy as heat:

1) Viscosity

Viscosity is in parallel with the muscle. The velocity of the viscosity is proportional to the force the muscle is exerting. Viscosity absorbs energy whenever there is a rapid movement of the muscle. As the foot lands there is a sudden stretching of the muscle and spring and an increase in viscosity energy. Then there is another sudden length change in the muscle and the spring as the foot takes off again, the muscle contracts and the spring recoils. Which therefore results in a second burst in the viscosity energy (envis), therefore two spikes are seen (see figure 1.9 and 1.10). More energy is absorbed on landing (muscle is stretched), than in take-off (muscle shortening), thus the viscosity energy spike is smaller in the latter than the former. From figure 1.16b, it can be seen that viscosity is hardly having any effect.

2) Muscle

The energy in the muscle is equal to the total energy minus the energy that went into the viscosity.

Opportunities for the muscle to waste energy are if the muscle spends a long time:
i) In stretch being active. When a muscle is stretched, energy is dissipated as heat in the mechanical stretching and this energy has to be resupplied from ATP splitting by the muscle subsequently when it shortens.

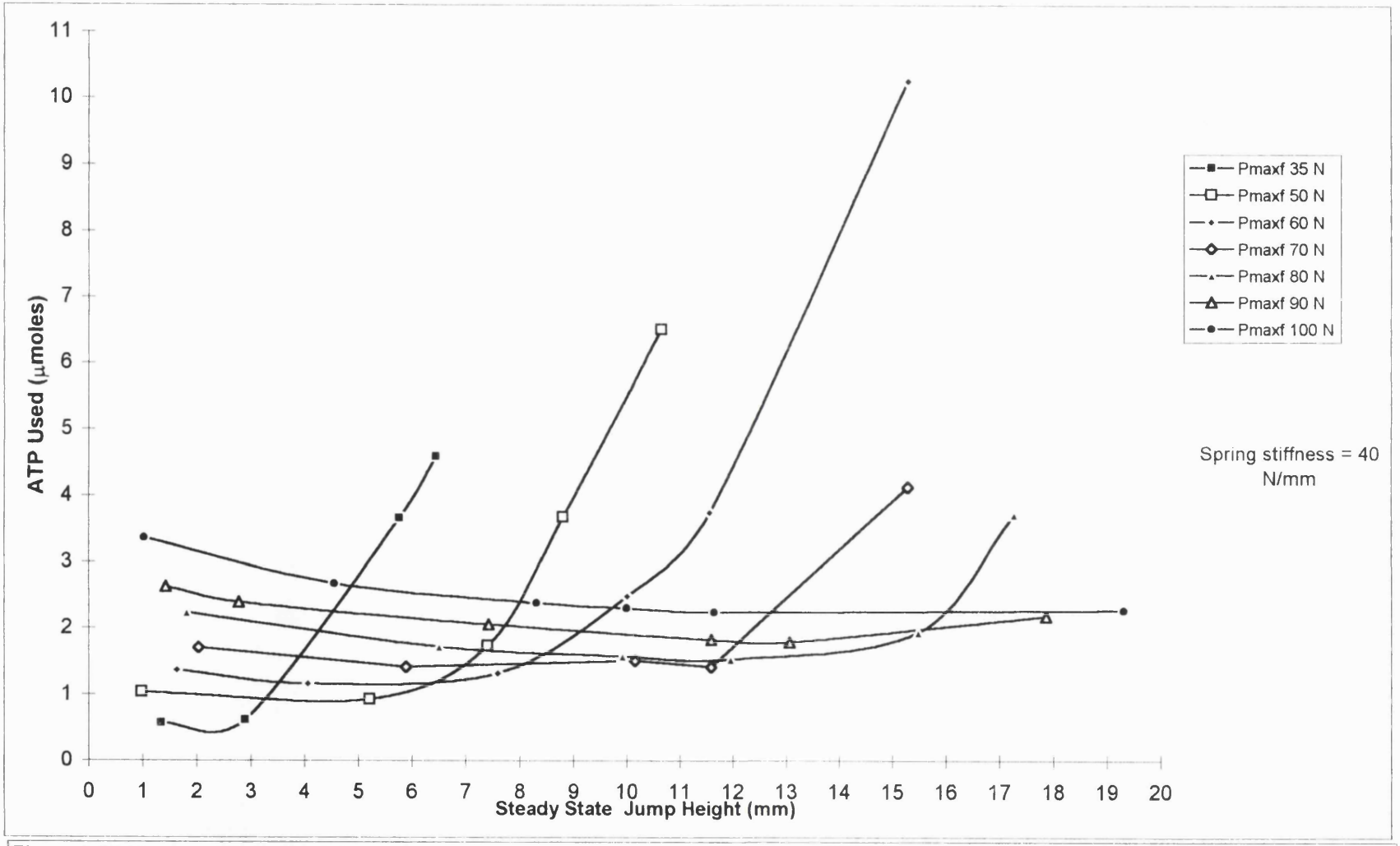

Figure 1.15. A series of steady state jumps for different Pmaxf values. The amount of ATP used in one jump is plotted as a function of jump height. Pmaxf is defined on page 45.

A

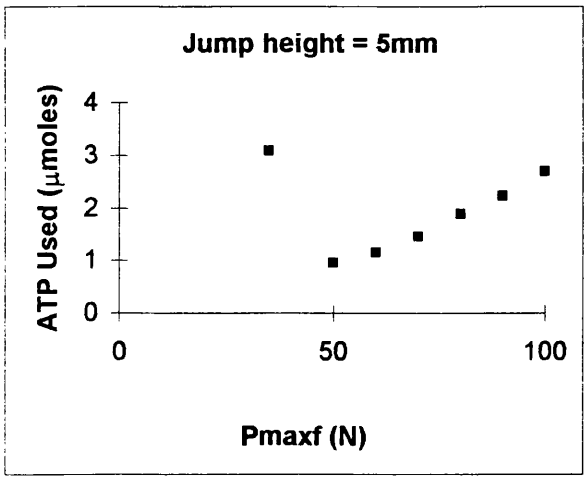

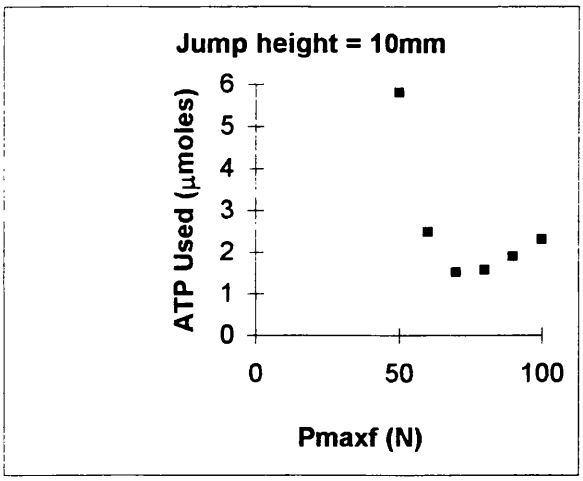

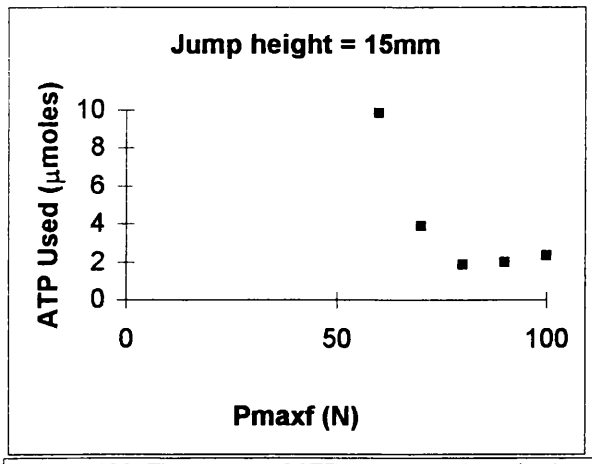

B

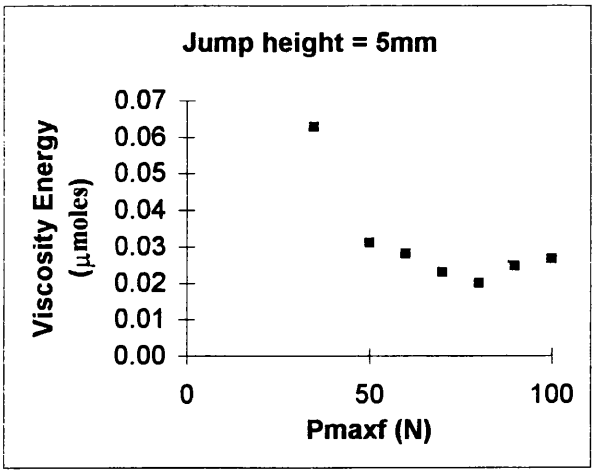

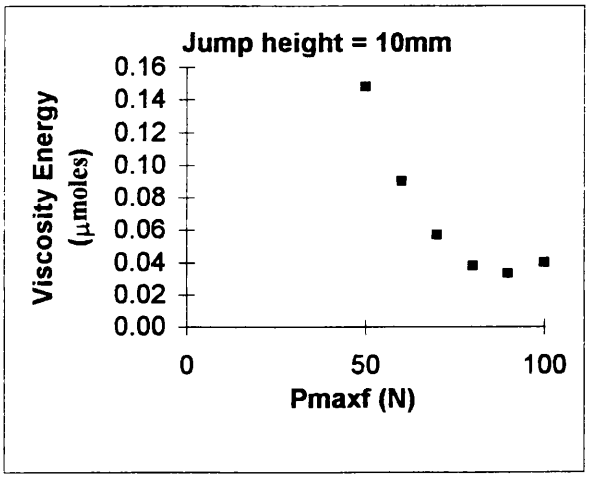

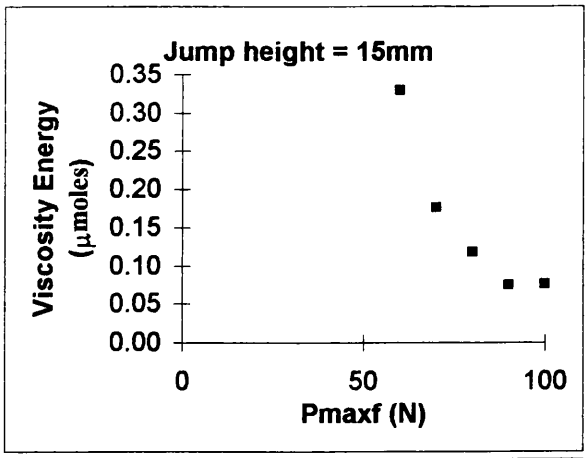

Figure 1.16A. The amount of ATP used in one jump is plotted as a function of Pmaxf. Three different steady state jump sizes are shown.

Figure 1.16B. The energy dissipated in the viscosity for one jump is plotted as a function of Pmaxf. Three different steady state jump sizes are shown.

Spring stiffness = 40 N/mm.
Pmaxf is defined on page 45.

ii) A very long time in isometric contraction. The muscle has to be kept active, in order to hold on to the other end of the spring. The ATP used here is dissipated as heat.
iii) Shortening very rapidly wastes ATP.

The model runs for the optimum muscle (Pmax 70N), too little muscle (Pmax 60N) and too much muscle (Pmax 100N) (spring stiffness 40N/mm) were compared in more detail, at a point where the foot was on the ground (see figure 1.7). The values for the variables "n" in the model instructions (see appendix 1) were given values from the long run, that corresponded to this start point. This enabled more data to be plotted on the shortened run.

What sets the optimum seems to be the balance between shortening and lengthening of the muscle. The lowest energy cost is obtained in Pmaxf 70N because the muscle is almost isometric (i.e. the muscle velocity line, is not very negative thus the muscle is hardly using any energy, see figure 1.18). Therefore the hypothesis is that if more or less muscle is used than the optimum, the muscle is doing more lengthening and shortening and is thus throwing power away. Looking at, figure 1.17, it can be seen that the muscle is absorbing almost as much power as it is producing. It seems the muscle is using energy when it is producing power. Too little muscle for a given spring stiffness, uses more energy at the end of the contraction i.e. at take-off, compared to the optimum muscle amount. This is because initially in decelerating the body the muscle does less work against the SEC, than the optimum muscle amount. Therefore in the acceleration of the body phase, the muscle has to stay fully active, which costs energy. Therefore the total energetic cost of the hop is greater than for the optimum muscle amount (see figures 1.20, 1.21 and 1.22).

A muscle amount greater than the optimum however, uses too much energy in the decelerating phase. This results in the time that the muscle is on for is less. Therefore the relative force in the deceleration phase is high (this is a sign of muscle relaxation). If the muscle is not active enough at take-off the muscle is excessively stretched, which results in energy being dissipated. At the time of take-off the muscle has to be active, for the energetic cost to be minimized. This is because the muscle is holding one end of the spring. The spring is absorbing work from the falling body (see figures 1.23,

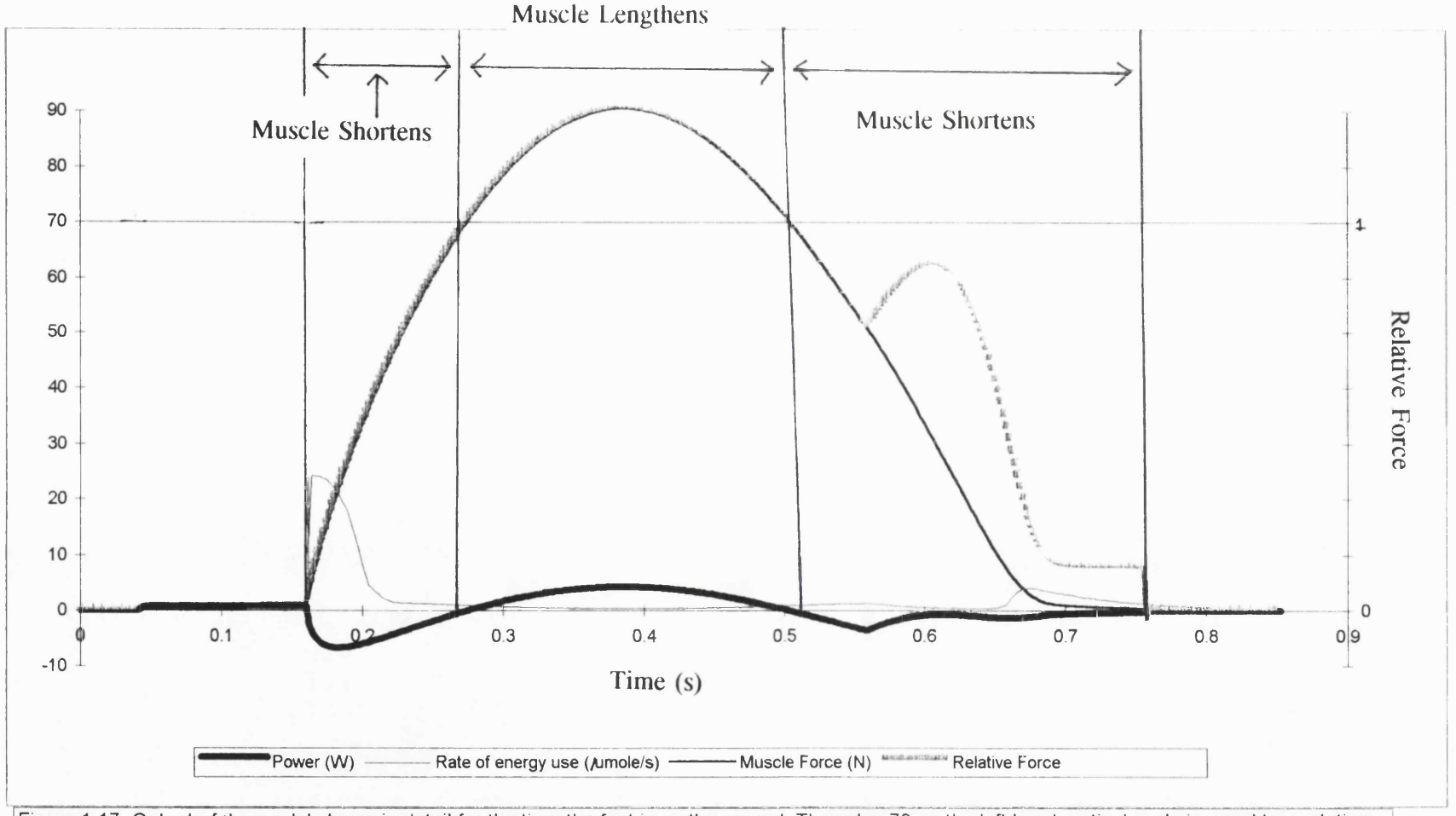

Figure 1.17. Output of the model shown in detail for the time the foot is on the ground. The value 70 on the left hand vertical scale is equal to a relative force of 1, i.e. the muscle is isometric.

Optimum muscle mass: Pmaxf 70 N.
Spring stiffness = 40 N/mm.

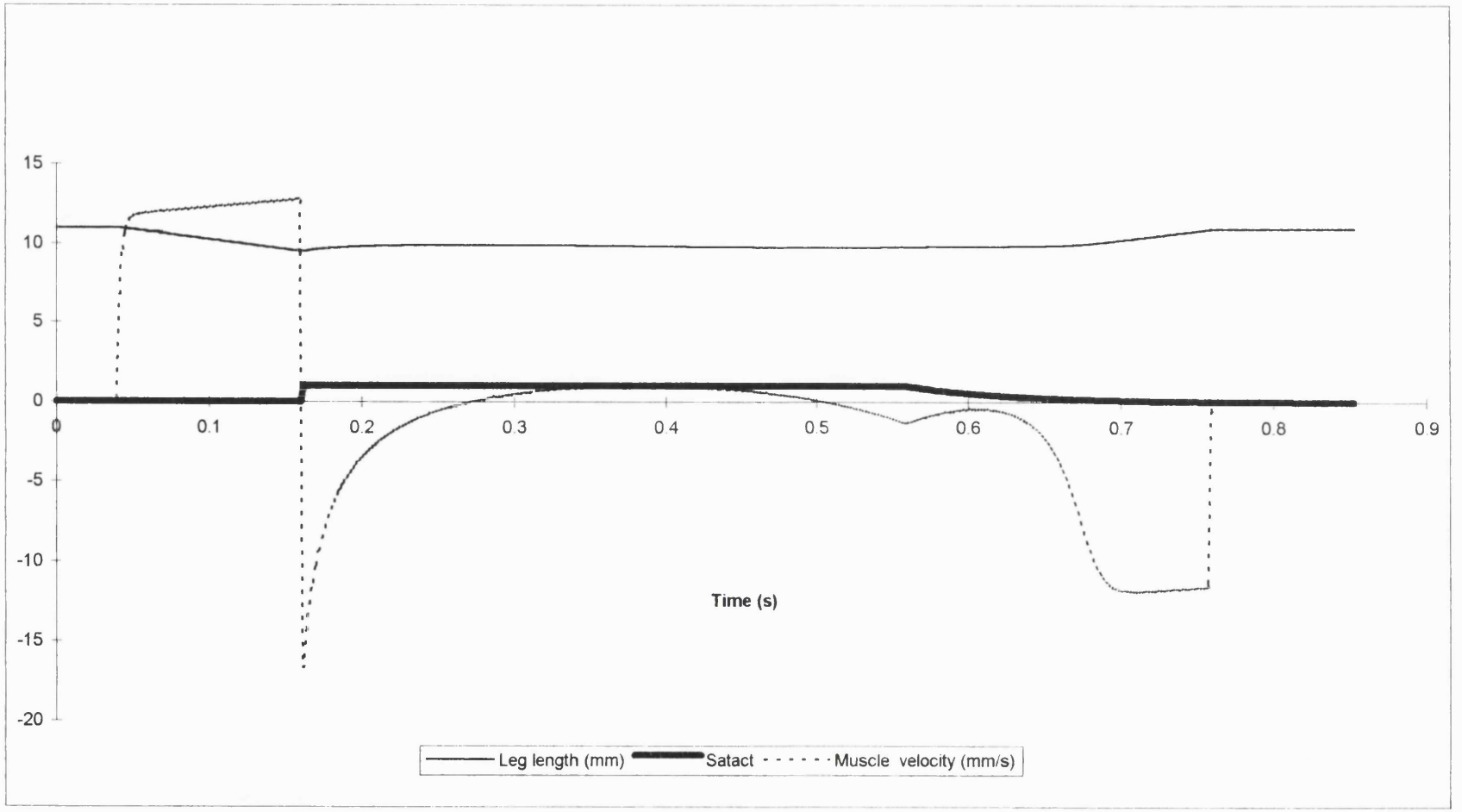

Figure 1.18. Output of the model shown in detail for the time the foot is on the ground. See page 104 for a definition of satact.

Optimum muscle mass: Pmaxf 70 N.
Spring stiffness = 40 N/mm.

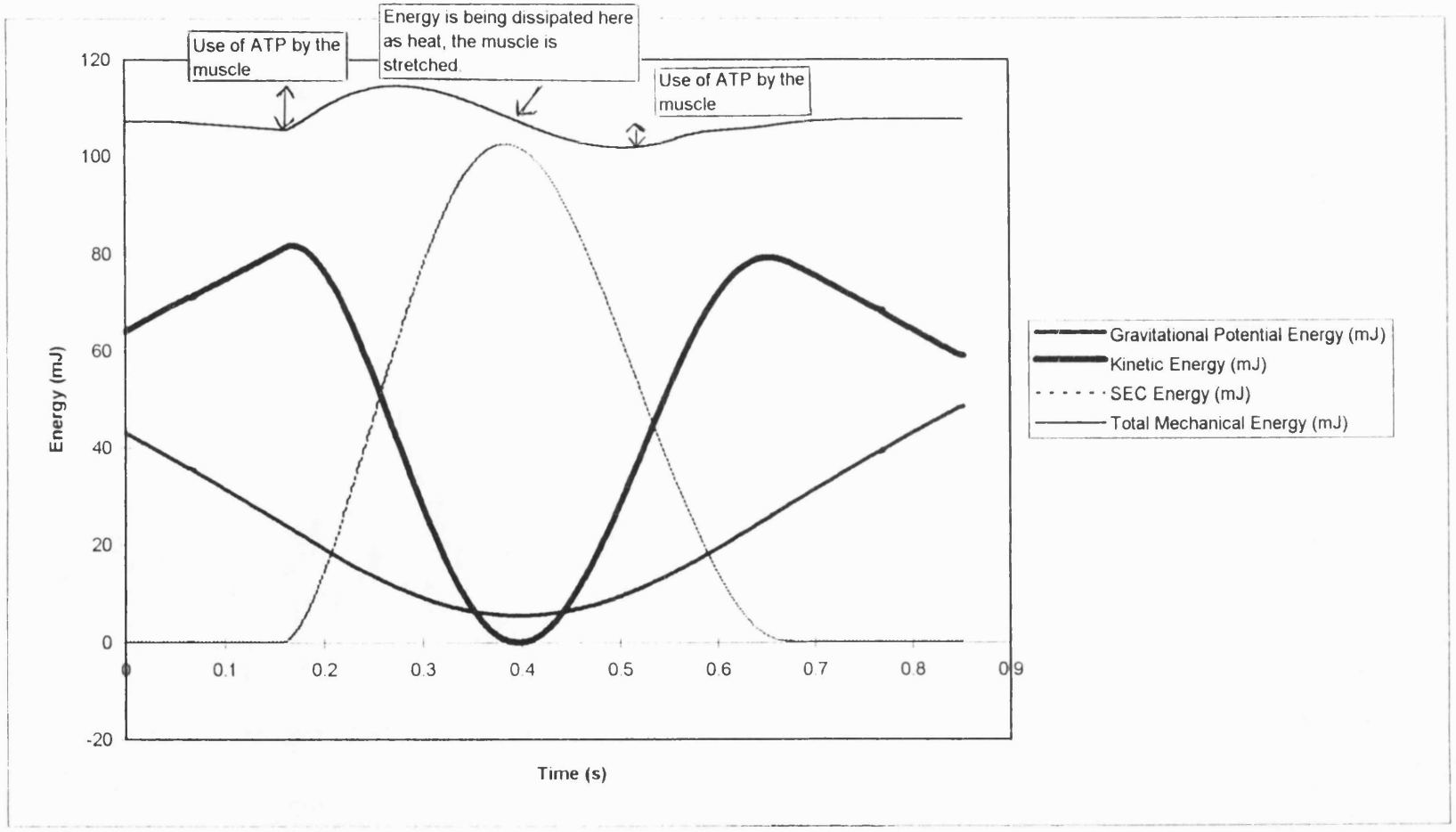

Figure 1.19. Output of the model shown in detail for the time the foot is on the ground. Since viscosity energy is negligible it has not been plotted on this graph. Total mechanical energy is equal to the sum of the gravitational, kinetic and SEC energy.

Optimum muscle mass: Pmaxf 70 N.
Spring stiffness = 40 N/mm.

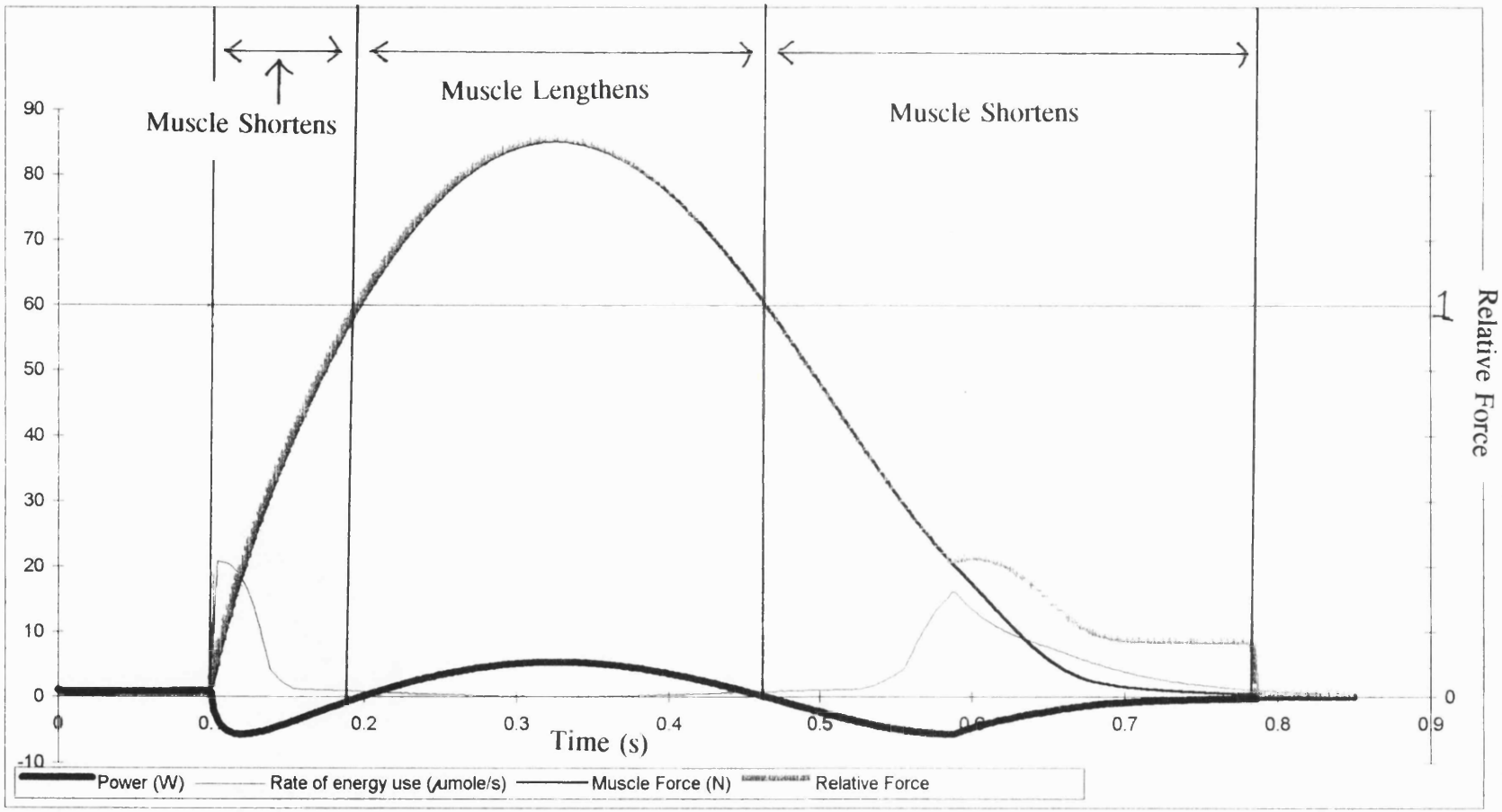

Figure 1.20. Output of the model shown in detail for the time the foot is on the ground. The value 60 on the left hand vertical scale is equal to a relative force of 1, i.e. the muscle is isometric.

Below the optimum muscle mass: Pmaxf 60 N.
Spring stiffness = 40 N/mm.

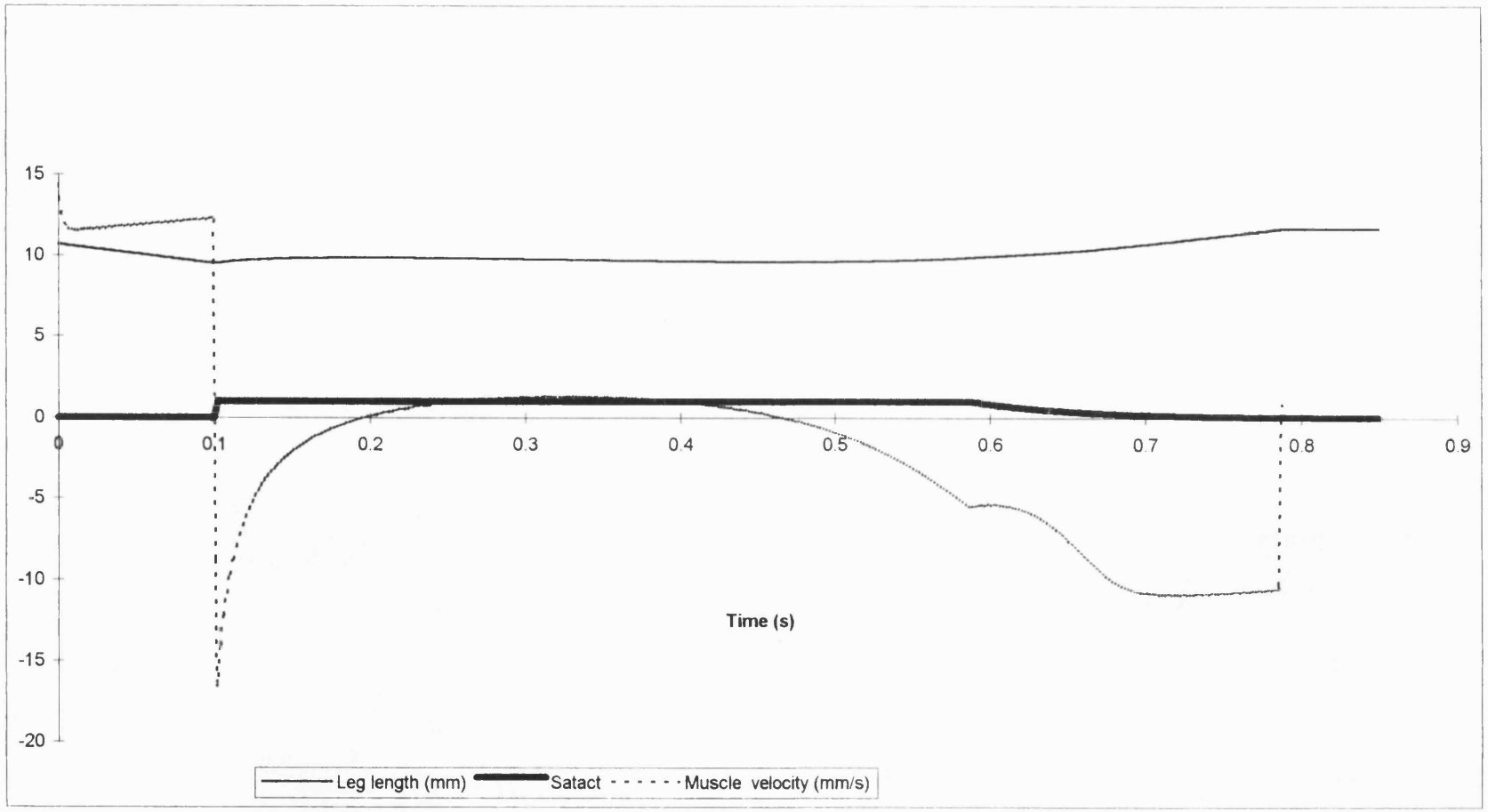

Figure 1.21. Output of the model shown in detail for the time the foot is on the ground. See page 104 for definition of satact.

Below the optimum muscle mass: Pmaxf 60 N.
Spring stiffness = 40 N/mm.

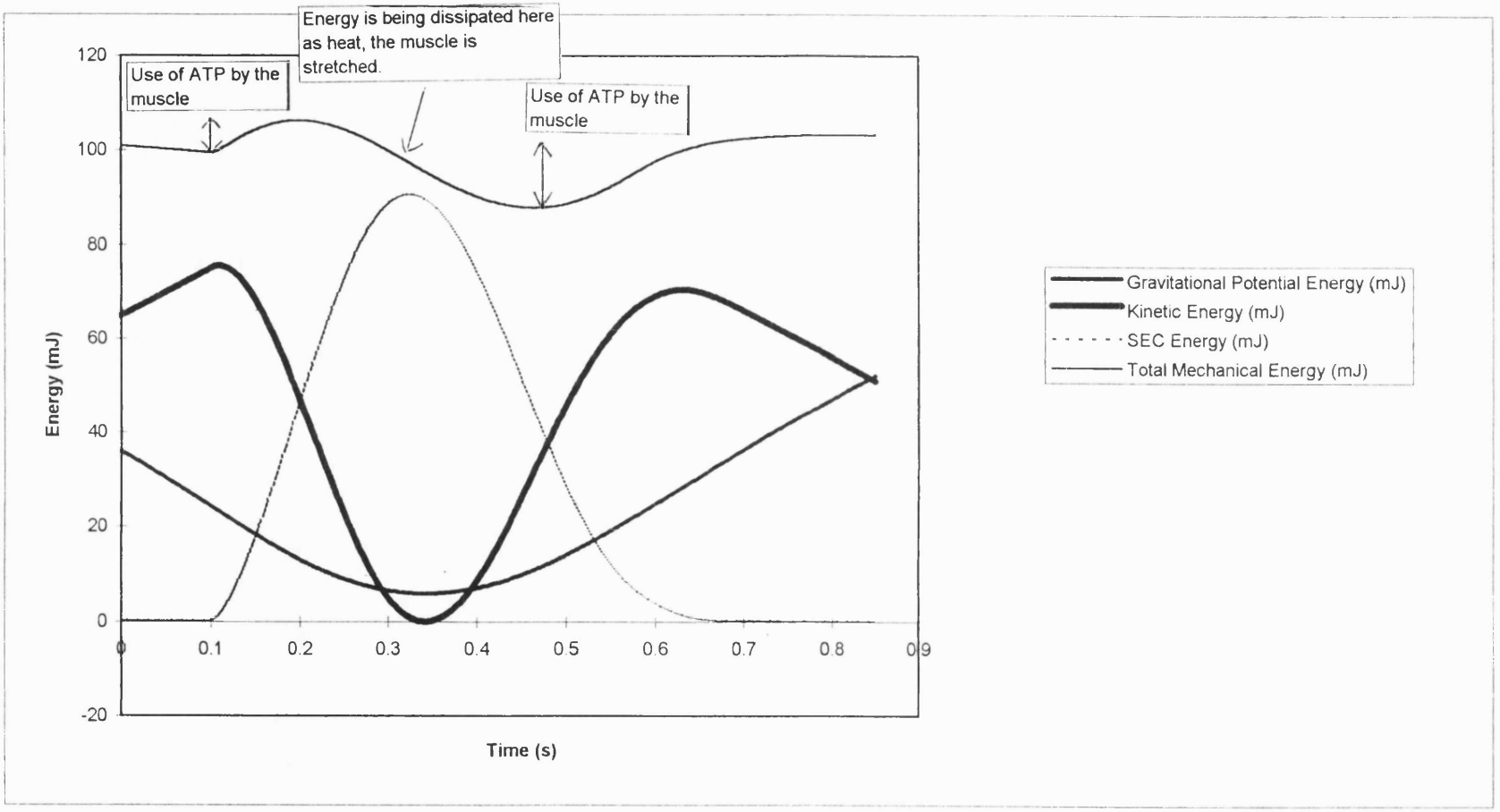

Figure 1.22. Output of the model shown in detail for the time the foot is on the ground. Since viscosity energy is negligible it has not been plotted on this graph. Total mechanical energy is equal to the sum of the gravitational, kinetic and SEC energy.

Below the optimum muscle mass: Pmaxf 60 N.
Spring stiffness = 40 N/mm.

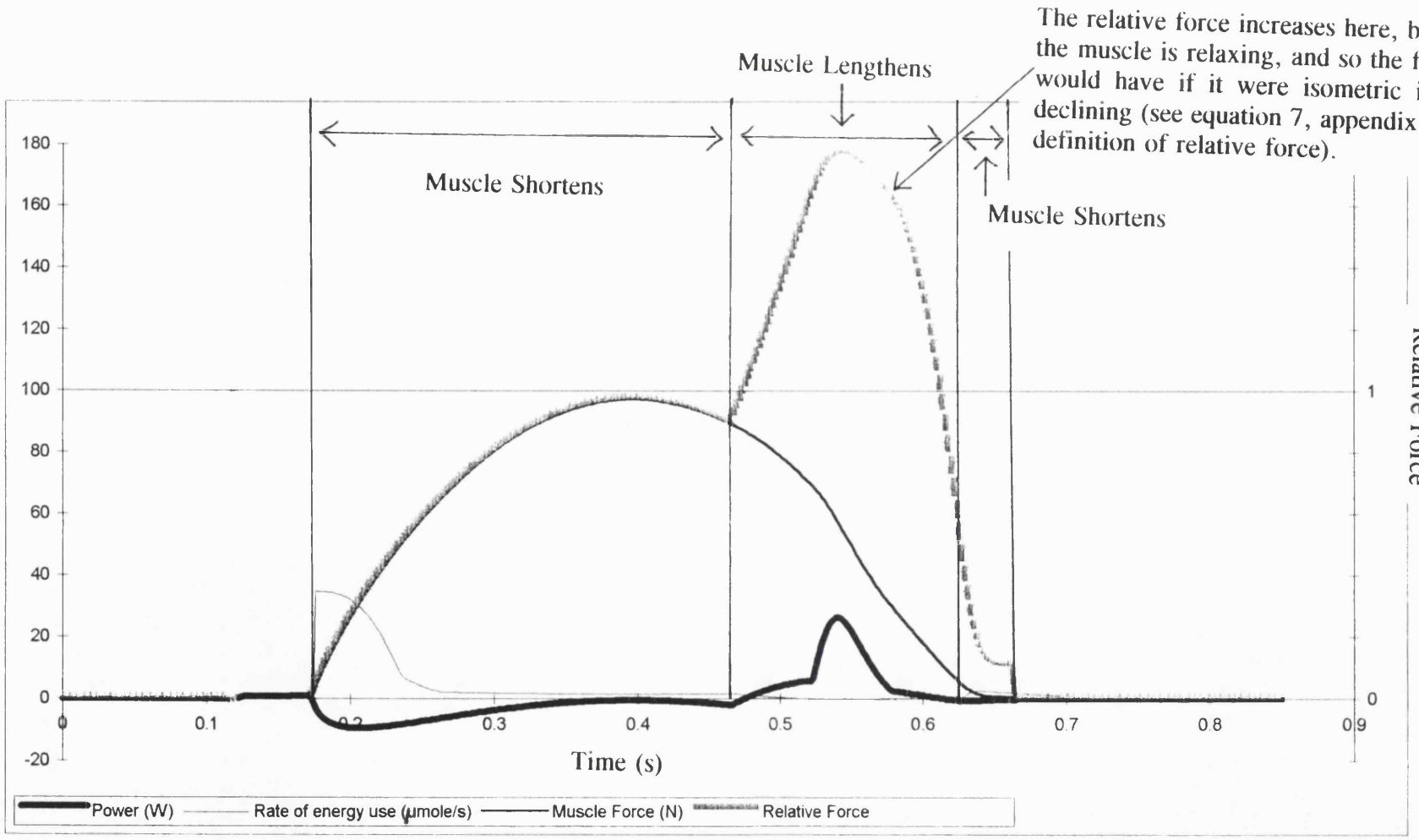

Figure 1.23. Output of the model shown in detail for the time the foot is on the ground. The value 100 on the left hand vertical scale is equal to a relative force of 1, i.e. the muscle is isometric.

Above the optimum muscle mass: Pmaxf 100 N.
Spring stiffness = 40 N/mm.

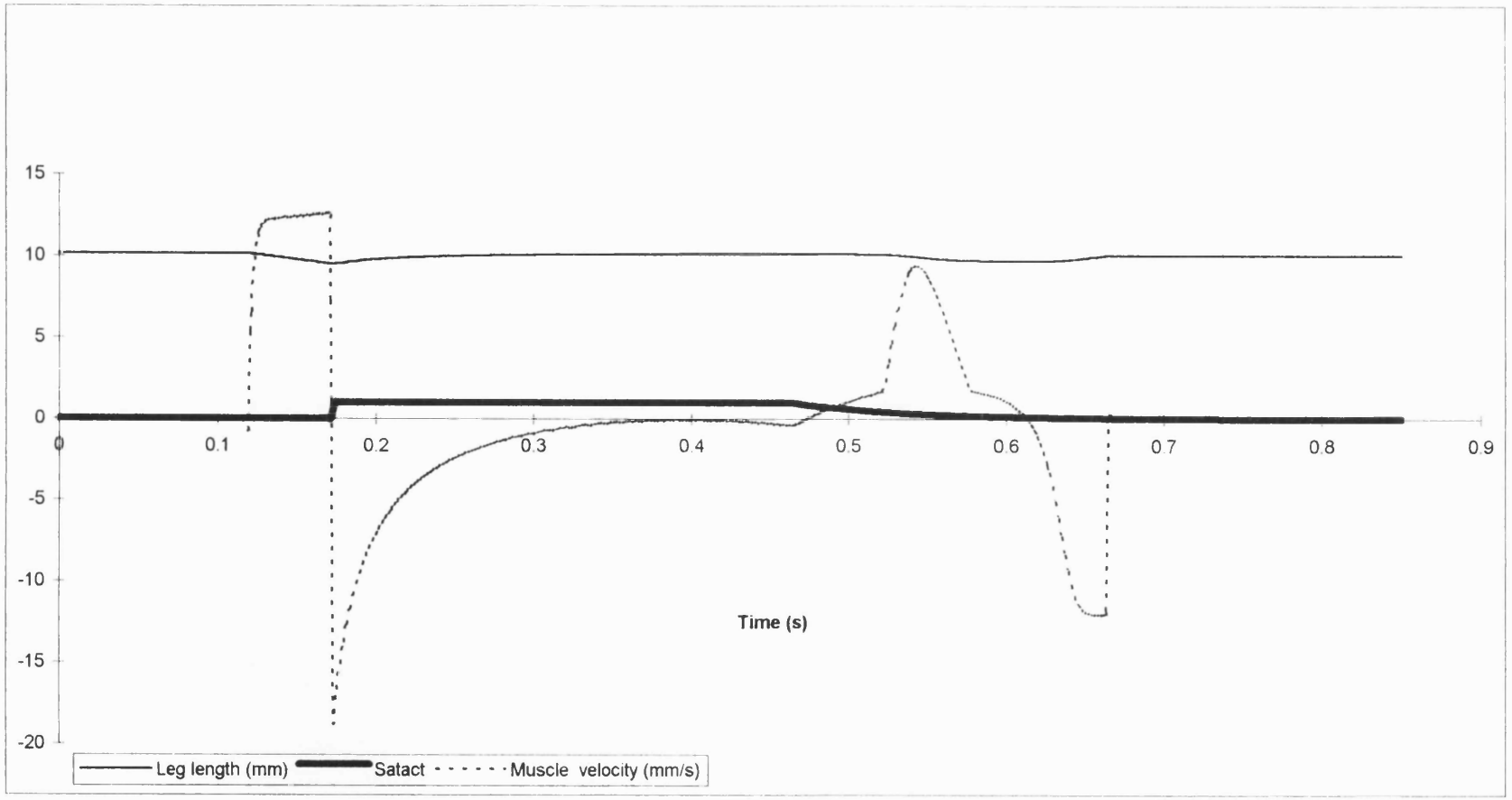

Figure 1.24. Output of the model shown in detail for the time the foot is on the ground. See page 104 for definition of satact.

Above the optimum muscle mass: Pmaxf 100 N.
Spring stiffness = 40 N/mm.

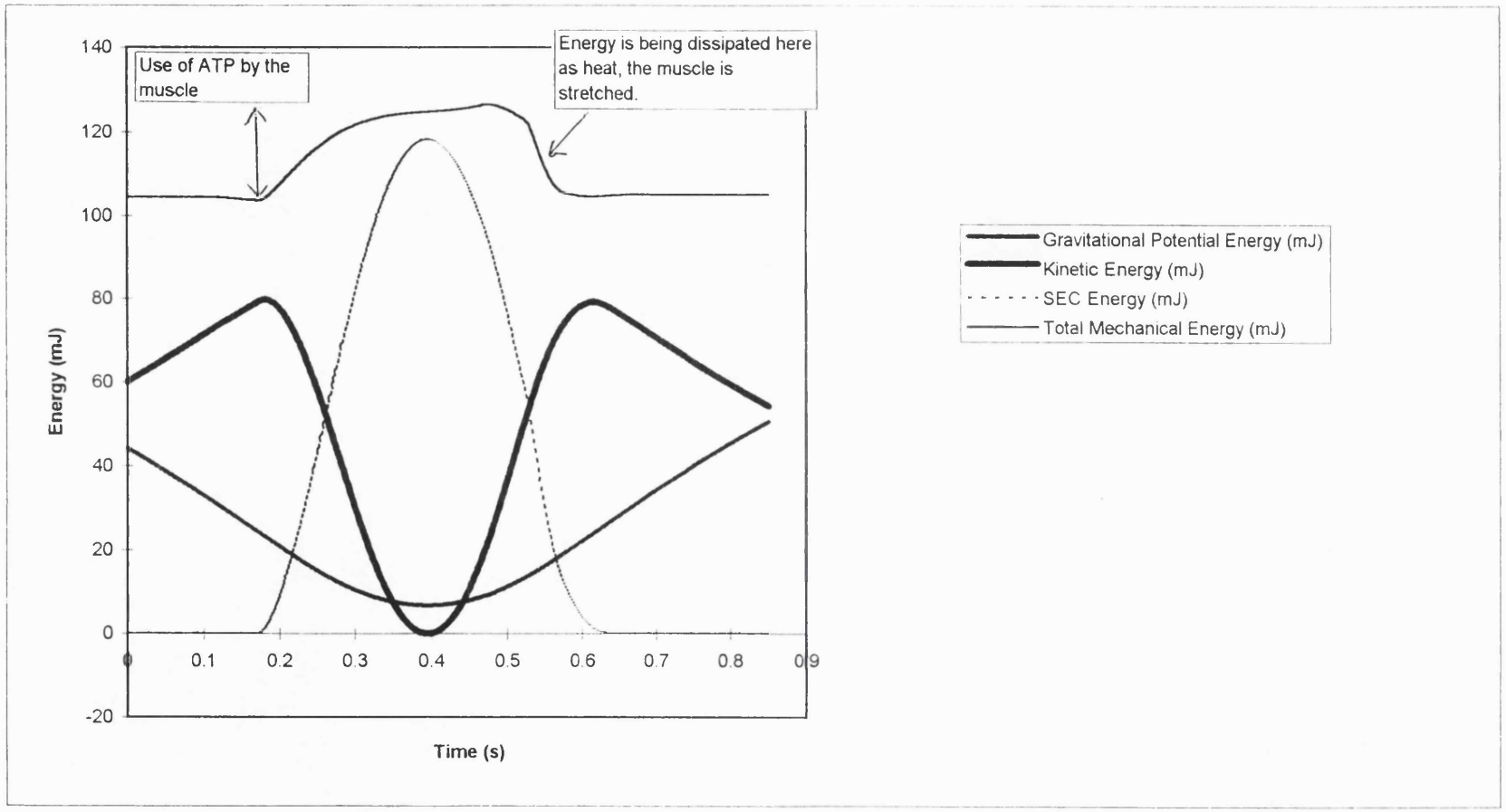

Figure 1.25. Output of the model shown in detail for the time the foot is on the ground. Since viscosity energy is negligible it has not been plotted on this graph. Total mechanical energy is equal to the sum of the gravitational, kinetic and SEC energy.

Above the optimum muscle mass: Pmaxf 100 N.
Spring stiffness = 40 N/mm.

1.24 and 1.25).

Once the muscle has done work against the SEC in decelerating the body, the ideal situation is for the muscle to be isometric as far as possible, since this is less energetically costly than shortening contractions. The energy stored in the SEC is bigger in the optimum muscle amount than in the too little muscle amount. In the too much muscle amount the energy stored in the SEC is even bigger, however this is what causes the muscle to switch off too early.

The criteria for a series of steady hops (ignoring the parallel viscosity, which is a minor factor), is that the work done by the muscle and the work done on the muscle have to be equal. Otherwise the amount of energy in the take-off would be different from landing. Thus the amount of energy in each hop is the same, i.e. the amount of mechanical energy in the system is conserved whilst the "beast" is on the ground. The energy is just converted from one form of energy to another, i.e. from kinetic energy to gravitational energy, to stored elastic energy. The SEC cannot store energy till the muscle is turned on. Only the muscle can cause an increase in total mechanical energy by splitting ATP (see figures 1.19, 1.22 and 1.25).

1.2.5. Optimum Spring Stiffness Simulations

The effect of spring stiffness on the energetic cost of hopping was investigated, in order to find the optimum spring stiffness and muscle ratio. The variable chconst was varied to obtain a 10mm jump for each of the stiffness values. The optimum spring muscle ratio was found to be spring stiffness 20N/mm to Pmaxf 50N. A stiffness of 10N/mm was found to be below the optimum and 40N/mm was found to be above the optimum spring stiffness (see figure 1.26). A spring stiffness of 10N/mm (optimum muscle mass = Pmaxf 40N), is worse at storing energy than the optimum stiffness because the muscle is being suddenly stretched whilst it is active. Thus it can be seen that the late spike in relative force is very large and the muscle velocity line goes positive. Thus energy is dissipated as heat, which is similar to the situation of too much muscle (see figure 1.27, 1.28 and 1.29).

For the spring stiffness of 40N/mm (optimum muscle mass = Pmaxf 70N), greater than

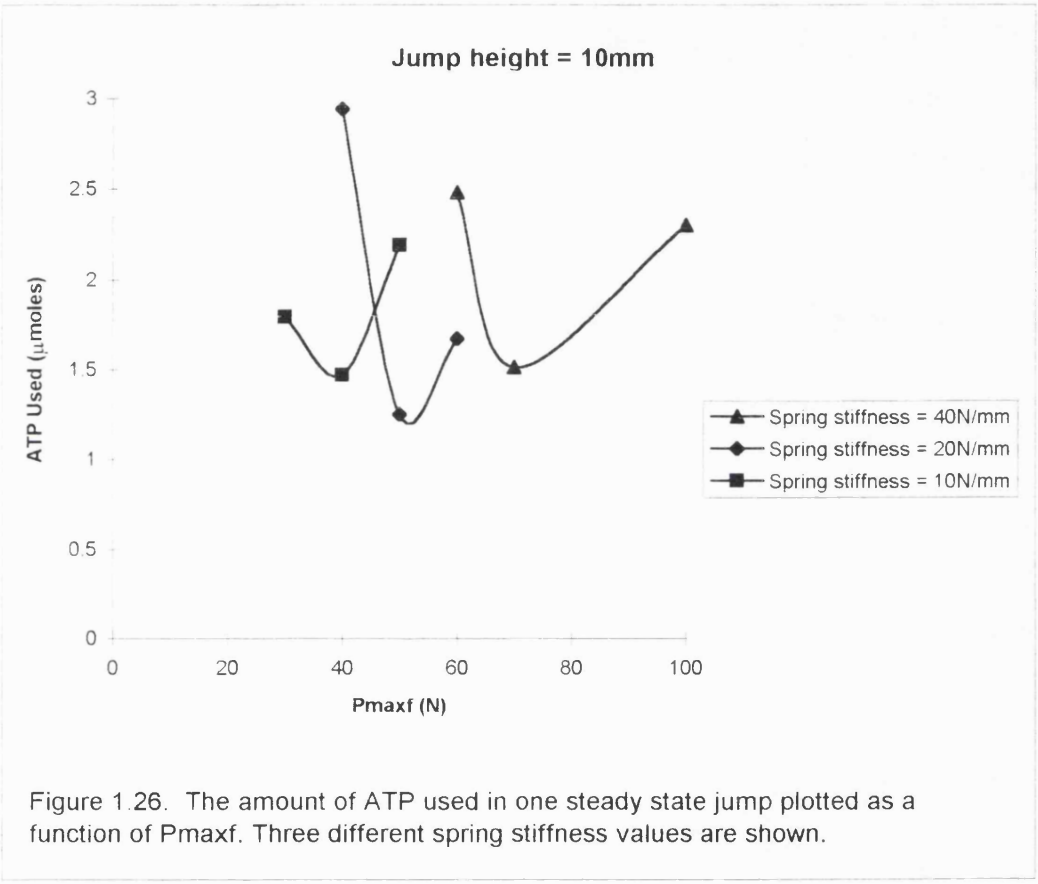

Figure 1.26. The amount of ATP used in one steady state jump plotted as a function of Pmaxf. Three different spring stiffness values are shown.

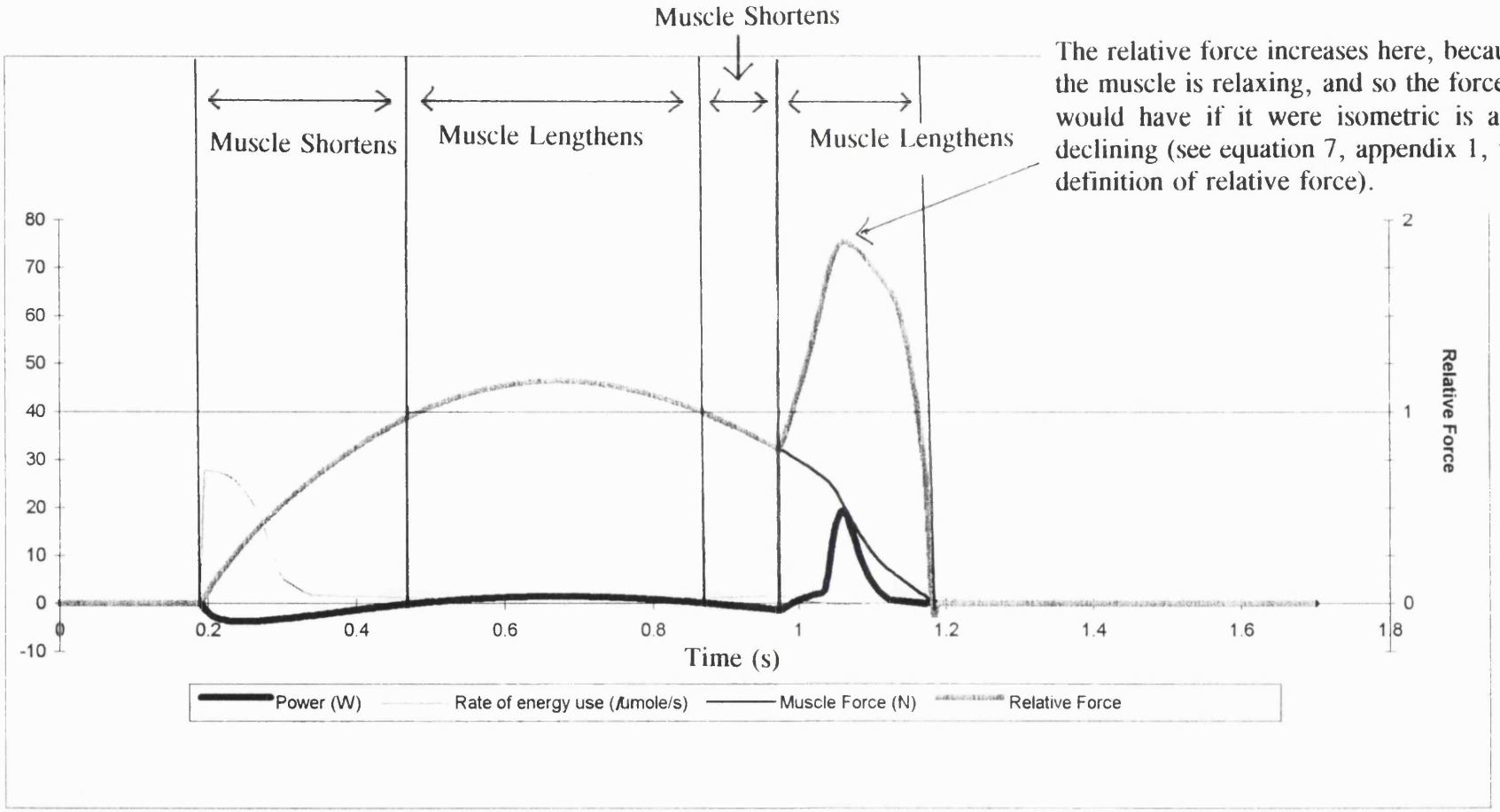

Figure 1.27. Output of the model shown in detail for the time the foot is on the ground. The value 40 on the left hand vertical scale is equal to a relative force of 1, i.e. the muscle is isometric.

Optimum muscle mass: Pmaxf 40 N.
Spring stiffness = 10 N/mm.

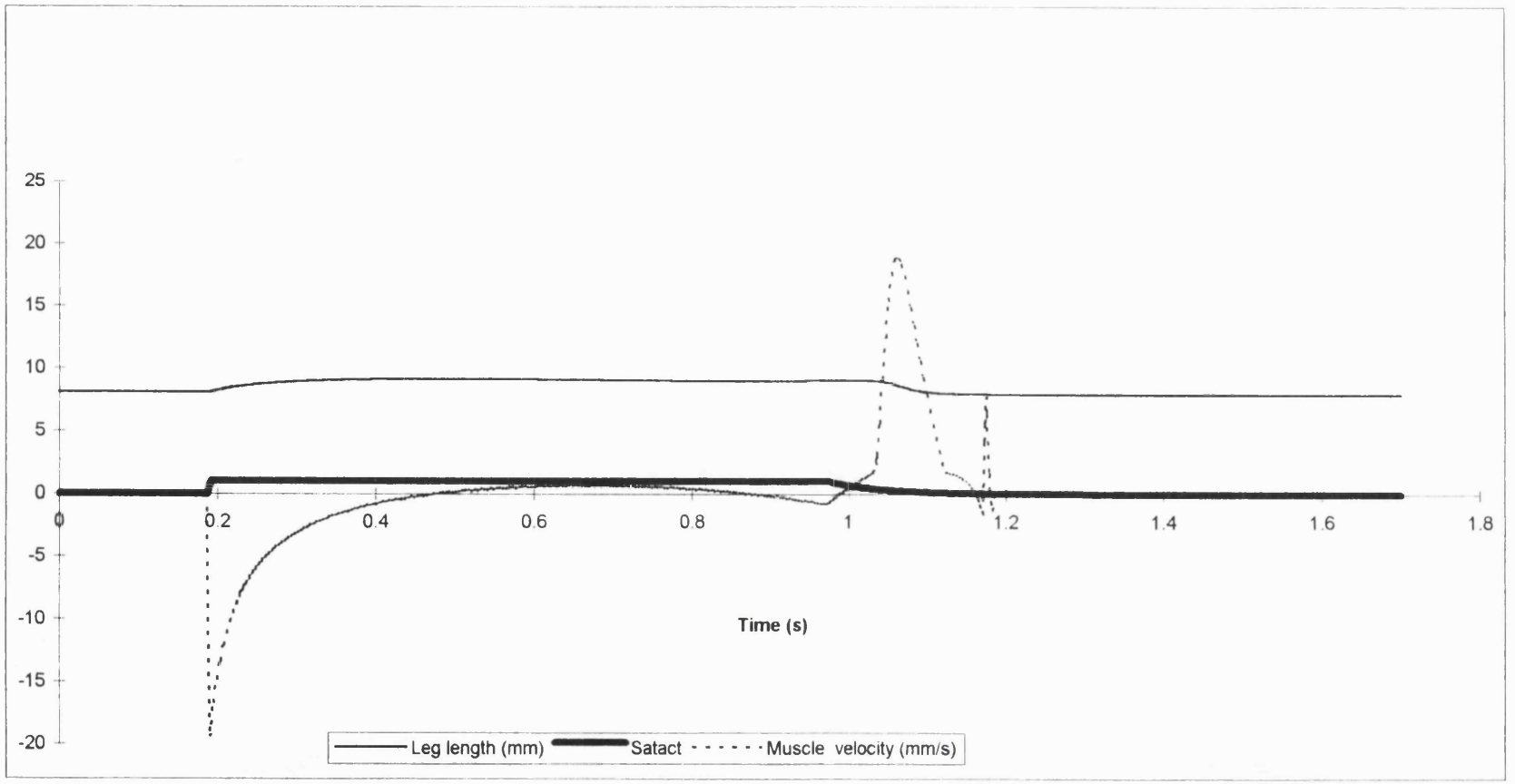

Figure 1.28. Output of the model shown in detail for the time the foot is on the ground. See page 104 for definition of satact.

Optimum muscle mass: Pmaxf 40 N.
Spring stiffness = 10 N/mm.

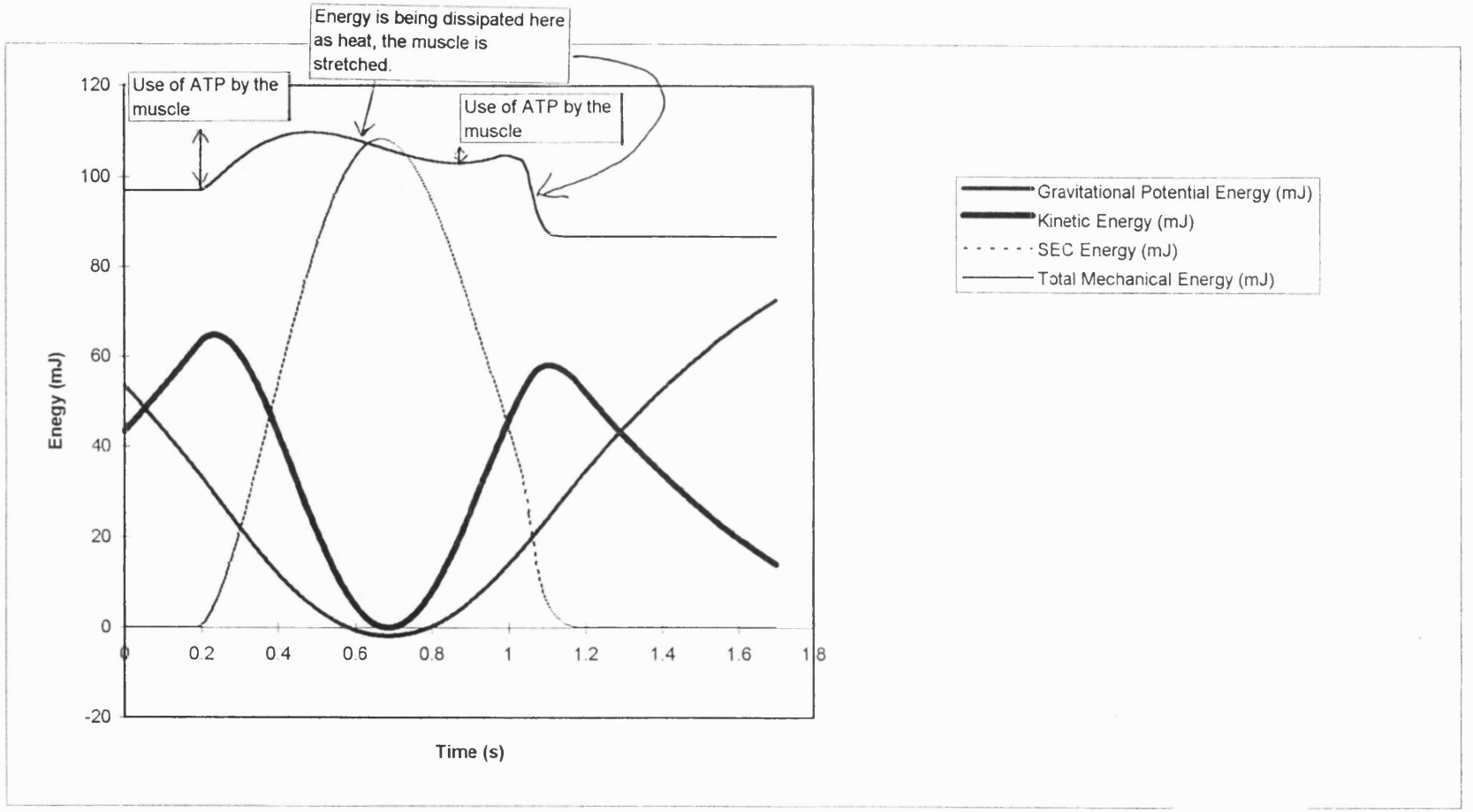

Figure 1.29. Output of the model shown in detail for the time the foot is on the ground. Since viscosity energy is negligible it has not been plotted on this graph. Total mechanical energy is equal to the sum of the gravitational, kinetic and SEC energy.

Optimum muscle mass: Pmaxf 40 N.
Spring stiffness = 10 N/mm.

the optimum, it can be seen that, late shortening of the muscle occurs for a duration of approximately 0.15s (see muscle velocity line on figure 1.18), which is energetically costly.

For the optimum spring stiffness of 20N/mm (optimum muscle mass = Pmaxf 50N), it can be seen that the late phase of shortening is very small, approximately for 0.05s (see figures 1.30, 1.31 and 1.32). It is likely that if the real optimum could be defined more closely there would be no length change of the muscle at this time. However the limitations of the model have been reached and the general point that is being shown is that the energetic cost is less when these late changes in muscle length are small. Substantial shortening uses ATP. Substantial lengthening of the muscle whilst active dissipate energy as heat, because the muscle acts as a brake absorbing the power to oppose the movement, thus it turns energy into heat. It would be possible to find the optimum muscle amount and spring stiffness more precisely, if the energy use and the velocity in the model were more precisely defined.

If there is no spring there can be no energy storage. When the "beast" lands the muscle is stretched, and if there is no spring this results in the dissipation of all the kinetic energy that was stored at the moment of landing as heat. The muscle will have a high force, but as soon as it starts shortening the large force is immediately lost. So the work that has to be put in (in the form of kinetic energy) for take-off to occur, has to be produced by the muscle in the same way it did in the first contraction. If a spring is added however, on landing the energy is stored in the spring, and as a result of the presence of the spring the force in the muscle will not rise as high, thus the muscle will dissipate less energy. The spring therefore allows length changes to occur in the muscle without a very large force being developed. The property of the spring is thus to lower the force in the muscle. If the velocity of the stretch is increased more force is produced and therefore more energy is stored in the spring. If the stretch is slow a low force is generated, because energy is being dissipated as it is stretched, so not much ends up being stored.

1.2.6. Definitions Of Efficiency

There are many definitions of efficiency:

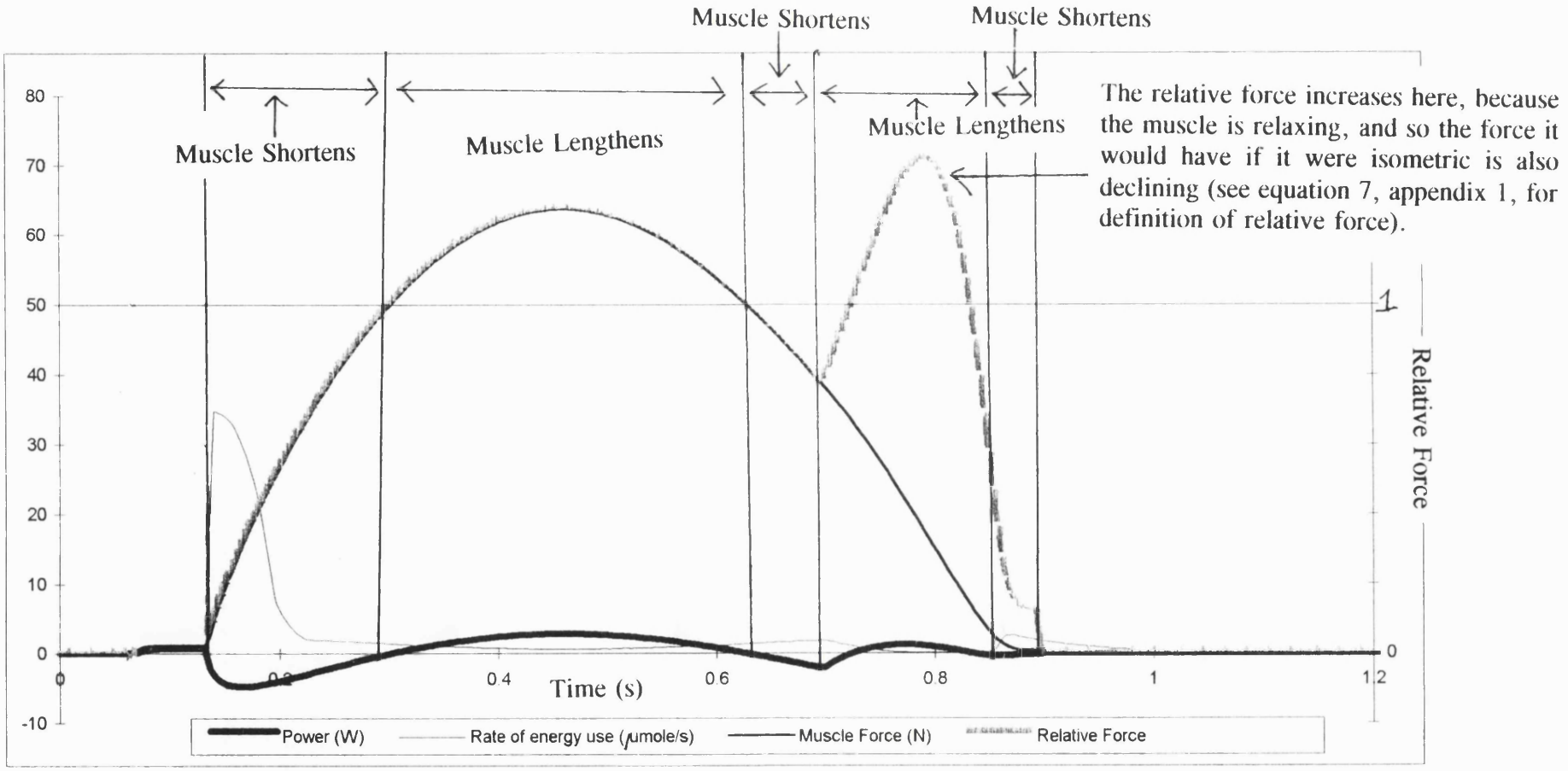

Figure 1.30. Output of the model shown in detail for the time the foot is on the ground. The value 50 on the vertical scale is equal to a relative force of 1, i.e. the muscle is isometric.

Optimum spring stiffness = 20 N/mm.
Muscle mass: Pmaxf 50 N.

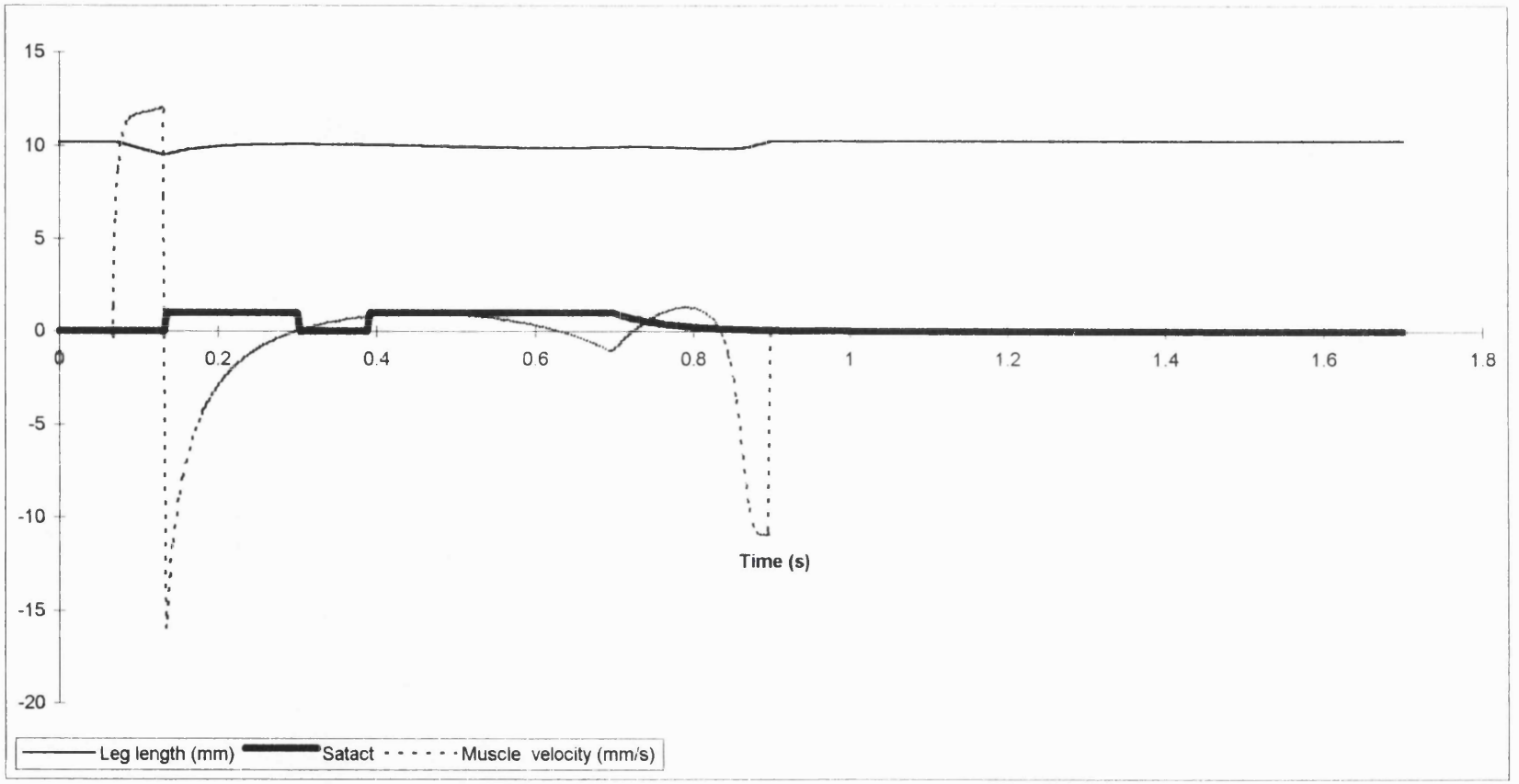

Figure 1.31. Output of the model shown in detail for the time the foot is on the ground. See page 104 for definition of satact.

Optimum spring stiffness = 20 N/mm.
Muscle mass: Pmaxf 50 N.

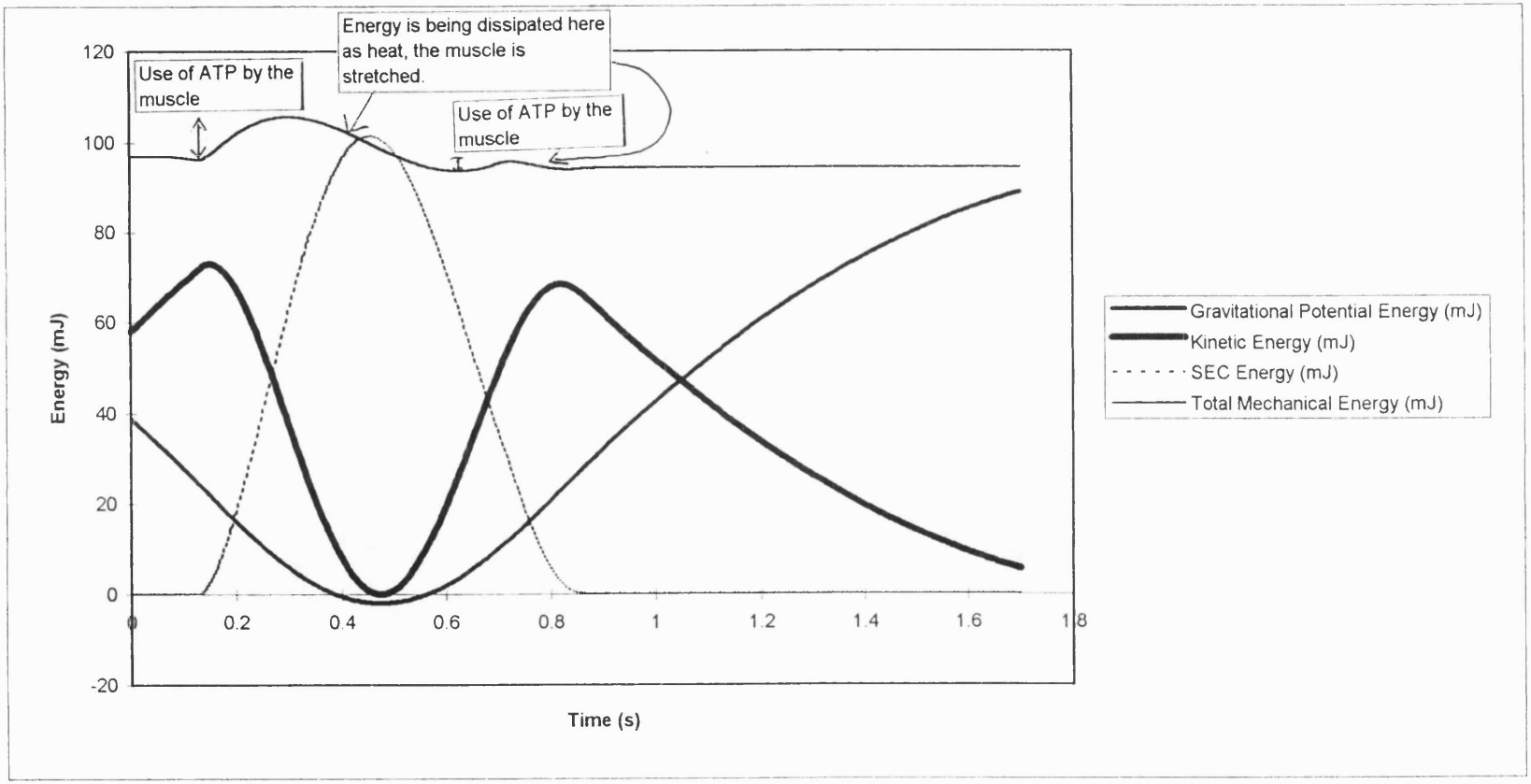

Figure 1.32. Output of the model shown in detail for the time the foot is on the ground. Since viscosity energy is negligible it has not been plotted on this graph. Total mechanical energy is equal to the sum of the gravitational, kinetic and SEC energy.

Optimum spring stiffness = 20 N/mm.
Muscle mass: Pmaxf 50 N.

1) The efficiency of the muscle alone is equal to the power produced by the muscle divided by the energy used by the muscle.
From figure 1.33, it can be seen that the maximum efficiency of the muscle is rather low at 0.118, it is influenced by the choice of Kapt of 5 and a Vmax of 2 muscle lengths/s. This low efficiency however does not effect the over all model conclusions, and it is not outside of the range of properties discovered for muscle.

2) The efficiency of the overall system is equal to the total energy needed for the jump divided by the energy used.
This definition of efficiency allows a value greater than 1, because of the recycling of energy. The increase in total mechanical energy shows how much has come from the muscle, the rest has been recycled.

3) The efficiency of the recycling mechanism = (Total energy - Energy that came from the muscle) / Total energy.

4) Efficiency of the muscle working in this machine is equal to the energy that came from the muscle divided by the energy cost.

From figure 1.34, it can be seen the optimum spring stiffness (20N/mm) and optimum muscle amount (Pmaxf 50N), has the highest efficiency of the overall system, due to it having the highest efficiency of the recycling mechanism. The efficiency of the muscle working in the machine is not the highest for the optimum spring to muscle amount ratio. However this fact is compensated for by the use of the recycling energy, where an efficiency of greater than 1 is obtained for the efficiency of the whole system.

1.2.7. Vmax Optimization

Having found the optimum ratio of muscle (Pmaxf 50 N) to spring stiffness (20 N/mm) to give the lowest energetic cost (1.25 μmoles) for a 10mm jump, Vmax was varied. An optimum Vmax was found in the model (Vmax -1 Lo/s) giving an energetic cost for a 10mm jump of 0.77μmoles. A faster muscle can exert more force at a given speed, therefore less muscle is required to obtain the same mechanical effect. However since the muscle is using APT at a faster rate, the cheaper energetic cost of using less muscle

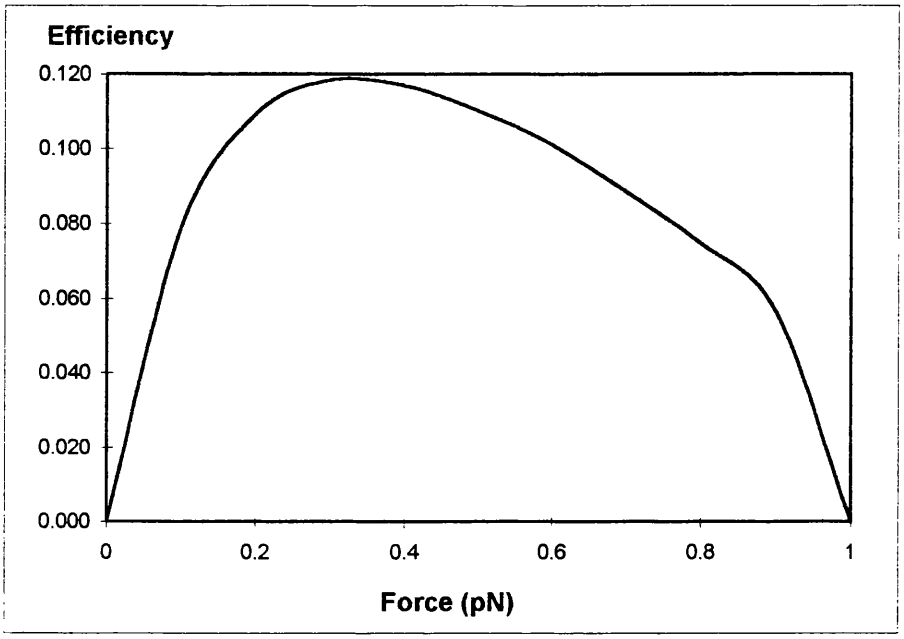

Figure 1.33. The efficiency of the model muscle during steady shortening under different loads, shown as a function of the force it exerts. Effiiciency of the muscle is defined on page 67.

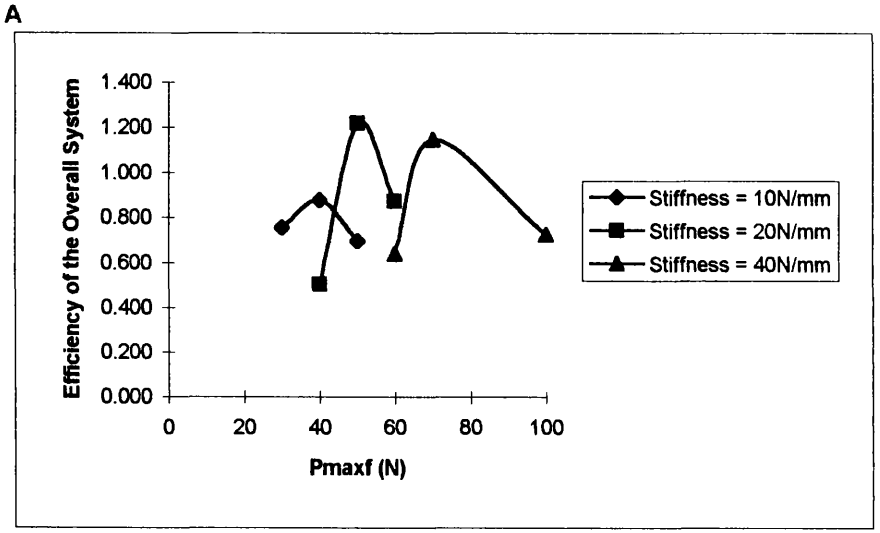

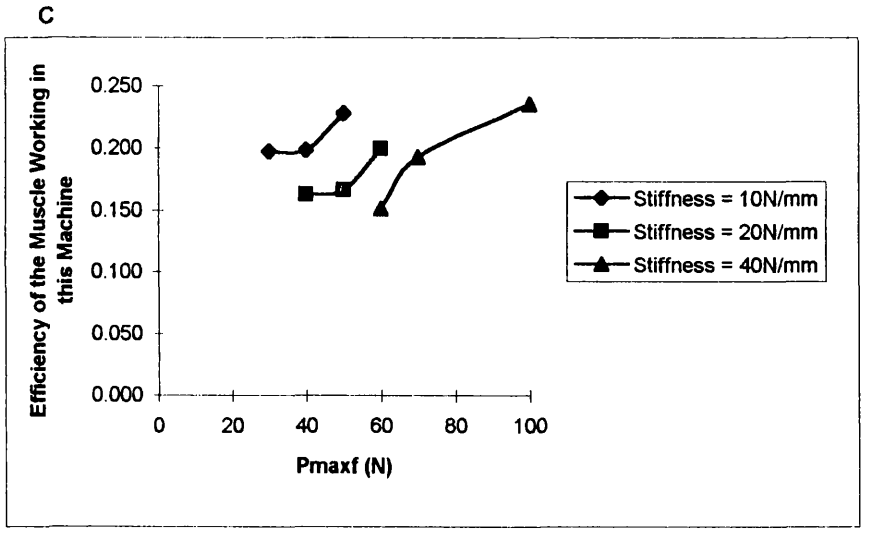

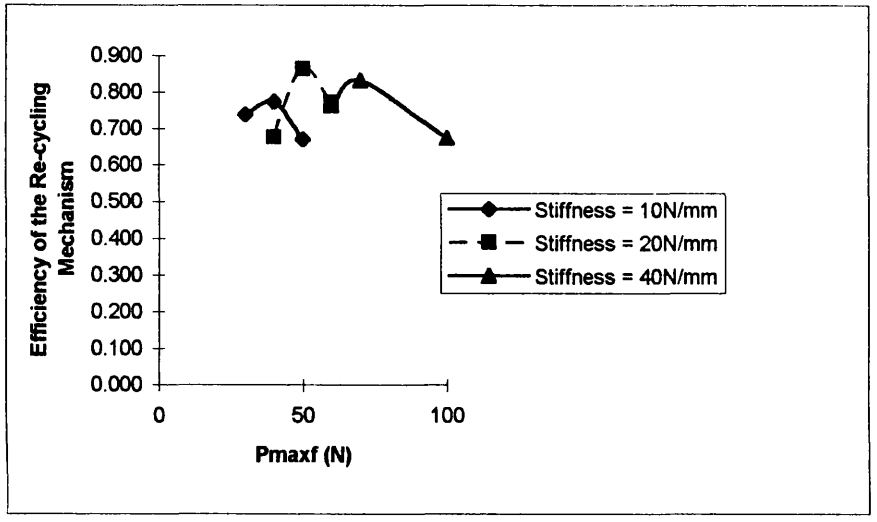

Figure 1.34. Efficiency for one jump plotted as a function of Pmaxf, for three spring stiffness values.

A: Efficiency for one jump of the overall system.
B: Efficiency for one jump of the re-cycling mechanism.
C: Efficiency for one jump of the muscle working in this machine.

See page 67 for the definitions of efficiency.

A

Stiffness 10 N/mm				
Jump Height 10mm				
	Pmaxf N	% Change from optimum Pmaxf	ATP Used µmole	% Change from optimum ATP Used
	30	-25	1.79	22
Optimum	40	0	1.47	0
	50	25	2.19	49
Stiffness 20 N/mm				
Jump Height 10mm				
	Pmaxf N	% Change from optimum Pmaxf	ATP Used µmole	% Change from optimum ATP Used
	40	-20	2.94	135
Optimum	50	0	1.25	0
	60	20	1.67	34
Stiffness 40 N/mm				
Jump Height 10mm				
	Pmaxf N	% Change from optimum Pmaxf	ATP Used µmole	% Change from optimum ATP Used
	60	-14	2.48	64
Optimum	70	0	1.51	0
	100	43	2.3	52

B

Jump Height 10mm					Optimum
	Stiffness N/mm	% Change from optimum Stiffness	ATP Used µmole	% Change from optimum ATP Used	Pmaxf N
	10	-50	1.47	18	40
Optimum	20	0	1.25	0	50
	40	100	1.51	21	70

Table 1.1. Optimum Pmaxf and spring stiffness values for "beast" of mass 1Kg.

A) For a given spring stiffness, there is a sharp optimum for the amount of muscle.

B) For a given mass of "beast", there is an optimum spring stiffness.

is cancelled out to some degree, thus an optimum Vmax exists. Varying the spring stiffness in either direction was found to increase the energetic cost of a 10mm jump. Similarly varying the muscle amount in either direction was found to increase the energetic cost of a 10mm jump. Thus it was concluded that a triple optimum (optimum spring stiffness, muscle amount and Vmax) had been obtained (see table 1.2).

1.3. Ageing Simulation

The results from the human ageing study in chapter 2, have shown that the F/CSA decreases by 30% in men aged 80 years compared to men under 40 years. The results from the stretching experiments on mouse EDL tendon (see chapter 4) have shown that tendon stiffness increases 18% in middle aged mice (15 months) as compared to young mice (3-5 months). The triple optimum simulation was run with a muscle amount (Pmaxf) decreased by 30% and a spring stiffness increased by 18%. In order to achieve the same jump height the muscle had to be kept on longer (i.e. chconst had to be greatly increased) (see figure 1.35a & b). The energetic cost for a 10mm jump was found to be 8.6 μmoles, for the simulated aged muscle, which is a 1018% increase in cost. Looking at figure 1.35b it can be seen that the muscle on landing is stretching (energy dissipating) on landing and then at take-off is undergoing a large contraction (energy requiring). Whereas the length change in the spring on landing is less than in the case with the optimum muscle amount (see figure 1.35a). In real life it would be more efficient for the person to utilize a greater muscle mass, than to keep the muscle on for longer. In the model a force of Pmaxf 51N is required to achieve a jump height of 10mm, when the spring stiffness is increased by 18%. Thus a 46% increase in muscle force is required to re-optimise the muscle to the increased spring stiffness. The energetic cost in this case however is only 0.92 μmoles (see table 1.3). The muscle length changes slightly more and the spring length slightly less than in the triple optimum situation. This option is of course subject to there being more muscle available. People also suffer muscle atrophy (Essen-Gustavsson & Borges, 1986: Kallman *et al.*, 1990: Vandervoort & McComas, 1986) at the same time as the decrease in muscle F/CSA and increase in tendon stiffness. When this happens the person has no option but to keep the muscle on for longer, which as shown in figure 1.35b, results in a huge increase in energetic cost.

1Kg "beast"	Spring Stiffness N/mm	Pmaxf N	Chconst	Jump Height mm	ATP Used µmoles	Vmax Lo/s	% Change of Vmax From The Optimum	% Change of ATP Used From The Optimum
	20	50	65000	9.97	0.95	-0.5	-50%	23%
Triple Optimum	20	50	9000	10.47	0.77	-1	0%	0%
	20	50	4815	9.93	1.25	-2	100%	62%

Table 1.2a. An optimum Vmax exists for a given muscle mass and spring stiffness. A point of triple optimum has been arrived at, showing optimum spring stiffness, muscle mass and Vmax. The triple optimum conditions give the lowest energy cost for a 10mm jump.

1Kg "beast"	Spring Stiffness N/mm	Pmaxf N	Chconst	Jump Height mm	ATP Used µmoles	Vmax Lo/s	% Change of Spring Stiffness From The Optimum	% Change of ATP Used From The Optimum
	10	50	150000	10.05	1.49	-1	-50%	94%
Triple Optimum	20	50	9000	10.47	0.77	-1	0%	0%
	25	50	900000	10.00	3.83	-1	25%	397%

Table 1.2b. An optimum spring stiffness exists for a given muscle mass and Vmax. Varying the spring stiffness in either direction increases the energy used in a 10mm jump.

1Kg "beast"	Spring Stiffness N/mm	Pmaxf N	Chconst	Jump Height mm	ATP Used µmoles	Vmax Lo/s	% Change of Muscle Amount From The Optimum	% Change of ATP Used From The Optimum
	20	45	480000	9.92	2.58	-1	-10%	235%
Triple Optimum	20	50	9000	10.47	0.77	-1	0%	0%
	20	60	2800	9.95	1.03	-1	20%	34%

Table 1.2c. An optimum muscle amount (Pmaxf) exists for a given spring stiffness and Vmax. Varying the muscle amount in either direction increases the energy used in a 10mm jump.

Triple optimum
Muscle Length Change = 0.51mm
Spring Length Change = 3.16mm
MTC Length Change = 3.66mm

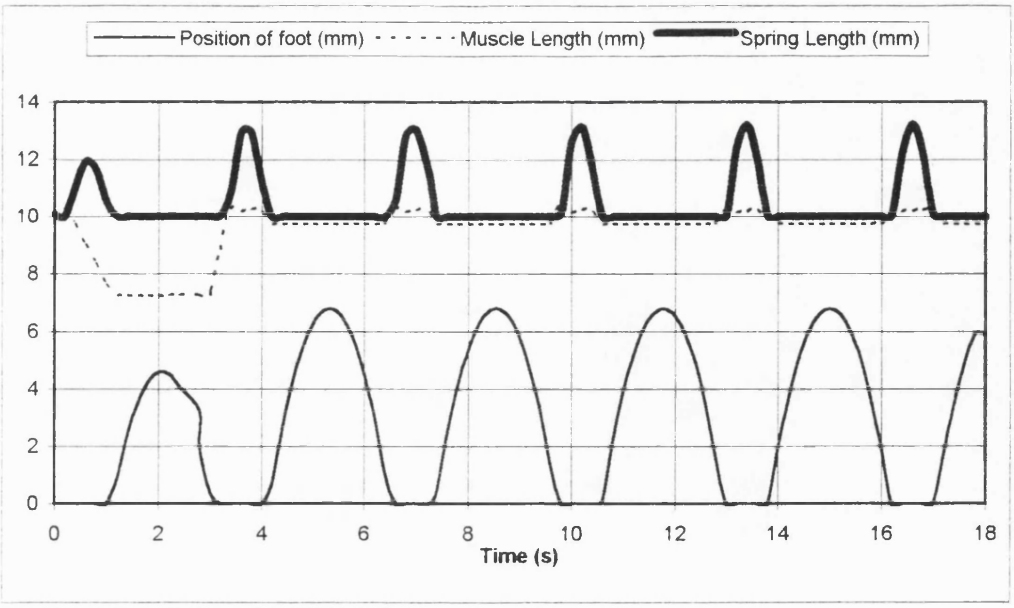

Figure 1.35a. Triple optimum run.

Jump height = 10.47 mm
Energy used = 0.77μmoles
chconst = 9000
Pmaxf = 50 N
Spring stiffness = 20 N/mm
Vmax -1 Lo/s

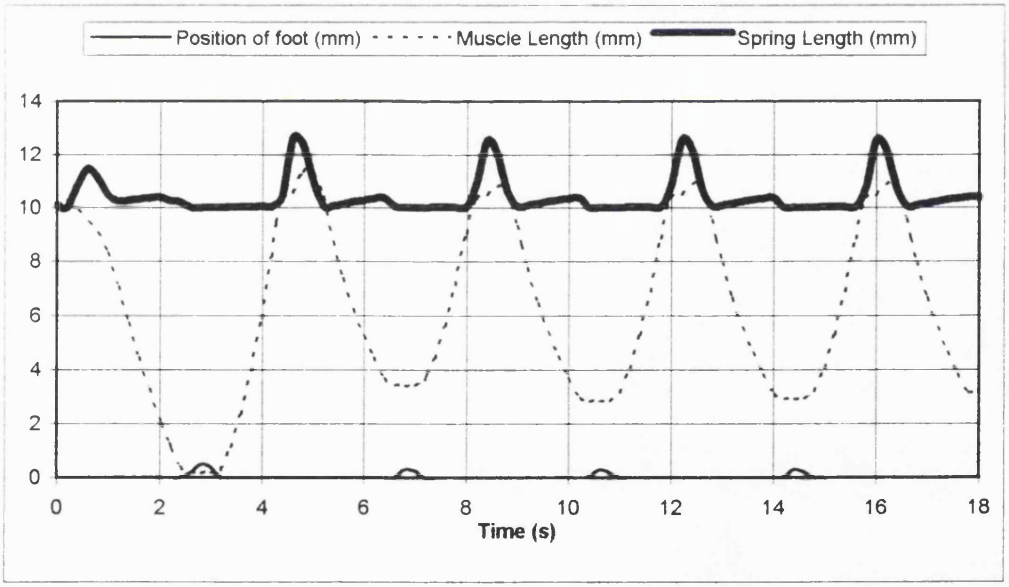

Figure 1.35b
Simulation of an aged muscle and tendon. Muscle force (Pmaxf) has been reduced by 30% from the optimum and spring stiffness has been increased 18% from the optimum. The muscle had to be kept on longer to achieve a 10mm jump.

Jump height = 10.43 mm
Energy used = 8.62 μmoles
chconst = 2×10^{13}
Pmaxf = 35 N
Spring stiffness = 23.60 N/mm
Vmax -1 Lo/s

		Triple Optimum	Old Muscle Muscle on for longer	Old Muscle Muscle amount increased
Jump height	mm	10.47	10.43	10.41
Energy Used	μmoles	0.77	8.62	0.92
Muscle Length Change	mm	0.51	8.06	1.18
Spring Length Change	mm	3.16	2.57	2.92
MTC Length Change	mm	3.66	10.63	4.1
Pmaxf	N	50	35	51
Spring Stiffness	N/mm	20	23.6	23.6
Vmax	Lo/s	-1	-1	-1
Chconst	arbitrary units	9000	2×10^{13}	9000

Table 1.3.
The situation of an aged muscle and tendon is simulated. F/CSA is reduced by 30% and tendon stiffness is increased by 18%.

In order to achieve a 10 mm jump the "beast" can either keep the muscle on for longer or it could increase the amount of muscle used.

The fact that the increase in spring stiffness is having a smaller effect on the energetic cost than the decrease in F/CSA can be seen by considering the situation of the ovariectomized / castrated mouse, where the F/CSA of the muscle decreases by 30%, but the stiffness of the tendon remains the same. In this case the animal has to produce a Pmaxf of 50N, a 43% increase, to achieve the same jump height as before the decrease in F/CSA.

1.4. Re-scaling

The model of mass 1kg was scaled down to 100g and up to 70Kg. The initial lengths of the "beasts" components were scaled in the model to the cube root of the change in mass (Alexander, 1988) (see table 1.4). A triple optimum was found for each of the two masses in the same manner as that for the 1kg model (described on P.47, P.62 and P.71) (see table 1.5, 1.6, 1.7 & 1.8). For each optimum model mass the length change in the MTC (muscle length plus tendon length change) was determined when jumping to the jump height investigated for each mass. A dimensionless number was determined for the triple optimum conditions for each mass:

(Optimum Stiffness (N/mm) X Length Change of MTC (mm)) / Optimum Po (N)

70Kg Model (see table 1.8)
500 (N/mm) X 11.94 (mm) / 4000 (N) = 1.5

1 Kg Model (see table 1.2)
20 (N/mm) X 3.66 (mm) / 50 (N) = 1.5

100g Model (see table 1.6)
2.5 (N/mm) X 2.23 (mm) / 4 (N) =1.4

The scaling has shown that the dimensionless number is the same for each of the "beast" masses, therefore the model is mass independent. Alexander (1995), in his mechanical jumping model showed that increasing the length of the leg increased the height of the jump (Alexander, 1995). However the current model is operating as if it does not have a leg at all (see section 1.5), it contains only a mass, a muscle and a spring in series.

Mass	Kg	1	70	0.1
Mass change factor			70	10
Linear scale			4.12	2.15
Spring Length	mm	10	41.2	4.6
Muscle length	mm	10	41.2	4.6
Muscle On length	mm	9.5	39.2	4.4
Leg Length	mm	10	41.2	4.6
Body Position	mm	19.9	82.0	9.2
Jump Height	mm	10	41.2	4.6

Table 1.4. The "beast" of mass 1Kg was scaled down to 100g and up to 70Kg.

Length scales to the cube root of the change in mass (Alexander, 1988).

A

Stiffness 1.25 N/mm Jump Height 4.6mm	Pmaxf N	% Change from optimum Pmaxf	ATP Used µmole	% Change from optimum ATP Used
	2	-20	0.50	178
Optimum	2.5	0	0.18	0
	5	100	0.31	72
Stiffness 2.5 N/mm Jump Height 10mm				
	Pmaxf N	% Change from optimum Pmaxf	ATP Used µmole	% Change from optimum ATP Used
	2.5	-38	0.49	410
Optimum	4	0	0.10	0
	10	150	0.55	473
Stiffness 5 N/mm Jump Height 10mm				
	Pmaxf N	% Change from optimum Pmaxf	ATP Used µmole	% Change from optimum ATP Used
	5	-50	0.80	208
Optimum	10	0	0.26	0
	20	100	1.04	300

B

Jump Height 4.6mm	Stiffness N/mm	% Change from optimum Stiffness	ATP Used µmole	% Change from optimum ATP Used	Optimum Pmaxf N
	1.25	-50	0.18	88	2.5
Optimum	2.5	0	0.10	0	4
	5	100	0.26	171	10

Table 1.5. Optimum Pmaxf and spring stiffness values for "beast" of mass 100g.

A) For a given spring stiffness, there is a sharp optimum for the amount of muscle.

B) For a given mass of "beast", there is an optimum spring stiffness.

100g "beast"	Spring Stiffness N/mm	Pmaxf N	Chconst	Jump Height mm	ATP Used µmoles	Vmax Lo/sec	% Change of Vmax From The Optimum	% Change of ATP Used From The Optimum
	2.5	4	8.00E+13	4.8	0.76	-0.25	-75%	900%
Triple Optimum	2.5	4	7.50E+03	4.6	0.076	-1	0%	0%
	2.5	4	3.00E+03	4.6	0.096	-2	100%	26%

Table 1.6a. An optimum Vmax exists for a given muscle mass and spring stiffness. A point of triple optimum has been arrived at, showing optimum spring stiffness, muscle mass and Vmax. The triple optimum conditions give the lowest energy cost for a 4.6mm jump.

100g "beast"	Spring Stiffness N/mm	Pmaxf N	Chconst	Jump Height mm	ATP Used µmoles	Vmax Lo/sec	% Change of Spring Stiffness From The Optimum	% Change of ATP Used From The Optimum
	1.5	4	2.50E+04	4.60	0.097	-1	-40%	28%
Triple Optimum	2.5	4	7.50E+03	4.60	0.076	-1	0%	0%
	3.5	4	5.00E+10	4.34	0.81	-1	40%	966%

Table 1.6b. An optimum spring stiffness exists for a given muscle mass and Vmax. Varying the spring stiffness in either direction increases the energy used in a 4.6mm jump.

100g "beast"	Spring Stiffness N/mm	Pmaxf N	Chconst	Jump Height mm	ATP Used µmoles	Vmax Lo/sec	% Change of Muscle Amount From The Optimum	% Change of ATP Used From The Optimum
	2.5	3	4.00E+13	4.60	0.68	-1	-25%	795%
Triple Optimum	2.5	4	7.50E+03	4.60	0.076	-1	0%	0%
	2.5	6	800	4.50	0.127	-1	50%	67%

Table 1.6c. An optimum muscle amount (Pmaxf) exists for a given spring stiffness and Vmax. Varying the muscle amount in either direction increases the energy used in a 4.6mm jump.

Triple optimum
Muscle Length Change = 0.39mm
Spring Length Change = 1.84mm
MTC Length Change = 2.23mm

A

Stiffness 100 N/mm Jump Height 41mm	Pmaxf N	% Change from optimum Pmaxf	ATP Used µmole	% Change from optimum ATP Used
	1500	-25	185	7
Optimum	2000	0	173	0
	2500	25	237	37
Stiffness 500 N/mm Jump Height 41mm				
	Pmaxf N	% Change from optimum Pmaxf	ATP Used µmole	% Change from optimum ATP Used
	3500	-13	178	26
Optimum	4000	0	141	0
	4500	13	157	11
Stiffness 2000 N/mm Jump Height 41mm				
	Pmaxf N	% Change from optimum Pmaxf	ATP Used µmole	% Change from optimum ATP Used
	7000	-7	170	13
Optimum	7500	0	150	0
	9000	20	165	10

B

Jump Height 4.6mm	Stiffness N/mm	% Change from optimum Stiffness	ATP Used µmole	% Change from optimum ATP Used	Optimum Pmaxf N
	100	-80	173	23	2.5
Optimum	500	0	141	0	4
	2000	300	150	6	10

Table 1.7. Optimum Pmaxf and spring stiffness values for "beast" of mass 70Kg.

A) For a given spring stiffness, there is a sharp optimum for the amount of muscle.

B) For a given mass of "beast", there is an optimum spring stiffness.

70Kg "beast"	Spring Stiffness N/mm	Pmaxf N	Chconst	Jump Height mm	ATP Used µmoles	Vmax Lo/sec	% Change of Vmax From The Optimum	% Change of ATP Used From The Optimum
	500	4000	1.00E+11	40	135	-0.25	-75%	47%
Triple Optimum	500	4000	1.00E+07	40	92	-1	0%	0%
	500	4000	7.00E+06	41	141	-2	100%	53%

Table 1.8a. An optimum Vmax exists for a given muscle mass and spring stiffness. A point of triple optimum has been arrived at, showing optimum spring stiffness, muscle mass and Vmax. The triple optimum conditions give the lowest energy cost for a 41mm jump.

70Kg "beast"	Spring Stiffness N/mm	Pmaxf N	Chconst	Jump Height mm	ATP Used µmoles	Vmax Lo/sec	% Change of Spring Stiffness From The Optimum	% Change of ATP Used From The Optimum
	100	4000	2.00E+12	40.00	346	-1	-80%	338%
Triple Optimum	500	4000	3.50E+07	41.00	79	-1	0%	0%
	1000	4000	1.00E+09	41.00	467	-1	100%	491%

Table 1.8b. An optimum spring stiffness exists for a given muscle mass and Vmax. Varying the spring stiffness in either direction increases the energy used in a 41mm jump.

70Kg "beast"	Spring Stiffness N/mm	Pmaxf N	Chconst	Jump Height mm	ATP Used µmoles	Vmax Lo/sec	% Change of Muscle Amount From The Optimum	% Change of ATP Used From The Optimum
	500	3000	3.50E+10	40.00	304	-1	-25%	285%
Triple Optimum	500	4000	3.50E+07	41.00	79	-1	0%	0%
	500	6000	3.00E+05	42.00	161	-1	50%	104%

Table 1.8c. An optimum muscle amount (Pmaxf) exists for a given spring stiffness and Vmax. Varying the muscle amount in either direction increases the energy used in a 41mm jump.

Triple optimum
Muscle Length Change = 1.66mm
Spring Length Change = 10.3mm
MTC Length Change = 11.94mm

If real geometry was put into the model the optimum conditions might be modified. The optimum Vmax in the model scaling was found to be the same for each model mass. However the Vmax of large and small animals in life is very different, for example for a human it is 0.2 - 4.1 Lo/s (Larsson & Moss, 1993) and for a mouse it is approximately 6 Lo/s (Woledge *et al.*, 1985). This maybe because of different geometric constraints that exist between a mouse and a human e.g. different leg lengths.

The dimensionless number obtained from the model is compared to that obtained with the isometric muscle force (Po) of soleus muscle and the stiffness of EDL tendon and its aponeurosis (see P.166, paragraph 3). The muscle experiments were performed on soleus muscle and the tendon experiments on EDL tendon, therefore in comparing these results it is assumed EDL and soleus tendon have the same stiffness. It seems likely they would have the same stiffness, since the Po of EDL muscle and soleus muscle are known to be similar (Brooks & Faulkner, 1991). Soleus and gastrocnemius are the muscles attached to the Achilles tendon which plays a role storing elastic energy in running. Therefore, in using the soleus muscle for this calculation it is assumed soleus and its tendon, are typical of a MTC are involved in running in a mouse.

Dimensionless Number For A Mouse MTC
(Stiffness of EDL tendon & aponeurosis (N/mm) X Maximum Length Change of MTC (mm)) / Po of Soleus muscle (N)

(0.94 N/mm X 1.4mm) / 0.36 N = 3.67 (see appendix 2)

Dimensionless Number For A Human MTC
(Stiffness of human Achilles tendon & gastrocnemius aponeurosis (N/mm) X Maximum Length Change of MTC (mm)) / Po of gastrocnemius muscle (N)

(131 N/mm X 16mm) / 1567 N = 1.34 (see appendix 3)

When the dimensionless number from the model is compared with that obtained from experimental data from a mouse or literature data from a human, the number obtained for the mouse is larger and for a human is smaller, although it is within the same order

of magnitude. The reason for this is not clear but could include the following:

1) Geometric constraints

2) safety factors

1.5. Models of the MTC Developed By Other Workers Compared To The Current Model

The objective of the current model was for it to be as simple as possible, but for it to possess realistic muscle properties. Therefore the current model has a realistic muscle, but very little else, its other components are just a mass (located at one point) and a spring. The leg in the model is of variable length, the component that is holding it at a fixed length is the muscle. In a way the leg in the model does not really exist, as the leg cannot sustain force without the muscle. Therefore the muscle can be considered just to be in series with the spring. There has to be a mass, as locomotion has been redefined, as the oscillation of the mass on a spring. The current model is simple in terms of mechanics but is sophisticated in terms of energetic. The objective of the current model is to predict the energy cost. At high forces the muscle lengthens, the extent to which this occurs will determine the cost of locomotion, since all energy lost has to be replaced by muscle transducing energy from ATP. The current model agrees with other models that there is an optimum spring stiffness.

The current model shows that with repeated jumps there is a substantial storing of energy in the spring which results mainly in the progressive saving of energy rather than the ability to jump higher and higher. The fact that compliance is having a greater effect on energy storage than jump height can be illustrated by looking at three identical simulations where only compliance is altered (see table 1.9). Looking at figure 1.36 and 1.37, it can be seen that more energy is stored in the spring (105mJ) with a compliance of 20N/mm, as opposed to with a lower compliance of 40N/mm (68mJ). Therefore because more energy is stored in the spring with a higher compliance the "beast" is able to jump higher. However if a higher jump is not required then the "beast" is able to use less muscle, due to the presence of compliance, resulting in a decreased energetic cost of the jump. Looking at the total mechanical energy (TME) shown on figure 1.36, it can be seen that with a higher compliance the work put in by the muscle is less, than when the compliance is lower (see figure 1.37). The work done on the mechanical

	Spring Stiffness N/mm	Pmaxf N	Chconst	Jump Height mm	ATP Used µmoles	% Change of Jump Height From The Optimum	% Change of ATP Used From The Optimum
	40	50	9000	6.85	2.09	-35%	171%
Optimum	20	50	9000	10.47	0.77	0%	0%
	10	50	9000	2.37	1.96	-77%	155%

Table 1.9. An optimum compliance exists to obtain a jump with a low energetic cost. The addition of compliance to the model up to the optimum, has a larger effect on reducing the ATP used than on increasing jump height.

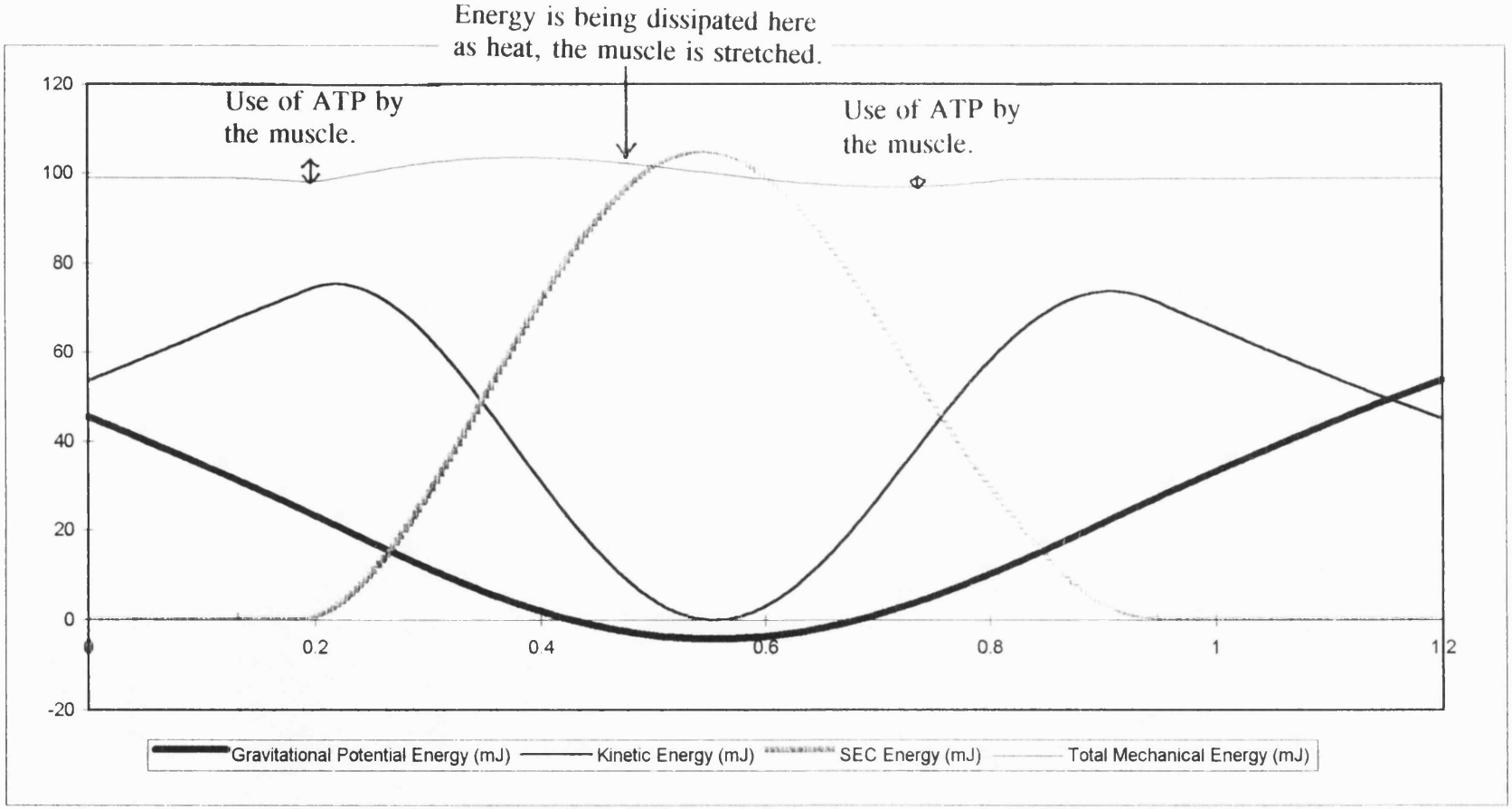

Figure 1.36. Output of the model shown in detail for the time the foot is on the ground. Total mechanical energy is equal to the sum of the gravitational, kinetic and SEC energy.
Triple Optimum:
Optimum muscle mass: Pmaxf 50 N.
Spring stiffness = 20 N/mm.
Vmax -1 Lo/s

Jump height = 10.47 mm.

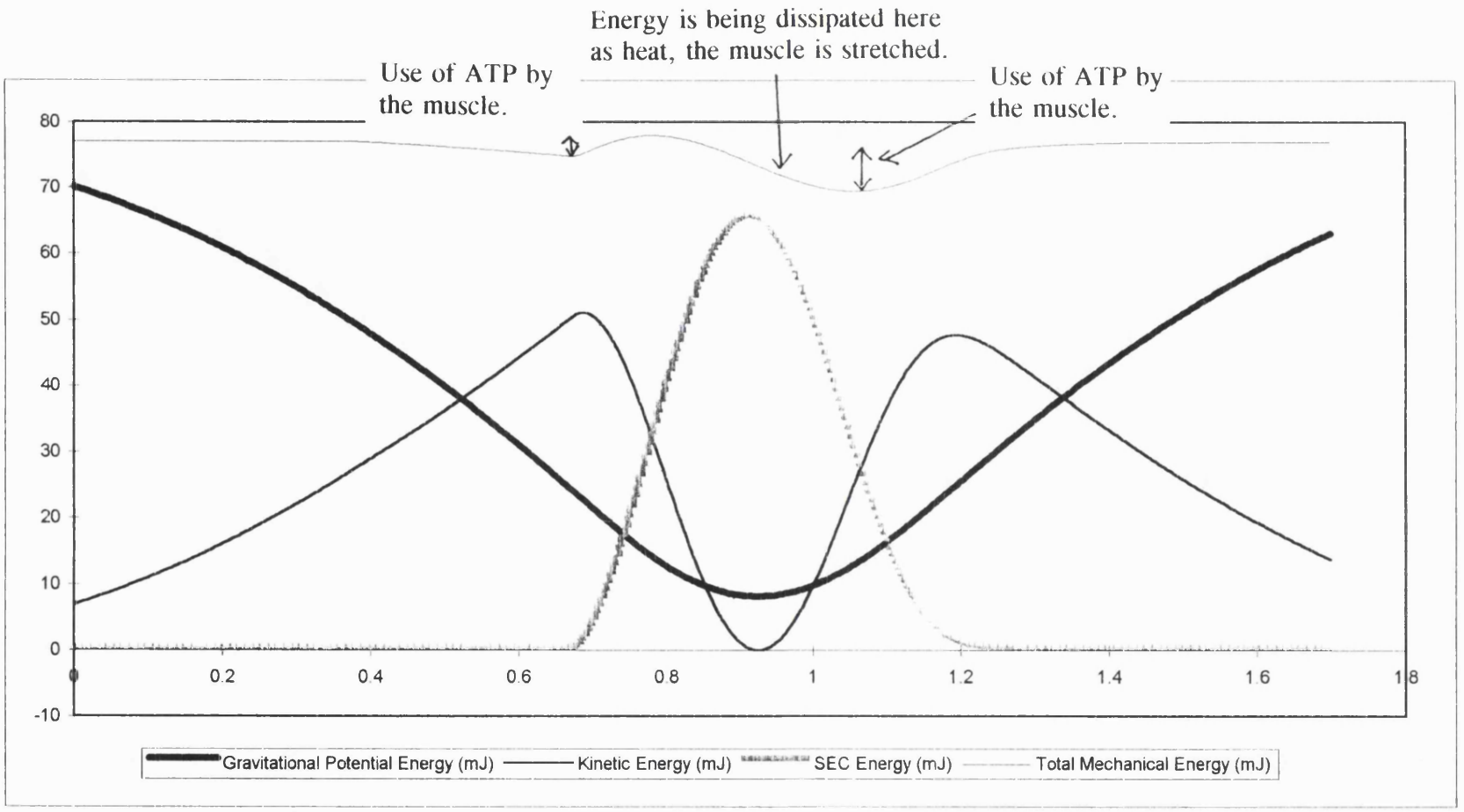

Figure 1.37. Output of the model shown in detail for the time the foot is on the ground. Total mechanical energy is equal to the sum of the gravitational, kinetic and SEC energy.

Optimum muscle mass: Pmaxf 50 N.
Spring stiffness (above optimum stiffness) = 40 N/mm.
Vmax -1 Lo/s

Jump height = 6.85 mm.

system is equal to the increases in TME. TME decreases because energy is dissipated, the site of energy dissipation is the muscle when it is being stretched whilst active. These two diagrams show that when the spring is doing more work the muscle is doing less work, which is similar to the results of Anderson and Pandy (1993) discussed below.

1.5.1. Anderson & Pandy (1993) Optimum Control Model

Anderson and Pandy (1993) presented an analysis of muscle-tendon action during a maximum-height squat jump (SJ) and a maximum-height countermovement jump (CMJ). They have done this by comparing experimental data and computed optimal control solutions to simulated maximal jumping of a four link segment model driven by eight musculo-tendon actuators. They found that tendon compliance does not affect jump height significantly. For both the CMJ and the SJ, increasing tendon compliance to extremes produced only a 3% increase in jump height. The increase in tendon compliance did augment the amount of energy delivered to the skeleton by the elastic tissues, but it simultaneously decreased the amount of energy delivered by the contractile elements (Anderson & Pandy, 1993). Thus Anderson and Pandy concluded, that in the context of jumping, the findings suggest that elastic energy storage and utilization affects efficiency much more than jump height (Anderson & Pandy, 1993). Which is in accordance with the findings of the current model, that as shown in table 1.9, the addition of compliance has a greater effect on energy efficiency than increasing jump height.

1.5.2. Alexander's 1995 Jumping Model

Alexander's model showed that SEC does increase jump height. In this model Alexander does not incorporate energetic properties. Alexander's paper looks at how jump performance depends on muscle properties, on the distribution of mass in the legs and on the number of leg segments. The height of a jump was found to depend on the maximum shortening speed of the muscles and the series compliance. As expected larger muscle forces were found to give higher jumps. For constant isometric force, faster muscles and higher compliances gave higher jumps (Alexander, 1995). It is also true in the current model that increasing Vmax increases the jump height (see table 1.10). In Alexander's model this is because faster muscles can exert more force, at given rates

	Units	Triple Optimum	Lower Vmax
Jump height	mm	10.47	9.20
Energy Used	μmoles	0.77	0.45
Muscle Length Change	mm	0.51	0.20
Spring Length Change	mm	3.16	2.96
MTC Length Change	mm	3.66	3.16
Pmaxf	N	50.00	50.00
Spring Stiffness	N/mm	20.00	20.00
Vmax	Lo/s	-1.00	-0.50
Chconst	arbitrary units	9000	9000

Table 1.10. Simulates the effects of Vmax on jump height. Increasing Vmax increases the height of the jump.

of shortening and series elastic elements can exert more force, at given rates of shortening (Alexander, 1995). This is true in the current model since the force in the muscle is the same as the force in the spring, due to the muscle and spring being in series (see appendix 1, equation 6). In the current model the force in the muscle is higher with a faster Vmax (see table 1.10), because the length change in the spring is larger from equation 6.

The highest jumps were achieved when the legs were given no mass. Mass in the legs reduces the height of the jump because some of the work done by the muscles is required to provide internal kinetic energy (energy associated with movement of parts of the body relative to the centre of mass). Unlike the external kinetic energy (associated with movement of the centre of mass), this energy does not become potential energy as the animal rises to the peak of the jump, so does not contribute to the jump's height (Alexander, 1995). In the model used in this thesis the legs did not have any mass as all of it was concentrated in the body to simplify the model. Longer legs were also found to give higher jumps. The longer the limb is, the faster the movement is, that the muscle produces. Therefore to achieve a particular velocity at the end of the limb, the rate of shortening of the muscle can be lower. Since the rate of shortening is lower, the muscle can exert more force and do more work (Alexander, 1995).

1.5.3. Limb Mechanics

The current model is not investigating how the mechanics of the limbs effects jumping, it is only considering the effects of muscle. To keep the model simple, the model muscle has a flat length tension curve, i.e. the model muscle has been given potentially infinite length, however the length of the muscle has been controlled by giving the leg length limits. This is of course not like real muscles, but means effectively the model muscle is working within the optimum sarcomere length plateau of the length tension curve. The current model does not consider the effect of the lever scaling properties of limbs and their relationship to the length tension curve, since they are not age dependent.

Changing Vmax in the current model is equivalent to changing the lever scaling properties. Limbs make muscles faster but weaker. The current model has showed that

the muscle can be made faster and weaker by increasing Vmax or stronger and slower by decreasing Vmax. An optimum Vmax was found in the model for a given muscle mass and spring stiffness. A faster muscle can exert more force at a given speed, therefore less muscle is required to obtain the same mechanical effect. However since the muscle is using ATP at a faster rate, the cheaper energetic cost of using less muscle is cancelled out to some degree, thus an optimum Vmax exists.

1.5.4. Cook (1993) Model

Cook (1993) compared experimental results obtained on imposing stretch-shortening cycles (SSC) on an intact human MTC (the first dorsal interosseus muscle), to a modification of a simple Hill model of the MTC as a SEC and a CC in series. Cook (1993) found for small amplitude stretches the MTC behaves almost like a perfect spring with the fraction of the energy returned extrapolating to 1 at zero cycle amplitude. However when a delay between the stretch and shortening is present, as occurs in many movements, it was found that not all of the energy is returned. Thus when a delay is present, energy is lost and the MTC does not behave like a perfect spring. In addition it was found both with and without a delay the amount of energy lost, increased with increased amplitude. This is a consequence of the fact that with increasing amplitude crossbridge detachment occurs, energy is dissipated and the MTC no longer behaves as a simple spring (Cook, 1993). The findings of the current model agree with this, illustrated by the existence of an optimum spring stiffness and muscle amount. The current model shows that a spring stiffness below the optimum, is worse at storing energy because the muscle is being suddenly stretched whilst it is active. Thus it can be seen that the late spike in relative force is very large and the muscle velocity line goes positive (see figure 1.27 & 1.28). Thus energy is dissipated as heat (see figure 1.29), which is similar to the situation of too much muscle.

1.5.5. Relationship Between Body Mass and Biomechanical Properties of Tendons

Pollock & Shadwick (1994a) measured the elastic modulus and hysteresis of distal limb tendons from a large size range of quadrupedal mammals to determine what scaling relationship might exist in the material properties of these tendons. A second objective of their study was to determine if the digital extensor tendons (a low-stress muscle-tendon unit) of adult mammals were mechanically similar to those tendons that act as

springs (i.e. the digital flexors and ankle extensors), and whether these properties varied with body size.

The findings of Pollock & Shadwick (1994a) were as follows:
1) The digital flexor and ankle extensor tendons (those likely to act as springs during the support phase of locomotion) have on average the same material properties (i.e. elastic modulus and hysteresis) as the digital extensors (those not likely to function as springs) and therefore the same inherent capacity for elastic energy storage. Second, the material properties of these anatomically and functionally distinct tendons are uniform over a range of species and body mass.

Consequently, if metabolic energy savings due to elastic energy storage increase with body mass in running mammals, as previously suggested by Alexander *et al.*, (1981), this does not result from a scaling of tendon material properties. Rather, differences in the level of tensile loading imposed on these tendons in larger animals must occur. These observations suggest the general finding that adjustments in the structural properties of the skeletal system in terrestrial mammals to accommodate increasing body size occur by changes in dimensions or shape, not material properties. This point further investigated in a companion study by Pollock & Shadwick (1994b), which considered the structural properties of muscle-tendon units in the hindlimbs of mammals as a function of body mass. It was concluded that the springlike tendons of large mammals can potentially store more elastic strain energy than those of smaller mammals because their disproportionately stronger muscles can impose higher tendon stresses.

The findings of the current model; that for a given mass of "beast", there is an optimum spring stiffness for a given muscle amount, is similar to the findings of Pollock & Shadwick (1994b). They found that the tendons of large mammals can potentially store more elastic strain energy than those of smaller mammals. This is because in the smaller mammals the tendons are proportionally thicker than those of the large mammals for the forces they are subjected to. Thus the findings of Pollock & Shadwick (1994b) agree with the findings of the current model, that for a given mass of "beast" there is an optimum tendon stiffness. It is for a given mass of "beast" because the spring deals with the weight of the animal. The reason for this in the Pollock & Shadwick (1994b) study

is that the corresponding muscles of the tendons in the smaller mammals are not able to stress the tendons sufficiently. It is suggested that these small animals, are highly specialized for saltatory locomotion. The maximum forces exerted on the ground when, for example, Kangaroo rats jump to heights as great as 50cm are 3 times greater than those exerted when they hop at their fastest steady speed. The forces produced to achieve the accelerations recorded when the animals jumped would place thinner tendons at great risk of being ruptured. It appears large animals may move more frequently at steady speeds (conditions best suited for elastic storage and recovery). Whereas small animals appear to place grater reliance on their ability to accelerate (or decelerate) rapidly. In which elastic energy saving is not important (Biewener & Blickhan, 1988).

In the current model a spring stiffness greater than the optimum spring stiffness, simulates a situation whereby the muscle force is insufficient to stretch the spring, thus the spring absorbs less of the landing force. Pollock & Shadwick do not discuss a situation where tendon compliance is below optimum. In the model the compliance of the spring was altered not by changing the size of the spring, but by changing its elastic modulus. However Pollock & Shadwick (1994a) found that the material properties of anatomically and functionally distinct tendons were uniform over a range of species and body mass. Thus adjustments in the structural properties of the skeletal system in terrestrial mammals to accommodate increasing body size were found to occur by changes in dimensions or shape, not material properties (i.e. smaller mammals have proportionally larger tendons than larger mammals). However, despite these differences in ways of altering tendon compliance the practical outcome will be the same.

1.5.6. Ground Contact Time

Farley *et al.*, (1991) modelled the body as a simple spring-mass system. They measured the properties of the spring by use of a force platform, when human subjects hopped forward on a treadmill over a range of speeds and in place over a range of frequencies (Farley *et al.*, 1991). The subjects used nearly the same frequency (the "preferred frequency", 2.2 hops/s) when they hopped forward on a treadmill and when they hopped in place. At this frequency the body behaved like a simple spring-mass system. The body was also found to behave like a simple spring-mass system when the subjects hopped at higher frequencies, up to the maximum they could achieve. However, at

higher frequencies, the time available to apply force to the ground (the ground contact time) was shorter. Experiments by Kram and Taylor (1990), have shown that metabolic rate during running is inversely proportional to the ground contact time over a range of speed and size. Cost triples as a horse, dog, or kangaroo rat increase speed, and the ground contact time is cut to one-third. When the ground contact time is shorter (at higher speeds), muscular force must be generated faster, requiring faster fibres with crossbridges that cycle and consume ATP at higher rates (Huxley, 1974). At the preferred frequency during both normal and maximum height hopping, the ground contact time is longer than at higher frequencies and, presumably, the cost of generating muscular force is lower (Farley *et al.*, 1991). At frequencies below the preferred frequency, the body did not behave in a springlike manner, and it appeared likely that the storage and recovery of elastic energy was reduced. Farley *et al.*, (1991) concluded that people choose the frequency at which they rebound from the ground in a springlike manner and at which the time available for force generation (the ground contact time) is maximized, thus minimizing the cost of generating muscular force (Farley *et al.*, 1991).

The current model is not just like a simple mass spring system as there is a ballistic phase and a muscle on phase. When the muscle is switched on, the "beast" behaves as a spring mass system (i.e. a certain mass and a certain spring stiffness, oscillates at a certain frequency, only viscosity in the air will cause it to come to rest). The current model once it is off the ground, is behaving ballistically. Once the "beast" is in the air, how long it stays in the air, is a consequence of how much energy was present at take-off. When the muscle is switched off, the spring effectively is not present, therefore the energy stored in the spring is lost, and only the energy stored in the moving mass is present. When the "beast" hits the ground, it can use a little muscle or a lot of muscle which will control how long it stays on the ground.

The current model, has shown that it is possible to use more muscle on for less time, or less muscle on for more time to achieve a particular jump height. For a given spring stiffness an optimum muscle amount exists, thus an optimum "muscle on" time exists. The model "muscle on" time is equivalent to ground contact time (the time force is exerted on the ground), since no force can be generated when the muscle is switched

off, as there is no pressure on the ground. As discussed by Farley *et al.*, (1991) above, when the ground contact time is shorter than the optimum (i.e. at higher hopping speeds), muscular force must be generated faster, requiring faster fibres with crossbridges that cycle and consume ATP at higher rates (Huxley, 1974). Similarly in the current model, when the "muscle on" time is shorter than the optimum, more muscle needs to be used thus the energetic cost increases.

1.6. Non-Linear Spring Simulation

The triple optimum run for the 1 Kg "beast"was re-run with a non-linear spring. Equations 2 and 6 (see appendix 1), in the linear triple optimum run were raised to the power of 1.72 (see figure 1.38). The value for spring stiffness was set at 7 N/mm, this value was chosen because it gives a similar stiffness in the working range to the triple optimum linear run (in this case spring stiffness was 20N/mm) (see figure 1.39). A non-linear spring increases the cost of the jump slightly (25% increase in energetic cost was found for a 10mm jump). In principal all calculations might be repeated with the non-linear spring. However this introduces another degree of freedom, i.e. the degree of non-linearity, therefore it is likely a quadruple optimum would exist.

1.7. Conclusions:

1) For a given spring stiffness, there is a sharp optimum for the amount of muscle. For the 1Kg "beast", increasing the muscle amount (for spring stiffness 20 N/mm) by 20% from the optimum increases the ATP used by 34% (see Table 1.1a).

2) For a given mass of "beast", there is an optimum spring stiffness, but it is not a sharp optimum. For the 1 Kg "beast", increasing the spring stiffness by 100% from the optimum, increases the ATP used by only 21% (see Table 1.1b).

3) For the optimum spring stiffness and optimum muscle amount, an optimum Vmax exists. For the 1Kg "beast" increasing Vmax by 100% from the optimum, increases the ATP used by 62% (see table 1.2a).

4) The ageing simulations (simulating a muscle with 30% reduction in F/CSA, and a 18% increase in tendon stiffness) show it would be more efficient for a person to utilize

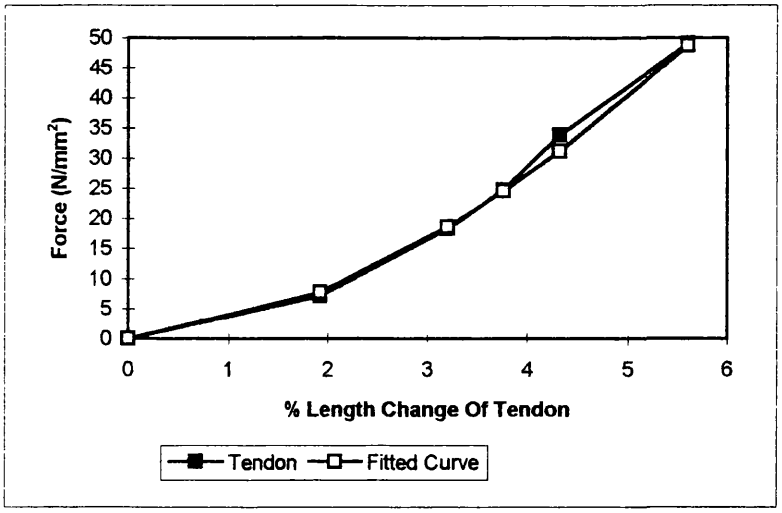

Figure 1.38.

The curvature of the length extension curve for the model non-linear spring was determined by fitting a curve to the experimental data obtained from the tendon experiments (shown in figure 4.13).

The curve was fitted via a power law equation, with two degrees of freedom (k and e):

k X Length change^{e}

The curvature of the fitted line was found to be 1.72.

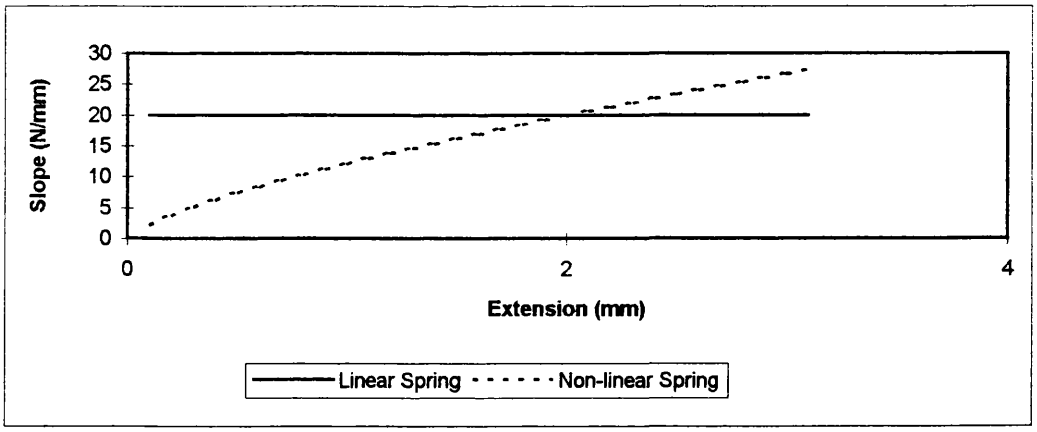

Figure 1.39
The slope of the linear and non-linear spring are plotted against spring extension. The spring stiffness value for the non-linear run was set at 7N/mm, as it gives a similar stiffness in the working range to the triple optimum linear run (stiffness = 20N/mm).

a greater muscle mass, than to keep the muscle on for longer, in order to achieve a set task (see table 1.3). This option is subject to there being more muscle available, if more muscle is not available this results in a large increase in energetic cost.

5) The increase in tendon stiffness has a smaller effect on the energetic cost than the decrease in F/CSA (see section 1.3).

Appendix 1- The Model equations

1) a lgsel.k=fifge(losel,pnbdy.k-pnfot.k-lgleg.k,tkoff.k,0.5)

The length of the spring (lgsel) is equal to the position of the body (pnbdy) minus the position of the foot (pnfot) minus the length of the leg (lgleg) (see figure 1.4).

2) a fcbdy.k=(mass*grav/1000)-stse*(lgsel.k-losel)

The force on the body (fcbdy) is equal to:
[its mass multiplied by gravity / 1000] minus the force due to the spring. The force due to the spring is equal to the spring stiffness (stse) multiplied by (the length of the spring minus the initial length of the spring).

3) r acbdy.kl=fcbdy.k/mass

The acceleration of the body (acbdy) is equal to the force on the body (fcbdy) divided by the mass.

4) l vybdy.k=vybdy.j+dt*(acbdy.jk)

The velocity of the body (vybdy) is obtained by integrating the acceleration of the body (acbdy).

5) l pnbdy.k=pnbdy.j+dt*(vybdy.j)

The position of the body (pnbdy) is obtained by integrating the velocity of the body (vybdy).

6) a fcmus.k=-stse*(lgsel.k-losel)

The force on the muscle (fcmus) is equal to the stiffness of the spring (stse) multiplied by the length of the spring (lgsel) minus the initial length of the spring (losel). Thus the force in the muscle is the same as the force in the spring, i.e. the spring and muscle are in series.

7) a fcmrv.k=fcmus.k/(pmax.k*satact.k+0.00000001)

The relative force on the muscle (fcmrv) is the actual force (fcmus) divided by the force that would exist if the muscle was isometric. Pmax (the amount of muscle that produces maximum isometric muscle force) multiplied by satact is the amount of muscle

isometrically activated at that time. The figure 0.00000001 is required to be put into the program for mathematical reasons to prevent the force from becoming infinite. Thus the relative force in the muscle is the force in the muscle relative to the maximum force it can produce.

8) a etarel.k=eta/(pmax.k*satact.k+0.00000001)

The relative viscosity (etarel) is the actual viscosity (eta) expressed relative to the force the muscle would exert if it were isometric at that time. (Viscosity is in parallel with the muscle).

9) a vyrep.k = (-(fcmrv.k * gcon + etarel.k + 1) + sqrt((fcmrv.k * gcon + etarel.k + 1)*(fcmrv.k * gcon + etarel.k + 1) - 4 *(etarel.k * gcon)*(fcmrv.k-1)))/ (2*(etarel.k * gcon)).

a vyren.k = (-(fcmrv.k - 2.3 - 1.42 * etarel.k) - sqrt ((fcmrv.k - 2.3 - 1.42 * etarel.k) *(fcmrv.k - 2.3 - 1.42 * etarel.k) - 4 * etarel.k * (2.266 - 1.42 * fcmrv.k)))/(2 * etarel.k).

a Vyrep and vyren are solutions to simultaneous equations (shown on figure 1.6). Vyrep refers to the positive velocity (muscle shortening) and vyren to the negative velocity (muscle stretching). The minimum of these two values is taken so that the parts of the curve, that do not represent the force velocity curve are ignored.

10) a vyvisc.k=fcmus.k/(eta*lomus*vmax)

Velocity of the viscosity (vyvisc) = force in the muscle / (viscosity X muscle length (lomus) X Vmax).

(see figure 1.6).

11) a vyrel.k = fifge (min (vyrep.k, vyren.k), vyvisc.k, satact.k, 0.05)

The relative velocity (vyrel) is determined by the viscosity when the muscle is switched off, and by a combination of the viscosity and force velocity properties when the muscle is switched on.

12) l lgleg.k=lgleg.j+dt*(-vymus.jk)

The length of the leg (lgleg) is obtained by integrating the velocity of the muscle (vymus). The length of the leg was made to be equal to the initial muscle length.

13) r vyfot.kl=fifge(vybdy.k+vymus.kl,0,tkoff.k,0.5)

The velocity of the foot (vyfot) is equal to the velocity of the body (vybdy) and the velocity of the muscle (vybdy), if take-off is true.

Or

The velocity of the foot is equal to zero if take-off is false.

14) l pnfot.k=pnfot.j+dt*(vyfot.jk)

The position of the foot (pnfot) is obtained by integrating the velocity of the foot (vyfot).

15) l enmus.k=enmus.j+dt*(atpas.jk)

The amount of ATP (enmus) used by the muscle is obtained by integrating the rate of ATP usage (atpas) by the muscle.

16) l envis.k=envis.j+dt*(endis.jk)

The viscosity energy (envis) is obtained by integrating the rate energy is dissipated (endis).

17) l tkoff.k = tkoff.j + dt * (1/dt) * (fifge (fifge (fifge (1, 0, vybdy.j, 0), 0, 0, fcmus.j), fifge (0, -1, pnfot.j, 0), 0.5, tkoff.j)).

Take-off has two values: Take-off = 1 (True), or Take-off = 0 (False). If take-off is true then it stays true, i.e. the beast is flying through the air and remains flying. If take-off is false then it stays false, i.e. the beast has landed and remains landed. Take-off changes from false to true if the velocity of the body is greater than 0 and the force in the muscle is less than 0, i.e. the beast takes off. Take-off changes from true to false if it has not already landed (i.e. it has a value less than 0.5) and the foot has touched the ground.

18) r atpas.kl = 0.014 * Pmax.k * satact.k * katp * tabxt (aptab, fcmrv.k, 0, 1,

0.05)

t aptab = 5 / 4.95 / 4.94 / 4.9 / 4.8 / 4.6 / 4.25 / 3.8 / 3.1/ 2.1 / 1 / 0.7 /0.45 /0.3 / 0.28 / 0.27 / 0.26 / 0.25/ 0.23 / 0.22 / 0.20.

The rate of ATP used (atpas) in shortening, stretching and isometric contractions is equal to the product of the following terms: 0.014 x Pmax x satact x Katp x tabxt.

0.014 is the number of micro moles of myosin activated to produce 1N of force. It was calculated in the following way:

Each myosin produces 1pN of force. Therefore 1 mole of myosin produces: $(6 \times 10^{23}) \times (1 \times 10^{-12}\ N) = 6 \times 10^{11}\ N$

The sarcomere is 2.4 μm long, the muscle fibre is 10mm long (parallel fibre muscle). Therefore there are 10mm / 2.4×10^{-3}mm = 4167 sarcomeres. Therefore there are 8334 half sarcomeres in series. Therefore a typical mole of myosin arranged in a 10mm muscle fibre produces 6×10^{11} N / 8334 = 7.1×10^{7} N.

Therefore the number of micro moles of myosin activated to produce 1N of force is: $1 / 7.1 \times 10^{7} = 1.389 \times 10^{-8}$ moles = 0.014 μmoles

Pmax is the maximum amount of muscle that can be activated.

Satact determines whether the muscle amount (Pmax) is fully on or not.

Katp refers to how fast the turn over of ATP is when the muscle is on.

Tabxt refers to the table called Aptab, a table of empirical values of the rate of ATP splitting as a function of the rate of shortening. When the muscle is shortening at its maximum speed it uses ATP 5 times faster than in the isometric state. When the muscle is stretching at its maximum speed it uses ATP at 0.2 times the isometric rate. In the isometric contraction each mole of myosin splits 5 ATP/second/site. The model calculates the rate of ATP use from the force in the muscle (fcmrv) from its lowest to highest value (0 to 1 in 0.05 intervals) (see figure 1.5). The units of ATPas are μmoles/s.

19) r vymus.kl=lomus*vmax*vyrel.k

The velocity of muscle (vymus) is equal to the initial length of the muscle (lomus) multiplied by Vmax (muscle lengths / second) multiplied by the relative velocity (vyrel) (between -1 and +1). A negative velocity is the muscle shortening. A positive velocity is the muscle lengthening.

20) r endis.kl=eta*vymus.kl*vymus.kl

The rate of energy dissipation (endis) is the product of the viscosity (eta) and the velocity of the muscle squared.

21) a Pmax.k=fifge(Pmaxf,Pmaxi,time.k,2.0)

The amount of muscle that produces maximum isometric force (Pmax) is equal to the final Pmax (Pmaxf) if the time is greater than or equal to 2.0 seconds.

Or

Pmax is equal to the initial Pmax if the time is less than 2.0 seconds.

Section to Control Activation

22) l act.k=act.j+dt*((go.j*chconst/dt)-relrat*act.j)

The activation (act) of the muscle occurs when the decision to "go" is made, and thus a "charge" (chconst) is put into the muscle. All of the time the "charge" is decaying with a relaxation rate (relrat) of 15/s. Thus "act" is a running account of how long there is to go before the muscle switches off (see figure 1.14).

23) a satact.k=min(1,act.k)

Satact is a value that varies from 0 (no activation) to 1 (full activation). If "act" is greater than 1, then satact is set to 1. If "act" is less than 1 then satact follows the "act" decay curve (see figure 1.14). Satact thus determines what percentage of the maximum muscle amount (Pmax) is being used.

24) a go.k = fifge (0, fifge (0, fifge(0, 1, pnfot.k, 0.01), lgleg.k, onlng), act.k, 0.01).

To turn the muscle on:

1) The foot must be on the ground (i.e. the foot position must be less than 0.01).

2) The muscle should not be already active (i.e. act must be less than 0.01).

3)The leg length must be less than the on length (onlng).

If "go" is off no stimuli can reach the muscle. The number 0.01 at the end of the equation means, if the muscle is still on a bit i.e. 1.0%, then it is left on.

Savper - This equation specifies the time interval with which the model plots the data.

List of names for the model

Names prefixed by a "p" are constants in a run of jumps. Names prefixed by "n" vary with the run.

p katp = 5 ATP/second/site in isometric contraction. The rate of ATP turn over when the muscle is on.

p losel = 10 mm. Initial length of the spring.

p Vmax = -2 muscle lengths/s. Maximum velocity of the muscle.

p mass = 1Kg. Mass of the body.

p grav = -9800mm/s^2. Acceleration due to gravity.

p lomus = 10mm. Initial length of the muscle.

p stse = 40N/mm. Stiffness of the spring.

p Pmax = maximum isometric force of the muscle

p Pmaxf = 50N. Final Pmax.

p Pmaxi = 100N. Initial Pmax.

p Chconst = 1000. Determines how much "charge" the muscle receives, which determines how long the muscle is on for.

p onlng = 9.5mm. The length at which the muscle is turned on.

p gcon = 4. The curvature of the force velocity curve, ie the constant in the Hill equation.

p eta = 0.1 N/(mm/s). Viscosity.

p relrat = relaxation rate = 15/s. Therefore the time constant is 1/15s.

n lgleg = Initially the leg of the leg is 10mm.

n pnbdy = Initially the position of the body is 19.9mm.

n vybdy = 0mm/s. Initially the body is stationary thus the velocity of the body is zero.

n pnfot = 0mm. Initially the position of the foot is on the ground.

n enmus = 0 μmole. Energy used by muscle

n envis= 0 mJ. The viscosity energy.

n tkoff = 0mm/s. Take-off velocity.

n act = 0. Activation.

dt = Integration time interval.

Appendix 2

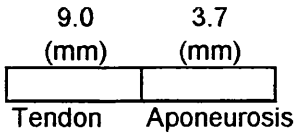

Total Length = 12.7 mm

If the tendon and aponeurosis is subjected to the isometric force of 0.36N, the tendon and aponeurosis are stretched by 3% (see P.166, paragraph 3).

3 % of 12.7 mm = 0.38 mm

$$\frac{0.36\ \text{N}}{0.38\ \text{mm}} = 0.94\ \text{N/mm}$$

The change in joint angle was determined for a mouse when its foot is moved to maximum extension. The mouse leg was placed on its side under a microscope in mouse Ringer, the fur was removed to reveal the Achilles tendon. A landmark on the Achilles tendon was observed as the foot was moved to maximum extension. 2.8mm was found to be the maximum extension, thus this is the maximum extension that can occur in running. However it is unlikely that a mouse would perform a maximum extension of the foot when running. Therefore a value of half this was used in the dimensionless number calculation.

Dimensionless Number

$$\frac{0.94\ \text{N/mm} \times 1.4\ \text{mm}}{0.36\ \text{N}} = 3.67$$

Appendix 3

1) Estimate of the stiffness of Achilles tendon and gastrocnemius aponeurosis.

Extension of human Achilles tendon in running = 18mm

Force in the tendon = 4700 N Alexander & Bennet-Clark, (1977)

Stiffness of Achilles tendon: 4700N / 18mm = 261 N/mm.

From the experiments on mouse soleus muscle and EDL tendon the stiffness of the tendon and aponeurosis in mouse has been found to be the same (see P.166, paragraph 3). It is assumed this is the case for human Achilles tendon and gastrocnemius aponeurosis. Therefore stiffness of gastrocnemius aponeurosis is: 4700N / 18mm = 261 N/mm.

Since the tendon and aponeurosis are in series their compliances add up, therefore the combined compliance is:

1/261 + 1/261 = 2/261

Stiffness is the reciprocal of compliance, therefore the combined stiffness of the tendon and aponeurosis is: 261/2 = 131

2) Estimate of the force in the gastrocnemius muscle.

If equal stresses acted in the gastrocnemius and soleus, gastrocnemius would exert one third of the force in the Achilles tendon.

4700 X 1/3 = 1567 N

Alexander & Vernon, (1975)

3) Estimate of the change in joint angle.

i) Fixing the leg and rotating the foot about the ankle joint, a human foot (at the ball of the foot) moves approximately 8cm.

ii) The lever ratio from the ball of the foot to the ankle was calculated from data given in Alexander (1988). The force on the ball of the foot when a 70Kg man runs is 1.9kN and in the Achilles tendon is 4.7kN.

4.7 kN / 1.9 kN = 2.47

Therefore the lever ratio from the ball of the foot to the ankle is 2.47. Thus the maximum length change of the MTC in running is approximately:

80mm / 2.47 = 32 mm

It is likely that in running the length change in the MTC would not be maximal, therefore half this value was used for the length change of the MTC in the dimensionless number calculation.

4) Dimensionless number for the human MTC: 131 (N/mm) X 16 (mm) / 1567 (N) = 1.34.

Chapter 2. MUSCLE WEAKNESS WITH AGE

2.1. Introduction

Muscle weakness associated with ageing has two components. There is a weakness due to muscle atrophy (Essen-Gustavsson & Borges, 1986: Kallman *et al.*, 1990: Vandervoort & McComas, 1986). In addition it has also been found that there is a reduction in the maximum voluntary force (MVF) per cross-sectional area (CSA) of the muscle with age. Brooks and Faulkner (1988) compared the contractile properties of soleus and extensor digitorum longus (EDL) muscles from young, adult and aged mice. They found the force (F) per CSA was reduced in muscles from aged mice during both isometric and shortening contractions, by about 20%, independent of shortening velocity.

It has also been shown that the MVF/CSA of the skeletal muscles of men and women after the age of 75 years are approximately 30% lower than in young men and women (20-40 years) (Bruce *et al.*, 1989a). Thus with old age skeletal muscle strength decreases not only due to muscle atrophy but also due to a reduction in F/CSA. Twitch interpolation studies have shown that elderly subjects can fully activate their muscles, therefore the reduction in MVF/CSA in elderly subjects is not due to the inability to fully activate their muscles (Phillips *et al.*, 1992). This technique relies on the principle that the size of the twitch response that is recorded from a muscle after single electrically stimulated shocks applied to the motor nerve, depends on the degree of concomitant activation in the muscle. The maximal twitch height is recorded when there is no voluntary force being produced; as the proportion of voluntary force is increased, the superimposed twitch height decreases towards zero, as the muscle becomes fully activated (Phillips *et al.*, 1992).

The cause of the reduction in F/CSA at present is unknown. In women the reduction in MVF/CSA has been shown to occur at the time of the menopause (Phillips *et al.*, 1993a). The time course of the reduced MVF/CSA in men is not known. The present study set out to investigate the age-related changes in MVF/CSA of the thumb adductor muscle (adductor pollicis) in men between the ages of 17 and 85 years.

2.1.1. Why The Adductor Pollicis Was Used In This Study

The adductor pollicis muscle was used for the following reasons:

1) The fibres are relatively parallel, i.e. the fibre length is a large proportion of muscle length. Therefore the CSA of the muscle is similar to the summated CSA of all the fibres. Thus a good correlation of force with CSA (R = 0.90) is obtained (Bruce *et al.*, 1989b).

2) There is not much disuse atrophy of the adductor pollicis. In normal daily activity the adductor pollicis muscle will be used both dynamically and isometrically. The muscle is very important for gripping or holding on to objects that will mainly require submaximal isometric contractions, and this is reflected in the fibres that are type I, fatigue resistant (Phillips *et al.*, 1992). This is a cross sectional study not a longitudinal study. Therefore it is possible the CSA of the adductor pollicis in one person might change with age. Changes in the population will affect the graph (see figure 2.6) e.g. people are generally getting bigger. However the limitations of the study suggest there is not much atrophy.

3) It is an easy muscle to determine the MVF because the insertion of the muscle is close to the point of force measurement. Thus the measurement is less likely to be affected by difference in lever ratios between subjects. For example, force measurements of the quadriceps muscle are usually taken at the ankle, which is some distance from the muscle insertion (Phillips *et al.*, 1992).

2.1.2. Method For Determining The CSA Of The Adductor Pollicis

The method of determining the CSA of the adductor pollicis muscle was that used by Bruce *et al.*, (1989b). The CSA was determined by measuring the thickness of the hand in the plane that bisects the adductor pollicis muscle by the difference in outputs between two linear potentiometers which were moved over the skin. A third potentiometer monitored the position of the hand.

An anatomical dissection of a cadaver hand, conducted by Bruce *et al.*, (1989b), through the same plane confirmed that the results of these measurements should approximate to the CSA of adductor pollicis together with the part of first dorsal

interosseous. In further studies they found the area measured by the hand profiles, were well correlated (r=0.937) with measurements of muscle CSA obtained from computer-assisted tomography (CAT) and nuclear magnetic resonance (NMR) images through the same plane (see figure 2.1). The estimated CSA obtained from the hand profiles was found to be only 60% of the actual muscle CSA, as determined by the imaging methods. This was not seen to be a problem, since the results were based on comparing the ratio between force and CSA, and did not depend on the absolute value of the ratio (Bruce *et al.*, 1989b).

The discrepancy in area is partly due to the fact that some of the muscle is proximal to the bases of the metacarpal bones and is therefore not included in the hand profile CSA measurement (see figures 2.2a and b). There is also a small compressing effect of the springs holding the potentiometers against the two surfaces of the hand (Bruce *et al.*, 1989b). However despite these limitations it has been shown that the Bruce *et al.*, (1989b) method of measuring CSA although not equal to, is highly correlated with the true CSA of adductor pollicis. The relationship between the force registered by the force transducer and the CSA of the muscle might be complex, i.e., geometric considerations such as the angle each fibre pulls on the thumb. Nevertheless assuming the architecture of the adductor pollicis is basically similar in different human individuals, one would expect a good relationship between CSA and force.

2.2. Methods

2.2.1. Subjects

Subjects were recruited from staff and students of University College London. Elderly subjects were recruited from three sources. Firstly, from retired staff of University College London, the Chelsea Pensioners of the Chelsea Royal Hospital and a sports centre in London. All together 159 men between the ages of 17 and 85 were tested.

2.2.2. The Protocol

The protocol was similar to that previously described in Bruce *et al.*, (1989a & b). A questionnaire modified from a Department of Health & Social Security questionnaire (Wickham *et al.*, 1989) was used to determine health and activity levels of subjects over 60 years of age. Subjects with pain or stiffness of movements of the thumb or specific

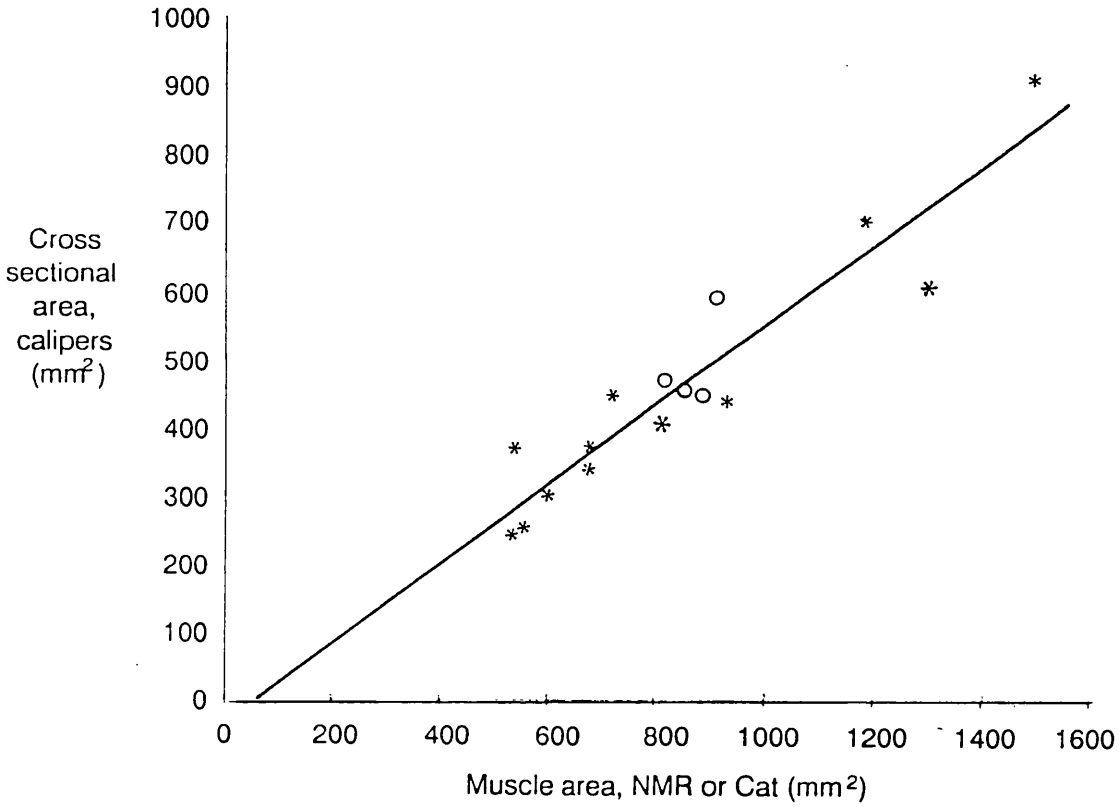

Figure 2.1. Relationship between muscle area measured from nuclear magnetic resonance (NMR) (*, n=12) or computer-assisted tomography (CAT) (o, n=4) images and CSA as measured by the method described in the text. The line is the regression line: y=0.58x-33.

From Bruce *et al.*, (1989b).

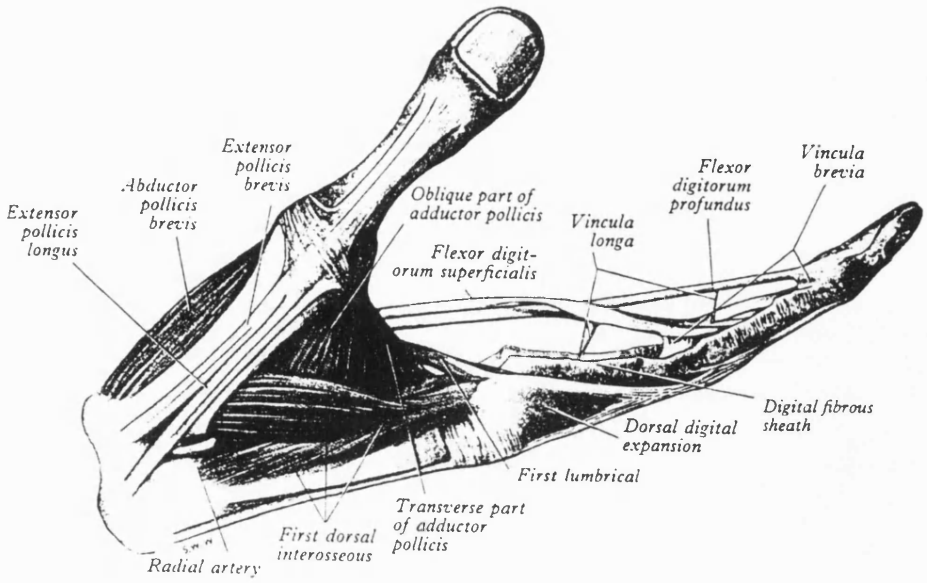

Figure 2.2a. Lateral part of the right hand showing the oblique and transverse part of the adductor pollicis. From Gray's Anatomy (1989).

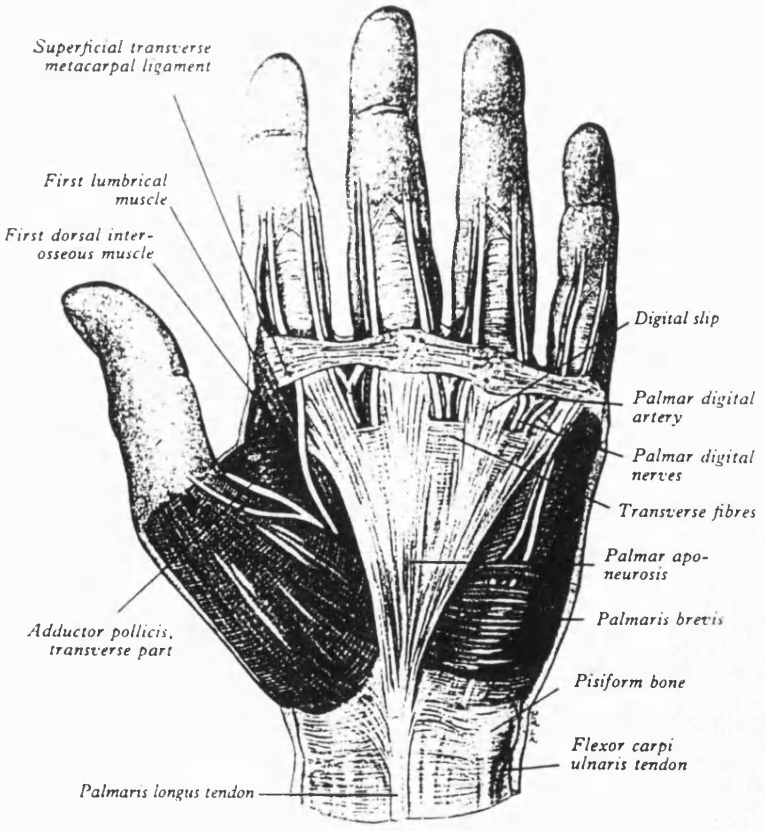

Figure 2.2b. The left palm, showing the transverse part of the adductor pollicis. From Gray's Anatomy (1989).

wasting of the hand muscle were excluded as were those with cardiovascular, generalized neuromuscular or thyroid disease, or those regularly taking medication likely to affect muscle function or motivation. The project was approved by the ethical committee at University College London.

2.2.3. Force And CSA Measurements

MVF of the adductor pollicis of the right hand was measured using a force transducer mounted on a metal bar placed between the bases of the proximal carpal bone of the thumb and the metacarpal bone of the index finger (Phillips *et al.*, 1992). The fingers and inter-phalangeal joint of the thumb were kept maximally extended throughout the measurements, to minimize contribution to the recorded force from the flexor muscles of the fingers. The subjects were requested to squeeze the bar as hard as possible against the metacarpal of the index finger. The point of opposition of the adduction of the thumb was chosen because it is close to the attachment of the adductor pollicis muscle and because it is proximal to the attachments of the flexor muscles of the thumb. Therefore differences in lever ratio between individuals were minimized. The force measured was therefore largely due to activity of adductor pollicis and a contribution from first dorsal interosseous (Bruce *et al.*, 1989b). Each subject was requested to make nine 2s maximum contractions. A rest of 30s was given in between each contraction. No habituation was seen. The subjects whilst performing the maximum voluntary contraction (MVC) were able to watch the computer screen on which the results were collected, and were also encouraged verbally to squeeze the bar harder.

The apparatus for measuring CSA is shown in figure 2.3a. The thumb was placed so that it was fully abducted. CSA was determined by measuring the thickness of the hand in the plane that bisects the adductor pollicis muscle, by the difference in outputs between two linear potentiometers which were moved over the skin. The shafts of the potentiometers were held by springs against the two surfaces of the hand. A third potentiometer monitored the position of the hand from the start point. The start point was determined for each subject as the point between the bases of the metacarpal bones of the thumb and index finger (see figure 2.3a). An X-Y plot of thickness against distance moved thus represents a profile of the hand (see figure 2.3b). Four profiles were obtained for each subject, the subject removed the hand from the apparatus

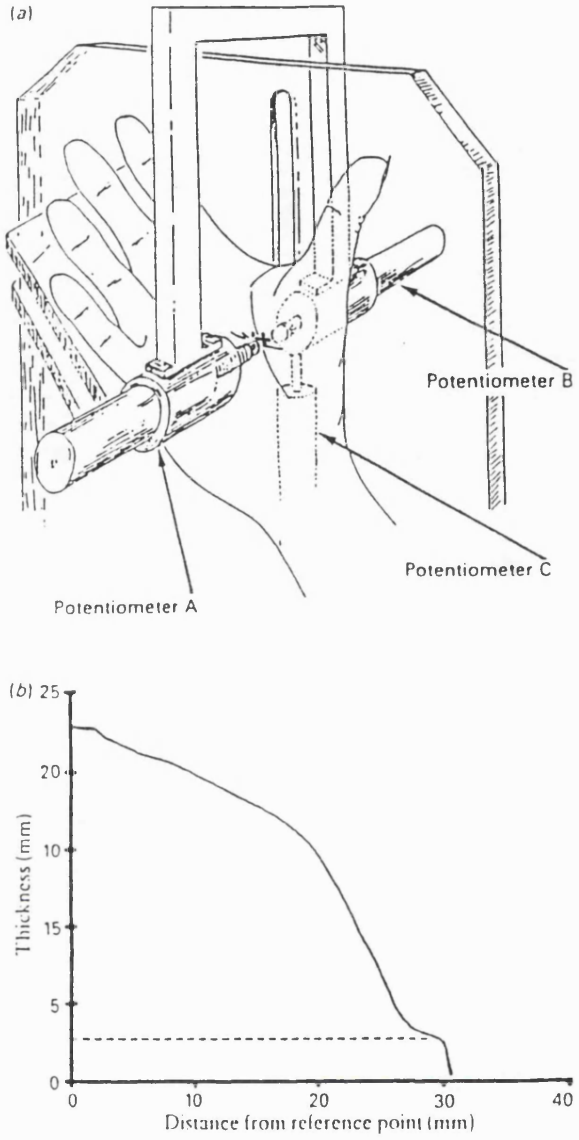

Figure 2.3a. Apparatus for estimating cross-sectional area (CSA) of adductor pollicis. Hand thickness was measured by the difference between the outputs of potentiometers A and B, and distance from the start point (*) by the output of potentiometer C. The resulting X-Y plot is shown in (b).

b) Profile of the hand as measured by the apparatus shown in (a). Hand thickness is shown plotted as a function of distance from the reference (start) point. The area above the broken line is taken to represent the CSA of adductor pollicis. The area below the broken line represents the skin and subcutaneous fat.
From Bruce *et al.*, (1989b).

between each measurement. The profiles were integrated after allowing for skin and subcutaneous fat thickness (see figure 2.3b). For each subjects the MVF is a mean of 9 maximum voluntary contractions and the CSA is a mean of 3-4 measurements. It took approximately 30 minutes to test one subject.

2.3. Results

For each subject MVF and CSA was highly reproducible resulting in a coefficient of variation of $<3\%$ and $<6\%$ respectively for up to 9 contractions and 3-4 CSA measurements respectively. This was also found to be the case for the women's measurements obtained by S.K. Phillips. Measurements of MVF and CSA made on the same subject by myself and S.K. Phillips were found to be the same. Five subjects were tested 3 times by each investigator on separate occasions, to establish if the method was reproducible. The mean coefficient of variation for MVF was found to be 3% and for CSA was 5.9%. Thus it was considered justifiable to compare the men's and women's results.

Figure 2.4, shows MVF plotted against CSA for men (17-60 years), and for pre-menopausal women (22-45 years, obtained by S.K. Phillips). MVF and CSA were found to be strongly correlated in both groups (men: $n=117$, $r=0.70$, $p<0.001$; pre-menopausal women: $n=30$, $r=0.63$, $p<0.001$). Combining the data was not found to alter significantly either the regression lines ($n=147$, $r=0.75$, $p<0.001$) nor the mean MVF/CSA. Figure 2.5, shows MVF/CSA against age for male subjects (17-85 years). It can be seen that the MVF/CSA starts to decline in men at about 65 years of age.

The CSA was not found to vary significantly with age and is summarized in figure 2.6 and table 2.1. As discussed in section 2.4.2, a 24% loss of muscle fibres at age 70 has been found in human muscle, however in the current study no atrophy in the adductor pollicis is found with age. From age 65 to 85 the CSA appears to increase slightly from 400 to 484 mm^2 (see table 2.2). However this increase was not found to be significant (see table 2.1b). In the age range 81-85 years there are five subjects, one of which has a very large CSA (see figure 2.6). This large CSA from one subject could be skewing the data in this group to produce a large mean CSA. This age group had the least number of subjects, due to the difficulty in finding healthy subjects of this age.

CSA of the adductor pollicis was found to increase generally with an increase in the height of the person (men aged 17-60 years) ($n=117$, $r=0.08$), although the correlation was not significant (see figure 2.7). The obesity index of the subjects was determined, it is the ratio of weight (Kg)/(height)^{2}m. A value of less than 25 signifies the person is not obese. A value of 25-29.9 = grade 1 obesity, 30-40 = grade 2 obesity and a value greater than 40 is grade 3 obesity (Garrow, 1983). The percentage fat of the hand was determined from the X-Y plot. It is the area below the dotted line divided by the area above the dotted line multiplied by 100 to give a percentage (see figure 2.3b). Plotting the percentage fat against the obesity index (men aged 17-60 years) a slight correlation was found, however it was not significant ($n=117$, $r=0.13$) (see figure 2.8). Table 2.2, summarizes the results for all the subjects grouped into 5 year age groups. In addition one castrated (due to testicular cancer) subject was tested his MVF/CSA was found to be very low 0.0897 N/mm^2, this result however was not included in the graphs, due to it being from only one subject.

The results of the time course of the decrease in MVF/CSA for the men were compared to results for women previously obtained by S.K. Phillips using the same apparatus and method. The time course of the decrease in MVF/CSA in men and women with age was found to be very different and is shown in figure 2.9a and b. The men and women were grouped into 5 year age groups (e.g. 21-25, 26-30 years etc). The mean group number for the men was 11.7 $\pm$ 0.90 and for the women was 8.4 $\pm$ 1.18 (mean $\pm$ sem). The group 86-90 year old men were obtained previously in a separate investigation by Bruce *et al.* (1989a) using the same apparatus, they were added to the graph to indicate that the decline in F/CSA with age does not continue to decrease but reaches a plateau. No difference MVF/CSA in men and women was found up to the time of the menopause. However after the menopause in women there is a dramatic decline in MVF/CSA (average age 51 years), in men by contrast there is a gradual decline which begins at about 65 years. A Student's unpaired t-test performed on the data showed for the four age groups between 51 and 70 years of age, that the MVF/CSA for the women was significantly lower than for the men of the same age group. At the age of 75 plus the MVF/CSA of men and women once again reached the same level (see table 2.3).

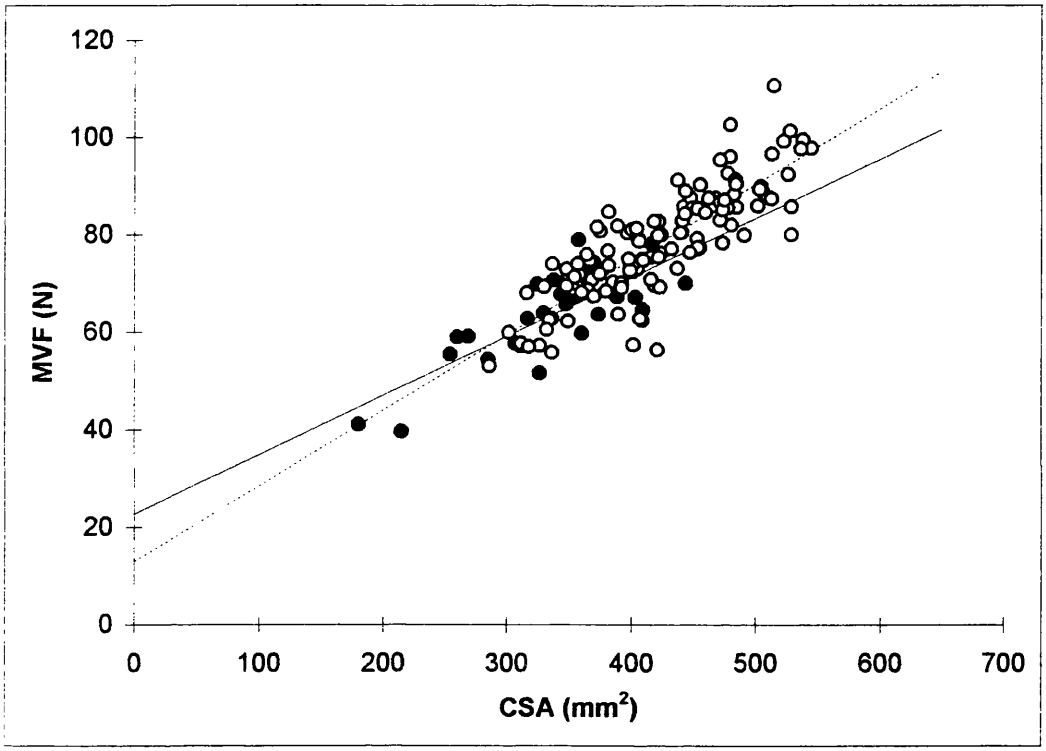

Figure 2.4. Relationship between maximum voluntary force (MVF) and cross-sectional area in men (17-60 years) (o) and pre-menopausal women (22-45 years) (●). The regression lines for men (- - -) and women (—) are also shown.

The intercept does not go through zero (y-intercept for men = 13), because in plotting the regression line it is assumed that all the error is in the y-axis. However there is also error in the x-axis, plotting the regression line the other way the intercept on the y-axis is negative (y-intercept for men = -15). The positive and negative intercepts are approximately equal and opposite (Snedecor & Cochran, 1976).

Correlation coefficients:
Men: n=117, r=0.70, p<0.001
Women: n=30, r=0.63, p<0.001
Men and Women combined (line not shown): n=147, r=0.75, p<0.001

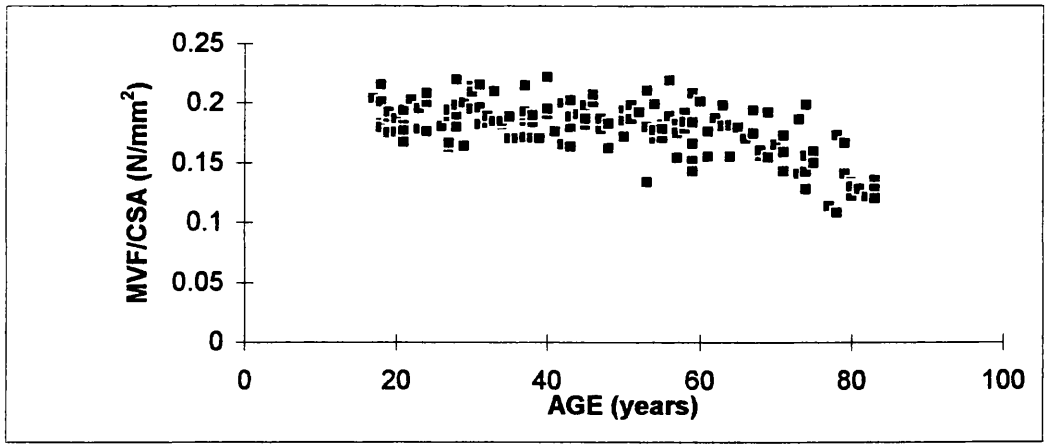

Figure 2.5. Relationship between maximum voluntary force (MVF) per cross-sectional area (CSA) and age for male subjects. Individual points for each subject are shown. n=159.

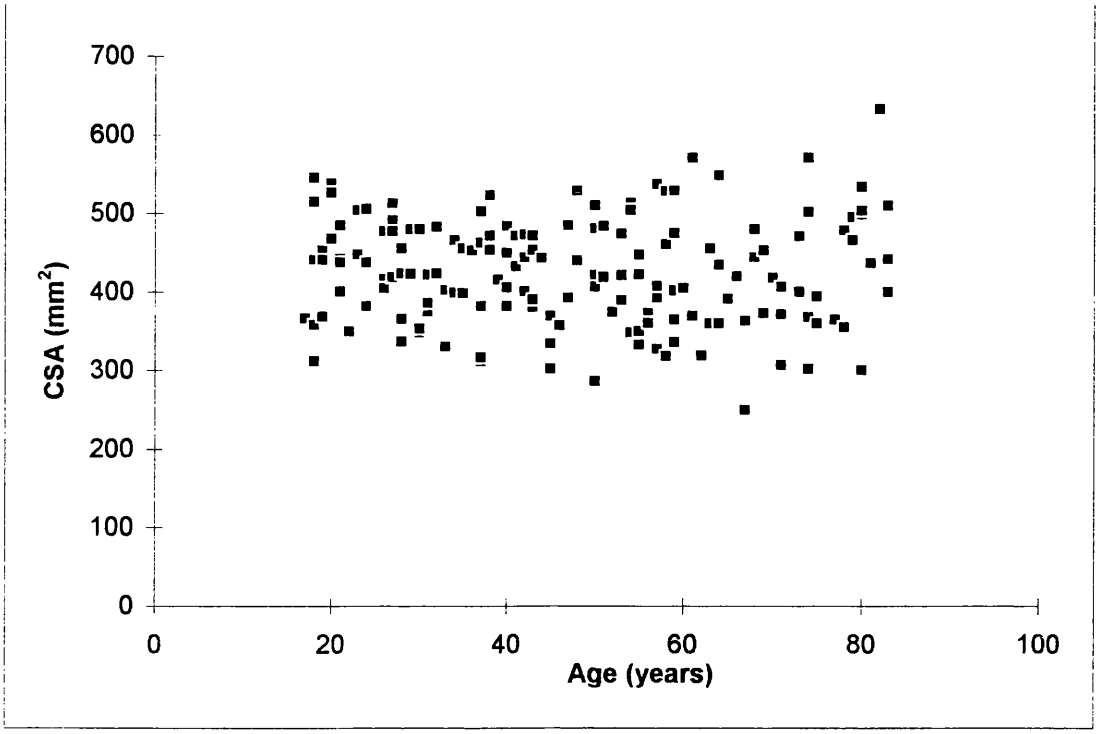

Figure 2.6. Relationship between cross-sectional area (CSA) and age for male subjects. Individual points for each subject are shown.
n=159.

Under 60 years mean CSA	Under 60 years group number	Over 60 years mean CSA	Over 60 years group number	Mean CSA under 60 years - over 60 years	% Mean of Difference	Under 60 years SEM	Over 60 years SEM	SEM of Difference	t	DF	P
424.466	117	425.529	42	-1.063	-0.250	5.680	12.783	13.988	-0.08	157	ns

Table 2.1a. Statistical analysis of the data using a Student's unpaired t-test, showing CSA of the adductor pollicis does not vary with age. The under 60 year age group contained men aged from 17 to 60 years. The over 60 year age group contained men from 61 to 85 years.

66-70 years mean CSA	66-70 years group number	81-85 years mean CSA	81-85 years group number	Mean CSA 66-70 years minus 81-85 years	% Mean of Difference	66-70 years SEM	81-85 years SEM	SEM of Difference	t	DF	P
400	8	484	5	-84	-21	26	41	48.55	-1.73	11	ns

Table 2.1b. Statistical analysis of the data using a Student's unpaired t-test, showing CSA of the adductor pollicis does not vary with age. The 66-70 year age group for men is compared to the 81-85 year age group.

DF = Degrees of freedom.

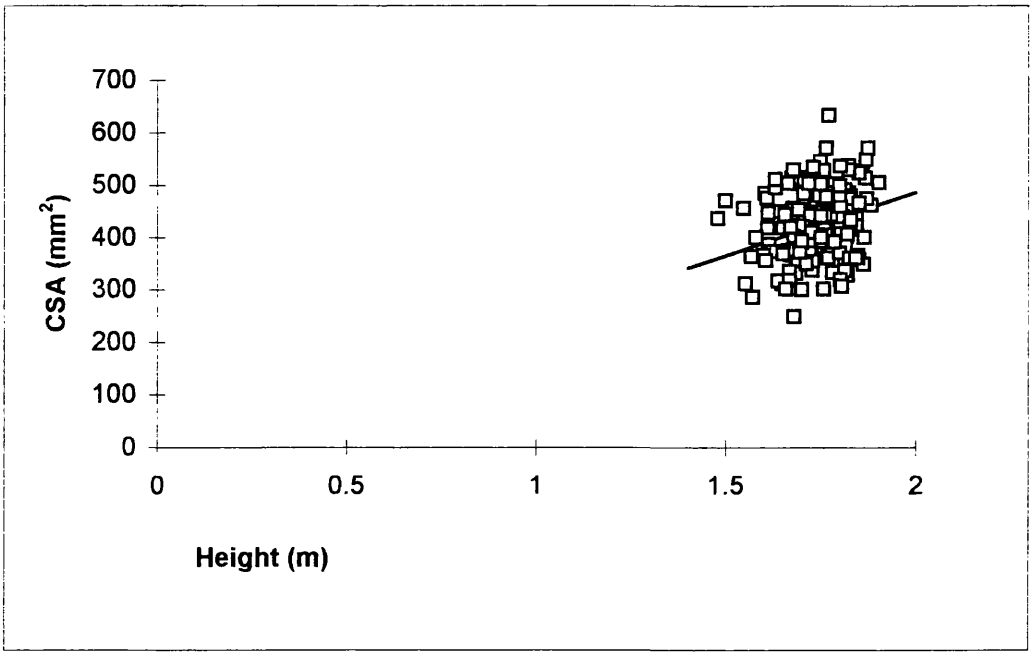

Figure 2.7. Relationship between cross-sectional area (CSA) and height in men (aged 17-60 years) (individual points and regression line shown).

Correlation coefficient:
n=117, r=0.08, p= < 0.1 (The correlation coefficient is not significant).

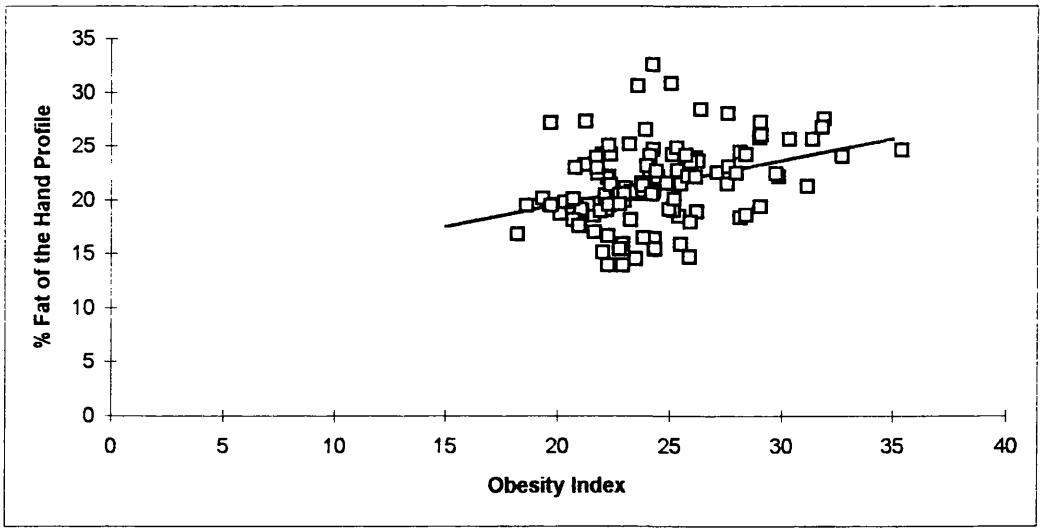

Figure 2.8. Relationship between the percentage fat of the hand profile and the obesity index in men (aged 17-60 years) (individual points and regression line shown).

Correlation coefficient:
n=117, r=0.13, p= < 0.1 (The correlation coefficient is not significant).

Table 2.2. Summary of the results for men.

MVF = Maximum voluntary force.
CSA = Cross-sectional Area.
O.I. = Obesity Index.
% Fat = % Fat of the hand profile.

Age Range 17 -20 years	MVF(N)	CSA (mm ^{2})	Height (m)	Weight (kg)	Age (years)	MVF/CSA	O.I.	% FAT
mean	83.8	444	1.744	72.4	18.67	0.1890	23.69	19.6
n	12	12	12	12	12	12	12	12
sd	14.7	79	0.084	9.5	0.98	0.0121	1.64	3.6
sem	4.3	23	0.024	2.7	0.28	0.0035	0.47	1.1

Age Range 21 -25 years	MVF(N)	CSA (mm ^{2})	Height (m)	Weight (kg)	Age (years)	MVF/CSA	O.I.	% FAT
mean	82.2	439	1.795	74.6	22.40	0.1881	23.10	19.4
n	10	10	10	10	10	10	10	10
sd	8.0	51	0.064	12.4	1.35	0.0140	3.14	3.8
sem	2.5	16	0.020	3.9	0.43	0.0044	0.99	1.2

Age Range 26 -30 years	MVF(N)	CSA (mm ^{2})	Height (m)	Weight (kg)	Age (years)	MVF/CSA	O.I.	% FAT
mean	80.7	429	1.771	70.4	27.88	0.1887	22.45	19.46
n	16	16	16	16	16	16	16	16
sd	11.5	56	0.059	6.5	1.41	0.0171	1.87	2.85
sem	2.9	14	0.015	1.6	0.35	0.0043	0.47	0.71

Age Range 31 -35 years	MVF(N)	CSA (mm ^{2})	Height (m)	Weight (kg)	Age (years)	MVF/CSA	O.I.	% FAT
mean	77.9	413	1.723	73.3	32.82	0.1895	24.66	20.86
n	11	11	11	11	11	11	11	11
sd	6.3	44	0.068	12.8	1.54	0.0131	4.05	1.77
sem	1.9	13	0.020	3.9	0.46	0.0040	1.22	0.53

Age Range 36 -40 years	MVF(N)	CSA (mm ^{2})	Height (m)	Weight (kg)	Age (years)	MVF/CSA	O.I.	% FAT
mean	80.3	429	1.739	76.9	38.14	0.1881	25.40	22.75
n	14	14	14	14	14	14	14	14
sd	10.7	64	0.075	11.3	1.41	0.0157	3.30	3.24
sem	2.8	17	0.020	3.0	0.38	0.0042	0.88	0.87

Age Range 41 -45 years	MVF(N)	CSA (mm ^{2})	Height (m)	Weight (kg)	Age (years)	MVF/CSA	O.I.	% FAT
mean	76.8	412	1.736	77.9	42.93	0.1869	25.79	22.8
n	14	14	14	14	14	14	14	14
sd	10.8	53	0.052	14.7	1.38	0.0133	4.42	4.7
sem	2.9	14	0.014	3.9	0.37	0.0036	1.18	1.2

Age Range 46 -50 years	MVF(N)	CSA (mm ^{2})	Height (m)	Weight (kg)	Age (years)	MVF/CSA	O.I.	% FAT
mean	77.5	424	1.751	80.3	48.36	0.1845	26.10	21.0
n	11	11	11	11	11	11	11	11
sd	10.4	74	0.077	13.8	1.69	0.0134	3.68	3.5
sem	3.1	22	0.023	4.2	0.51	0.0040	1.11	1.1

Age Range 51 -55 years	MVF(N)	CSA (mm ^{2})	Height (m)	Weight (kg)	Age (years)	MVF/CSA	O.I.	% FAT
mean	76.1	421	1.717	73.5	53.46	0.1813	24.83	22.35
n	13	13	13	13	13	13	13	13
sd	11.4	61	0.083	11.4	1.45	0.0185	2.39	2.62
sem	3.2	17	0.023	3.2	0.40	0.0051	0.66	0.73

Table 2.2. continued.

Age Range 56 - 60 years	MVF(N)	CSA (mm ^{2})	Height (m)	Weight (kg)	Age (years)	MVF/CSA	O.I.	% FAT
mean	74.5	414	1.746	72.6	57.88	0.1804	23.77	22.92
n	16	16	16	16	16	16	16	16
sd	14.4	72	0.074	8.8	1.20	0.0202	2.24	4.10
sem	3.6	18	0.019	2.2	0.30	0.0050	0.56	1.03

Age Range 61 - 65 years	MVF(N)	CSA (mm ^{2})	Height (m)	Weight (kg)	Age (years)	MVF/CSA	O.I.	% FAT
mean	73.7	423	1.786	77.83	63.00	0.1742	24.29	22.99
n	9	9	9	9	9	9	9	9
sd	16.9	87	0.095	12.11	1.41	0.0158	2.61	2.46
sem	5.6	29	0.032	4.04	0.47	0.0053	0.87	0.82

Age Range 66 - 70 years	MVF(N)	CSA (mm ^{2})	Height (m)	Weight (kg)	Age (years)	MVF/CSA	O.I.	% FAT
mean	67.9	400	1.666	70.9	68.00	0.1710	25.50	22.00
n	8	8	8	8	8	8	8	8
sd	11.8	72	0.068	9.1	1.31	0.0152	2.29	2.27
sem	4.2	26	0.024	3.2	0.46	0.0054	0.81	0.80

Age Range 71 - 75 years	MVF(N)	CSA (mm ^{2})	Height (m)	Weight (kg)	Age (years)	MVF/CSA	O.I.	% FAT
mean	62.7	405	1.731	80.7	73.18	0.1578	26.87	23.19
n	11	11	11	11	11	11	11	11
sd	7.6	81	0.107	14.1	1.54	0.0210	3.29	2.24
sem	2.3	24	0.032	4.2	0.46	0.0063	0.99	0.67

Age Range 76 -80 years	MVF(N)	CSA (mm ^{2})	Height (m)	Weight (kg)	Age (years)	MVF/CSA	O.I.	% FAT
mean	59.9	444	1.705	76.88	79.00	0.1355	26.6	22.68
n	9	9	9	9	9	9	9	9
sd	12.9	82	0.088	9.15	1.12	0.0220	4.1	3.37
sem	4.3	27	0.029	3.05	0.37	0.0073	1.4	0.79

Age Range 81 -85 years	MVF(N)	CSA (mm ^{2})	Height (m)	Weight (kg)	Age (years)	MVF/CSA	O.I.	% FAT
mean	61.2	484	1.642	71.6	82.40	0.1266	26.9	22.4
n	5	5	5	5	5	5	5	5
sd	10.8	92	0.121	7.1	0.89	0.0061	4.3	3.0
sem	4.8	41	0.054	3.2	0.40	0.0027	1.9	1.3

Castrated Subject	MVF(N)	CSA (mm ^{2})	Height (m)	Weight (kg)	Age (years)	MVF/CSA	O.I.	% FAT
n=1	29.6	329	1.65	57.9	84	0.0898	21.3	19.1

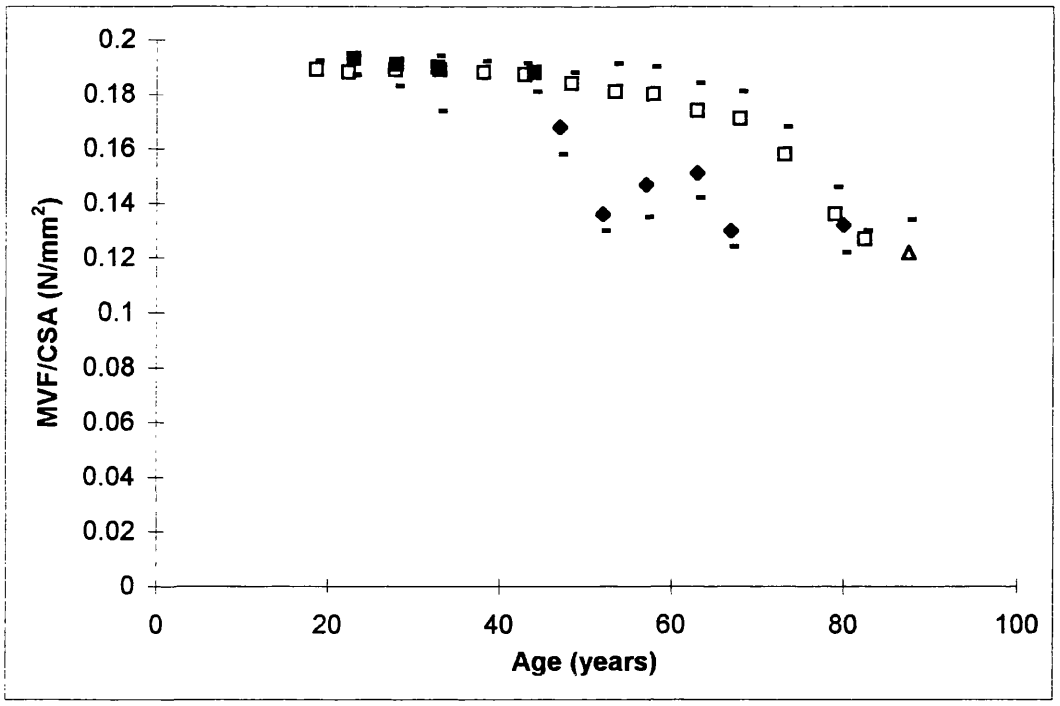

Figure 2.9a. Relationship between maximum voluntary force (MVF) per cross-sectional area (CSA) and age for three groups of subjects: men (□), pre-menopausal women (■) and peri- or post-menopausal women (◆). MVF/CSA is expressed as the mean value for the subjects in the age group, the sem has been plotted on the graph. The mean group number for the men was 12, and for the women was 8. Male subjects obtained by Bruce et al., (1989a) (△) are also plotted.

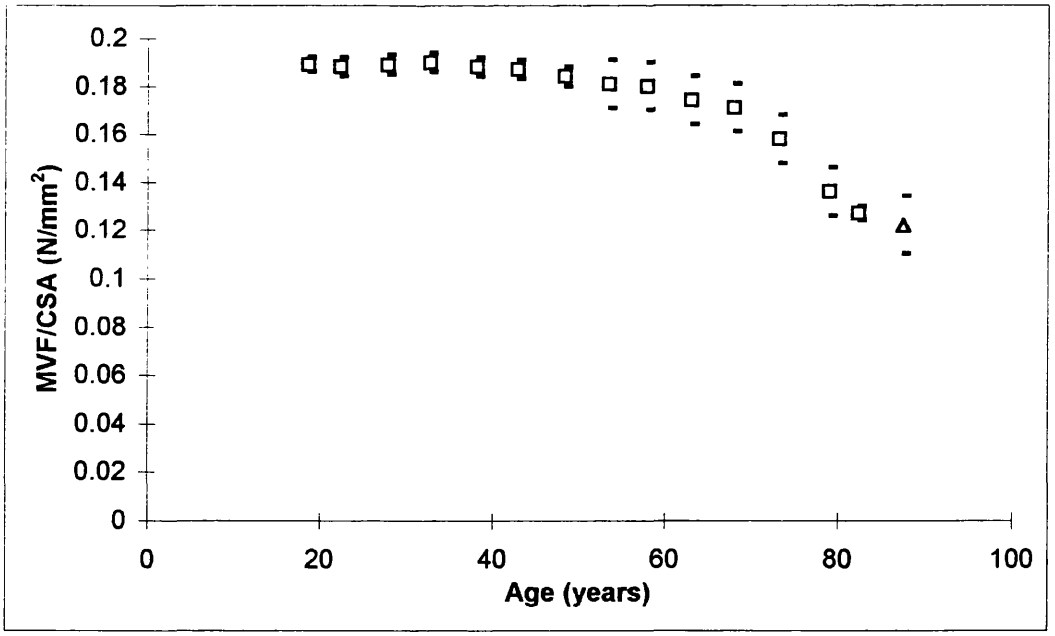

Figure 2.9b. Relationship between maximum voluntary force (MVF) per cross-sectional area (CSA) and age for male subjects (□). MVF/CSA is expressed as the mean value for the subjects in the age group, the sem has been plotted on the graph. The mean group number for the men was 12. Male subjects obtained by Bruce et al., (1989a) (△) are also plotted.

	Mean F/CSA	Group No.	Mean F/CSA	Group No.	Mean F/CSA							
Age Group (years)	Men	Men	Women	Women	Men - Women	% Mean of Diff	Men SEM	Women SEM	SEM of Diff	t	DF	P
21-25	0.188	10	0.193	9	-0.005	-2.660	0.004	0.006	0.007	-0.69	17	NS
26-30	0.189	16	0.191	5	-0.002	-1.058	0.004	0.008	0.009	-0.22	19	NS
31-40	0.190	25	0.189	4	0.001	0.526	0.003	0.015	0.015	0.07	27	NS
41-45	0.187	14	0.188	5	-0.001	-0.535	0.004	0.007	0.008	-0.12	17	NS
41-50 (post-menopausal women), 46-50 (men)	0.184	11	0.168	9	0.016	8.696	0.004	0.010	0.011	1.49	18	0.2
51-55	0.181	13	0.136	13	0.045	24.862	0.005	0.006	0.008	5.76	24	0.001
56-60	0.180	16	0.147	8	0.033	18.333	0.005	0.012	0.013	2.54	22	0.02
61-65	0.174	9	0.151	11	0.023	13.218	0.005	0.009	0.010	2.23	18	0.05
66-70	0.171	8	0.130	5	0.041	23.977	0.005	0.006	0.008	5.25	11	0.001
76-85	0.132	14	0.132	15	0.000	0.000	0.005	0.012	0.013	0.00	27	NS

Table 2.3. Shows statistical analysis of the data using a Student's unpaired t-test, comparing the results from the men to those obtained for women by Phillips *et al*., (1993a).

D.F. = degrees of freedom.
N.S. = non significant at the 0.05 level of significance.

2.4. Discussion

The present study shows the time course of the decrease in F/CSA in men and women is very different. In women the decrease begins after the menopause (average age 51 years) (Phillips *et al.*, 1993a), whereas in men the decrease begins at about 60 years of age. It has been shown that post-menopausal women (45-85 years) not taking hormone replacement therapy (HRT) have a reduced MVF/CSA similar to that of men over 75 years of age. In contrast post-menopausal women receiving HRT do not show any reduction in MVF/CSA (Phillips, *et al.*, 1993a).

2.4.1. Oestrogen And Testosterone Changes With Age

At the time of the menopause there is a dramatic reduction in oestrogen levels (McKinlay, 1989). Beginning a few years prior to the menopause, the ovaries exhibit a progressive decline in ability to secrete oestrogen and progesterone, resulting in an elevation in secretion of gonadotropic hormones. In the post-menopausal period, the ovaries atrophy and lose their follicles and ova, and a further elevation occurs in secretion of gonadotropic hormones. Thus in women after the menopause the only source of oestrogen is that produced from adrenal androgens (Harman & Talbert, 1985). HRT consists largely of oestrogen administration, thus it seems that oestrogen in some way prevents the reduction in MVF/CSA associated with the menopause (Phillips *et al.*, 1993a).

A corresponding hormone in men to provide this function is possibly testosterone. Evidence suggests free testosterone levels start to decline in men at about 60 years of age (McKinlay, 1989), which is consistent with the time course of reduced MVF/CSA shown in the present study. In ageing men, the decreased secretion of testosterone by the testes, also results in a rise in gonadotrophins, although these do not reach the high levels seen in post-menopausal women (Harman & Talbert, 1985). This suggests that reduced testosterone levels in men might be responsible for the reduced MVF/CSA associated with old age. In normal men, the peripheral aromatization of androgens is an important source of oestrogens. At present it is not clear what happens to the levels of both androgens and oestrogens with age in men (McKinlay, 1989). In order to investigate the possible role testosterone plays in maintaining MVF/CSA, levels of androgens and oestrogens must also be measured.

2.4.2. Muscle Atrophy With Age

The cause of the muscle atrophy associated with old age is not well understood. There is evidence for a loss muscle fibres (Lexell *et al.*, 1983) and a decrease in fibre size (Essen-Gustavsson & Borges, 1986). Essen-Gustavsson & Borges (1986), took muscle biopsies from healthy men and women from the ages of 20 to 70 years. They did not find any change in the fibre type composition with age. However the 70 year old men and women showed significantly reduced areas of both type I and type II fibres compared with the 60 year olds. Lexell *et al.*, (1983), estimated that there was a 24% reduction in the mean number of vastus lateralis muscle fibres in men aged 70-73 years. The reduction in the number of muscle fibres raises the question of whether this is due to a loss of complete motor units or whether each unit comprises a diminishing number of muscle fibres. Stahlberg & Fawcept (1982) found an increase in fibre number per motor unit with age, which was found to be more pronounced in distal than proximal muscles.

A study by Tzankoff & Norris (1977) found a decrease of about a third of the muscle mass after the age of 50 years in healthy adults. Brooks & Faulkner, (1988) reported a decrease of 20% in the mass of soleus muscle and of 13% in the mass of EDL muscle, from aged mice as compared to young mice. The dry muscle mass/wet mass ratio has been reported to be 0.25 in the soleus and omohyoid muscles of rats of all ages. This therefore indicates that in spite of significant decreases in mass with age, that the losses in protein and water were proportional (Brooks & Faulkner, 1988).

2.4.3. Reduced Force Per CSA With Age

Various explanations have been put forward:

1) There is a reduced ability to activate the muscles. However it has been shown by Phillips *et al.*, (1992), using the technique of twitch interpolation studies, that healthy, active elderly subjects with a low MVF/CSA could fully activate their muscles.

2) The second possibility is that a change in gross muscle architecture could have occurred, such as a change in the pennation angle of the muscle fibres. This would render the interpretation of F/CSA measurements difficult (Bruce *et al.*, 1989a). However the study by Bruce *et al.*, (1989a) was conducted on the adductor pollicis

muscle, a relatively parallel-fibred muscle. A reduction of approximately 30% in the MVF/CSA of this muscle from elderly subjects was found compared to young adult subjects. Thus indicating that a change in the pennation angles of the muscle fibres is unlikely to be responsible for such a large reduction in MVF/CSA associated with ageing.

Muscle architecture could also be changed by replacement of muscle by non-muscle tissue, i.e. a reduction in the number of active myosin sites. This would lead to an over estimate of muscle CSA by the current method of determining CSA. Supporting this an increased prominence of fat cells and connective tissue and the presence of lipofuscin has been described in ageing muscle (Jennekens *et al.*, 1971). However further studies using ^{31}P nuclear magnetic resonance (Taylor *et al.*, 1984) have shown that there is no diminution in concentrations of ATP, phosphocreatine and inorganic phosphate with age. Which does not support the hypothesis that the reduction in MVF/CSA in ageing muscle is due to a replacement of muscle with non-muscle tissue. In addition as is explained later, the MVF/CSA reduction with age was found not to occur during rapid stretching of active muscle. Thus if the force loss were due to a reduction in the number of active myosin sites, one would expect the force loss in stretching, isometric and shortening contractions to be the same (Phillips *et al.*, 1991). In addition the study by Taylor *et al.*, (1984) showed that the time to resynthesize ATP in the recovery period measured by the time to replete phosphocreatine (PCR) was also not different between young adult (20-45 years) and elderly subjects (70 - 80 years). This suggests that the ageing process does not affect the metabolic ability of human skeletal muscle to respond to exercise and that the changes found in muscle of the elderly are not due to alterations in energy production (Taylor *et al.*, 1984).

3) It has been suggested that the reduced F/CSA in aged muscle is a consequence of selected atrophy of fast twitch (type II) muscle fibres (Caccia *et al.*, 1979; Aniansson *et al.*, 1986). Based on the assumption that the intrinsic strength of type II fibres is 1.8 times greater than type I fibres, presumably due to the myosin type (Young 1984; Grindrod *et al.*, 1987). However the adductor pollicis muscle is almost entirely (approximately 80%) composed of type I fibres (Round *et al.*, 1984). Thus a selected atrophy of type II fibres would not be expected to significantly reduce the MVF/CSA

of this muscle, and so it seems unlikely to be the cause of the reduced MVF/CSA in the adductor pollicis muscle. In addition Phillips *et al.*, (1993b), found no change in the native myosin in mouse soleus and EDL mouse with age. Thus the reduced F/CSA in the aged mouse muscle could not be due to the expression of a weak force generating myosin, neither do these results support the hypothesis that fibre types change with age in mice (Phillips *et al.*, 1993b).

4) Reduced F/CSA has also been described under conditions of increased intracellular inorganic phosphate (P_i) (Elzinga *et al.*, 1989), when the intracellular pH (pH_i) is lowered (Curtin, 1990) and under conditions of hypertonicity (Howarth, 1958). However, a study by Phillips *et al.*, (1993b), has shown that there is no difference in the resting muscle pHi, P_i, ATP or PCR levels with age, in both mouse soleus and EDL muscle. Although it is possible that hormonal influences could alter perhaps the sensitivity of the crossbridges to such metabolites or that some other factor affects the crossbridge reducing force development with ageing. Evidence by Phillips *et al.*, (1993a) has shown that oestrogen, when administered to post-menopausal women is able to prevent the action of this unknown factor, and thus prevent the reduction in MVF/CSA with age.

It is unlikely that myofibrils of ageing mice are in a hypertonic environment. However a consequence of hypertonicity is that it may reduce the actomyosin lattice spacing and thus cause a reduction in force. Therefore it is possible that perhaps there is a change in the environment that is increasing the net charge on the proteins and therefore altering the lattice spacing. Thus the lattice spacing should therefore be measured in muscles from young and aged mice to see if it has changed (Phillips *et al.*, 1991).

Fatigued muscle produces a reduced force but the force during shortening is affected to a greater extent than the isometric force (de Haan *et al.*, 1989). However with ageing the reduction in F/CSA is the same proportion in both shortening and isometric contractions (Phillips *et al.*, 1991).

5) Evidence suggests the reduced F/CSA is not a result of a decreased number of attached crossbridges, but a consequence of less force being produced per crossbridge.

It has been shown in isolated soleus muscle from aged mice that the reduced F/CSA in old muscle is absent during rapid stretching. Whereas the force produced during shortening is reduced by approximately 13.3%. This results in a change in the force velocity curve for aged muscle as compared to young muscle (Phillips *et al.*, 1991).

The effect of stretching an active muscle is thought to move more of the crossbridges into a high force state as opposed to a low force state (Lombardi & Piazzesi, 1990). Thus it seems likely that the cause of reduced F/CSA in ageing is a result of the myosin molecule favouring the low force state. This low force can be identified as the state suggested by Pate and Cooke, (1989) as having P_i bound to the active site, whereas the high force state does not. Phillips *et al.*, (1993b) found that changes in muscle performance demonstrated in the aged mouse are not due to the expression of a weak force generating myosin because the native myosin does not change with age.

A study of womens' menstrual cycle by Phillips *et al.*, (1993c) found on day 14, that the ratio of stretch to isometric force was significantly lower ($15.5 \pm 5.8\%$, $n=7$, $P<0.05$) on day 14 than day 1 or day 21. Resulting from the fact that the isometric force was found to be greater by about 20% on day 14 than day 1 or day 21, but no difference in stretch force during the cycle was found. During the menstrual cycle both oestrogen and progesterone levels change. Mid cycle, at ovulation (day 14), there is a large oestrogen peak, which is consistent with the idea that muscle strength can be affected by oestrogens (Phillips *et al.*, 1993c). Possibly by forcing the crossbridge into a high force state, by some unknown mechanism. Since as stated previously, in the active stretch all the crossbridges are forced into a high force state.

2.5. Conclusions

Phillips *et al.*, (1993d) conducted a study to determine whether the reduction in MVF/CSA in women after the menopause was the same as that seen in old age. They compared the maximum isometric force and active stretch force from the soleus muscles of young, ovariectomised and control mice. The control mice were the same age as the ovariectomised mice, but were not operated on. They also compared post-menopausal women and pre-menopausal (control) women. The isometric MVF/CSA was found to be significantly reduced in the ovariectomised mice and the post-menopausal women as

compared to the controls. In contrast, active stretch MVF/CSA was not found to be different. Therefore indicating that in both old age and oestrogen deficient muscle, stretch can remove the reduction in MVF/CSA that is found in isometric and shortening contractions. Which suggests that the cause of the force loss is due to changes in the behaviour of the myosin molecule favouring the low-force state (Phillips *et al.*, 1993d). Although to my knowledge no stretch studies have been conducted on elderly men, it seems probable that it would have the same effect. Thus it seems likely that the mechanism of muscle weakness is the same in muscles from old mice, ovariectomised mice, post-menopausal women and elderly men.

The mechanism by which oestrogen and testosterone might maintain F/CSA in old muscle, by maintaining the myosin molecule in a high force state, is not known. Although there are known to be oestrogen receptors in skeletal muscle (Dahlberg, 1982), it is possible that the effect of oestrogen may not be direct but via a growth hormone or insulin-like growth factor (Phillips, *et al.*, 1993d). Dihydrotestosterone (DHT) is the most potent androgen in most tissues. It is produced by the local conversion of testosterone, and androgen receptors usually have a greater affinity for DHT than testosterone. However in skeletal muscle the cytoplasmic receptor mainly binds testosterone rather than DHT, which suggests that testosterone exerts a direct effect on muscle (Florini, 1987).

Both oestrogen and testosterone replacement therapy have been shown to restore bone mass in osteoporosis (Marcus, 1991). It has been found by Jones & Rutherford (1990), that the force produced, by a given CSA of the quadriceps muscle, was found to be lower in women with osteoporosis compared to those without. It is not known if it is by direct action on the bone that oestrogen and testosterone can maintain bone mass (Marcus, 1991). It is possible thus that the effects of these hormones on bone mass maybe an indirect result of increased mechanical stress placed on the bone due to increased force of the attached muscle, due to increased F/CSA.

The similarities between mouse and human muscle ageing, that have been quoted in this chapter indicate that mouse muscle is an appropriate model for human muscle ageing. A female mouse model of oestrogen deficiency and a male mouse model of castration

could be used to study further the possible cellular mechanisms responsible for muscle weakness at old age and the menopause.

2.6. Further Experiments

The full force velocity curve should be measured in old and young men to determine whether there is a small transition jump from shortening to lengthening. This has been measured in old and young mice, where no transition jump from shortening to lengthening was found (Phillips *et al.*, 1991). The data should be analyzed using the modelling techniques of Lombardi & Piazzesi (1990) (which describes the behaviour of muscle during stretch), in conjunction with the ideas of Pate & Cooke (1990) (which explains the two force states).

Chapter 3. Mechanical Experiments On Whole Muscle

3.1. Introduction

In these experiments the compliance of mouse soleus muscle was investigated. There are three components in series: the tendon, the aponeurosis and the crossbridges. The compliancies of these springs add up since they are in series. The current series of experiments aims to quantify the compliance of each of the components.

The stiffness of a muscle fibre can be measured by very rapidly changing its length while recording the tension. Unstimulated fibres have a low stiffness, suggesting that thick and thin filaments can move past each other with little restraint. When the muscle fibre is stimulated it becomes very much stiffer. The stiffness varies with filament overlap in approximately the same way as tension. The stiffness rises with about the same time course as the tension but somewhat faster, because the crossbridge is put in place and then pulls. This suggests that relative movements of the thick and thin filaments are restrained in the active muscle by the crossbridges between them (Huxley & Simmons, 1971).

The classic work in this field is that of Huxley and co-workers on single frog muscle fibres (Tibialis anterior, lateral head) (Ford et al., 1977). Thus when a contracting muscle is rapidly shortened the force falls as the compliant portions of the crossbridge (S2 portion) are unloaded. If the release is completed within 0.2-1.0 ms a very rapid initial recovery of force follows from T_1 to T_2 lasting 2-5 ms, followed by a slower phase during which the force returns to the isometric tension (see figure 3.1). The explanation proposed, is that the rapid phase of force recovery is due to rotation of the S1 heads of the unloaded bridges thereby re-stretching the compliant S2 component (Huxley & Simmons, 1971) (see figure 3.2). The slow phase of force recovery, from T_2 to full isometric force, is ascribed to detachment and reattachment of crossbridges, so that the conditions of the isometric contraction are re-established (Huxley & Simmons, 1971). A length step thus results in the following four sequential phases of change in tension (see figure 3.1).

T_0 is the maximum isometric tension just before the release, T_1 is the extreme tension reached during the release: T_2 is the tension reached during early recovery phase.

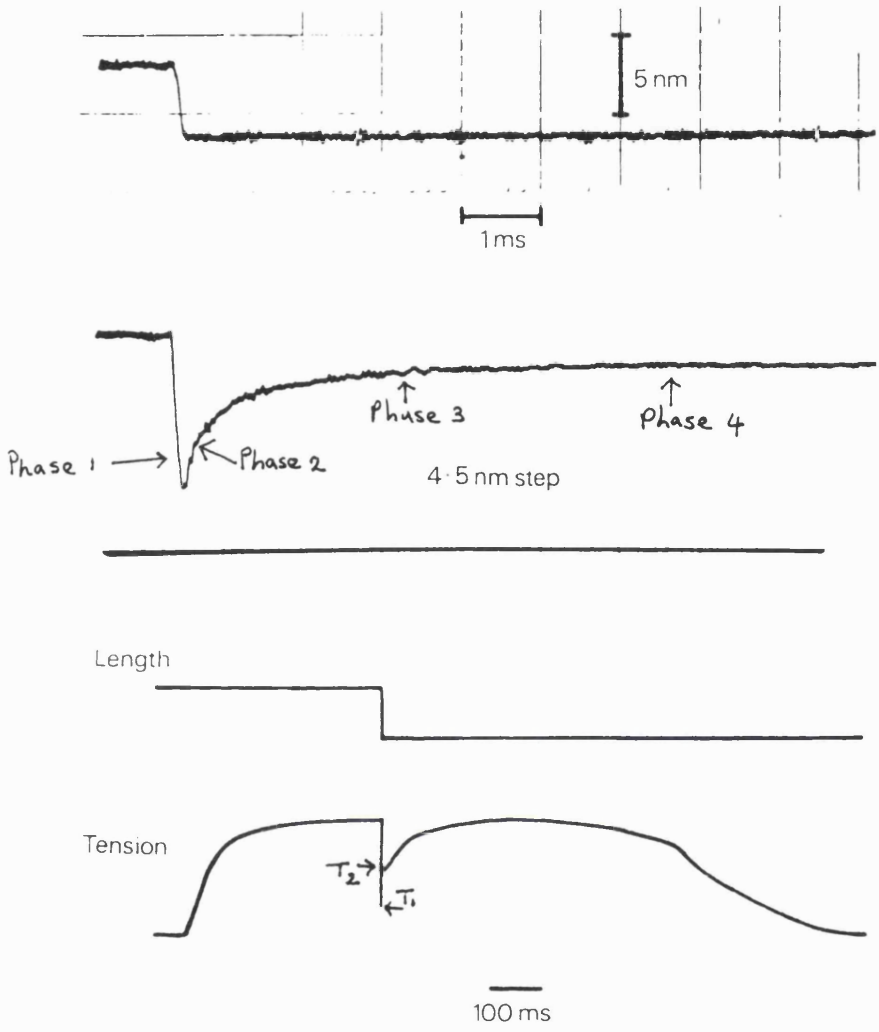

Figure 3.1. "Tension transient", i.e. time course of change of tension in response to a sudden change of length. Lower pair of traces: length and tension on a slow time scale, so as to show the whole tetanic contraction. The initial phase of tension recovery after the step is so fast that the downstroke and upstroke appear as a single line. Upper records: a part of a similar contraction which includes the step, on a time scale approximately 100 times faster, to show the early recovery phase. Length change 4.5nm per half-sarcomere. Steep parts of records retouched. Frog muscle fibre, approximately 0°C. Records obtained in collaboration with Simmons and Ford.

From A.F. Huxley , (1980)

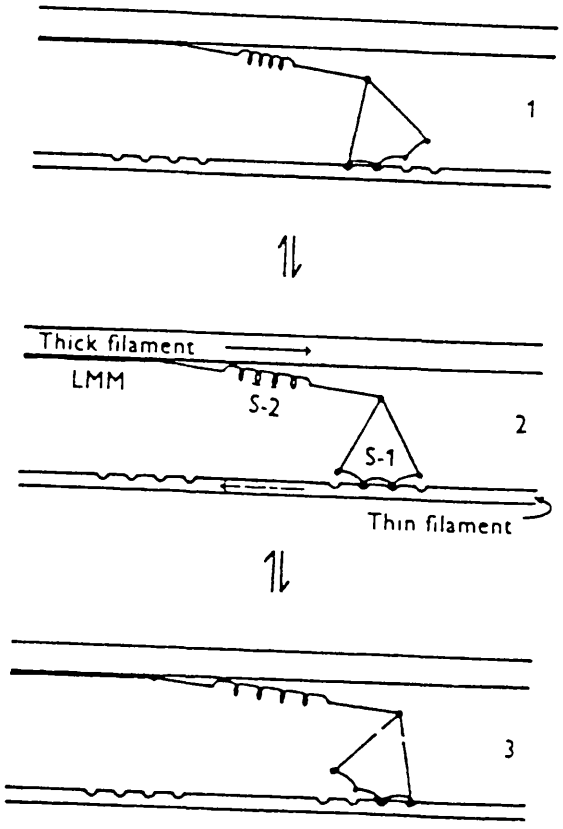

Figure 3.2. Huxley and Simmons model of the crossbridge, incorporating an elastic element and a stepwise shortening element. Here the elastic element is equated with the S2 portion of the myosin molecule and the stepwise shortening element with the S1 portion and its combination with actin.

From A.F. Huxley (1974)

Phase 1. A sudden drop in tension to T_1 occurs during the length change.
Phase 2. Immediately after the length change there is a rapid rise in tension to T_2, this phase lasts for 2-5 ms (the larger the release, the faster the transition).
Phase 3. The recovery of tension is greatly slowed or even reversed, the duration of phase 3 is between 10-50 ms at 0°C.
Phase 4. The recovery tension gradually reaches the original tension (Ford *et al.*, 1977).

Experiments by Ford *et al.*, (1977) using length steps of different sizes produced a T_1 and T_2 curve graph (see figure 3.3). The T_1 curve represents the tension at the end of the first phase and the T_2 curve, at the end of the second phase. Huxley and Simmons, (1971) proposed a theory to explain the shape of the T_1 and T_2 curves, which can be visualized as described below. The crossbridge is thought to consist of a tail and a head joined by a hinge (see figure 3.4). The tail part contains an undamped spring and the head part of the crossbridge can attach to actin at a number of angles. Due to the presence of the spring the head can move between the different angles without detaching and without relative movement of actin and myosin. The force exerted by the crossbridge depends on two variables x and z. x is the displacement of the myosin S1 head from the optimum binding position. z is the angle with which the S1 head binds to actin. Relative movement of the filaments changes x, but not z; rotation of the head changes z, but not x.

If the muscle is released very rapidly (0.2ms step release), so that there is no time for rotation of crossbridge heads to occur, the observed stress-strain curve is that of the spring itself. This gives the T_1 curve which is found to be experimentally nearly linear. The T_2 curve however has a plateau; tension falls very little for small length changes, but more for large length changes where the curve becomes almost parallel to the T_1 curve but displaced by about 6nm per half sarcomere. This suggests that T_2 represents the properties of the tension generator in the crossbridges, i.e. the S1 heads. The plateau is thought to correspond to the range of movement over which rotation of the myosin head can fully take up the slack in the S2 portion. The S1 head attaches to a site on the actin filament and rotates about it. In doing so the S1 head pulls on the elastic S2 subfragment that connects the S1 head to the backbone of the myosin filament. Thus each S1 head is able to take up about 6nm of slack (Huxley & Simmons, 1971).

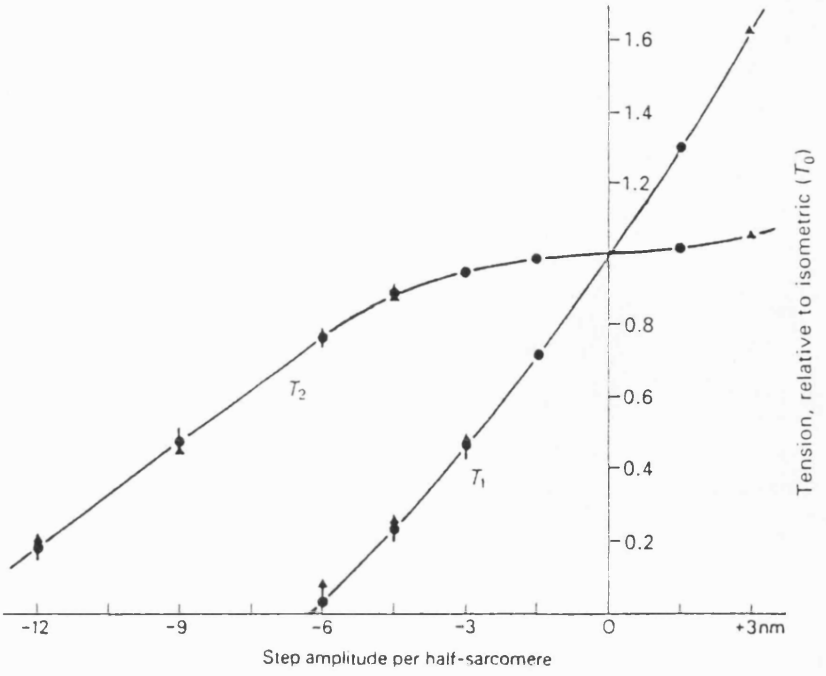

Figure 3.3. Curves of T_1 (extreme tension) and T_2 (tension approached during early recovery phase) in length-control steps of various amplitudes, both expressed as a fractions of T_0, the isometric tension immediately before the step. Negative values of step size indicate releases; positive values stretches.

From Ford *et al.*, (1977)

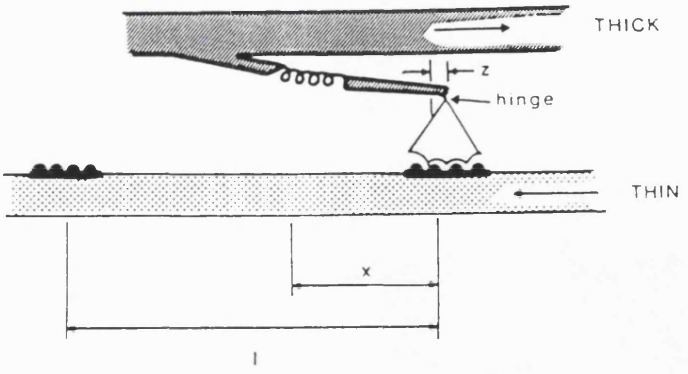

Figure 3.4. The modification to the 1957 theory suggested by Huxley and Simmons (1971). The head of the crossbridge can bind to the actin in a number of stable configurations at different angles, and therefore with different values of Z. The length of the spring in the crossbridge is now dependent on two variables, x and z. I is equal to the distance between the actin binding sites.

From Woledge *et al.*, (1985)

To determine the structures responsible for the passive elasticity Huxley and Simmons measured the T_1 and T_2 curves at different degrees of filament overlap, i.e. different muscle lengths. It was found that both curves scaled down in proportion to the number of crossbridges that can be formed (see figure 3.5). Hence it was concluded that this elasticity resided in the crossbridges (Huxley & Simmons, 1971).

3.2. Vmax (Maximal Velocity of Shortening).

A contracting muscle is rapidly shortened by a known distance (at a velocity greater than Vmax) so that the fibres become slack and will then shorten with no external load. The time for the fibre to take up the slack and to begin pulling on the force transducer gives a measure of the velocity of unloaded shortening (Edman, 1979). Vmax is independent of filament overlap (Edman, 1979), which means Vmax is independent of crossbridge number. To normalize Vmax (μm/s/half sarcomere) the number of half sarcomeres in series therefore needs to be measured. This then takes into account the thin filament lengths in different muscles. For example, if the thin filaments are longer fewer sarcomeres can be packed into a fibre of given length, thus the un-normalized Vmax is less. Vmax when normalized per half sarcomere, reflects the rate at which crossbridges can turnover, attach and detach, when unloaded and is characteristic of the proteins themselves and not of the arrangement.

3.3. Methods

The experiments were performed on soleus muscle dissected from mice, killed by dislocation of the neck. Both male and female mice of Balb/c strain aged 2-8 months were used. The mice had unrestricted access to a standard diet.

The muscle is attached to the bone by long tendons. After dissection aluminium foil (150 μm thick) 'T' clips were clamped on to each tendon as close to the muscle as possible to eliminate much of the tendon compliance. The more usual technique is to tie threads around the tendon and then to attach these to the apparatus but this contributes considerable series elasticity. Since the present experiment is trying to determine the amount of series elasticity in different locations of the muscle, it is not desirable that more series elasticity should be added to the muscle. Soleus muscle are slightly pennate, the fibres length is approximately 70% of the muscle length (Brooks

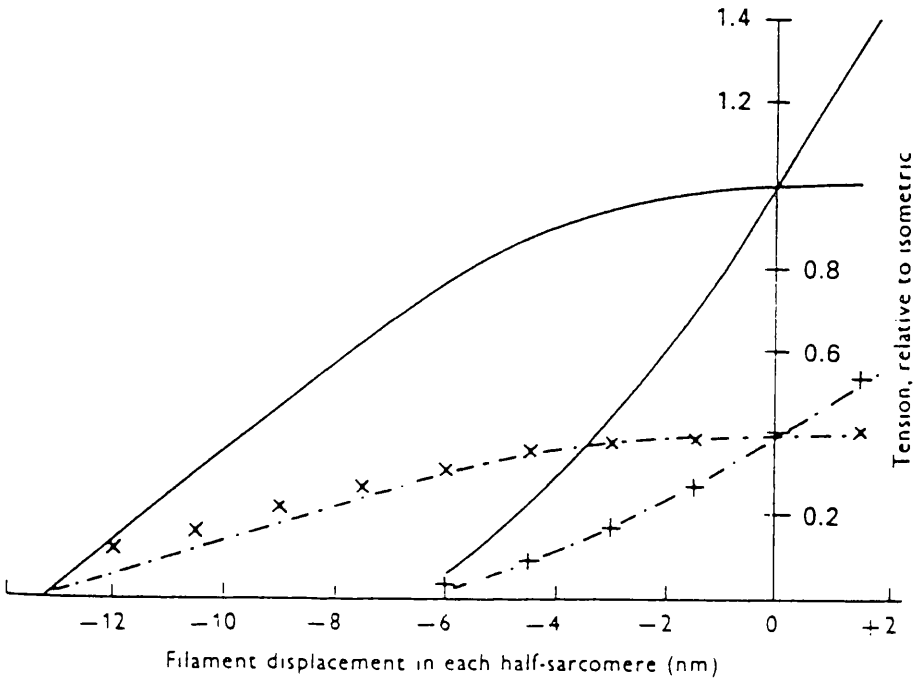

Figure 3.5. T_1 and T_2 curves from the same frog muscle fibre at two different lengths. The continuous curves were obtained when the sarcomere length was 2.2μm, at which all the crossbridges would be overlapped by thin filaments. The crosses show T_1 and T_2 curves from the same fibre when stretched to give a sarcomere length of 3.1μm, at which the overlap would be reduced to about 39%. The interrupted curves are simply the continuous curves scaled down to 39%.

From A.F. Huxley, (1974)

and Faulkner, 1988).

3.3.1. Bathing Solution

The Ringer solution contained 122.5mM NaCl, 5mM KCl, 1mM $MgCl_2$, 2mM $CaCl_2$, 1mM NaH_2PO_4, 24mM $NaHCO_3$ and 20mM Na-pyruvate. Pyruvate was chosen as the substrate instead of glucose because previous experience has shown that the muscles seem to last longer. The solution was gassed continuously with 95% O_2, 5% CO_2, the bath temperature was maintained at 25 $\pm$ 0.5°C and the mean pH of the bathing solution was 7.5. The osmolarity was measured to be 306 $\pm$ 0.8 ($\pm$ sd) mOsM, which is in accordance with the measured osmolarity of mouse blood (approximately 300 mOsM) (Yin, 1990). The K^+ and Na^+ ion concentrations were measured and were found to be 4.94 $\pm$ 0.15 and 160.8 $\pm$ 3.34 ($\pm$ sd) mM respectively. These measured values are in accordance with the calculated values for K^+ And Na^+ ions concentrations of 5 and 167.5 mM respectively.

Experimental Set Up

3.3.2. Muscle Stimulation

Muscles were stimulated directly using bright platinum electrodes connected to an electrical stimulator. The electrodes were placed either side of the muscle close to it but not touching it (see figure 3.6). The stimulation pulse was a square wave of 0.1-0.2 ms duration. Maximal stimulation was used which was between 50 and 60 volts. This was determined from measuring tetanus force while increasing stimulus strength until force increased no further. The optimum muscle length for maximal isometric tetanic force production was first determined for each muscle. Tetanic stimulation was given at a rate of 80Hz for 600ms. This frequency was chosen because it gave maximal tetanic force at the optimum muscle length. The muscle was given 1 minute rest in between stimulations. The isometric force produced at the end of each experiment was found to be the same as at the beginning of the experiment. Thus it was assumed the muscle was behaving satisfactorily through the duration of the experiment (approximately one hour).

3.3.3. Muscle Force Measurement

The foil 'T' clips attached to the muscle were placed over hooks in the muscle bath, one a fixed hook attached to the muscle bath and the other on the lever of the force

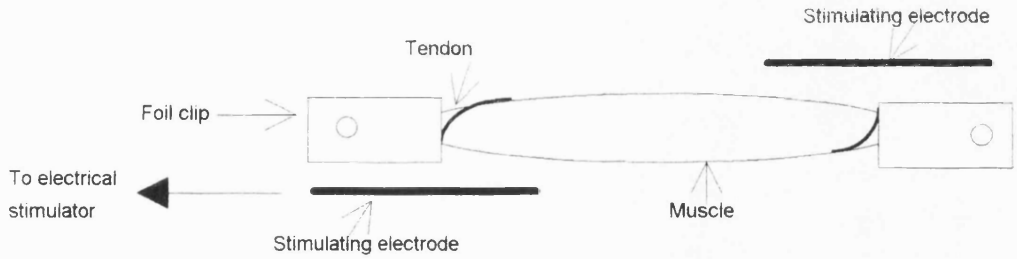

Figure 3.6. The muscle and stimulating electrode arrangement.

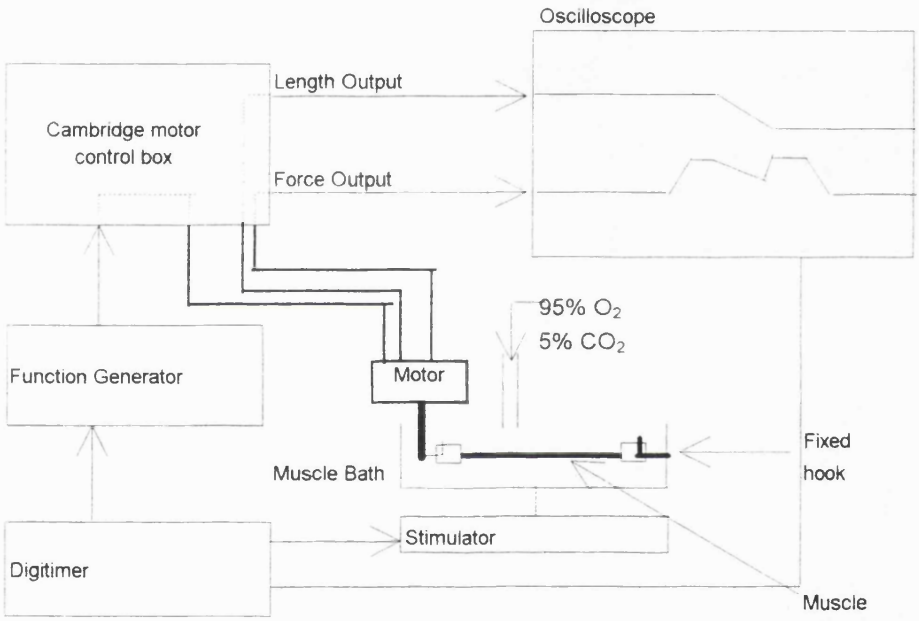

Figure 3.7. A schematic diagram of the experimental apparatus used in the quick length release experiments

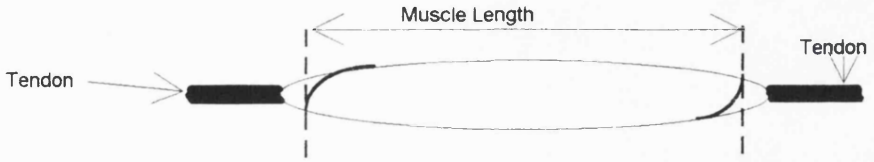

Figure 3.8. The length of soleus muscle was determined as the length between the dotted lines.

transducer, which is connected to a micrometer gauge for accurate length adjustments and was controlled by a dual mode motor (Cambridge Technology Inc. USA., Model No. 350). The Cambridge motor output was displayed, analyzed and stored on an oscilloscope (Nicolet 420). This arrangement is shown in figure 3.7.

The force transducer was calibrated by hanging known weights on the steel hook to which the muscle would normally be attached. The weights ranged from 5 to 20g. The weights were successively increased then decreased and the output voltage was recorded for each weight.

The motor performance was tested by making some releases on a small steel spring so that the force in the spring is dropped to half by the release. The spring was made from a piece of stainless steel wire wound round a pin. The external spring diameter was 2mm, the wire thickness was 0.25mm and the spring length was 1.6cm. The spring was surrounded by silicone oil to provide damping. The force and length trace obtained had the same shape which indicates the motor was performing well.

3.3.4. Muscle Length

The length of the muscle could be adjusted by the micrometer gauge attached to the force transducer. This measures changes in muscle length. The absolute muscle length was measured using the microscope eyepiece graticule. The microscope was calibrated with a stage micrometer. Dry weight was obtained by removing the tendons and leaving the muscle to dry in a desiccator until constant weight was obtained. The arrangement of the fibres in soleus muscle is pennate thus muscle length was measured as in figure 3.8. The muscles were normalized for size, by taking account of fibre length and dry muscle weight. The force normalized for muscle size is expressed as force/(weight/length) i.e. Nm/g.

3.3.5. Sarcomere Length Measurement

A sarcomere has regions of different refractive index (McCarter, 1981) with a periodicity along the fibres. Light wavelengths similar to this periodicity will be diffracted. The diffracted light is collected on a screen behind the muscle (described as a Fresnel diffraction pattern). The pattern seen, is a series of lines on either side of the

zero-order line. The distance between the zeroth-order line and the first order line (D) was measured as shown in figure 3.9. This is determined by the sarcomere length and wavelength of light (λ) related by the equation:-

$$S.L = \lambda / \sin (\tan^{-1} D/L)$$

Where L is the distance between the muscle and the screen, the wavelength was 0.6328 μm. D was measure in several places along the muscle fibre bundle for a mean value of sarcomere length. L was calculated by measuring the distance of the screen from the fibre bundle.

The spindle shaped soleus muscle is thick and dense, this makes the whole muscle unsuitable for laser diffraction. At the end of the experiment the muscle was pinned out in a petri dish at the optimum muscle length and placed in 2% gluteraldehyde in Ringer and left overnight. In order to obtain a clear diffraction pattern small bundles of fibres were teased from the fixed muscle, using iodide stain which enhances contrast between the fibres and connective tissue and 50% glycerol which softens the fibres. The bundles contained about 3-10 fibres. Fibre length was measured at this point, followed by sarcomere length measurement by laser diffraction, using a beam of Helium-Neon laser light about 1mm wide

3.3.6. Quick Releases

The stiffness of the whole mouse soleus muscle was measured by imposing quick length releases (amplitudes of -20 to -420 μm) (approximately 0.25 to 5.38% of the fibre length) on the muscle whilst it was being maximally tetanically stimulated. The point of the experiment was to work on whole muscle, thus the experiments were conducted on whole muscle as opposed to fibre bundles. However, because the experiments are conducted on a lot of fibres, the results obtained are an average result for the whole assembly. Soleus muscle is composed of different fibre types (60% slow and 40% fast fibres, Brooks & Faulkner, 1991). Thus it is likely that the fibres might have slightly different lengths or intrinsic properties. This is an inevitable limitation of the

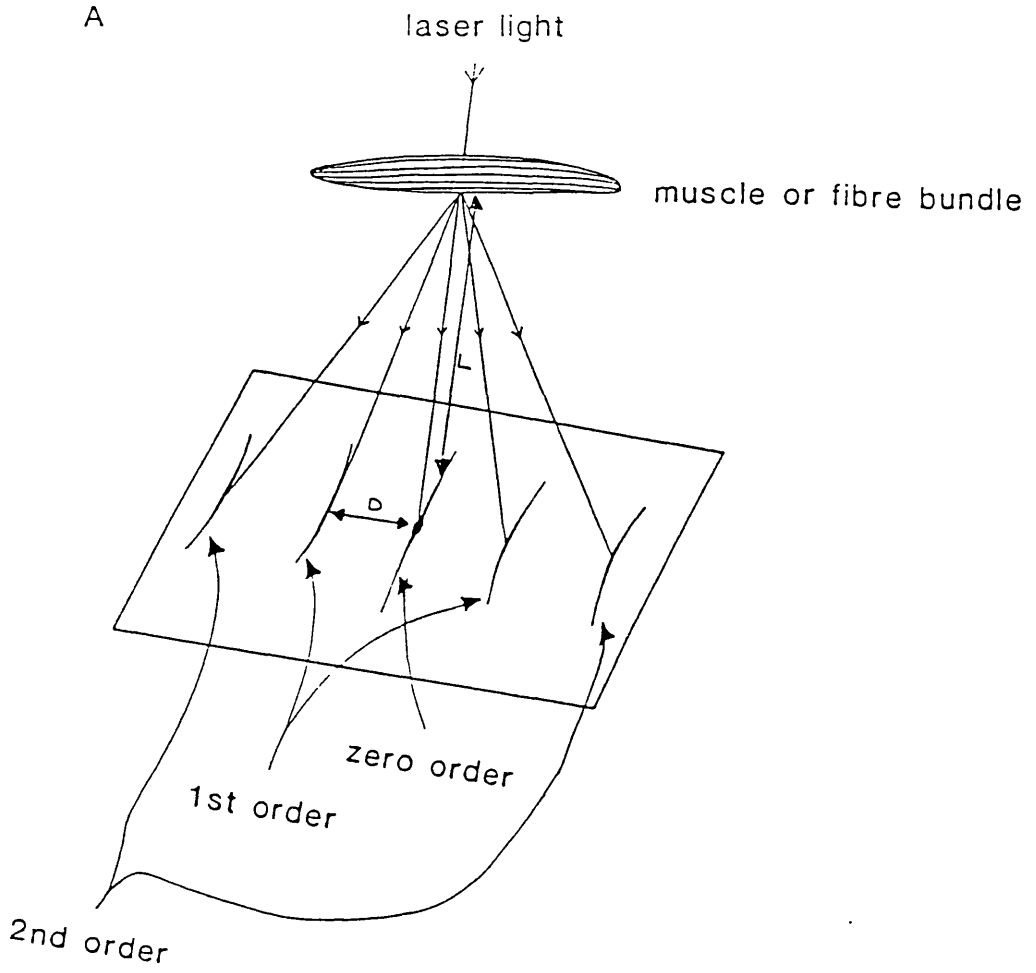

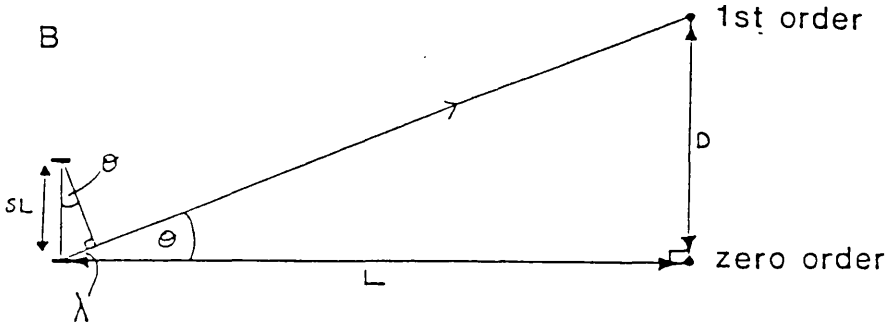

$\tan \theta = D/L$ $\quad \theta = \tan^{-1} D/L$ $\quad \sin \theta = \lambda/SL$

$SL = \lambda/\sin \theta$ $\quad SL = \lambda/\sin (\tan^{-1} D/L)$

Figure 3.9. Sarcomere length (SL) measurements by the laser diffraction technique (A) and a diagram of the diffraction of laser light by sarcomeres and how the SL is derived by trigonometry (B).
From Phillips, (1980).

experiments.

The length changes were imposed by the Cambridge motor which was controlled by a function generator. The length step time from 10 to 90% was 1.4ms (see figure 3.10). Unstimulated controls were done in order to ensure that the movement of the muscle itself did not cause any artifacts. A faster length step was not used because access to equipment that would measure a large force and produce the movement fast enough was not available.

In order to read T_1 a fast time base on the Nicolet is required (50 μs/point). The length step change also has to be fast, to determine crossbridge stiffness, and in addition the force transducer response needs to be equally fast. By looking at the enlarged force and length trace of a quick release (see figure 3.11b), it can be seen that the lowest point on the force trace corresponds to the lowest initial point on the length trace, indicating that the force transducer used in the current experiments was fast enough to record force changes induced by a 1.4ms step change.

3.3.7. Brenner Experiments

The muscle was subjected to a quick release, followed by an interval and then a quick stretch, which results in the breaking of the crossbridges (Brenner, 1984). The muscle was stimulated throughout this time (stimulation lasted for 850ms). Unstimulated controls were performed in order to see if the movement of the muscle itself caused any artifacts. Pre stretch the crossbridges S1 heads are rotating to re-stretch the compliant S2 portion, that has become slack as a consequence of the quick release. Some crossbridges are also detaching or detached. Post stretch the crossbridges are detached and are reforming. The stretch and the release were made in 1ms.

3.3.8. Vmax Measurements

The most direct way of measuring Vmax is the slack release method (Edman, 1979). A contracting muscle is rapidly shortened by a known distance (at a velocity greater than Vmax) so that the fibres become slack and will then shorten with no external load. By varying the distance of release the time for the fibre to take up the slack and begin pulling on the force transducer gives a measure of the velocity of unloaded shortening.

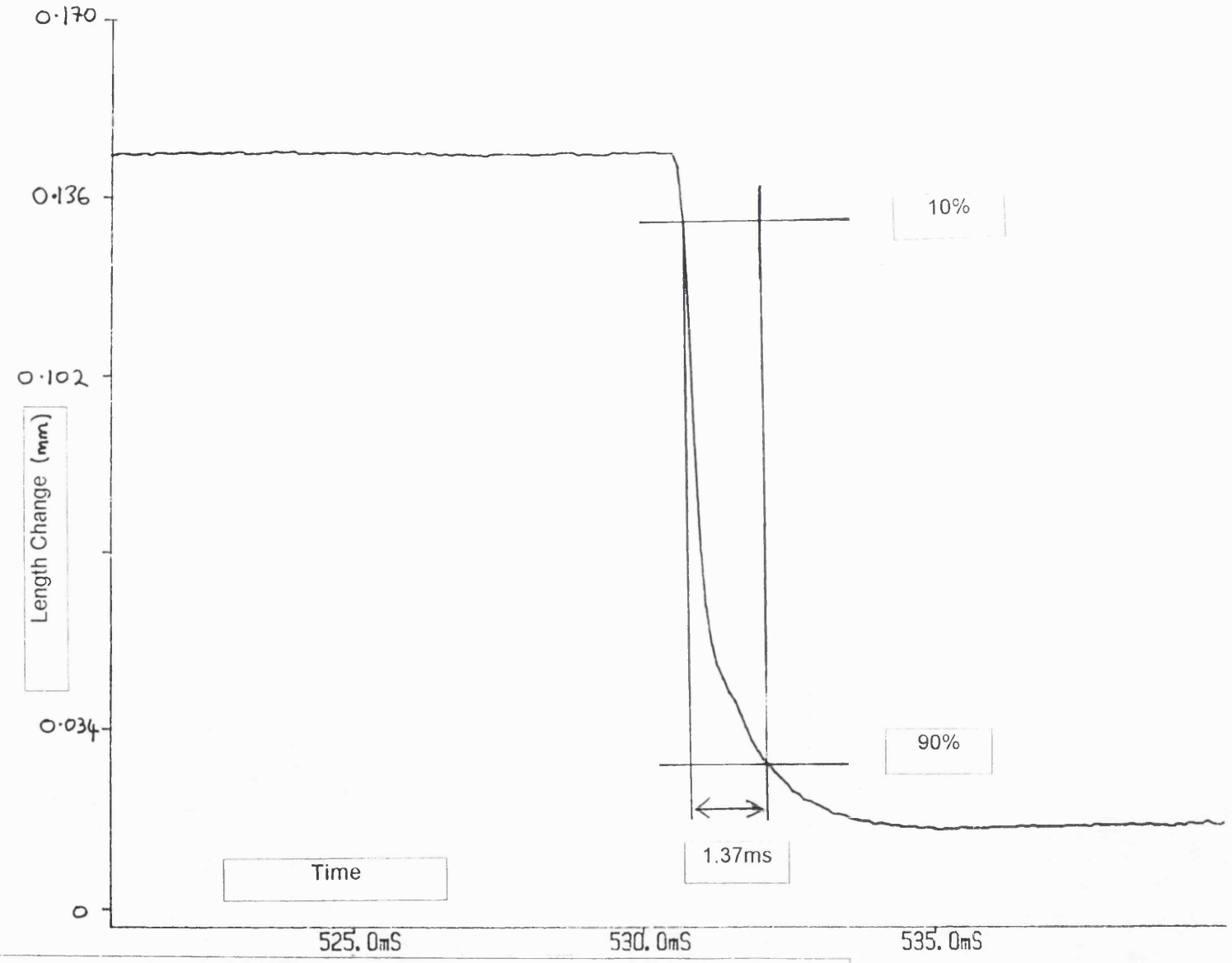

Figure 3.10. The length step time was measured from 10 to 90% of the length change.

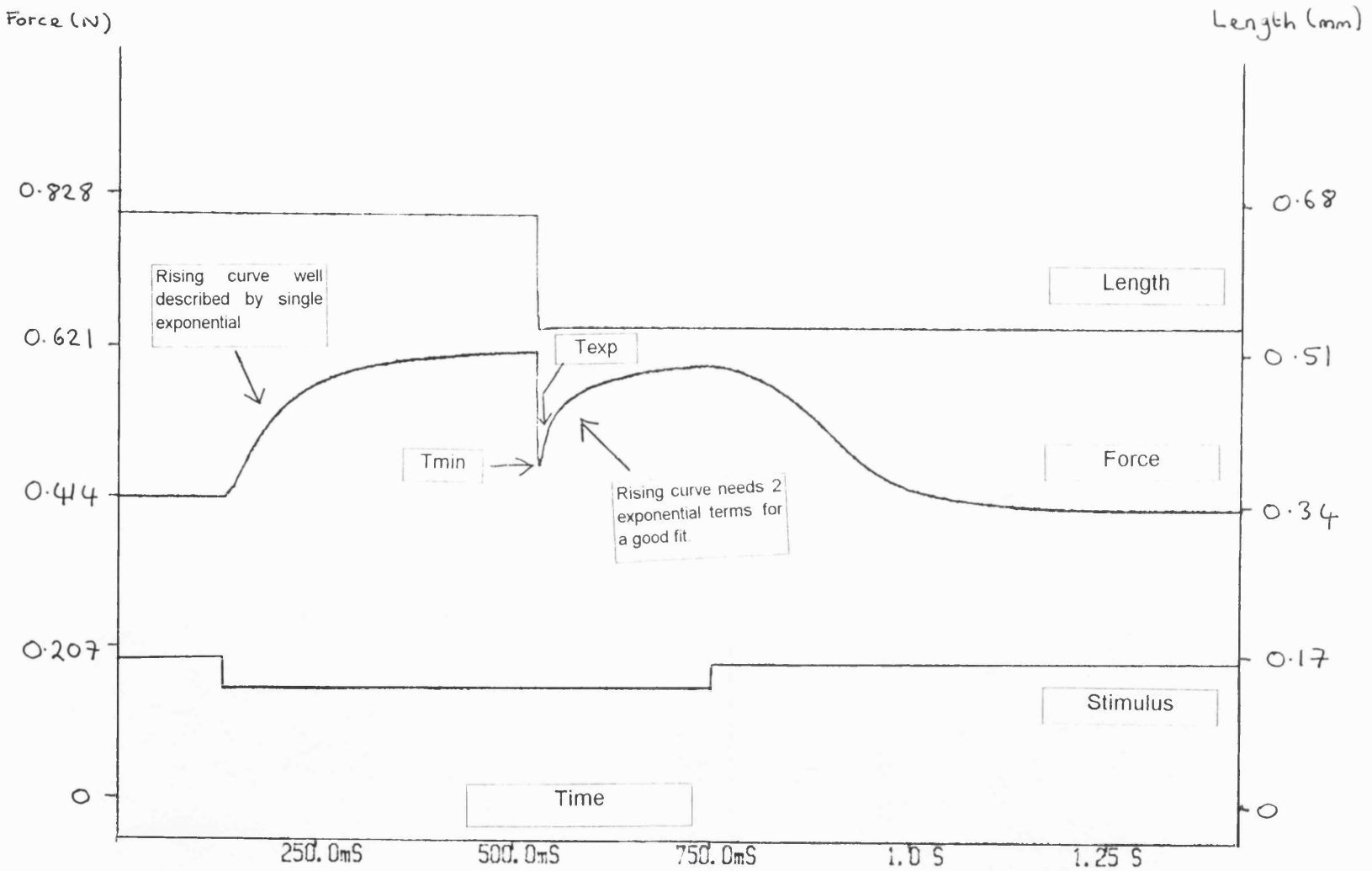

Figure 3.11a. A typical length and force record from a quick release experiment. See page 149 for definitions of Tmin and Texp.
Length step = 1.4ms. Stimulus duration = 600ms.

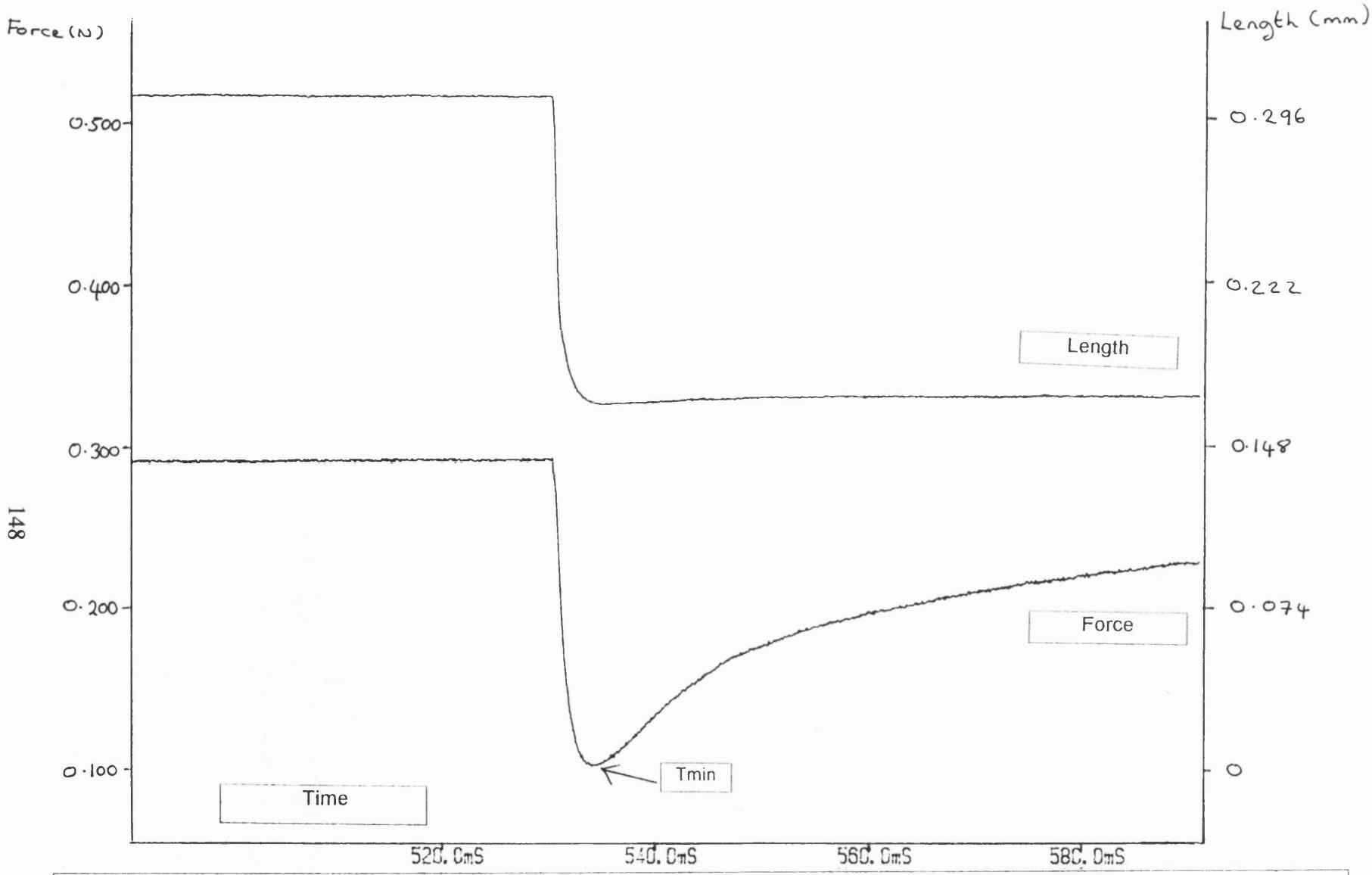

Figure 3.11b. A typical length and force record from a quick release experiment. The traces in Figure 3.11a are shown in an enlarged form. See page 149 for definition of Tmin.
Length step = 1.4ms. Stimulus duration = 600ms.

This time was determined as the point of divergence between superimposed traces of an unstimulated force trace with that of a stimulated force trace.

Large amplitude releases were imposed on the muscle in the range of 400 to 1080 μm (approximately 5 to 14% of the fibre length). The number of half sarcomeres in the muscle fibre was calculated by dividing the measured fibre length by the measured half sarcomere length. The slope of the graph of distance released against the time to redevelop tension gives Vmax.

3.4. Results

1) Figure 3.11a, shows a typical record of a quick length release performed on mouse soleus muscle. A tension minimum (Tmin) is obtained following the release followed by a recovery.

2) The Nicolet force traces from the quick release experiments were transferred into the spreadsheet Excel, to enable rising exponentials to be fitted to the initial tension rise and the tension recovery parts of the force trace. Figure 3.12 and figure 3.13 show typical records. The time and the force values for the first point of the selected area of the initial tension rise and the tension recovery were subtracted from all points of the selected area, to reset this point in each part of the trace to zero (see figure 3.14). It was found that two rising exponentials ($P(Q(1-e^{-t/tor1}) + (1-Q)(1-e^{-t/tor2}))$) could be fitted to the tension recovery after the quick release, indicating this consists of both a fast and a slow phase. However only one exponential ($P(1-e^{-t/tor})$) is needed to fit to the initial tension rise, indicating it is only composed of one component (see figure 3.11a). The observed points and the exponential predicted points superimpose, for both the initial rise and the tension recovery, thus the fit is good (see figures 3.12 and 3.13). A summary of these results is shown in tables 3.1 and 3.2.

3) The fitted value of the amplitude of the fast component of (PQ) from the tension recovery was added to the Tmin value, to obtain "T_2", which was termed Texp. Quotation marks have been placed around the name T_2 because, it is not certain if the Texp value obtained in the current results is a T_2. Table 3.3, shows the Tmin and Texp values from one experiment on mouse soleus muscle. Figure 3.15, shows Tmin and

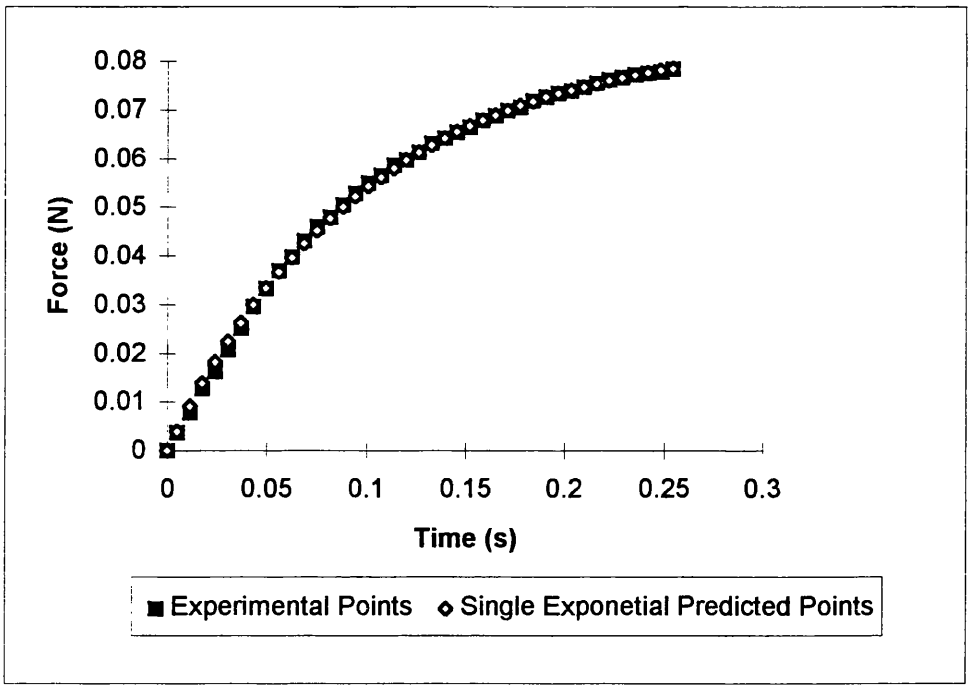

Figure 3.12. Initial force rise of mouse soleus muscle, a typical record. A single rising exponential has been fitted.

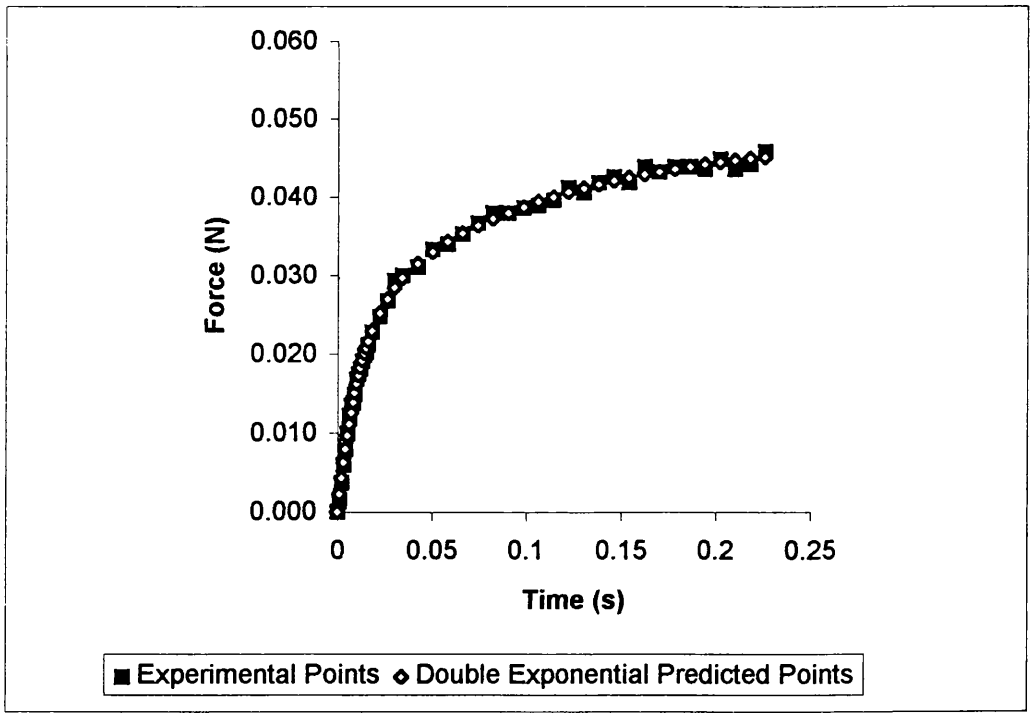

Figure 3.13. Tension recovery of mouse soleus muscle after a quick release (1.0ms step), a typical record. A double rising exponential has been fitted.

PQ = 0.023N
Tmin = 0.074N
Texp = 0.097N
See page 149 for definition of terms.

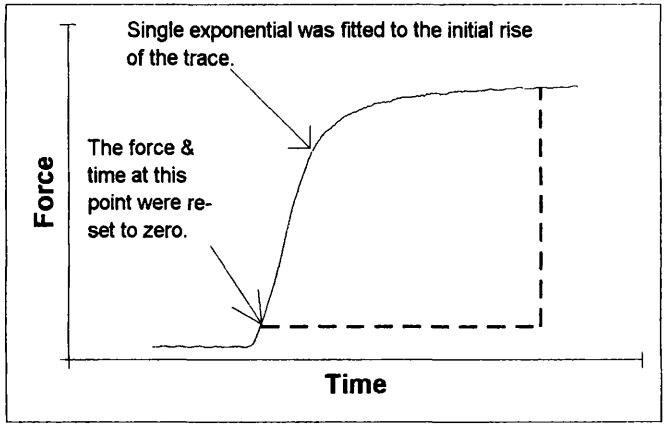

Figure 3.14. Shows to which part of the initial tension rise of a force record, the single exponential was fitted. The force at 6% rise and corresponding time, were re-set to zero.

Species	Mouse (whole muscle)	Frog (single fibre) *R.Temporaria*
Muscle	Soleus	Tibialis Anterior (lateral head)
Type	Slow twitch (predominantly)	Fast twitch
Temperature	25°C	1°C
	Traces obtained from current experiments.	Traces obtained from M.Linari.

Record	Time constant (ms)	Record	Time constant (ms)
1	93	1	57
2	85	2	73
3	84	3	58
4	99	4	59
Mean	90	Mean	62
sd	7	sd	7
sem	2.5	sem	2.6
n	4	n	4

Rate of rise (s^{-1}) = 11.10

Rate of rise (s^{-1}) = 16.19

Ratio of rate of rise of mouse to frog = 0.69

Table 3.1. A Single rising exponential was fitted to the initial tension rise of mouse and frog muscle records, to obtain the time constants for the initial tension rise. The records in each case are from 4 different muscles, each from a different mouse.

Muscle 1				Muscle 2				Muscle 3			
Distance Released (nm/hs)	Fast Time Constant (ms)	Slow Time Constant (ms)	Q	Distance Released (nm/hs)	Fast Time Constant (ms)	Slow Time Constant (ms)	Q	Distance Released (nm/hs)	Fast Time Constant (ms)	Slow Time Constant (ms)	Q
-3.85	10.7	218	0.57	-3.14	12	105	0.478	-3.01	13	97	0.506
-5.66	8	76	0.475	-5.96	14	98	0.511	-5.35	11	103	0.496
-8.61	13	96	0.505	-8.01	11	201	0.505	-8.92	13	107	0.547
-11.55	11	102	0.511	-11.32	9	108	0.498	-11.05	15	101	0.493
-13.82	12	107	0.517	-13.06	13	103	0.513	-13.28	11	93	0.504
-16.5	14	83	0.492	-16.23	11	106	0.504	-16.07	12	200	0.516
-20.85	14	115	0.544	-20.67	13	96	0.491	-20.8	9	105	0.498
-23.11	10.7	107	0.499	-23.35	11	113	0.523	-23.67	12	103	0.518
-25.83	13	107	0.544	-25.98	15	102	0.543	-25.39	13	101	0.507
-29.01	9.5	103	0.514	-29.54	13	101	0.495	-29.7	14	111	0.519
-33	13	99	0.509	-33.72	14	104	0.503	-33.53	10	105	0.507
-35.99	13	105	0.51	-35	11	106	0.513	-35.11	13	103	0.523
Mean	11.83	110	0.516	Mean	12.25	111.9	0.506	Mean	12.17	110.8	0.511
sd	1.87	36	0.026	sd	1.71	28.4	0.017	sd	1.70	28.5	0.015
sem	0.54	10	0.007	sem	0.49	8.2	0.005	sem	0.49	8.2	0.004
n	12	12	12	n	12	12	12	n	12	12	12
Student's paired t-test (fast - slow time constant)				Student's paired t-test (fast - slow time constant)				Student's paired t-test (fast - slow time constant)			
t	DF	P		t	DF	P		t	DF	P	
-9.4	11	0.001		-11.9	11	0.001		-12.0	11	0.001	

Mean data for the three muscles			
Muscle Number	Fast Time Constant (ms)	Slow Time Constant (ms)	Q
1	11.83	109.833	0.516
2	12.25	111.917	0.506
3	12.17	110.750	0.511
mean	12.08	110.833	0.51
sd	0.23	1.044	0.00
sem	0.13	0.603	0.0027
n	3	3	3

Table 3.2. Double rising exponentials were fitted to the tension recovery records after a quick release (step time = 1.4ms) (see figure 3.13). The equation for the double rising exponential is: $P(Q(1-e^{-t/tor1}) + (1-Q)(1-e^{-t/tor2}))$. The value Q, represents how big the fast component is as a proportion of the total. The table shows the distance released and the corresponding time constants and Q values obtained, for three different muscles (each from a different mouse).

A Student's paired t-test shows that the fast and slow components are significantly different at the 0.001 level of significance.
hs = half sarcomere DF = degrees of freedom

Distance Released nm/hs	T0 mN	Tmin mN	Fast component value mN	Texp mN	Tmin/T0	Texp/T0
0.00	102.7	102.7	0.0	102.7	1.00	1.00
-3.85	107.9	91.2	10.9	102.1	0.84	0.95
-5.67	105.8	78.3	11.3	89.6	0.74	0.85
-8.61	102.5	69.8	15.2	85.0	0.68	0.83
-11.56	102.7	61.8	20.3	82.1	0.60	0.80
-13.83	104.1	53.0	22.7	75.8	0.51	0.73
-16.55	103.3	46.4	23.5	69.9	0.45	0.68
-20.85	103.6	34.3	29.9	64.2	0.33	0.62
-23.12	104.7	30.8	29.5	60.3	0.29	0.58
-25.84	102.7	24.2	33.0	57.1	0.24	0.56
-29.01	102.7	12.3	33.9	46.2	0.12	0.45
-33.00	102.7	-0.3	37.0	36.7	0.00	0.36
-35.99	102.7	-11.7	38.0	26.3	-0.11	0.26

Table 3.3. Tmin and Texp values from one quick length change experiment on mouse soleus muscle. See page 149 for definitions of the terms on the table.

hs = half sarcomere

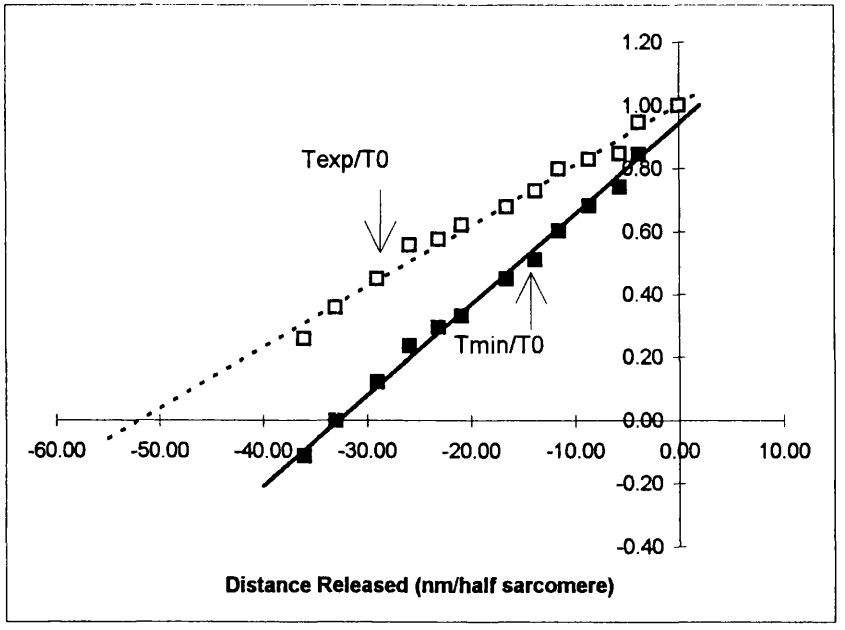

Figure 3.15. Data from one quick length change experiment on mouse soleus muscle (muscle number 1 on table 3.4). Tmin and Texp are plotted as a function of the length change. Both Tmin and Texp are expressed as a fraction of T0, the isometric force immediately before the step length change. Negative values of distance moved indicate release and positive values a stretch. See page 149 for definition of Tmin and Texp. The solid line is the regression line for Tmin, the dotted line is the regression line for Texp.

Texp, both expressed as a fraction of T_0, plotted as a function of the distance released, for one experiment. A summary of these results from all the experiments are shown in table 3.4.

4) The fast time constant of the tension recovery after a quick release, was found not to vary with the distance released. Figure 3.16, shows the average time constant ($\pm$ sem) from three muscles plotted, as a function of distance released.

5) The x-intercept of the Tmin curve from the quick release experiments (see figure 3.15) was found not to change over release speeds of 0.5 to 2ms (see figure 3.17a). The x-intercepts for the step release speeds of 0.5 to 2.0ms were obtained by the following method. The distance released in 0.5ms, was read from the length trace on the oscilloscope (see figure 3.17c). The corresponding force, for a step release of 0.5ms duration, was read from the force trace (see figure 3.17c). The force obtained was termed Tmin (for 0.5ms step speed). This procedure was performed on three different quick release traces for each muscle. A graph of $Tmin/T_0$ (for 0.5ms step speed) was plotted as a function of the distance released in 0.5ms. From this graph the x-intercept for 0.5ms step time was obtained (see figure 3.17b). This procedure was repeated for the step release times of 1.0ms, 1.5ms and 2.0ms. This analysis was performed on each of the nine muscles tabulated on Table 3.4.

6) The slack method (Edman, 1979) was used to determine the maximum velocity of shortening (Vmax). The graphs of distance released plotted as a function of time to re-develop tension were linear for distances between 5.53 $\pm$ 0.6% and 13.59 $\pm$ 0.8% ($\pm$ sem, N=9) of the fibre length; this indicates that the maximum velocity of shortening is constant over this range (figure 3.18 shows a typical record). The fibres may have been able to shorten at Vmax over longer distances but this was not tested. The mean ($\pm$ sem) Vmax was found to be 7.28 ($\pm$ 0.30) muscle lengths per second. These results are summarized in Table 3.5.

7) The aponeurosis length was calculated from the muscle length minus the fibre length. This slightly under estimates the aponeurosis length, since the muscle fibres are pennate rather than parallel. However it is only a small error since the fibre angle in the guinea

Muscle No.	T_{min}/T_0 Slope hs/nm	T_{min}/T_0 X-Intercept (nm/hs)	T_{exp}/T_0 Slope hs/nm	T_{exp}/T_0 X-Intercept (nm/hs)
1	0.029	-32.7	0.0193	-51.89
2	0.039	-26.64	0.0187	-50.91
3	0.029	-34.03	0.0192	-51.98
4	0.03	-33.80	0.0189	-54.23
5	0.029	-32.79	0.02	-50.33
6	0.031	-33.00	0.0179	-54.53
7	0.033	-31.42	0.0189	-52.59
8	0.035	-29.83	0.0199	-49.65
9	0.029	-35.90	0.0187	-54.35
Mean	0.0316	-32.24	0.0191	-52.272
sd	0.0035	2.69	0.0006	1.806
sem	0.0012	0.90	0.0002	0.602
n	9	9	9	9

Table 3.4. A summary of the results from the quick length release experiments on mouse soleus muscle (1.4ms step). The slope and intercept for T_{min}/T_0 and T_{exp}/T_0 plotted as a function of distance released are given. See page 149 for definitions of Tmin and Texp.

9 muscles were used, each from a different mouse.
hs = half sarcomere

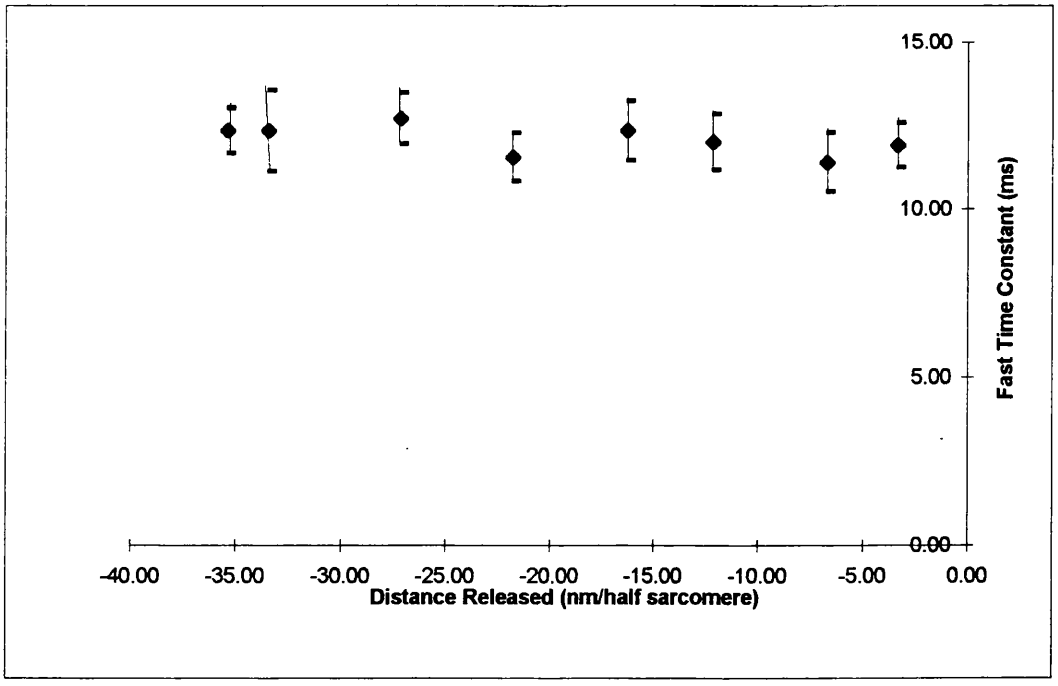

Figure 3.16. The fast time constant of the tension recovery after a quick release (1.4ms step), is plotted as a function of the distance released. The values shown are means (± sem) from the three experiments shown in table 3.2, grouped into distance released ranges of 0 to 5, 6 to 10 nm/half sarcomere, etc. The number in each group ranges from 3 to 6 (mean = 4.5).

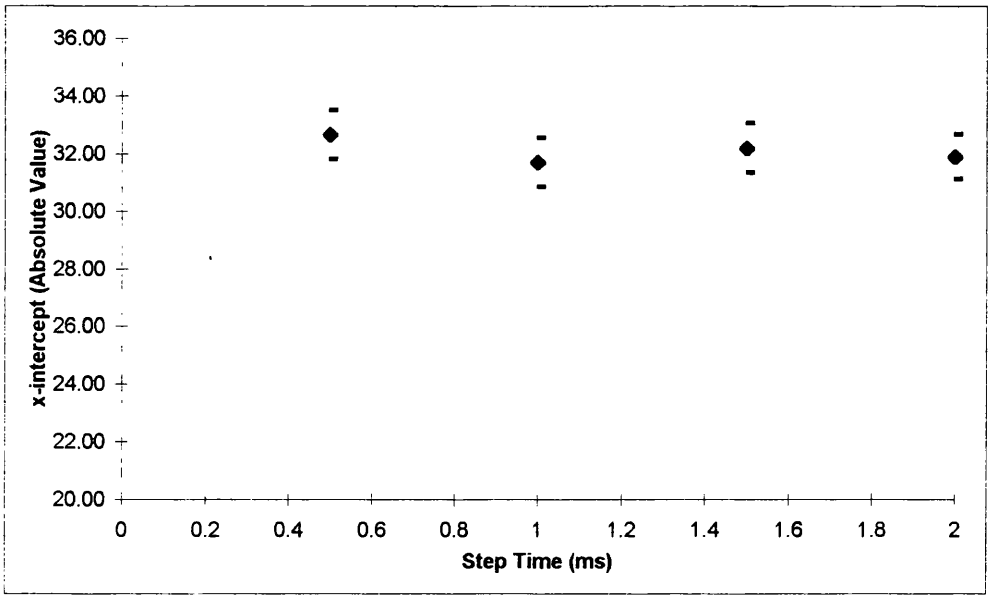

Figure 3.17a. The x-intercept (absolute value) for the $Tmin/T_0$ curve plotted as a function of distance released, is shown not to vary with step release speeds from 0.5ms to 2.0ms. The points plotted are the means (+ sem) for each step time (n=9). See page 154 for details of how the x-intercepts were obtained. The results were tabulated from nine muscles tabulated on table 3.4.

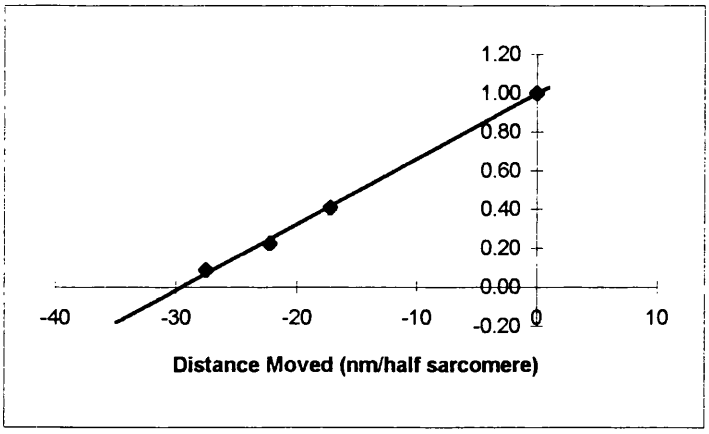

Figure 3.17b. $Tmin/T_0$ (for 2.0ms step speed) is plotted as a function of the distance released for the step time release of 2.0 ms. See page 154 for details of how the Tmin value was obtained.

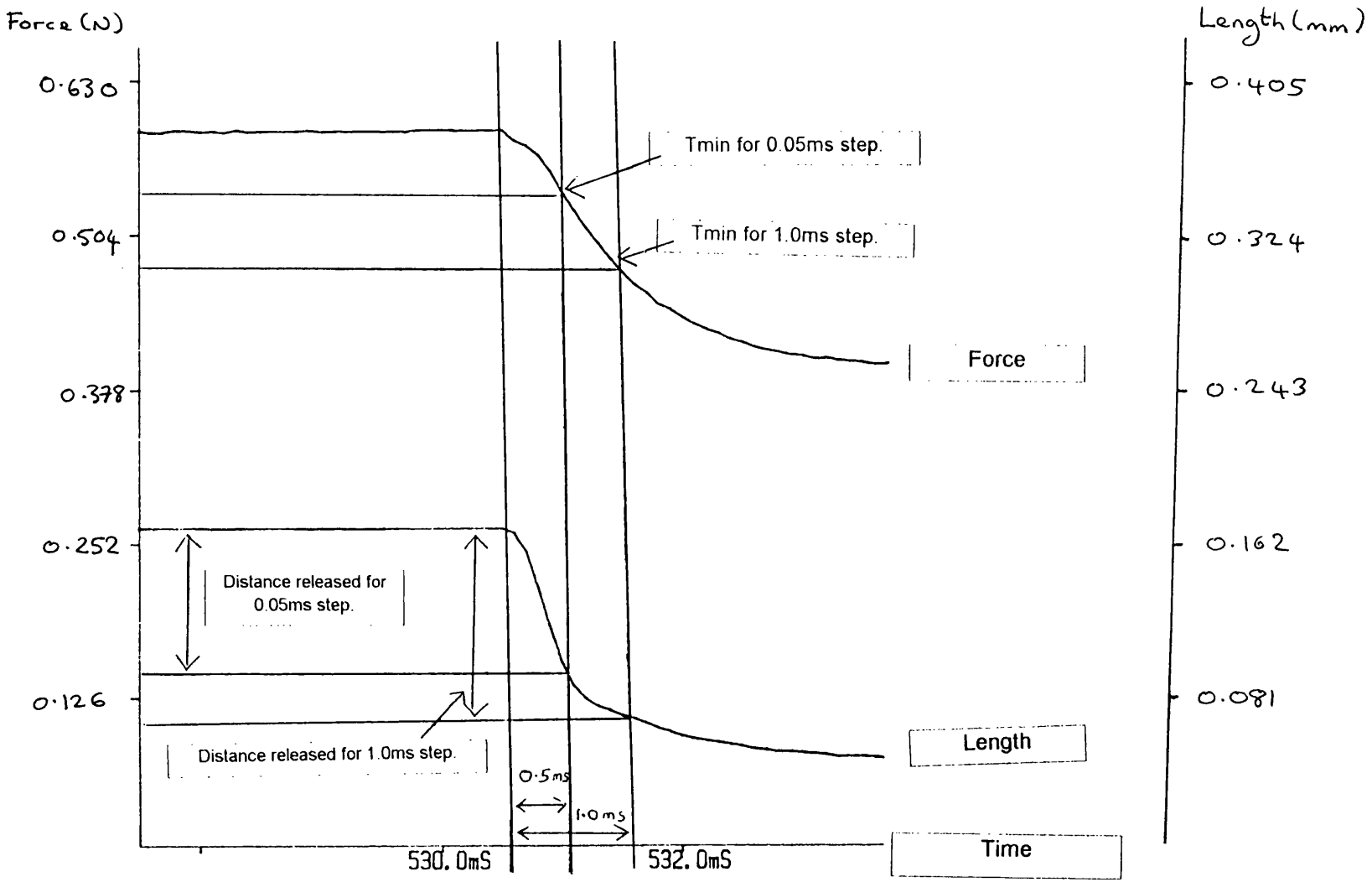

Figure 17c. An enlarged section of a length and force trace from a quick release experiment on mouse soleus muscle. Tmin for step speeds 0.5 and 1.0ms have been marked on the trace to illustrate how Tmin was determined. See page 149 for definition of Tmin.
Length step = 1.4ms.

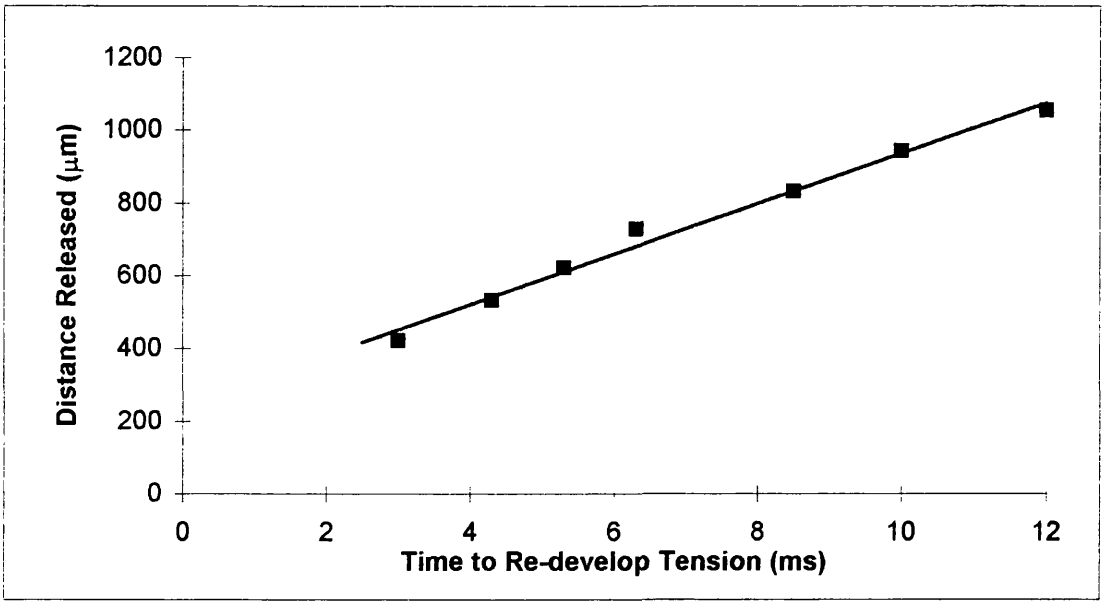

Figure 3.18. Maximum velocity of shortening (Vmax) was determined by the slack method (Edman, 1979) (see page 154 for details). Distance released is plotted as a function of the time to re-develop tension. the slope of the regression line gives Vmax. The record shown is the result from muscle number 3, in table 3.5.

Muscle No.	Slope (Vmax) (mm/s)	Slope (Vmax) (μm/s/hs)	Slope (Vmax) (lo/s)
1	95.7	13.82	8.47
2	82.4	14.24	7.23
3	69.4	11.40	6.31
4	73.1	12.07	6.54
5	74.8	15.42	8.88
6	74.7	13.18	7.41
7	68.9	13.55	7.55
8	69.9	14.20	6.47
9	72.2	12.04	6.68
Mean	75.7	13.32	7.28
sd	8.6	1.29	0.91
sem	2.9	0.43	0.30
n	9	9	9

Table 3.5. A summary of the results for maximum velocity of shortening (Vmax) of mouse soleus muscle at 25°C. Vmax is obtained from the slope of the regression line obtained in figure 3.18. Nine muscles were used, each from a different mouse.

hs= half sarcomere
lo= muscle length.

The number of half sarcomeres and muscle length for each muscle are shown in table 3.6.

pig soleus muscle has been measured to be 7° to the long axis of the muscle (Powell *et al.*, 1984). The cosine of 7° is 0.993, therefore assuming the fibre angle of mouse soleus muscle to be similar, the error in assuming the fibres to be at an angle of 0° to the long axis of the muscle is only 0.7% (see figure 3.19). The mean (± sem) aponeurosis length was found to be 3.7 mm (± 0.24) (see table 3.6).

8) Brenner experiments: The stimulated soleus muscles were subjected to a quick release, followed by an interval, then a quick stretch (Brenner, 1984). The stretch results in the crossbridges being broken. Rising double exponentials ($P(Q(1-e^{-t/tor1}) + (1-Q)(1-e^{-t/tor2}))$) were fitted to the tension recovery. After the quick stretch a fast and a slow phase is present in the recovery of tension (see figure 3.20). However in the initial tension rise only one exponential could be fitted ($P(1-e^{-t/tor})$), thus only a slow phase is seen (see figure 3.13). The shortening intervals of 2, 5, 10 ms were found to be too short to break all the crossbridges indicated by the fact the force did not drop very much after the stretch, therefore a shortening interval of 22ms was used (see figure 3.21a and b for a typical record). The results are summarized in table 3.7.

3.5. Discussion

The classic work in this field is that of Huxley and co-workers on single frog muscle fibres (Tibialis anterior, lateral head) (Ford et al., 1977). They showed if a step release is made very quickly (completed within 1 ms) a drop in force occurs (the lowest force point is termed T_1) followed by a rapid recovery (the force at the end of this rapid recovery is termed T_2) (see figure 3.1). It needs to be determined whether the current results from the quick release experiments performed on soleus muscle represent a T_1 or T_2 curve or an intermediate. In the interpretation of the present experiments it is presumed that mouse soleus muscle crossbridges will behave similarly to frog muscle crossbridges, but not necessarily at the same speed. What is not clear at the moment is whether the force measured at the lowest point (Tmin) is the force at the T_1 point or the T_2 point (see figure 3.11a). If the T_1-T_2 transition in mouse muscle is very quick, then the lowest force point will be T_2. If however the transition is slower than in frog muscle then the lowest point will be T_1.

Frog muscle fibres have been investigated under conditions where tendon compliance

Muscle No.	Muscle Length (ML) (mm)	Fibre Length (FL) (mm)	FL / ML	Aponeurosis Length (mm)	Number of half sarcomeres	Weight (Dry) (mg)	Weight / FL (mg/mm)	Isometric Force (N)	Isometric Force (Nm/g)	Sarcomere Length (μm)
1	11.3	7.1	0.63	4.20	6927	1.67	0.24	0.191	0.81	2.05
2	11.4	6.8	0.60	4.60	5787	1.65	0.24	0.189	0.78	2.35
3	11.0	7.3	0.66	3.70	6083	1.41	0.19	0.186	0.96	2.4
4	11.2	7.3	0.65	3.87	6058	1.44	0.20	0.177	0.90	2.41
5	8.4	5.8	0.69	2.63	4854	1.32	0.23	0.19	0.83	2.39
6	10.1	6.8	0.67	3.28	5667	1.46	0.21	0.191	0.89	2.4
7	9.1	6.2	0.68	2.92	5082	1.3	0.21	0.185	0.88	2.44
8	10.8	6.1	0.56	4.70	4919	1.21	0.20	0.16	0.81	2.48
9	10.8	7.4	0.69	3.40	5992	1.48	0.20	0.189	0.95	2.47
Mean	10.5	6.8	0.65	3.70	5708	1.44	0.21	0.1842	0.87	2.38
sd	1.0	0.6	0.04	0.72	669	0.15	0.02	0.0101	0.06	0.13
sem	0.3	0.2	0.01	0.24	223	0.05	0.01	0.0034	0.02	0.04
n	9	9	9	9	9	9	9	9	9	9

Table 3.6. Characteristics of mouse soleus muscle measured in the current experiments. The aponeurosis was calculated from the method shown in figure 3.19. The wet to dry muscle ratio was found to be 4:1.

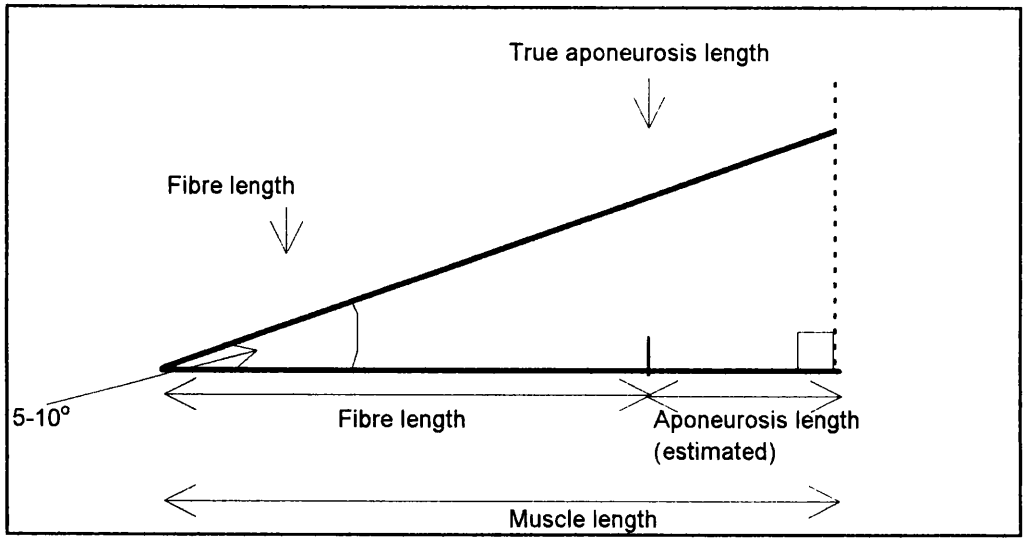

Figure 3.19. The aponeurosis length is slightly under estimated, in calculating it as the muscle length minus the fibre length. The fibre angle has been measured to be 7° to the long axis of the muscle (Powell *et al*., 1984). The cosine of 7° is 0.993, therefore the error in assuming the fibres to be at an angle of 0° is only 0.7%.

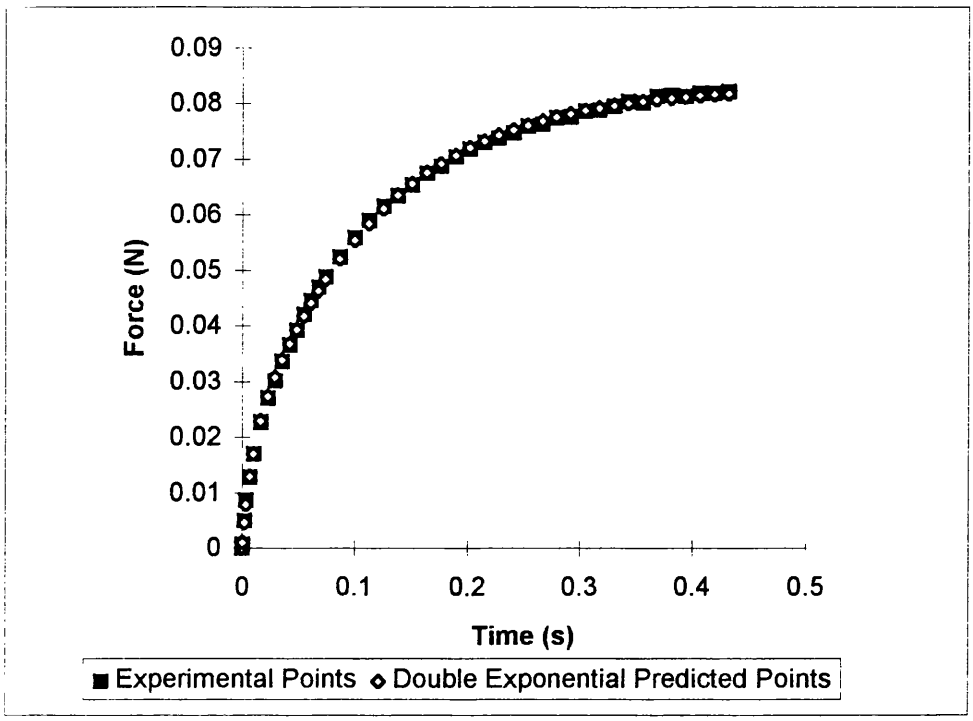

Figure 3.20. Tension recovery of mouse soleus muscle after a quick release followed by an interval and then a quick stretch. A double rising exponential has been fitted.

PQ = 0.067N
Tmin = 0N

See page 149 for definition of terms.

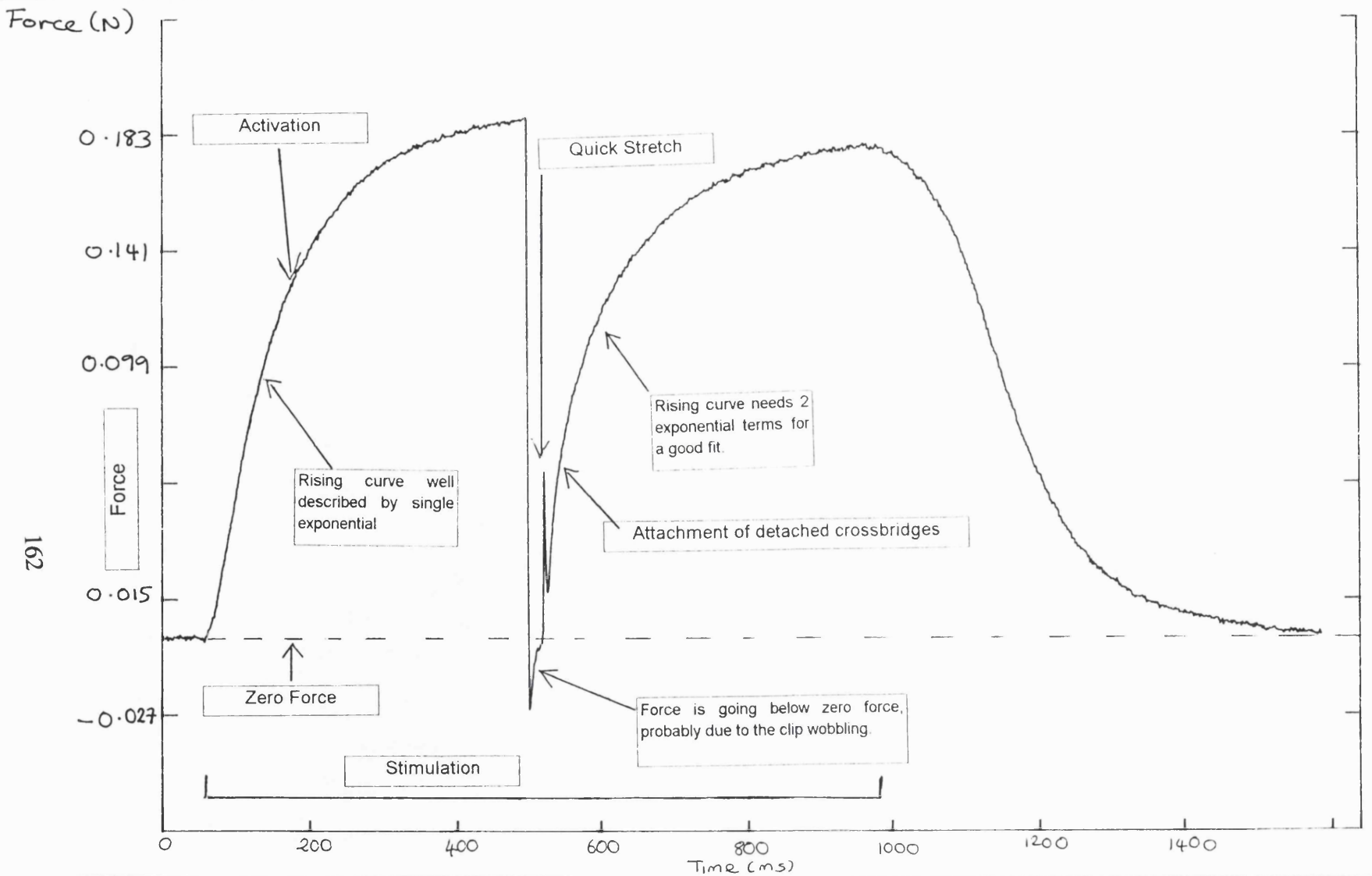

Figure 21a. Force trace from the Brenner experiment on mouse soleus muscle. The muscle whilst being stimulated was subjected to a quick release, followed by an interval and then a quick stretch.
Length step = 1.0ms. Stimulus duration 850ms. Pulse interval duration = 22ms. Amplitude of release and stretch = 0.75mm.

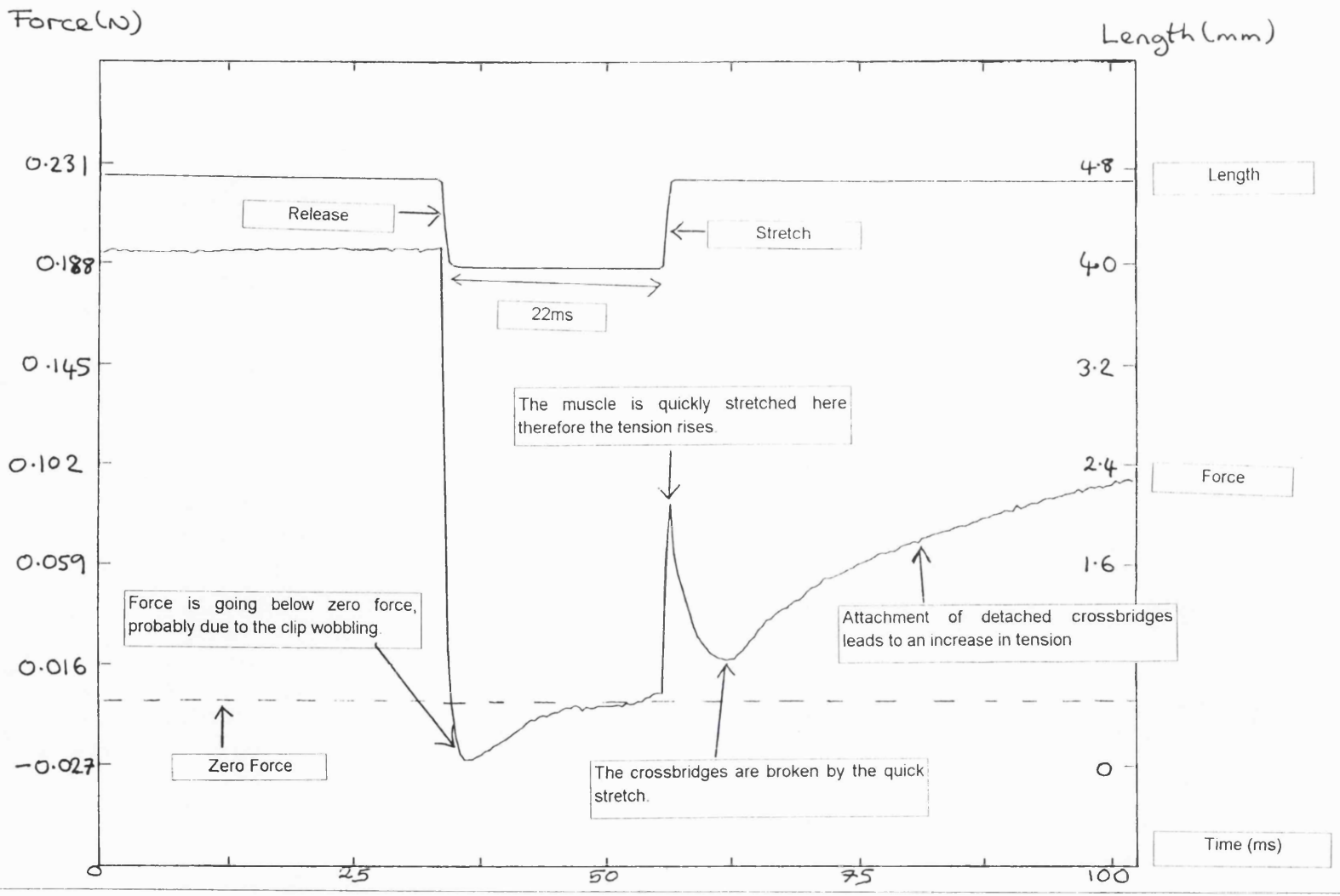

Figure 21b. Enlarged section of length and force trace from the Brenner experiment on mouse soleus muscle. The muscle whilst being stimulated was subjected to a quick release, followed by an interval and then a quick stretch.
Length step = 1.0ms. Stimulus duration 850ms. Pulse interval duration = 22ms. Amplitude of release and stretch = 0.75mm.

Muscle No.	Initial Tension Rise Time Constant (ms)	After Stretch Fast Time Constant (ms)	After Stretch Slow Time Constant (ms)	Q
1	95.7	10.9	105.25	0.5140
2	99.5	14.0	106.91	0.5090
3	95.6	8.3	112.11	0.5240
Mean	96.9	11.1	108.09	0.5157
sd	2.2	2.9	3.58	0.0076
sem	1.3	1.6	2.07	0.0044
n	3	3	3	3
Rate of rise (s^{-1}) =	10.32	90.36	9.25	

Difference:	Initial tension rise minus fast time constant after the stretch	
Muscle No.		
1	84.8	
2	85.5	
3	87.3	
Mean of the difference	85.87	
Sd of the difference	1.29	
Sem of the difference	0.74	
n	3	
Student's paired t-test		
t = Mean of difference / Sem of difference	DF	P
115.32	2	0.001

Table 3.7. The table shows results from three different muscles. Double rising exponentials were fitted to the tension recovery records after a quick stretch (see figure 3.20). The equation for the double rising exponential is: $P(Q(1-e^{-t/tor1}) + (1-Q)(1-e^{-t/tor2}))$. The value Q, represents how big the fast component is as a proportion of the total.

A single rising exponential was fitted to the initial tension rise.

3 muscles were used, each from a different mouse.

A Student's paired t-test shows that the slow and fast components from the initial tension rise and tension recovery, respectively are significantly different at the 0.001 level of significance.

is known to be negligible: that is using single fibres and placing metal clips over the ends so that tendon compliance is eliminated. In whole soleus muscle, used in the current experiments, aponeurosis exists and has significant compliance compared to the crossbridges. Thus the compliance of the muscle can be divided into:

1) The behaviour of the crossbridges

2) The behaviour of the tendons within the muscle.

If a length change is put in, it either goes into the sliding of the filaments or into the elastic structures. The tension in both of them is the same. The current experiments are trying to measure the internal compliance of both the muscle fibres and of the aponeurosis, this cannot be achieved until the timing of the T_1 to T_2 transition is known.

Looking at the quick release traces from the current experiments it appears as if a T_1-T_2 transition can be observed. It can be seen that after the end of a release, the force appears to rise to a plateau rapidly, then hesitate and then go on rising more slowly. This is what one would expect if it were a T_1-T_2 transition, since if T_2 has not been reached at the end of the step then a transition to it will be seen (see figure 3.11a).

The "T_2" values in the current experiments were obtained by fitting double exponentials to the recovery tension after the release. Double exponentials were fitted because they were found to describe the results well. Thus indicating that maybe there are two components present in the recovery tension trace; a fast component and a slow component.

Assuming that mouse crossbridges have a T_1-T_2 transition, and stiffness roughly similar to that of frog muscle crossbridges. Then three hypothesises can be considered for explaining the results (see figure 3.22):

3.5.1. Hypothesis A: T_1-T_2 is faster in mouse muscle than frog muscle.

If the T_1-T_2 transition is fast then it might have finished even before the fastest release (0.5ms) has been completed. In which case it is likely that the current Tmin curve is a T_2 curve (see figure 3.22).

The shape of the Tmin curve (approximately a straight line), obtained in the present

experiments needs to be explained (see figure 3.22). The T_2 curve obtained by Huxley and co-workers has a peculiar shape; it has a flat plateau and then falls steeply with increasing release size and is due to the rotation of the S1 heads. Whereas it is likely the Tmin curve from the current experiments, is due to the rotation of the S1 heads plus the aponeurosis compliance. So it is possible that the Huxley and Simmons behaviour is masked by the aponeurosis compliance that exists in the present results. It is likely that the aponeurosis has an exponential compliance, as tendon is known to have (see section 4.2.3.). That is the more it is stretched the stiffer it becomes, so a rising exponential curve is obtained (see figure 3.23). If the compliance caused by the aponeurosis curve and the curve caused by the rotation of the crossbridge heads (Huxley and Simmons T_2 curve) are added together they might give approximately a straight line. Resulting from the fact that one is curving up and the other is curving down as they approach isometric tension. So that the plateau that would be expected from a T_2 curve could be masked by the increasing stiffness of the tendon.

To further explore this point, the distance axis values of the Huxley and Simmons T_2 curve were subtracted from the current Tmin distance axis values (see figure 3.24). The shape obtained should be the shape of the aponeurosis compliance (the top of the subtracted trace has a strange shape and should be ignored, since the distances in this region are very small, and so are not reliable. In the current Tmin curve a linear decline to -32 nm/hs intercept is seen. The resultant subtracted trace has an intercept on the x-axis of around -19 nm/hs. Which is a length decrease of 2.9% of the aponeurosis length (see table 3.8). A length release of 2.9% in the aponeurosis drops the force to zero, from isometric force. Therefore a stretch of 2.9% raises the force to isometric force. In the tendon experiments, the isometric force (0.36N) stretches the tendon by 3% (see figure 4.16). The muscle experiments were performed on soleus muscle and the tendon experiments on EDL tendon, therefore in comparing these results it is assumed EDL and soleus tendon have the same stiffness. It seems likely they would have the same stiffness, since the isometric force of EDL muscle and soleus muscle are known to be similar (Brooks & Faulkner, 1991). Thus it seems 59% (-19nm/hs) of the x-intercept is due to aponeurosis compliance.

The total tendon length in series with mouse soleus muscle is about 9mm. Therefore the

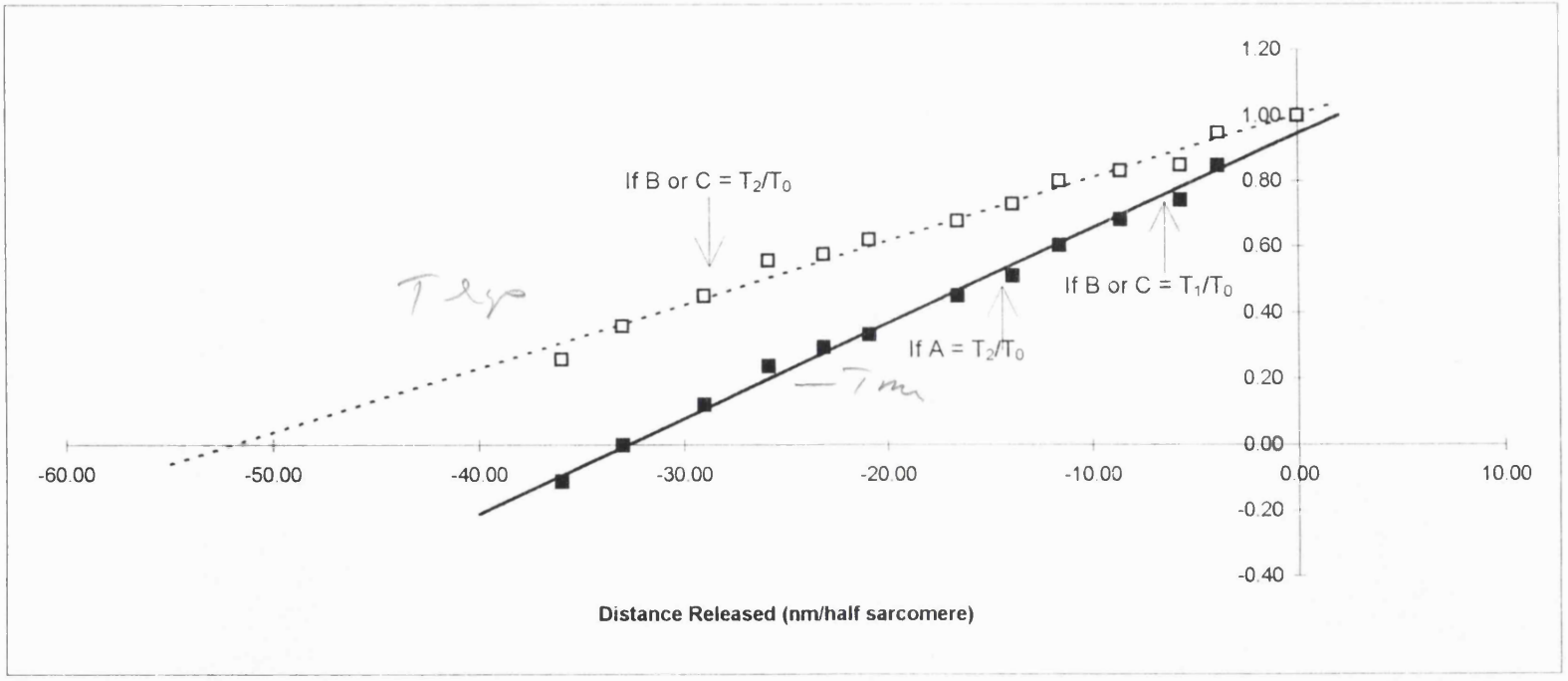

Figure 3.22. Data from one quick length change experiment on mouse soleus muscle, at 25°C. Tmin (■) and Texp (□) are plotted as a function of the length change. Both Tmin and Texp are expressed as a fraction of T_0, the isometric force immediately before the step length change. Negative values of distance moved indicate a release. See page 149 for definition of Tmin and Texp. The solid line is the regression line for Tmin, the dotted line is the regression line for Texp.

Three hypotheses can be considered to account for the identity of Tmin and Texp:
Hypothesis A: T_1-T_2 is faster in mouse soleus muscle than in frog muscle. The bottom curve (filled squares) is a T_2/T_0 curve.
Hypothesis B: T_1-T_2 is slower in mouse muscle than in frog muscle. The bottom curve is equal to T_1/T_0 and the top curve (open squares) is equal to T_2/T_0.
Hypothesis C: T_1-T_2 is the same speed in mouse and frog muscle. Bottom curve is equal to T_1/T_0 and the top curve is equal to T_2/T_0.

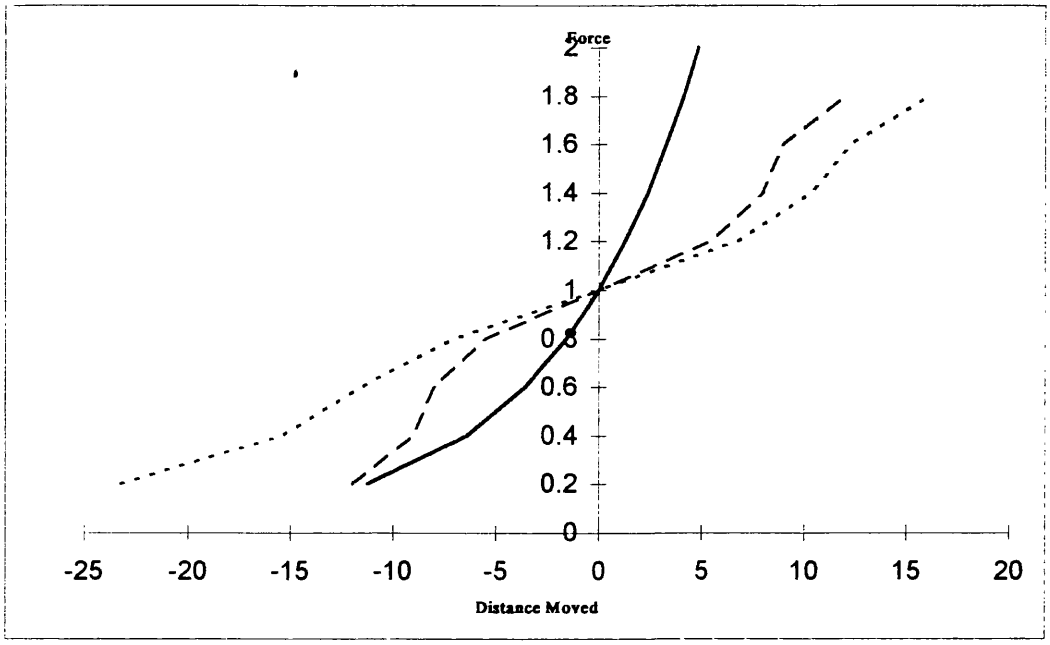

Figure 3.23. The effect of adding together two elastic components in the distance axis. The components are added together in this direction because they are in series. The solid line represents the rising exponential component, the series elasticity. The dashed line represents the T_2/T_0 curve, which is assumed to be symmetrical. The dotted line represents the effect of adding together in the distance axis the series elasticity and the T_2/T_0 curve.

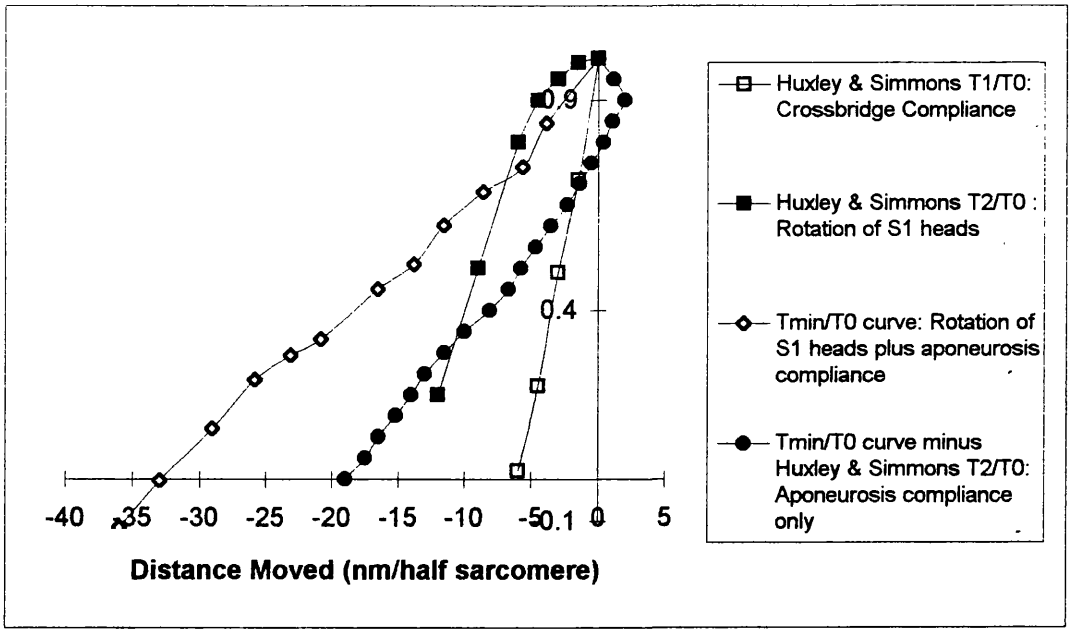

Figure 3.24. The distance axis values of the Huxley and Simmons T_2/T_0 curve (values used from figure 3.3) were subtracted from the distance axis values of the $Tmin/T_0$ curve obtained in the current experiments (values used from figure 3.15). The shape of the subtracted curve represents the shape of the aponeurosis compliance. The top of the subtracted curve should perhaps be ignored, since the distances are small in this region and so are not reliable.

total length in series; muscle fibres (6.8mm), aponeurosis (3.7mm) and tendon (9.0mm) is 19.5mm. Thus if a stress of the isometric force is applied, the muscle fibre length is changed by 0.051mm (0.8% of its length, see table 3.8), the aponeurosis length changes by 0.11mm (3.0% of its length, see table 3.8) and the tendon length changes by 0.3mm (3.0% of its length, see figure 4.16). Therefore the total length change is 0.46mm, of which 11% occurs in the muscle fibres, 24% in the aponeurosis and 65% in the tendon.

The tension recovery after the quick release appears to have two components (fast component = 12ms, slow component 111ms) (see table 3.2). The time constant for the initial rise of tension in mouse muscle is 90ms (see table 3.1), thus the fast component (approximately 12ms) is not present in the initial tension rise. It is possible that the time constant for the initial tension rise is the time course with which activation is occurring, i.e. calcium movements. To further explore this point the Brenner experiment was performed (Brenner, 1984). The muscle is stimulated, released and then stretched. The quick stretch is thought to break all the crossbridges.

The results from this experiment show that after the stretch (i.e. after the crossbridges have been broken) there is a fast phase (time constant = 11ms) and a slow phase (time constant = 108ms) in the recovery of tension. Whereas at the start of the contraction only the slow phase (time constant = 97ms) is seen (see table 3.7). Thus a fast component is present in the recovery of tension when the muscle is active. This fast component is therefore not due to T_1-T_2 transition, since there can be no T_1-T_2 transition when there are no crossbridges attached. The fast time constant obtained after the stretch in these experiments was 11ms. Which is the same as the fast time constant obtained after a quick release (12ms) (see table 3.2). Thus the Brenner experiments seem to indicate that the Texp curve is not a T_2 curve, but is the fast phase of attachment of detached crossbridges (see figure 3.22). Thus indicating that the Tmin curve is a T_2 curve.

An analysis was done to see if the x-intercept on the Tmin curve changed over the release speeds of 0.5 to 2ms (see figure 3.17a). In frog single muscle fibres it has been found that the x-intercept (absolute value) is 33% smaller with a release speed of 0.2ms compared to 1.0ms release, indicating the fibre is stiffer and therefore the crossbridges

Average Muscle Length	Average Fibre Length	Average Aponeurosis Length	Aponeurosis/Fibre	Average Sarcomere Length	Average Number of Sarcomeres	Average Number of Half Sarcomeres (hs)	Average Tmin/T0 x-intercept
(mm)	(mm)	(mm)		(μm)			(nm/hs)
(see table 3.6)	(see table 3.6)	(see table 3.6)		(see table 3.6)			(see table 3.4)
10.5	6.8	3.7	0.55	2.38	2840	5681	-32

x-intercept for aponeurosis	Length change of the aponeurosis	% Length change of the aponeurosis	x-intercept for Huxley & Simmons (1ms step)	Length change of the Muscle	% Length change of the fibre length
(nm/hs)	(mm)		(nm/hs)	(mm)	
(see figure 3.24)					
-19	-0.108	-2.9	-9	-0.0511	-0.76

Table 3.8. An X-intercept of -19nm/hs for aponeurosis compliance (see figure 3.24) represents a length decrease in the aponeurosis of 2.9%. An x-intercept of -9nm/hs represents a length decrease in the muscle fibre length of 0.76%.

The average number of half sarcomeres was obtained in this table by dividing the average fibre length by the average sarcomere length.

are stiffer (Ford et al., 1977) (see figure 3.25). This is because in the slower releases some of the T_1-T_2 transition is occurring during the release, thus the slower the release the greater the distance of release needs to be to drop the force to zero. It is possible that approximately half of the x-intercept in the present results is due to aponeurosis compliance. In which case it is likely that the step release time range of 0.5 to 2ms has no effect on varying tendon compliance.

In the tendon experiments two step speeds were used: 2 and 100ms. The tendon was found to be on average 14% stiffer at 2ms than at 100ms step speed (see table 4.8). Thus extrapolating from this one would expect the stiffness of the aponeurosis to increase less than 0.2% at 0.2ms step time, than at 1.4ms step time, which can be considered negligible (see figure 3.26). Thus the change in the x-intercept due to the change in the crossbridge stiffness in whole mouse soleus muscle over the step time range 0.5 to 2ms, would be partially masked by the tendon compliance, which has a large (59%) influence on the x-intercept. Thus one would expect a decrease in the x-intercept of 14% rather than 33%, when the step speed is increased from 1.0 to 0.2ms (see table 3.9). However in the present experiments no statistically significant variation was found in the x-intercept over this speed range. Indicating that either T_1-T_2 is over or that it has not started by the end of the release.

The recovery speed, for the recovery of tension after a quick release (see figure 3.16), was found not to vary with the size of the release. One would expect that the bigger the release the faster the recovery speed (i.e. the time constant would be lower), in accordance with the findings of Ford et al., (1977). The S1 crossbridge head has to overcome an activation energy, before it can rotate to restore the tension. The activation energy is larger when the force in the crossbridge is higher. The force in the crossbridge is higher after a small release, since the compliant S2 portion has not been unloaded as much, thus x is greater (see figure 3.27). The larger the activation energy, the slower the rate constant is, therefore the recovery process is slower after a small release. If the recovery phase is not a T_1-T_2 transition then the fact that recovery speed does not vary with release size is easily understood, as there is no reason for it to vary. This finding fits in with hypothesis A.

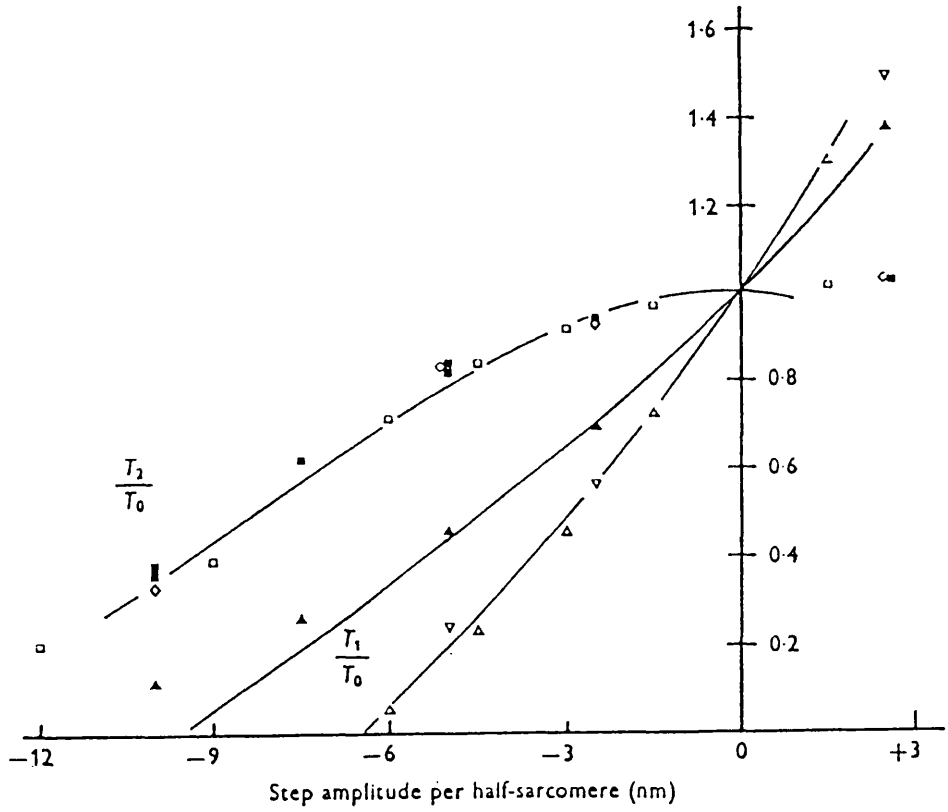

Figure 3.25. Curves of T_1 (triangles) and T_2 (squares) obtained with the standard step completed in 0.2ms (open symbols), and with a step completed in 1.0ms (filled symbols).

From Ford *et al.*, (1977)

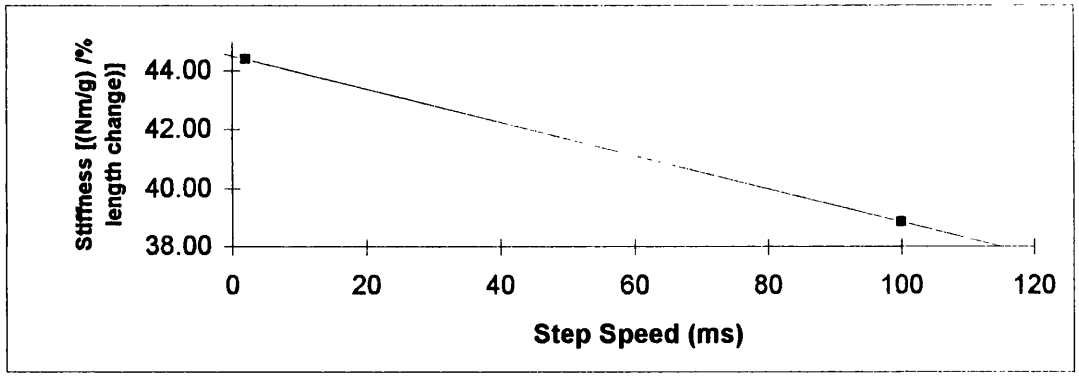

Step time speed ms	Stiffness Nm/g (dry)/% length change
2	44.40
0	44.51
Stiffness increase =	0.2%

Figure 3.26. Stiffness of EDL tendon plotted as a function of the step release speed. Each tendon was subjected to release speeds of 2ms and 100ms. The mean stiffness value for each speed have been plotted (see table 4.8). The y-intercept is 44.51 Nm/g (dry weight), thus the increase in tendon stiffness from step speeds of 0ms to 2ms, is 0.2%, which can be considered negligible.

	Step Time 1ms			Step Time 0.2ms				
	Total x-Intercept nm/hs	Crossbridge x-Intercept nm/hs	Aponeurosis x-Intercept nm/hs	Total x-Intercept nm/hs	Crossbridge x-Intercept nm/hs	Aponeurosis x-Intercept nm/hs		
Huxley & Simmons		-9			-6		% decrease of crossbridge x-intercept	33%
Hypothesis A: 59 % of the x-intercept is due to aponeurosis compliance.								
Aponeurosis			-19			-19	% decrease of aponeurosis x-intercept	0%
Soleus Muscle	-32	-13	-19	-28	-9	-19	% decrease of total x-intercept	14%
Hypothesis B: 72 % of the x-intercept is due to aponeurosis compliance.								
Soleus Muscle	-32	-9	-23	-29	-6	-23	% decrease of total x-intercept	9%

Table 3.9. The x-intercept for the graph T_{min}/T_0 against distance released, is influenced by the aponeurosis that is present in whole muscle. The table calculates the effect of the aponeurosis on the x-intercept of the muscle at two step speeds. Two hypothesis are considered: a) 59% of the x-intercept is due to aponeurosis compliance, b) 72% of the x-intercept is due to aponeurosis compliance.

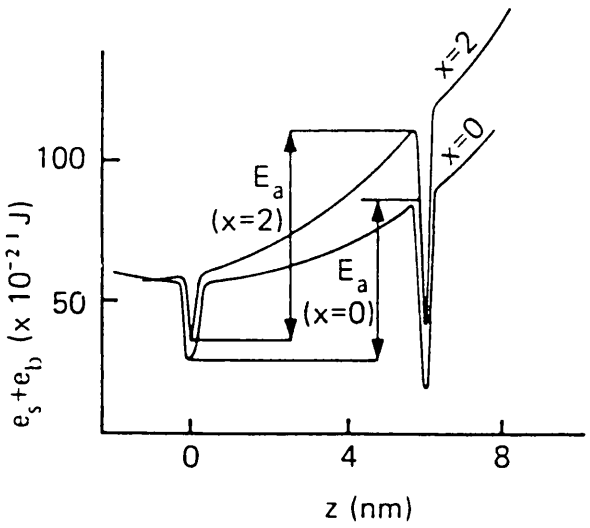

Figure 3.27. Basic free energy of a crossbridge as a function of z. The two curves are for two different values of x. The vertical arrows show the activation energy (E_a) for the transition from z = 0 to z = 6; note it is greater for the larger value of x.

es= energy in the spring

eb= energy of binding

From Woledge et al., 1985

The other question that needs to be determined is the speed of the muscle. A comparison of the various time dependent properties of mouse and frog muscle suggests that mouse muscle is "faster" than frog muscle. Table 3.10, compares time dependent properties obtained from mouse muscle in the current experiments with published data from that of frog muscle. A reasonable estimate can be obtained from a comparison between the Vmaxs. The mean ($\pm$ sem) Vmax of the mouse muscle was found to be 7.28 $\pm$ 0.30 muscle lengths/s at 25°C (see table 3.5). This is faster than the Vmax of frog muscle at 0°C which has been found to be approximately 1.86 muscle lengths/s (Ritchie & Wilkie, 1958). Table 3.10, shows that all the other time dependent properties of mouse and frog muscle, except for the initial rate of tension rise, are faster in mouse muscle (25°C) than in frog muscle (0-3°C). It is likely that the higher temperature makes the values three times faster in the mouse than in frog muscle. The average difference in speed of the values is also around three times larger. So it is possible if the mouse and frog measurements could be performed at the same temperature they would have the same speed. However the results from the current experiments are comparing mouse muscle at 25°C and frog muscle at 0°C, in which case mouse muscle is about 3 times faster than frog muscle. Which indicates that the T_1-T_2 transition is likely to be faster in mouse muscle than in frog muscle.

The T_1-T_2 transition time is a consequence of the crossbridges responding to a certain rate constant at a particular force. The initial rate of tension rise will have no effect on the T_1-T_2 transition since it has no effect on the rate of the transition of the crossbridge moving from a high force state to a low force state. Fusion frequency is to do with activation and so has nothing to do with the crossbridges, and so will not influence the T_1-T_2 transition. Isometric tetanus heat production, Vmax, maximum mechanical power output, rate of fall and isometric crossbridge turnover all reflect the same underlying processes that the T_1-T_2 transition is a consequence of. Since they are all approximately three times faster in mouse than in frog muscle, it indicates that the T_1-T_2 transition is three times faster in mouse than frog muscle.

In frog muscle at O°C the T_1-T_2 transition (known as phase 2) lasts for 2-5 ms (the transition is faster with increasing release size) (Ford et al., 1977). Therefore in mouse muscle at 25°C it is possibly lasts for 0.6 to 1.7ms, which means the T_1-T_2 transition is

	Units	Mouse	Muscle	Twitch Type	Reference	Frog	Muscle	Species	Twitch Type	Temp	Reference	Mean for the mouse and frog values	SD for the mouse and frog values	Ratio of mouse to frog values
Isometric tetanus heat production	mW/g (dry)	26	Soleus	slow	Phillips, 1988	6.4	Semitendinosus	R.Temporaria	Fast	0°C	Curtin & Woledge, (1981)	16.2	13.86	4.06
Vmax	Muscle lengths / second	7.28	Soleus	slow	Current experiments	1.86	Sartorius	R.Temporaria	Fast	0°C	Ritchie & Wilkie, (1958)	4.57	3.83	3.91
Maximum power output	W/Kg	629	Soleus	slow	Current experiments	102	Semitendinosus	R.Temporaria	Fast	1 -2.5°C	Calculated from the equation in the legend.	365.5	372.65	6.17
Rate of tension rise	s^{-1}	11.1	Soleus	slow	Current experiments	16.19	Tibialis anterior	R.Temporaria	Fast	1°C	Traces obtained from M. Linari	13.645	3.60	0.69
Rate of tension fall	s^{-1}	39.4	Soleus	slow	Current experiments	17.3	Tibialis anterior	R.Temporaria	Fast	1°C	Traces obtained from M. Linari	28.35	15.63	2.28
Fusion frequency (for maximum force)	Hz	50	Soleus	slow	Current experiments	18	Tibialis anterior	R.Temporaria	Fast	1°C	M. Linari (personal communication)	34	22.63	2.78
Isometric crossbridge turnover / crossbridge	s^{-1}	0.682	Soleus	slow	Current experiments	0.168	Tibialis anterior	R.Temporaria	Fast	1°C	Calculated from the equation in the legend.	0.425	0.36	4.06

Table 3.10. Various time dependent properties are shown for mouse and frog muscle. The values for the mouse muscle (25°C) were obtained from the current results, the values for the frog muscle are from published data.

Maximum power (M^2) as a fraction of Po.Vmax was calculated from the equation $M^2 = (2 + G\text{-}2\ (1+G))/G^2$ (in mW, when Po is in N and Vmax is in mm^{-s}) (G=Po/a, Po= isometric tetanus force, a=constant in the Hill equation) (Woledge *et al*., 1985).

Rate of tension fall was obtained by fitting double falling exponential (P(Qe-t/tor1 + (1-Q)e-t/tor2)) to the exponential part of the falling tension trace (n=4, for both the mouse and frog muscle). The rate of fall that is reported is that of the positive exponential term (see figures 3.28a & b, and table 3.11).

The isometric crossbridge turnover per crossbridge = rate of energy liberation (mW/g wet weight) divided by the product of the energy output per PCr split (mJ/μmol) and the number of crossbridges per gram of muscle (μmol/g wet weight) (Woledge et al., 1985).

A

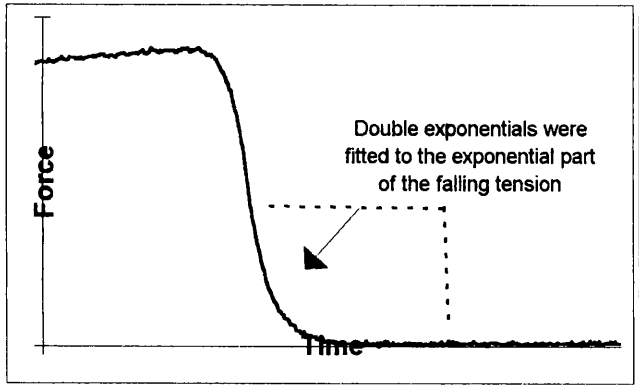

Figure 3.28a. A double falling exponential was fitted to the exponential part of the falling tension trace. Since this portion of the trace is influenced by the switching off of the crossbridges. Whereas the initial section of the tension fall is due to the taking up of Ca^{2+} into the sarcoplasmic reticulum.

Figure 3.28b. Shows a typical record of tension fall in mouse soleus muscle, to which a double falling exponential has been fitted.

B

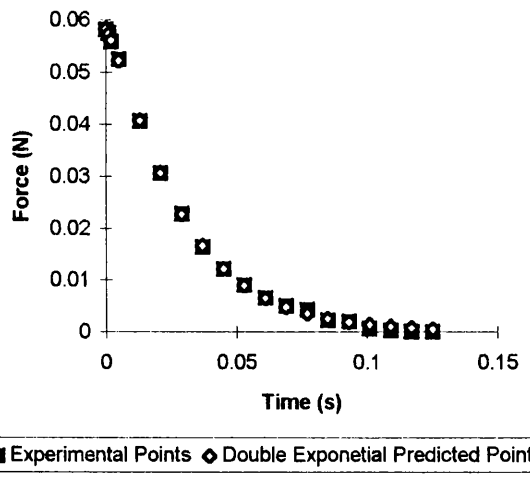

Species	Mouse (whole muscle)	Frog (single fibre) *R.Temporaria*
Muscle	Soleus	Tibialis Anterior (lateral head)
Twitch Type	Slow twitch	Fast twitch
Temperature	25°C	1°C
	Traces obtained from current experiments.	Traces obtained from M.Linari.

Record	Time constant (ms)	Record	Time constant (ms)
1	25	1	46
2	27	2	62
3	21	3	47
4	29	4	77
Mean	25	Mean	58
sd	3	sd	14
sem	1.2	sem	5.1
n	4	n	4

Rate of fall (s^{-1}) = 39.41

Rate of fall (s^{-1}) = 17.26

Ratio of rate of fall of mouse to frog = 2.28

Table 3.11. A double falling exponential ($P(Qe^{-t/tor1} + (1-Q)e^{-t/tor2})$) was fitted to the exponential part of the tension fall of mouse and frog muscle records, to obtain the time constants for the tension fall.

The value of Q is negative, the time constant that is reported here is that of the positive exponential term. The records in each case are from 4 different muscles. A Student's unpaired t-test shows the time constants from the mouse muscle traces are significantly faster than those from the frog muscle traces ($p<0.001$). This indicates the switching off of the crossbridges is faster in mouse than in frog muscle.

Student's unpaired t-test

t= -6.24

n= 8

Degrees of freedom = 6

P= 0.001

probably finished before the end of the release.

The reason the rate of initial isometric tension rise is slower in the mouse than in frog muscle (see table 3.1), is likely to be due to two reasons: firstly the slowness of the calcium released from the sarcoplasmic reticulum. It is known from the results of the Brenner experiments that the initial rate of tension rise (calcium is rate limiting) of mouse muscle is 10/s, whereas the rate of the redevelopment of tension after all the crossbridges have been broken by a stretch (calcium is not rate limiting), is 90/s (see table 3.7). Therefore it is likely that the slow process in the initial rate of tension rise is due to activation, i.e. the rate of the release of calcium from the sarcoplasmic reticulum and the binding of calcium to troponin. This point is further illustrated by the fact that the twitch of mouse soleus muscle is very small compared to the tetanus, whereas in frog muscle the twitch is not much smaller than the tetanus. Thus showing in the mouse soleus muscle many stimuli are required before enough calcium is released.

The second reason for the slowness of the initial tension rise is likely to be due to the presence of internal compliance. This slows the rate of rise, because the spring has to be extended. It is likely that the initial tension rise in whole frog muscle would be about half as slow as frog single fibres. Thus ignoring aponeurosis compliance, the initial rate of tension rise in mouse soleus muscle is likely to be half as slow as in single frog fibres, this would give a value of 8/s. This value is very similar to the value obtained for whole mouse soleus muscle of 11/s (see table 3.1). Mouse soleus muscle is known to consist of 60% slow fibres and 40% fast fibres (Brooks & Faulkner, 1991). Electromyographic studies of cat soleus muscle, have shown that it is active during both standing and walking (Goslow et al., 1973). It is a tonic muscle and is active all the time, required to keep the ankle at right angle for standing. Thus only a little calcium is required to be released for each contraction.

3.5.2. Hypothesis B: T_1-T_2 is slower in mouse than frog muscle.

Tmin curve = T_1, Texp curve = T_2

If the T_1-T_2 transition is slower in mouse than it is in frog, then it is likely that the Texp

curve is in fact a T_2, supported by the fact that two exponentials can be fitted to the recovery trace.

From the work of Huxley and Simmons, it is known that 9nm/hs (1.0ms step time) is required to drop the force produced by the frog muscle crossbridges (T_1) to zero. Thus if the Tmin curve is a T_1 curve then (32 - 9 = 23nm/hs) 72% of the intercept is due to the tendon compliance. However if 72% of the x-intercept in the current experiments is due to aponeurosis compliance, this provides an explanation for the fact that the x-intercept was not found to vary with release speed (0.2-1.0 ms). Since increasing the tendon stiffness between release speeds of 0.2-1.0 ms is negligible (see figure 3.26), and thus the x-intercept for the whole muscle would be expected to decrease by 9% instead of 33% (see table 3.9) for muscle fibres. The large amount of internal compliance could also be responsible for masking the absence of the expected effect of larger releases producing faster recovery tension.

The fact that the mouse muscle appears faster than frog muscle (see table 3.10) makes it difficult to explain why conversely in mouse muscle the T_1-T_2 transition should be slower than in frog muscle.

3.5.3. Hypothesis C: T_1-T_2 transition is the same speed in mouse muscle as in frog muscle.

The differences between the current experimental results and Huxley and Simmons results might be all explained by the presence of compliance in the current results. One would expect the same series compliance to be added to both the T_1 and T_2 curve, thus the shift on the length axis of each curve would be expected to be equal. If this were not true it would mean the compliance in the muscle was damped; i.e. it was not the same at different speeds of release. From the current experiments the Tmin curve is shifted by about 23nm/hs and the Texp curve by about 38nm/hs from the Huxley and Simmons curves (1.0ms step). These two shifts are quite dissimilar, so it is not expected this method of adding compliance would work very well.

In frog fibres the time constant of the fast process is 1ms. The presence of compliance in whole muscle is expected to make it twice as slow, which would give a time constant

of 2ms. However, in the current experiments the time constant of the fast process was found to be roughly 12ms (see table 3.2). Therefore assuming the speed of the T_1-T_2 transition in frog and mouse to be the same, the presence of compliance in whole muscle, does not account for all the difference in the time constants of the fast process between mouse and frog muscle. Since the process is still appearing 6 times slower in mouse than frog muscle. Thus it is concluded hypothesis C, does not apply.

3.6. Conclusions

The fast component of the tension recovery after a quick release, is the fast phase of attachment of detached crossbridges. The slow component is the slow phase of attachment of detached crossbridges. This is concluded from the results of the Brenner protocol, which has shown that after a stretch (i.e. after the crossbridges have been broken) there is a fast phase and a slow phase in the recovery of tension. The fast component cannot be due to a T_1-T_2 transition, since there can be no T_1-T_2 transition when there are no crossbridges attached. The slow component is not due to activation, but is due to crossbridge attachment. Therefore there is a slow and a fast phase in crossbridge attachment. Thus the Brenner experiments seem to indicate that the Texp curve is not a T_2 curve, but is the fast phase of attachment of detached crossbridges (see figure 3.22).

This implies the T_1-T_2 transition has already occurred in the present results, and thus the T_1-T_2 transition is faster in mouse soleus muscle than frog muscle. Therefore it is likely that T_1 has not been observed and thus possibly the Tmin curve in the current results is perhaps a T_2, i.e. hypothesis A applies. The T_1-T_2 transition appears to be very fast in mouse, this shows that the muscle can deliver work very quickly over short distances, since the T_1-T_2 transition indicates the speed of the spring through which all the force in the muscle passes. Thus it is concluded that 59% of the x-intercept of the quick release experiments is due to aponeurosis compliance.

CHAPTER 4. TENDON STRETCHING EXPERIMENTS

4.1. Introduction

The aims of these experiments on stretching tendons were:

1) To determine the compliance of the tendons.

2) To determine whether castration or ovariectomy affects the compliance of the tendon.

3) To determine whether the tendon stretches uniformly.

Knowing the compliance of the tendon gives an indication of how much energy can be stored in the tendon. The more compliant the tendon is, the more energy it can store at a given force. Compliance alone, however, does not give a complete description of the tendon, the linearity and hysteresis also need to be discussed. If the material possesses linearity then the material stretches in proportion to the force it is subjected to.

4.1.1. Previous Methods Of Investigating Tendon Stiffness

1) Observing Joint Movements (Dimery *et al.*, 1986).

Several of the distal leg muscles of horses have such extremely short muscle fibres that their changes in length in locomotion must be due almost entirely to elastic extension of their tendons. Thus it is possible to determine the degree of tendon stretch by observing the movements of the joints. Using this method it was determined that elastic strains of the order of 5% occur in the digital flexor tendons of horses in locomotion.

2) Studies measuring isolated tendon compliance (Ker, 1981; Dunn & Silver 1983; Rigby *et al.*, 1959; Woo et al., 1980).

A piece of tendon is attached to a fixed hook and a moving hook. The tendon is stretched and the force it develops is recorded on a strain gauge. The results obtained by this method, by previous investigators are summarized on table 4.1. This method was also used in the present experiments.

4.1.2. Ways Of Imaging The Tendon:

1) X-ray (Amis *et al.*, 1987).

X-ray film in subjects whose biceps muscles were injected with radio-opaque markers, showed in strong isometric contractions, the distal tendon of the long head of the biceps, lengthened by about 2% of its estimated rest length (Amis *et al.*, 1987). However this

Reference	Tendon	Age of Tendon	Young's Modulus Stress/Strain N/mm^2	Strain Rate % / min	Duration of stretch s	Yield point % strain	Energy stored/ gram of tissue For 3% stretch mJ/g	Compliance mm^2/N	Strain applied	Stress applied N/mm^2
Current study	Mouse EDL tendon	Adult, 3 - 5 months	1243	1.8×10^4 to 1.68×10^5	0.1	>7%	275	0.000805	0 to 7 %	0 to 50
Ker (1981)	Sheep Plantaris tendon	Adult, 5 years	1826	25 to 1230	0.05 to 2.3	Not given	660	0.000548	0 to 3.7 %	0 to 57
Dunn & Silver (1983)	Human psoas tendon	47 - 56 years	62	10	30	30%	None	0.0161	0 to 5 %	0 to 18
Rigby et al., (1959)	Rat tail tendon	Adult, 4 - 5 months	289	1 to 20	Not given	8%	130 (2% / minute strain rate)	0.00346	0 to 8%	0 to 18
Woo et al., (1980)	Pig digital extensor tendon	Adult, 1 year	882	0.26	Not given	6%	224	0.00113	0 to 6 %	0 to 40

Table 4.1. Data from the current experiment tabulated with data from previous studies of measuring tendon compliance.

method is only sensitive enough to detect tendon lengthening in maximum voluntary contractions.

2) Computed tomography (Reinig *et al.*, 1985).

Computed tomography (CT) can provide reasonable definition of the tendons and adjacent soft tissues and musculature but is limited by the lack of direct sagittal imaging, sagittal imaging is desirable since most tendons run in the sagittal plane. Although sagittal reconstructions can be performed, thin section images would have to be obtained at close intervals to yield optimal anatomical detail. This results in a long examination with a significant radiation dose (Reinig *et al.*, 1985). In addition sagittal reformatted CT images are inferior to magnetic resonance images in spatial and contrast resolution (Marcus *et al.*, 1989).

3) Magnetic Resonance Imaging (MRI) (Marcus *et al.*, 1989).

The definition of the soft tissue planes and muscular bundles is much better with MRI than any other imaging method. Sagittal imaging can easily be obtained so it is possible to show the two ends of the tendon in one image (Marcus et al., 1989). Other advantages compared with CT are the absence of ionising radiation or any other apparent biological hazard. Disadvantages of MRI are the high cost of the sophisticated machinery and the necessity for highly trained operator. It is also unsuitable for patients with cardiac pacemakers which can be adversely affected by the magnetic fields as can metallic clips or implants (Sutton, 1994). MRI and CT have only so far been used to image the tendon and not yet to determine the compliance of the tendon.

4.2. The Structure of Tendon

4.2.1. Collagen Fibres

Fibrous connective tissue forms tendons. The major component is collagen fibres (over 70% of the dry weight), surrounded by cells and amorphous ground substance (proteoglycans) and elastic fibres (Grant & Prockop, 1972). The tendon is relatively devoid of blood vessels. Collagen fibres are capable of only a slight degree of extensibility, they are therefore very resistant to tensile stress (Grant & Prockop, 1972). The collagen of a tendon is arranged in a wavy bundle called a fascicle (see figure 4.1). A fascicle varies from 50 to 300 microns in diameter. The fascicle is in turn composed

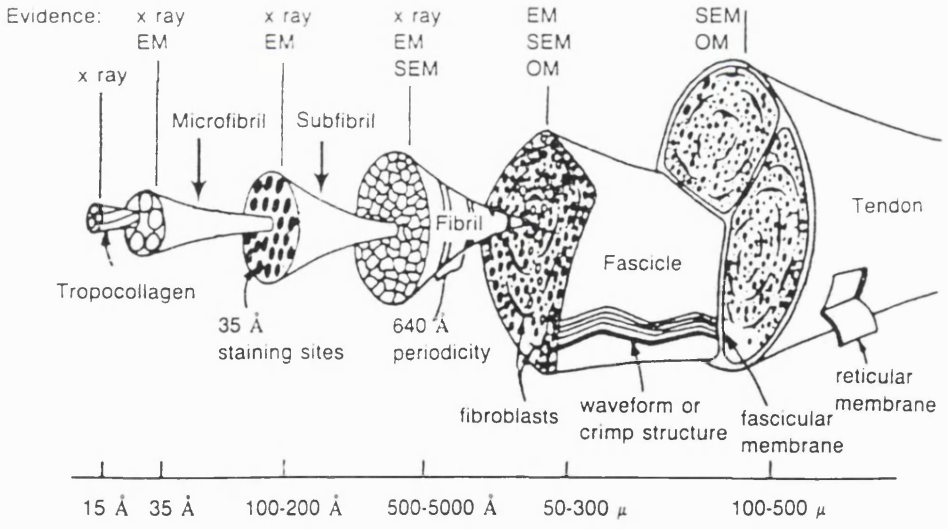

Figure 4.1. Collagen hierarchy.

From Kastelic *et al.*, (1978).

of bundles of fibrils, each of which is approximately 50 to 500 nm in diameter. The fibrils are in turn composed of bundles of collagen subfibrils, each of which is approximately 10 to 20 nm in diameter. Each subfibril is comprised of bundles of collagen microfibrils or filaments, each of which is approximately 3.5 nm in diameter. The diameter of the filament in a given tissue vary with age and the source (Diamant *et al.*, 1972).

The collagen microfibril is composed of regularly spaced, overlapping collagen molecule units (sometimes called tropocollagen) (see figure 4.2). The collagen molecule consists of three polypeptide chains (alpha chains) of equal length. Two of the chains (the $alpha_1$ chains) are identical and one (the $alpha_2$ chain) is distinct, and is known as type 1 collagen (Ramachandran, 1967). Each chain has a molecular weight of approximately 95 000. The individual chain forms a left handed helix, while the three chains are coiled around a central axis to form a right handed helix. The collagen molecule has the shape of a rod, about 290nm long and 1.5nm in diameter. Every third amino acid in the helical chain is glycine. The imino acids proline and hydroxyproline together account for about another 20% of the residues. Because of their rotational restrictions, the imino acids produce the helical conformation and the hydroxyproline stabilizes the triple helix by contributing to interchain hydrogen bonds (Oxlund, 1984).

The collagen molecules lie in parallel alignment with a staggered overlap of almost one fourth of their length. Actual measurements indicate that a gap or hole of about 41.9 nm occurs between the end of one collagen molecule and the beginning of the next in the same line. This overlapping is what causes the prominent cross-bands or striations. Collagen fibrils have a cross-band periodicity of 60 to 70 nm depending on the source and degree of hydration (Ramachandran, 1967). A major factor that adds tensile strength to collagenous structures is the presence of both intramolecular cross-links between the $alpha_1$ and $alpha_2$ chains of the collagen molecule and the intermolecular cross-links between collagen subfibrils, microfibrils, and fibres. In a sense, the cross-links act to weld the building blocks (i.e., the molecules) into a strong rope like unit. Generally the shorter the length between one cross-link and the next or the larger the number of cross-links in a given distance, the higher the resistance to stretch will be (Ramachandran, 1967).

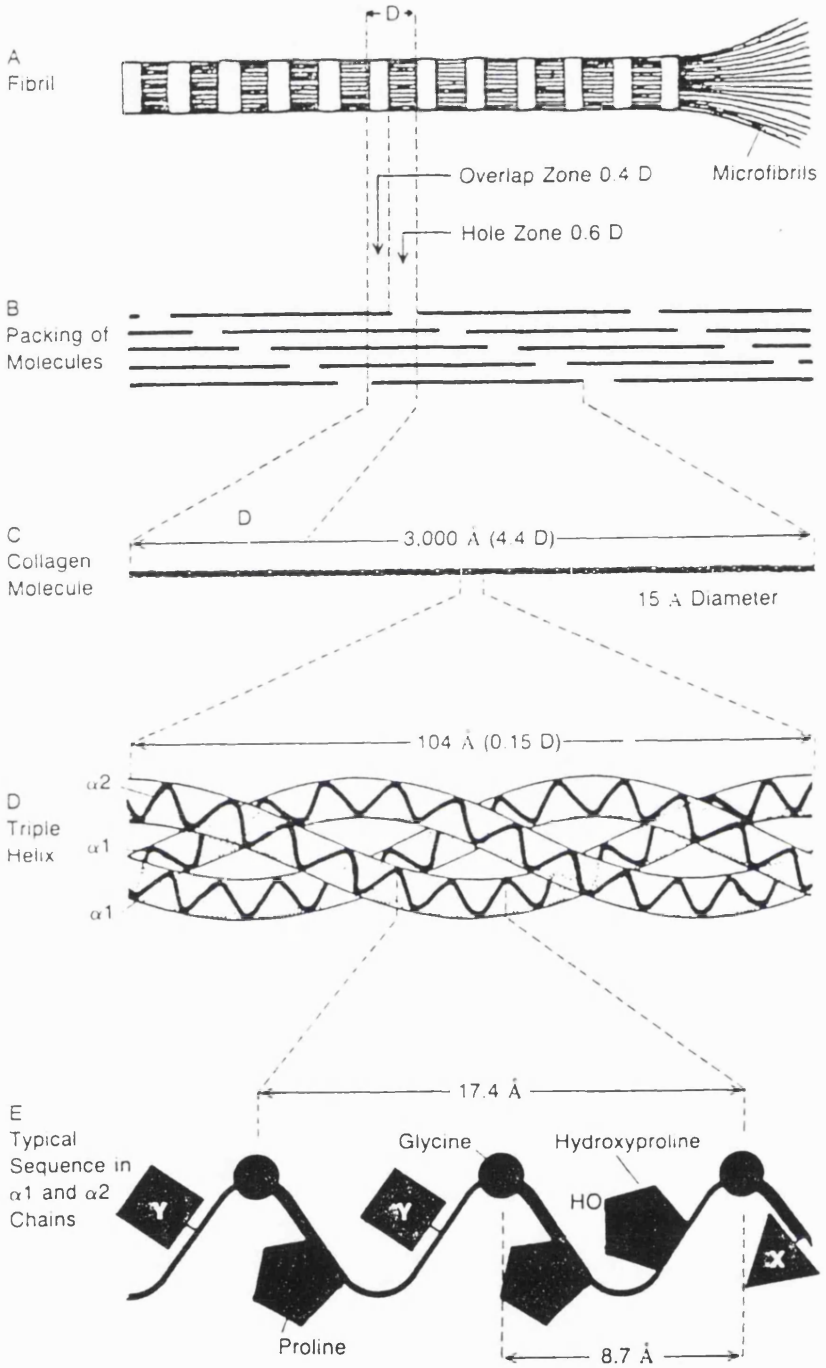

Figure 4.2. Collagen ultrastructure. Many tiny collagen fibrils make up a collagen fibre (a). The cross-striations in the fibril result from the overlapping of collagen molecules (b). The collagen molecule itself (c) is composed of three polypeptide chains that are organized into a rope-like triple helix (d). The amino acid sequence of these polypeptide chains is unique in having glycine as every third amino acid (e). The position following glycine is frequently proline and the y position preceding glycine is frequently hydroxyproline.

From Prockop and Guzman, (1977).

4.2.2. Elastic fibres

Tendon also contains elastic fibres (approximately 4.4g / 100g dry weight) (Grant & Prockop, 1972). Elastic fibres are composed of elastin. Elastin is a complex structure with a mechanical property of elasticity (the ability of a stretched material to return to its original resting state) due both to its biochemical composition and to the physical arrangement of its individual molecules (Hukins, 1984). Elastic fibres yield easily to stretching because they are composed of a network of randomly coiled chains joined by covalent cross-links. These cross-links impose a restriction on the elastic fibres such that, upon stretching, the individual chains are constrained and cannot slip past one another (Franzblau & Faris, 1981). However, the covalent interchain forces are weak and the cross-links widely spaced. As a result, minimal unidirectional force can produce extensive elongation of chains before cross-links begin to restrict movement. Thus, similar to the collagenous fibres, elastic fibres allow extensibility until the slack and spacing between the chains are taken up (Franzblau & Faris, 1981). It seems the tendon is elastic because the collagen after it is extended returns to its original length, rather than due to the small percentage of elastic fibres. The amount of elastic fibres has not been found to vary much between different tendon types (Hukins, 1984).

4.2.3. The Stress-Strain Curve

Tendons do not obey Hooke's Law *'ut tensio sic vis'* (Elliott, 1965). Rat tail tendon (RTT) in particular has been studied extensively, because of its highly organized structure. RTT is a uniaxial structure consisting of tendon fibres which are roughly parallel to the tendon axis (Rigby *et al.*, 1959). In RTT each fibre has a planar crimp which arises from its pattern of collagen fibre orientations. The planarity of the crimp in RTT has been demonstrated by polarised light microscopy (Diamant *et al.*, 1972) (see figure 4.3).

The stress-strain curve of a tendon can be divided into three regions (see figure 4.4, which was obtained from RTT): (1) a low modulus toe (curved) region, (2) a linear region during which the tangent to the stress-strain curve does not change, and (3) a yield and failure region where the modulus (tangent to the curve) is initially reduced (yield) and then markedly reduced before failure.

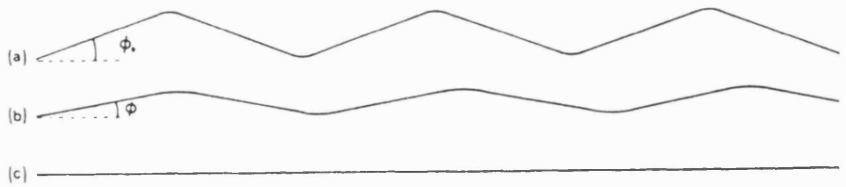

Figure 4.3. Diagrammatic representation of the crimp structure in rat tail tendon (a) unstretched, (b) at an intermediate stage and (c) under sufficient stress to remove the crimp.

From Hukins, (1984).

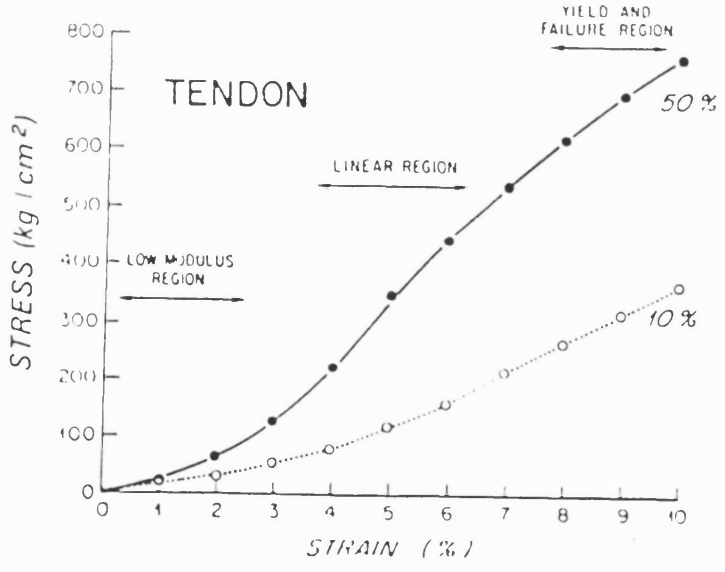

Figure 4.4. Stress-strain curves for wet rat tail tendon in tension at strain rates 10% and 50% per minute. The strain rate dependence is a result of viscoelasticity which is prominent in connective tissue. The early part of each curve, or toe region, represents straightening of the crimp pattern in collagen fibres while the collagen fibres are stretched during the linear region. Fibril disintegration occurs via a shear-slip mechanism in the yield and failure region.

From Trelstad and Silver, (1981).

1) In the "toe region" the slope or tangent modulus increases with strain until it reaches a constant value. Rigby *et al.* (1959), attributed straightening of the crimp observed in collagen fibres by polarized light microscopy as the physical basis of the toe region. In the RTT it has been shown that the low strain deformation of less than 3%, involves uncrimping of the collagen fibrils which requires very little stress (Rigby *et al.*, 1959).

The straightening of the crimp leads to the collagen fibrils reorientating in the direction of the applied stress (Elliott, 1965). A clear demonstration, by polarized light microscopy, of this reorientation has been reported by Diamant *et al.* (1972), on RTT. Ultimately, this results in an increase in crystallinity or orientation that strengthens the intermolecular bond and increases resistance to further elongation. Thus the crimp structure leads to a tendon that is compliant at low strains but stiffens when the strain increases (Elliott, 1965; Diamant *et al.*, 1972).

2) X-ray diffraction shows that the application of tension to a collagen fibril does not stretch the individual collagen molecules. Their conformation does not change when RTT is stretched by up to 20% of its original length (if the rate of straining is sufficiently slow; less than 1% per minute, extensions of up to 20% can be reached in RTT) (Rigby *et al.*, 1959). The linear region involves stretching of collagen fibres and therefore the stiffness in this region is indicative of the stiffness of the collagen fibre. The slope of the straight part of the stress-strain graph, i.e. tensile stress/tensile strain is termed Young's modulus (E). If a material has a large E, it resists elastic deformation strongly and a large stress is required to produce a small strain.

3) Mature tendon exhibits a yield region characterized by a decrease in the tangent modulus. In the yield region elongation is irreversible and permanent deformation remains after unloading. Small angle x-ray scattering studies suggest that within the yield region the crystalline pattern within the collagen fibres is destroyed (Silver, 1987).

In RTT, a strain of 4% is generally found to be the limits of the collagen fibres reversibility, this corresponds to the end of the toe region. Thus it is concluded RTT usually operates in the toe region. At strains of 4-8% the tendons surface waviness disappears. A point is reached where all intermolecular forces are exceeded, and so

RTT breaks at strains of around 8 to 10% (Rigby *et al.*, 1959). The ultimate tensile strength of tendon has however probably never been accurately measured because clamping cannot be achieved that will exert the applied stress uniformly across the fibril bundles and clamping itself probably damages the structure (Davison, 1982). The safety factor of the tendon is defined as the force required to break the tendon divided by the isometric muscle force. Generally the safety factor of the tendon has been found to be approximately 3-6 (Wainwright *et al.*, 1976).

The energy storage capacity of the tendon is not primarily due to the straightening out of the crimp, but to the elastic properties of the straightened collagen fibres (Ker, 1981). This is because the energy stored is equal to the area under the stress-strain curve (since the energy dissipated due to hysteresis is negligible). It can be seen from figure 4.4 that the area under the toe region (2%) is a small proportion of the area compared to the area under the linear region (47%). RTT is known to operate only in the toe region, i.e. below the 3% strain zone (Rigby *et al.*, 1959). Since only a small percentage of the energy is stored at this strain level, it seems to indicate that the purpose of the rat's tail is not to store energy.

4.2.4. Hysteresis

The force extension curve for a tendon is a loop. The graph shown in figure 4.5, was obtained from the gastrocnemius tendon of a wallaby. The upper line was drawn as the specimen was stretched and the lower line as it shortened. The loop is formed because some of the work done stretching the specimen is degraded to heat instead of being recovered in the recoil, this phenomenon is termed hysteresis. The area (A+B) under the rising line represents the work done stretching the specimen. The area B represents the work recovered in the elastic recoil and the loop area (A) the energy lost as heat. Thus the proportion of energy lost is A/(A+B). Here this energy dissipation can be seen to be small, about 0.07. This is important if tendons are to act as a store of energy (Alexander, 1988).

4.2.5. Viscoelasticity

The property of a material to show sensitivity to rate of stress loading is called viscoelasticity. With viscoelastic materials a quickly applied force meets with a higher

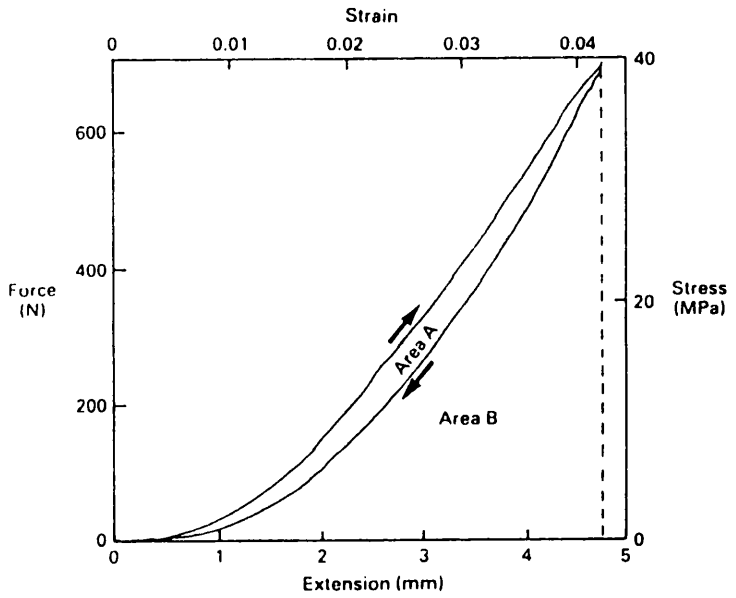

Figure 4.5. Graph of force against extension, obtained from the gastrocnemius tendon of a wallaby. The upper line was drawn when the tendon was stretched and the lower line as it shortened. The loop is formed because some of the work done stretching the specimen is degraded to heat instead of being recovered in the recoil. The area (A+B) under the rising line represents the work done stretching the specimen. The area B represents the work recovered in the elastic recoil and the loop area (A) the energy lost as heat. Thus the proportion of energy lost is A/(A+B). Here this energy dissipation can be seen to be small, about 0.07. Additional scales show stress and strain.

From Alexander, (1988).

resistance (Galley & Forster, 1990). More energy is dissipated during slow loading, so that less of the work done on the tissue stretches it, i.e. it is less stiff. If a tendon is stretched and held at a particular length, the load required falls with time. This viscoelastic behaviour is caused by the internal rearrangement of the molecules of the tendon, which tend to occupy a position of minimum strain energy. Therefore, the amount of recoverable energy stored in the tendon decreases with time, some has been converted to heat (Hukins, 1984).

4.2.6. Preconditioning

All connective tissues exhibit a phenomenon termed "preconditioning" which involves changes in the mechanical properties as a result of a series of loading and unloading cycles. Figure 4.6, shows a series of loading and unloading cycles for RTT, cycled between zero extension and a fixed force. The extension was limited to less than 2% which is the region in which mechanical properties are reproducible (Rigby, 1964). Cyclic deformation, was found to increase the tangent modulus (i.e. the tendon is becoming stiffer) in the linear region by 35% to 40%, while the energy loss in a cycle (hysteresis loop) is decreased. This is thought to be due to improved orientation of collagen fibres along the stress direction (Rigby, 1964).

4.2.7. Summary Of The Mechanical Properties Of Tendon

Thus to summarize the important mechanical properties of tendon, are:

1) The stress-strain curve of tendon is not linear, the stiffness is greater at higher strains.

2) The initial stage of tendon deformation (for strains of up to about 0.04 in RTT) involves straightening the crimp.

3)Tendon creeps under a constant applied stress.

4)The strain developed in the tendon depends on the rate at which stress is applied.

5)Tendon exhibits mechanical hysteresis i.e. it does not store all its deformed energy, but the proportion of energy lost is small.

6) After a rapid series of extension and relaxation cycles, the stiffness increases and the hysteresis is less marked.

7) When the strain exceeds the yield point (a value of around 0.04 in RTT) the tendon becomes plastically deformed (Hukins, 1982).

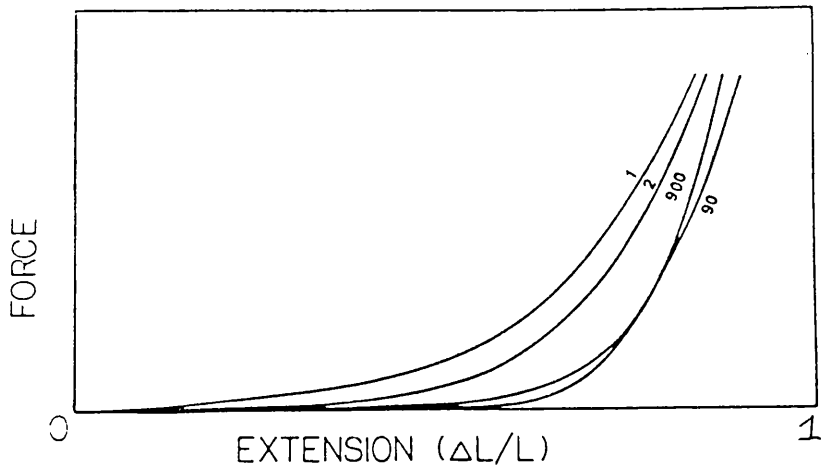

Figure 4.6. Force extension curves for rat tail tendon, illustrating changes in behaviour as a function of a number of cycles. The tendon has been cycled between zero extension and a fixed force. The number of cycles is written alongside each curve.
From Rigby, (1964).

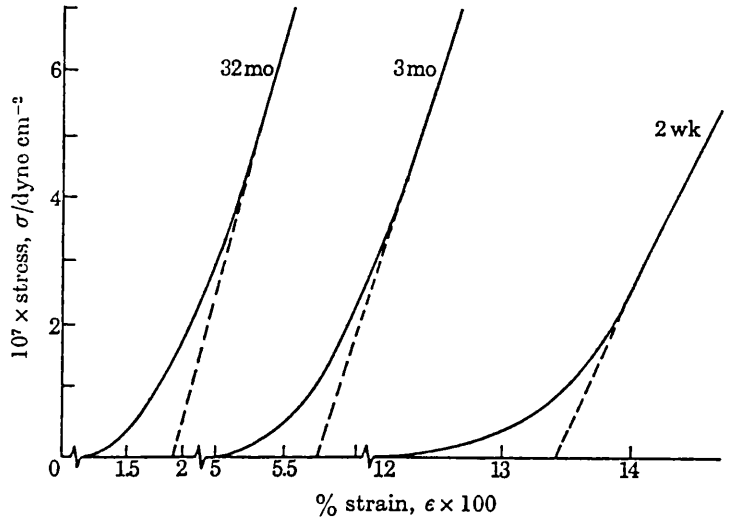

Figure 4.7. Typical experimental stress-strain curves in the toe region from young, mature and old tendons. The intercept of the extrapolated dotted line with strain axis marks the toe region. The toe region gets shorter and the slope of the linear portion gets steeper with age.

From Diamant et al., (1972)

4.3. Ageing

Collagen is one of the few proteins (together with elastin) which show clear changes with age. As an extracellular protein, it is not renewed during cell division, and consequently accumulates aging changes. Collagen content is known to increase with maturation and aging of the tissue (Everitt & Delbridge, 1976). Isotopic studies have shown that collagen can be separated into soluble and insoluble forms of collagen. It has been shown that the soluble collagens are completely converted to insoluble collagen (Lindstedt & Prockop, 1961). Although the body collagen taken as a whole, is metabolically inert, there appears to be small pools of collagen which are both synthesized and degraded rapidly. In addition rapid degradation of collagen can occur in special situations such as in the post-partum uterus and starvation (Lindstedt & Prockop, 1961).

Hydroxyproline is found in the tissues of vertebrates almost exclusively in collagen, except for a small amount of hydroxyproline in elastin. The content of hydroxyproline in elastin is only about one-tenth of the amount present in collagen, and the body contains far less elastin than collagen. Thus the unique distribution of hydroxyproline among proteins makes this amino acid a useful, and naturally occurring label for studying the metabolism of collagen. The endogenous free hydroxyproline and peptides containing hydroxyproline present in biological fluids have been shown to be derived from the degradation of collagen (Kivirikko, 1970).

Isotopic studies have indicated that both the rate of collagen synthesis and the rate of collagen degradation are more rapid in young animals than in old ones. Even though the total amount of collagen in the body is much greater in the older animal and adult human, the urinary excretion of hydroxyproline is one-third to one-sixth of the values seen in young animals or children (Kivirikko, 1970). In human subjects, a high excretion values for urinary hydroxyproline is observed in children, which gradually decrease to adult levels at the age of about 20 to 25 years, and then remain relatively constant between the ages of about 25 and 65 years. Only a few studies deal with changes in the urinary hydroxyproline values in subjects over 65 years of age. A study carried out in subjects on a hydroxyproline free diet have suggested that a decrease may take place after the age of about 65 or 70 years. These finding suggest that a further

decrease in the rate of collagen turnover may occur in old age (Kivirikko, 1970).

The mean diameter of collagen fibrils increases with age. An inverse relationship has been shown to exist between the carbohydrate content of collagen and fibril diameter. It has been shown that structural glycoproteins regulate the diameter of collagen fibrils by modulating the aggregation of tropocollagen molecules, an increase in diameter is preceded by a loss of structural glycoproteins (Cetta *et al.*, 1982). In addition the decrease in mucopolysaccharides and water with age in tendon, may in part explain the increased stiffness of tendon in old age. Since in the tendon of newborns, the collagen fibres are found to be separated from each other while in old tendon the fibres appear more closely packed (Ippolito *et al.*, 1980).

4.3.1. Cross-links

The amount of cross-links derived from the process of non-enzymic glycosylation has been found to increase with age (Naresh & Brodsky 1992). Cross-linking appears to: (a) increase the resistance of the collagen to degenerative enzymes and urea degradation (Davison, 1982); (b) increase its tensile strength; (c) decrease its elasticity and decrease its solubility (Verzar, 1963). The intensity of the fluorescence characteristic of sugar-derived cross-links in human tissues shows a linear relation with age, and this trend is accelerated in insulin-dependent type I diabetes (Monnier *et al.*, 1984). In accordance with this mechanical stiffness of collagen has been observed to be increased in experimentally induced diabetes in RTT (Andreassen *et al.*, 1981). In non-enzymic glycosylation, the small fraction of glucose molecules in the open chain aldehyde form reacts spontaneously with lysyl and hydroxylysyl residues of collagen, first forming a Schiff base and resulting in stable, fluorescent intermolecular cross-links via an undefined pathway (Reiser, 1991).

4.3.2. Hypophysectomy Inhibits Intermolecular Cross-linking Of Collagen

Hypophysectomy is the surgical removal or destruction of the pituitary gland (hypophysis) in the brain. It eliminates the pituitary hormones and greatly reduces the secretion of hormones from the thyroid, adrenal cortex, and gonads. Hypophysectomy is known to markedly decrease the rate of ageing in most tissues (Everitt, 1973). In hypophysectomized rats the breaking times of RTT were found to be approximately 50%

shorter. Thus the biological age of collagen fibres in these hypophysectomized rats approximately corresponds to that of controls half their chronological age (Olsen & Everitt, 1965). Age changes in collagen solubility are also abolished by hypophysectomy. In the rat it has been shown 2 years after hypophysectomy, that the collagen is "younger" than normal because it contains 20% insoluble or old collagen, compared with 40% in the intact control (Everitt & Delbridge, 1976). Normal age changes do, however, occur in the soluble collagen of the hypophysectomized rat; i.e. the mean diameter of the collagen fibres increases with age and a decrease of structural glycoproteins occurs (Everitt & Delbridge, 1976).

It appears therefore, that the site of the anti-aging action of hypophysectomy is not on soluble collagen, but on the insoluble fraction (Everitt & Delbridge, 1976). Shoshan *et al.*, (1972) showed that the cross-linking of collagen implants was inhibited in hypophysectomized rats. These results were interpreted by Shoshan *et al.*, as indicating that hypophysectomy inhibits the first step in intermolecular cross-linking of collagen by affecting the production or activity of lysyl oxidase, a pituitary-dependent enzyme (Shoshan *et al.*, 1972).

Food intake is an important factor in collagen ageing. The rate of the increase in collagen fibre tensile strength with age in RTT, is reduced by 30% in food-restricted rats (Everitt *et al.*, 1983). Food is required for the synthesis of collagen and for the ageing or cohesion of collagen fibres (Everitt *et al.*, 1983). Hypophysectomy also decreases the appetite thus the rats have a lowered food intake. When a comparison is made of the collagen age, as measured by the breaking time in urea of RTT fibres from hypophysectomized rats and food restricted rats eating the same amount of food, the hypophysectomized rats are found to be significantly "younger". Therefore the pituitary gland secretes a factor which accelerates the ageing of collagen independently of changes in food intake (Everitt & Delbridge, 1976). Thyroidectomy has a similar anti-ageing effect on collagen in RTT, and thyroxine accelerates these age changes (Everitt & Delbridge, 1976). The ageing process is also accelerated by Adrenocorticotrophic hormone (ACTH), which was shown by Arvay and Takacs (1965), to increase the ageing of collagen fibres in RTT. ACTH is released under conditions of stress, and stimulates the secretion of corticosteroid hormones from the adrenal cortex (Everitt &

Delbridge, 1976). Thus to summarise, the acceleration of collagen ageing is closely related to the amount of food consumed, which is regulated by pituitary and thyroid hormones. Corticosteroids also increase the ageing of collagen, but act independently of food intake (Everitt & Delbridge, 1976).

4.3.3. Exercise Increases The Breakdown Of Cross-Links In Tendon

Some research has suggested that exercise or mobilization may be a determining factor in preventing cross-linking (Woo *et al.*, 1982). Exercise has been shown to decrease the increased stiffness occurring in tendons with old age (Naresh & Brodsky, 1992). Despite the fact that exercise is known to increase the concentration of collagen in the tendons (Woo *et al.*, 1982). Indicating that exercise increases the breakdown of cross-links in the tendon. In immobilisation it has been shown that the tendons and ligaments around the knee lose significant quantities of their biochemical constituents, such as water and glycosaminoglycan concentrations. An increase in collagen cross-linking in these tissues has been found following a period of nine weeks of lack of motion (Woo *et al.*, 1982).

4.3.4. The Length Of The Toe Region Decreases With Increased Age

The length of the toe region in the stress-strain curve of the RTT decreases with increased age due to a systematic decrease in the crimp angle with age for RTT (Torp *et al.* 1975a). According to a model devised by Diamant *et al.*, (1972) a decease in the crimp angle decreases the strain at which the fibrils become perfectly oriented and, therefore, at which the tendon suddenly stiffens. Thus fibril reorientation accounts, at least in part, for the age-related increase in stiffness of the RTT which is demonstrated by mechanical testing in vitro (Diamant *et al.*, 1972). The tangent modulus in the linear region increases with increased age in the RTT indicating the stiffness of the collagen fibre is increased (Torp *et al.* 1975b). Torp *et al.*, 1975b found that in RTT a stiffness increase of 130% from rats aged 1.5 months to 23 months. Diamant et al., 1972 found 81% increase in stiffness in RTT in rats aged from 3 months to 32 months (see figure 4.7). With age in RTT it has been found the failure stress increases whereas the failure strain decreases (Torp *et al.*, 1975b).

4.4. Effects Of Oestrogen And Testosterone On Tendon

It is generally agreed that collagen formation is more pronounced in males than in

females (Kao, *et al.*, 1957). However to my knowledge, it is not known whether tendons are stiffer in males than in females. The collagen content of the uterus has been found to increase after oestradiol administration and pregnancy (oestrogen levels increase) (Harkness, 1964) and decrease after ovariectomy and delivery (oestrogen levels decrease) (Harkness *et al.*, 1954). The effect of ovariectomy and delivery upon the collagen content of the uterus may be inhibited by oestrogen administration (Deyl *et al.*, 1976). Ovariectomy at an early age in female rats, has been shown to slow the rate of collagen ageing in RTT (Arvay, 1976). Thus it is possible oestrogen could increase the collagen content of the tendon by increasing the collagen content directly, or by increasing the cross-links which leads then to an increase in the collagen content, due to decreased breakdown of collagen (Deyl *et al.*, 1976).

In castrated male rats, collagen formation has been found to be decreased in the skin (Deyl *et al.*, 1976). Correspondingly, Smith & Allison (1965) reported an increased collagen content of skin and femur in young female rats after testosterone administration. In addition an increased mechanical strength of wounds after testosterone treatment has been found (Deyl *et al.*, 1976). Similarly for tendon it has been shown that in the extracellular tendon matrix, the number of dysplastic (an abnormal growth of collagen fibres) collagen fibrils is significantly increased as a function of the duration of androgen administration. In accordance with this finding anabolic steroids are often used in the treatment of ruptured tendons (Michna & Hartmann, 1987). Testosterone is known to cause a general increase in the connective tissue of muscle, and is thought to occur simultaneously with the increase in muscle bulk brought about by androgens in men (Alnaqeeb *et al.*, 1974).

4.5. Current Experiments

The present series of experiments were conducted on extensor digitorum longus (EDL) tendons from young adult, castrated and ovariectomized mice to see if any difference in the stiffness in the tendons exists. Alexander (1988), has said it is hard to calculate the strains in the tendon because it is difficult to know where in the clip the tendon is being gripped and in addition the clamps severely distorted the tendon in order to grip it. If so, it should be equally hard to determine correctly the compliance of the tendon. Markers were therefore placed on the tendons from four young adult mice to divide it

into three sections. This was done in order to firstly determine whether the tendon maybe slipping in the clips or damaged by the clips and secondly to determine whether the tendon stretches uniformly.

4.6. Methods

The experiments were performed on EDL tendon dissected from mice, killed by dislocation of the neck. Two tendons were used from each mouse, one from each leg, taken from the third toe (see figure 4.8). The mice had unrestricted access to a standard diet. Various categories of mice were used:

1) Ovariectomized mice: aged 15 months, ovariectomized at 5 months. 15 months is about middle aged for a mouse, the average life span of a mouse is about 30 months.
2) Female control mice: aged 15 months, the same stock as the ovariectomized mice but not operated on.
3) Castrated mice: aged 15 months, castrated at 5 months.
4) Male control mice: aged 15 months, the same stock as the castrated mice but not operated on.
5) Young adult male and female mice aged 3-5 months.

After dissection aluminium foil (150 μm thick) 'T' clips were folded over and pressed down on to each end of the tendon. Aluminium clips were used rather than thread because they would not add any appreciable amount of series elasticity to the tendon. Since the present experiment is trying to determine the amount of tendon compliance, it is not desirable that more series elasticity should be added to the tendon. The experiments were conducted on the tendons on the same day they were dissected from the mice. The current experiments were performed at 25°C, Rigby *et al.* (1959), found that there was no alteration in RTT between 0 and 37°C.

4.6.1. Bathing Solution

The Ringer solution contained 115mM NaCl, 5mM KCl, 0.5mM $MgCl_2$, 2.5mM $CaCl_2$, 1mM NaH_2PO_4, 24mM $NaHCO_3$ and 11mM glucose. The solution was gassed continuously with 95% O_2, 5% CO_2, the bath temperature was maintained at a temperature of 25 $\pm$ 0.5°C and the mean pH of the bathing solution was 7.5.

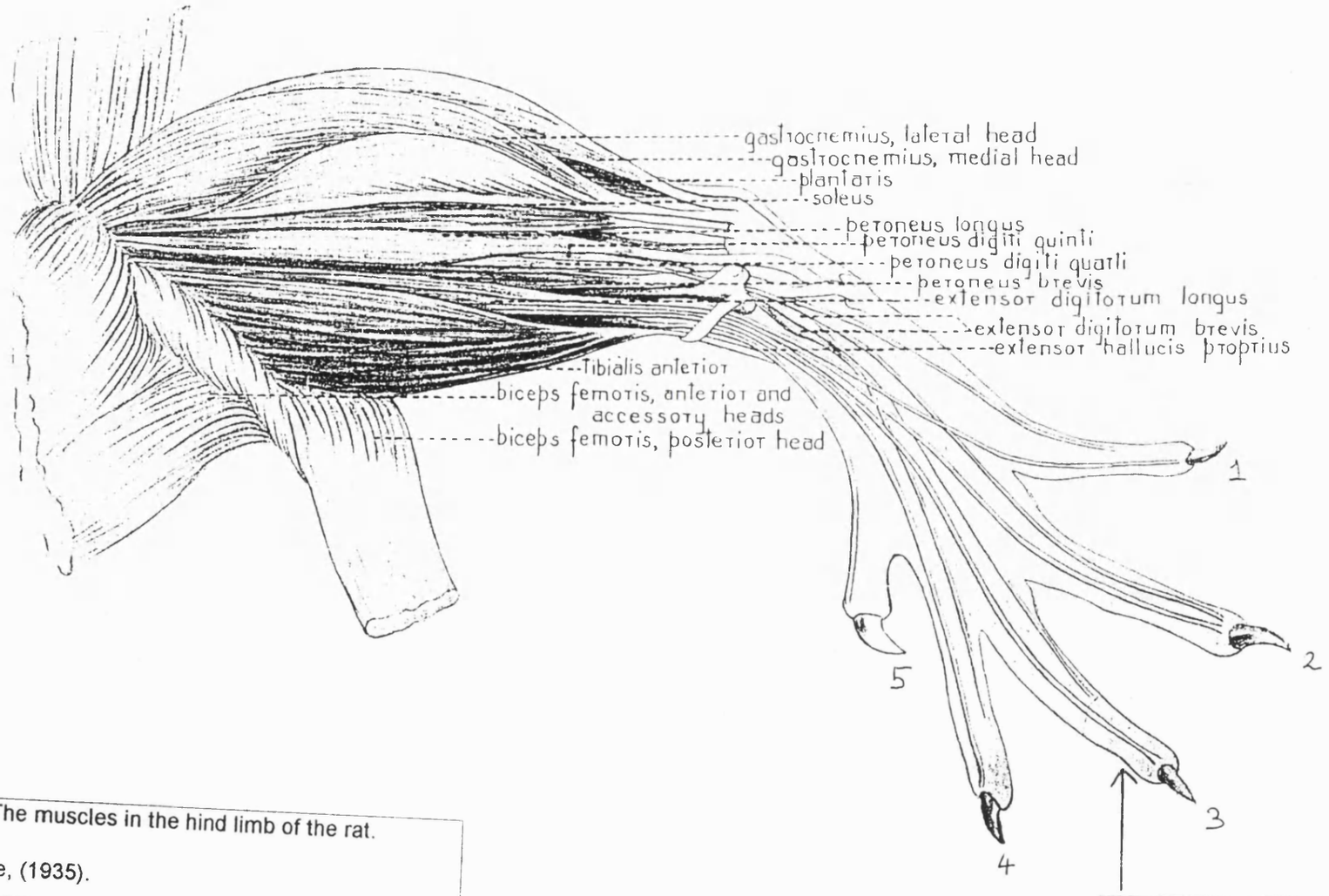

Figure 4.8. The muscles in the hind limb of the rat.

From Greene, (1935).

4.6.2. Tendon Force Measurement

The foil 'T' clips attached to the tendon were placed over hooks in the tendon bath, one a fixed hook attached to a force transducer and the other on the lever of the length transducer, which is connected to a micrometer gauge for accurate length adjustments and was controlled by a dual mode motor (Cambridge Technology Inc. USA., Model No. 350). The Cambridge motor output was displayed, analyzed and stored on an oscilloscope (Nicolet 420) (see figure 4.9). The force transducer was constructed of a nickel bar with a 2mm strain gauge (120 ohm) stuck on either side of it. The force transducer was calibrated by hanging known weights on the steel hook to which the tendon attaches. The weights (5-20g) were successively increased then decreased and the output voltage was recorded for each weight. For the tendon experiments the force was not measured from the same end as the motor. Since in this situation movement artifacts are created on the force trace. Although in the case of muscle measurements this artifact can be eliminated by doing an unstimulated control record for each trace and subtracting it from the stimulated record. However for the tendon it is not possible to do an unstimulated control, since the tendon can not be stimulated. Thus for the tendon experiments the force was measured at the opposite end to the motor.

4.6.3. Tendon Length

The length of the tendon could be adjusted by the micrometer gauge attached to the lever of the length transducer. The absolute tendon length was measured using the microscope eyepiece graticule, at a magnification of three times. The microscope was calibrated using a stage micrometer. The tendon weight wet was obtained by blotting the tendon briefly with a tissue. Dry weight was obtained by leaving the tendon to dry at approximately 30°C until a constant weight was obtained. A section of approximately 6mm long from the middle of the EDL tendon was used for the measurements. The tendons were normalized for size, by calculating the CSA of the tendon from the formula:

Tendon CSA = Tendon wet mass (mg) / Density (mg/mm^3) X Tendon length (mm)
Density was taken to be 1.12 mg/mm^3 (Ker, 1981).

The force normalized for tendon size is expressed as force/CSA i.e. N/mm^2. The tendon

length was measured as the length of tendon between the inside of the clips (see figure 4.10a).

4.6.4. Quick Length Changes

The stiffness of the tendon was measured by imposing quick length changes (around 0 to 7% of the tendon length) on the tendon. The stretch or the release was held for 100ms. The amplitude of the length change was increased from small to larger values, rather than vice versa, to avoid damaging the tendon with large stretches before observing the small ones. The tendon was given 1 minute rest in between length changes. The tendon was placed in the Ringer bath at an initial slack length, the tendon was then lengthened until it was no longer slack (as judged by microscopic observation), this length was defined as the unstretched tendon length. The tendon was then stretched by around a further 3-4%. The length changes were performed on the tendon starting at this 3-4% stretched length. This was done because, a reference point, is required to define where the tendon was stretched and released from. In order to facilitate the identification of this point it is desirable to start the releases and stretches on the tendon on the linear portion of its stress-strain curve. Thus although the starting stretch given to the tendons varied between 3-4%, this was taken to be preferable to starting the experiment with the tendon at 0% stretch, and having to determine the zero point from the asymptotic approach of the stress-strain curve to zero.

The releases and stretches were of such a range of magnitudes so as to represent the magnitude of force the tendon is subjected to whilst it is attached to its muscle. Although tendons are more compliant than muscle, the forces it is subjected to are the same as its muscle. The amplitude of the stretches were only taken up to a value that gave approximately two times the maximum isometric force of the EDL muscle (isometric force of EDL muscle is 0.36N, Brooks & Faulkner, 1991) so as not to damage the tendon fibres by excessive stretching.

The length changes were imposed by the Cambridge motor which was controlled by a ramp generator. The speed was kept constant when changing the size of the amplitude of the length change. The length step time from 10 to 90% was 2ms. In addition length steps of 100ms were also conducted on the tendons from young adult mice, to observe

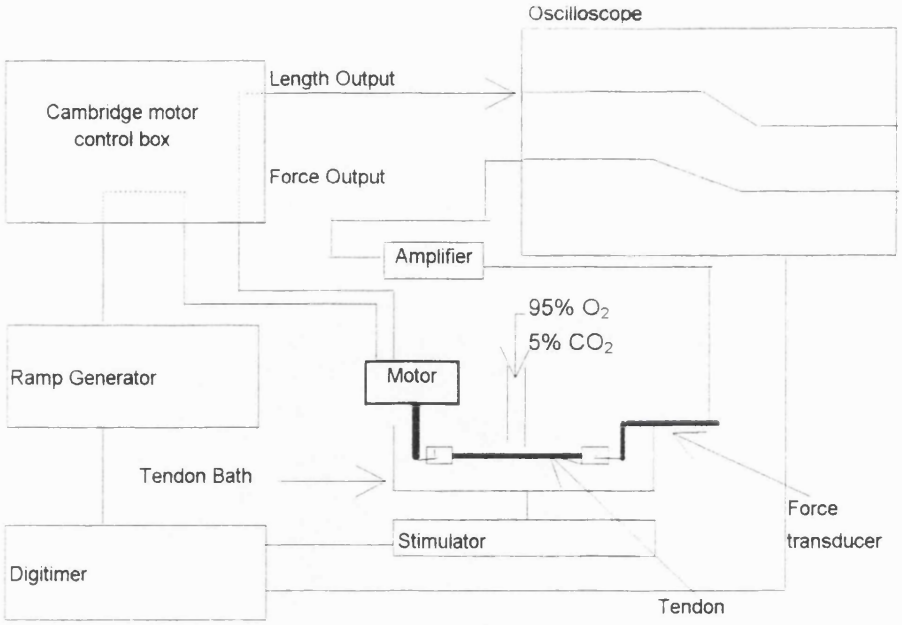

Figure 4.9. A schematic diagram of the experimental apparatus used for force and length measurements.

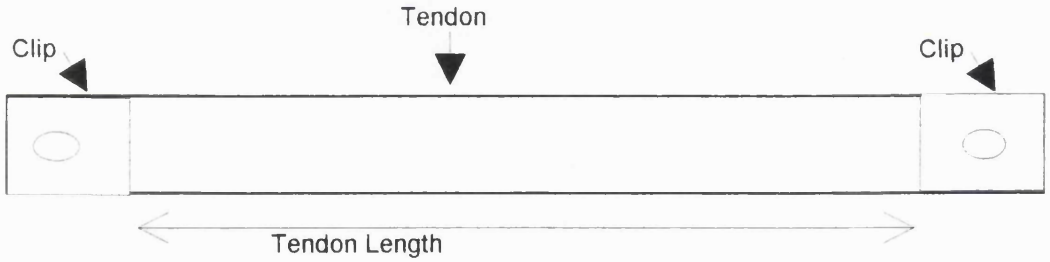

Figure 4.10a. A schematic diagram of the tendon, showing the how the length of the tendon was measured.

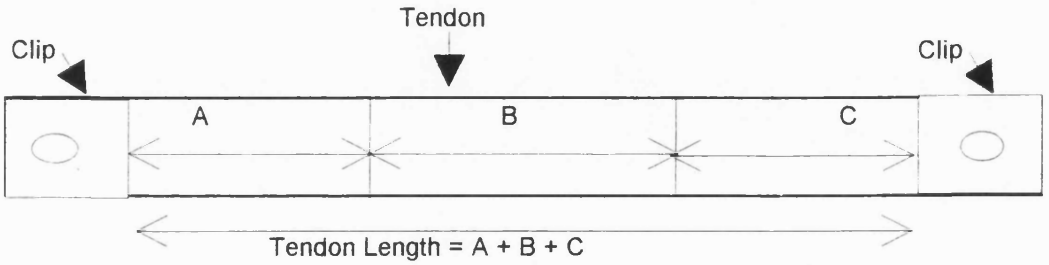

Figure 4.10b. A schematic diagram of the tendon, showing the position of the markers dividing the tendon up into sections.

the effects of changing the speed. Length changes of 2ms and 100ms were considered to represent a quick and slow movement. Landing for example is a 1ms event, this can be compared with a slow stretch which can take 100ms.

4.6.5. Markers

Markers were placed along the length of the tendons, from four young adult mice, to divide the tendon into three sections (of around 2mm in length) (see figure 4.10b). The most reliable method was found to be to place a thin line of black Dylon leather dye applied to the tendon with a fine pin, on to the tendon at its 3% stretched length. The dye did not penetrate the tendon, but stained the surface and it did not wash off in Ringer solution. One edge of the dye stain was used to give a sharply defined marker. The tendon was subjected to quick stretches and releases to determine the tendon stiffness, as previously described. The length of each section of the tendon during the stretches was determined by the microscope eyepiece, at 3 times the magnification. It was necessary to repeat the stretches a few times, in order to enable the length of each section of the tendon to be determined. The microscope eyepiece was calibrated using a stage micrometer.

4.7. Results

4.7.1. Stress-Strain Curve

The results of one tendon experiment are presented in detail: Figure 4.11, shows the force and length traces from one length change experiment, on a tendon from a young adult mouse. Figure 4.12, is a graph of the force change in the tendon (N/mm^2) plotted against the percentage length change of the tendon (the results are given as a percentage of the unstretched length of the tendon). The minimum force obtained (see table 4.2) was re-defined to be zero by subtracting the minimum force from all the forces. This was done because the experiment was performed with the tendon at an initial length of 3% stretched. The resultant force is called the transformed force. Similarly the largest length release was subtracted from all the length change values to re-define it to be zero. The resultant length changes are called the transformed % length change. Figure 4.13 shows the transformed % length change plotted as a function of the transformed force.

The relationship between tension change and length change in the tendon appears to be

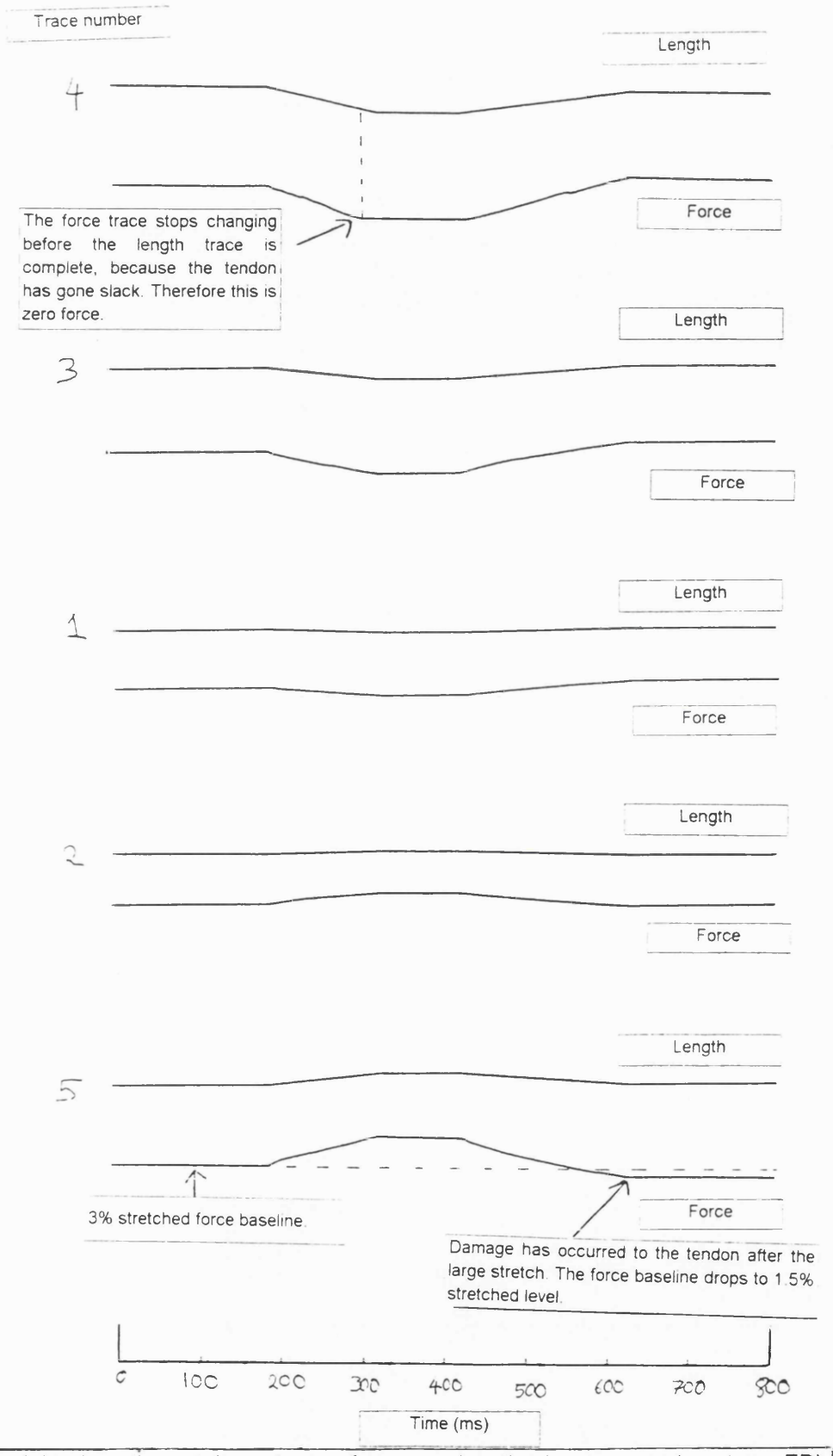

Figure 4.11. Length and force traces from one length change experiment on EDL tendon (plotted on figure 4.12.). The trace number refers to the number of the trace as plotted on figure 4.12.
Length step = 100ms.

Young adult tendon		
weight	0.033	mg
tendon length	6	mm
Weight/Length	0.0055	mg/mm
step speed	100	ms

Trace No.	% length change of tendon (unstretched length)	Force (N/mm^2)	Transformed % Length Change	Transformed force (N/mm^2)
4	-3.76	-24.82	0.00	0.00
3	-1.84	-17.67	1.92	7.15
1	-0.56	-6.55	3.20	18.27
Start point	0.00	0.00	3.76	24.82
2	0.56	9.03	4.32	33.85
5	1.84	24.22	5.60	49.04

Table 4.2. The results of one tendon stretching experiment are shown. See page 204 for definition of the terms.

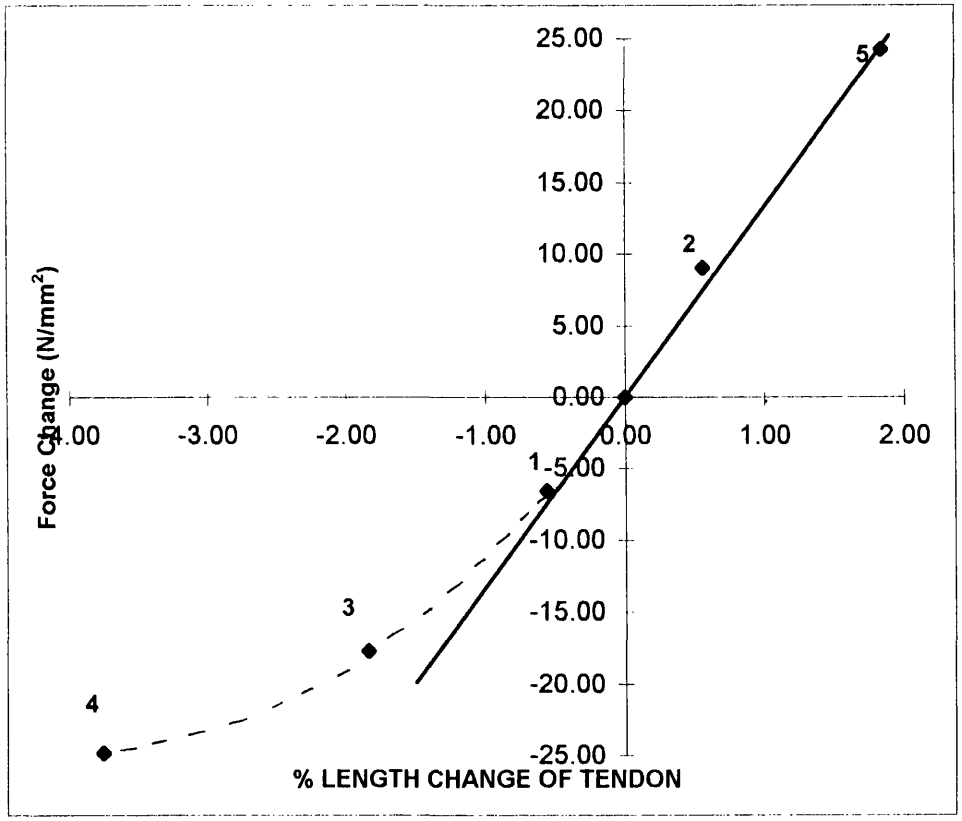

Figure 4.12. Data from the tendon stretching experiment, shown in table 4.2. Force developed in the tendon is plotted as a function of the percentage length change of the tendon. The numbers refer to the order in which the measurements were made.

Length step = 100ms.

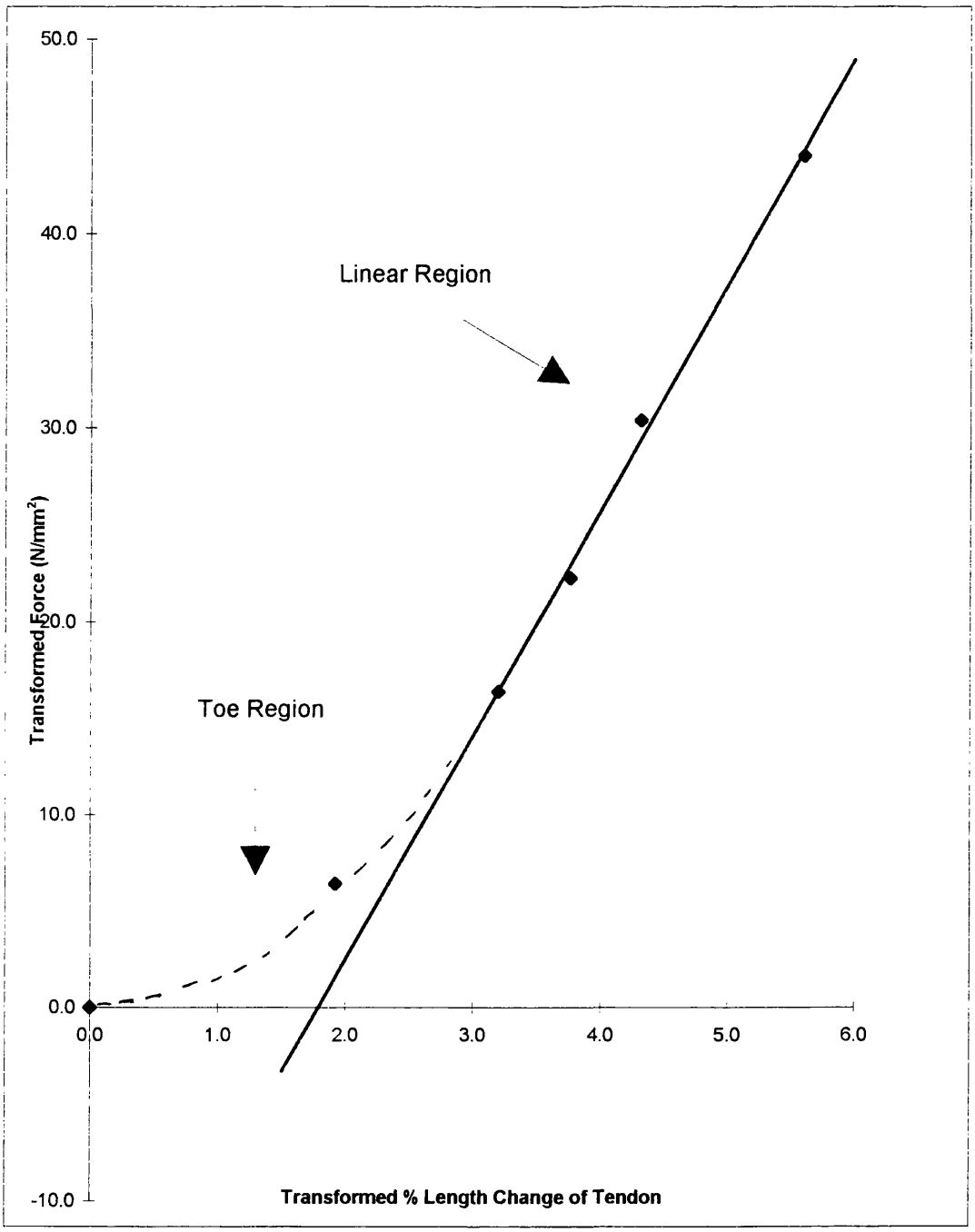

Figure 4.13. Data from the tendon stretching experiment, shown in table 4.2. Transformed force developed in the tendon is plotted as a function of the transformed percentage length change of the tendon. This is the same graph as that shown in figure 14.12, except that here the minimum length change and force observed have been re-defined to be zero (see page 204 for details). The regression line is fitted through the linear region.

Young's modulus (of linear region) 1162 N/mm^2.

Length Step = 100ms

S-shaped. There is a toe region, a linear region which shows the compliance and a yield region is known to exist. The regression line has been fitted to go through the linear region. The stiffness of the tendon is defined as the slope of the linear region, the reciprocal of this is the compliance. The yield point was not determined to avoid damaging the tendon, since the current experiments were primely concerned with determining tendon stiffness. The results from the rest of the experiments are tabulated in table 4.3.

4.7.2. Variability

Comparing Young's modulus for the tendon from one mouse to the next within the experimental categories, there seems to be large variations in Young's modulus between animals, the average coefficient of variation for all the groups was found to be 15%. However, as can be seen on figure 4.13, the experimental points lie well on the fitted regression line, which indicates that the line is fitted well to the points. Thus it seems that the variations are due to actual variations in the tendon stiffness between tendons. Similarly Ker, (1981) found a coefficient of variation of 15% between the stiffness of plantaris tendon of sheep. Comparing the variation in stiffness from tendons from the same animal smaller coefficient of variations are obtained, an average value of 4.2% was found (see table 4.4).

4.7.3. The Linear Region

No significant difference was found between the stiffness of the tendons from the control female and control male mice, therefore these two groups of mice were combined to make one group (see table 4.5). Similarly no significant difference was found between the ovariectomy and castrated mice, and thus these two groups were combined into one group. No statistically significant difference was found between the stiffness of tendons from the operated and young adult mice. The operated mice were then compared with the control mice. The tendons from the control mice were found to be 15.3% stiffer than the tendons from the operated mice, ($p < 0.005$) (see table 4.5). When compared separately the castrated to the control male tendons and the ovariectomized to the control female tendons, both groups were found to be less stiff, although the difference was not significant at the 0.05 level of significance for the ovariectomized mice ($p < 0.2$). The tendons from the control mice (15 months) were

Young Adult	(Age 3-5 months)			Step speed	2ms
Tendon No.	Young's Modulus N/mm^2	Weight mg	Length mm	Weight / length mg/mm	x- intercept (end of toe region)
A1	1482	0.0275	6.00	0.0046	1.63
A2	1511	0.0310	6.10	0.0051	1.61
B1	1012	0.0305	6.53	0.0047	1.81
B2	1226	0.0394	7.19	0.0055	1.97
C1	1429	0.0361	7.80	0.0046	1.68
C2	1295	0.0330	6.00	0.0055	1.79
D1	984	0.0255	6.84	0.0037	1.79
D2	1007	0.0330	5.85	0.0056	1.94
Mean	1243.15	0.0320	6.54	0.0049	1.78
sd	221.19	4.46E-03	0.69	6.41E-04	0.13
sem	78.20	1.58E-03	0.24	2.27E-04	0.05
n	8	8	8	8	8
cv	17.79%	13.94%	10.58%	13.05%	7.50%

Control Female (Middle aged mice - 15 months)				Step speed	2ms
Tendon No.	Young's Modulus N/mm^2	Weight mg	Length mm	Weight / length mg/mm	x- intercept (end of toe region)
A1	1587	0.0407	6.90	0.00590	1.64
A2	1519	0.0482	7.41	0.00650	1.73
B1	1531	0.0419	6.30	0.00665	1.69
B2	1490	0.0329	6.96	0.00472	1.73
C1	1616	0.0464	6.60	0.00704	1.61
C2	1595	0.0577	8.91	0.00648	1.61
D1	1098	0.0377	6.33	0.00595	1.61
D2	1136	0.0339	6.57	0.00516	1.56
Mean	1446.45	0.0424	7.00	0.0060	1.65
sd	207.81	8.23E-03	0.85	7.85E-04	0.06
sem	73.47	2.91E-03	0.30	2.78E-04	0.02
n	8	8	8	8	8
cv	14.37%	19.39%	12.21%	12.98%	3.68%

Mean Young's Modulus coefficient of variation 14.87%

Table 4.3. Summarizes all the data from the tendon experiments. The wet to dry weight ratio is 4 to 1.

Tendons numbered with the same letter were obtained from the same animal.

Table 4.3 is continued on the next page

Control male (Middle aged mice - 15 months)				Step speed	2ms
Tendon No.	Young's Modulus N/mm^2	Weight mg	Length mm	Weight / length mg/mm	x- intercept (end of toe region)
A1	1398	0.0336	6.84	0.0049	1.67
A2	1420	0.0577	8.91	0.0065	1.64
B1	1624	0.0474	6.39	0.0074	1.53
B2	1546	0.0300	6.39	0.0047	1.65
C1	1731	0.0427	7.02	0.0061	1.49
C2	1626	0.0535	6.63	0.0081	1.57
D1	1234	0.0402	6.99	0.0057	1.70
D2	1295	0.0397	6.30	0.0063	1.59
E1	1534	0.0600	7.11	0.0084	1.62
Mean	1489.82	0.0450	6.95	0.0065	1.61
sd	164.45	1.05E-02	0.79	1.30E-03	0.07
sem	54.82	3.49E-03	0.26	4.34E-04	0.02
n	9	9	9	9	9
cv	11.04%	23.27%	11.41%	20.18%	4.21%

Ovariectomized (Middle aged mice - 15 months)				Step speed	2ms
Tendon No.	Young's Modulus N/mm^2	Weight mg	Length mm	Weight / length mg/mm	x- intercept (end of toe region)
A1	1136	0.0360	6.96	0.0052	1.83
A2	1123	0.0200	6.93	0.0029	1.73
B1	1326	0.0450	6.81	0.0066	1.82
B2	1300	0.0330	6.48	0.0051	1.86
C1	1619	0.0480	7.23	0.0066	1.67
C2	1526	0.0390	6.87	0.0057	1.58
D1	1012	0.0250	6.93	0.0036	1.76
Mean	1291.78	0.0351	6.89	0.0051	1.75
sd	221.32	1.01E-02	0.22	1.42E-03	0.10
sem	83.65	3.83E-03	0.08	5.37E-04	0.04
n	7	7	7	7	7
cv	17.13%	28.81%	3.24%	27.87%	5.70%

Table 4.3 continued

Castrated (Middle aged mice - 15 months)				Step speed	2ms
Tendon No.	Young's Modulus N/mm^2	Weight mg	Length mm	Weight / length mg/mm	x- intercept (end of toe region)
A1	1542	0.0381	6.03	0.0063	1.75
A2	1418	0.0333	7.23	0.0046	1.72
B1	1352	0.0351	6.45	0.0054	1.79
B2	1109	0.0327	6.81	0.0048	1.62
C1	1285	0.0345	6.90	0.0050	1.83
C2	1383	0.0375	6.78	0.0055	1.72
D1	1095	0.0330	6.63	0.0050	1.79
D2	1141	0.0291	6.93	0.0042	1.84
E1	1022	0.0251	6.23	0.0040	1.79
Mean	1261	0.0332	6.67	0.0050	1.76
sd	176.50	4.04E-03	0.37	7.07E-04	0.07
sem	58.83	1.35E-03	0.12	2.36E-04	0.02
n	9	9	9	9	9
cv	14.00%	12.18%	5.61%	14.16%	3.83%

Table 4.3 continued

Young Adult	Age 3-5 months						
Tendon number	Young's Modulus	Tendon number	Young's Modulus	Tendon number	Young's Modulus	Tendon number	Young's Modulus
A1	1482	B1	1012	C1	1429	D1	984
A2	1511	B2	1226	C2	1295	D2	1007
Mean	1497		1119		1362		996
sd	20.506		151.321		94.752		16.263
sem	14.500		107.000		67.000		11.500
n	2		2		2		2
cv	1.37%		13.52%		6.96%		1.63%

Control Female	Middle aged - 15 months						
Tendon number	Young's Modulus	Tendon number	Young's Modulus	Tendon number	Young's Modulus	Tendon number	Young's Modulus
A1	1587	B1	1531	C1	1616	D1	1098
A2	1519	B2	1490	C2	1595	D2	1136
Mean	1553		1511		1606		1117
sd	48.08		28.991		14.849		26.870
sem	34.00		20.500		10.500		19.000
n	2		2		2		2
cv	3.10%		1.92%		0.92%		2.41%

Control Male	Middle aged - 15 months						
Tendon number	Young's Modulus	Tendon number	Young's Modulus	Tendon number	Young's Modulus	Tendon number	Young's Modulus
A1	1398	B1	1624	C1	1731	D1	1234
A2	1420	B2	1546	C2	1626	D2	1295
Mean	1409		1585		1679		1265
sd	15.56		55.154		74.246		43.13
sem	11.00		39.000		52.500		30.50
n	2		2		2		2
cv	1.10%		3.48%		4.42%		3.41%

Castrated	Middle aged Age 15 months						
Tendon number	Young's Modulus	Tendon number	Young's Modulus	Tendon number	Young's Modulus	Tendon number	Young's Modulus
A1	1542	B1	1352	C1	1285	D1	1095
A2	1418	B2	1109	C2	1383	D2	1141
Mean	1480		1231		1334		1118
sd	87.681		171.827		69.30		32.53
sem	62.000		121.500		49.00		23.00
n	2		2		2		2
cv	5.92%		13.96%		5.19%		2.91%

Ovariectomised	Middle aged - 15 months				
Tendon number	Young's Modulus	Tendon number	Young's Modulus	Tendon number	Young's Modulus
A1	1136	B1	1326	C1	1619
A2	1123	B2	1300	C2	1526
Mean	1130		1313		1573
sd	9.19		18.38		65.76
sem	6.50		13.00		46.50
n	2		2		2
cv	0.81%		1.40%		4.18%

Table 4.4. Young's modulus for tendon obtained from the same animal are compared. The average coefficient of variation for all groups is 4.2 %.

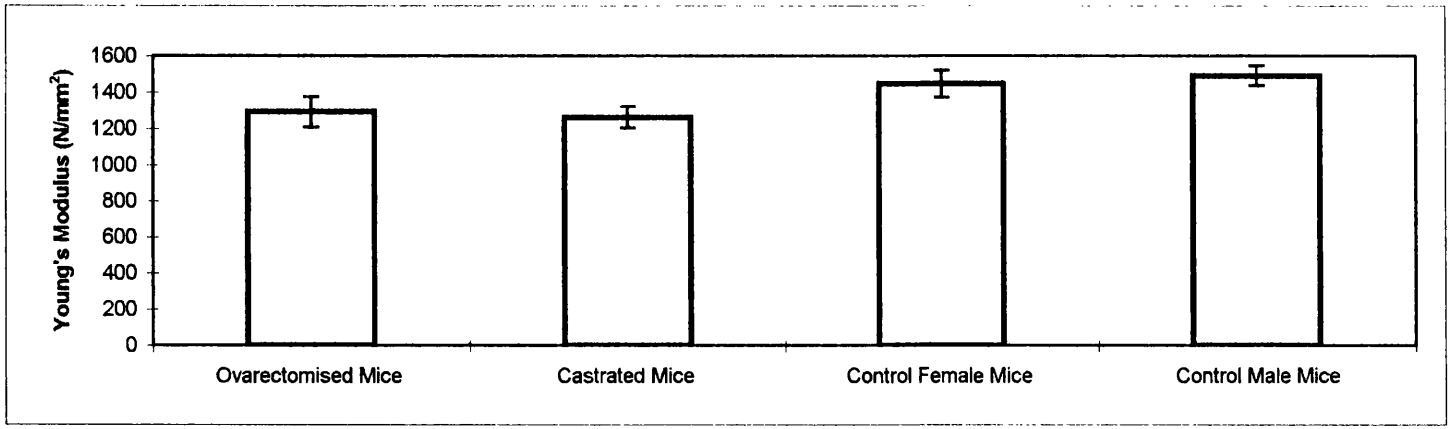

Figure ** Histograms of Young's Modulus for the various categories of mice. The value shown for each group is the mean (+/- sem). All categories of mice were middle aged mice (15 months).

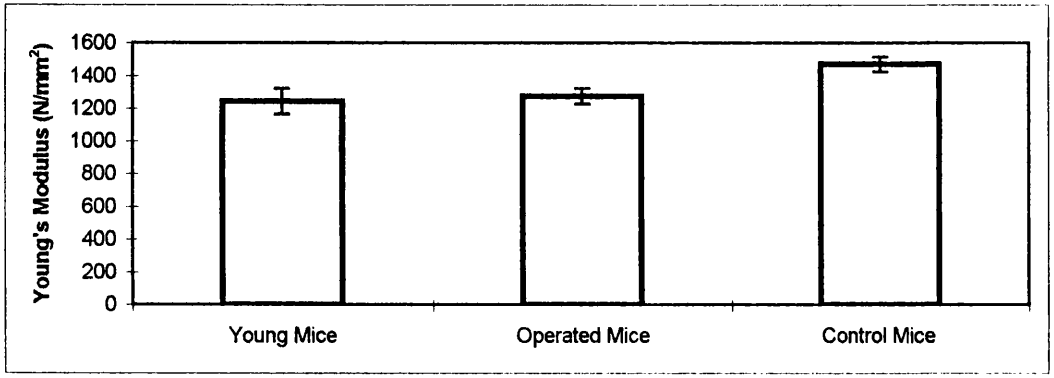

Figure 4.14. Histograms of Young's Modulus for the various categories of mice. The value shown for each group is the mean (+/- sem).

The operated and control categories of mice were middle aged mice (15 months).
The young mice aged3-5 months.

	Ovariectomized	*Control Female*
Mean	1292	1447
Observations	7	8
df	13	
t Stat	-1.395	
P(T<=t) two-tail	0.186	

	Castrated	*Control Male*
Mean	1261	1490
Observations	9	9
df	16	
t Stat	-2.849	
P(T<=t) two-tail	0.012	

	Control Female	*Control Male*
Mean	1447	1490
Observations	8	9
df	15	
t Stat	-0.480	
P(T<=t) two-tail	NS	

	Ovariectomized	*Castrated*
Mean	1292	1261
Observations	7	9
df	14	
t Stat	0.313	
P(T<=t) two-tail	NS	

	Operated	*Control Mice*
Mean	1274	1469
Observations	16	17
df	31	
t Stat	-3.010	
P(T<=t) two-tail	0.005	

	Young	*Operated*
Mean	1243	1274
Observations	8	16
df	22	
t Stat	-0.358	
P(T<=t) two-tail	NS	

	Control Mice	*Young*
Mean	1469	1243
Observations	17	8
df	23	
t Stat	2.715	
P(T<=t) two-tail	0.012	

Table 4.5. Student's unpaired t-test was performed on the Young's modulus data from the various categories of mice.
NS = non-significant at the 0.05 level.

In performing multiple t-tests it is possible that a significant result will be obtained by chance. The highest level of significance that occurs in the tests above is 0.005. This is a probability of 1 in 200 of obtaining the significant result. However seven tests have been performed, therefore there is a probability of 7/200, which is approximately a probability of 1/29 of obtaining a significant result by chance. Since this is a low probability it indicates the significant result in this case has not been obtained by chance.

found to be on average 18.2% stiffer ($p < 0.01$) than the tendons from the young adult mice (3-5 months). Thus indicating, as has previously been reported, ageing increases the stiffness of the tendons.

4.7.4. Toe Region

No significant difference was found between the length of the toe region of the stress-strain curve between the operated and young adult mice. The length of the toe region in the control mice was found to be approximately 6.8% smaller than in the operated or young adult mice (see figure 4.15, table 4.3 and table 4.6). The length of the toe region was determined to be the point at which the regression line of the linear region, intercepts the x-axis of the stress-strain curve (see figure 4.15).

4.7.5. Yield Point

The yield point was not determined so as not to cause too much damage to the tendon. All tendons were stretched to approximately 7% strain without the yield point occurring, although in some of the tendons at around 6% strain the force baseline after the stretch was found to be lowered (since the start point was 3% stretched), indicating damage had occurred to the tendon. Indicating this might be the beginning of the yield point. In RTT the yield point occurs at about 4% strain.

4.7.6. Weight / Unit Length

No significant difference was found between the weight / unit length between the tendons from the operated and young adult mice. The weight per unit length in the control mice was found to be approximately 26% larger than in the operated or young adult mice (see tables 4.3 and 4.7).

4.7.7. Viscoelasticity

The young adult tendons were subjected to two speeds of length change; 2ms and 100ms. These two speeds of release were imposed alternately on the tendon, the amplitude of the length change as described before was increased from small to larger values, to avoid damaging the tendon with large stretches before observing the majority of the results. Figure 4.16, shows the results from a typical experiment. The linear part of the curve is slightly steeper in the 2ms than in the 100ms step release. Showing that

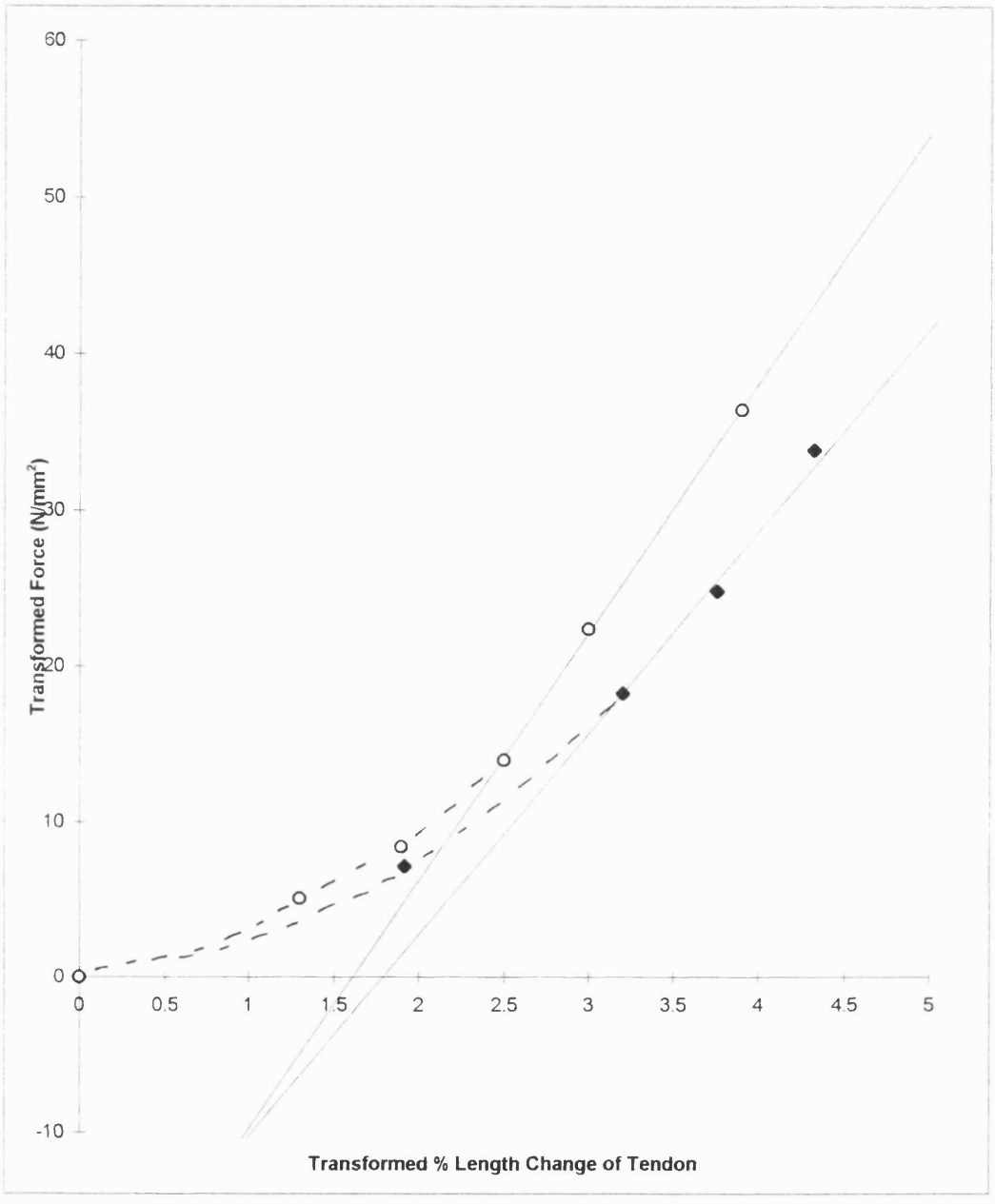

Figure 4.15. Force developed in the tendon plotted as a function of the % length change of the tendon. Results from a typical experiment for a tendon from a control female (middle aged - 15 months) (○) and young adult (3-5 months) (◆) mouse are shown. The length and force plotted are the transformed length and force (see page 204 for details). The regression lines are fitted through the linear parts of each trace. The toe region is shorter for the control female tendon than for the tendon from the young adult mouse. Length step = 2ms.

Young's modulus (linear region):
Control female tendon = 1595 N/mm^2
X-intercept = 1.61

Young adult tendon = 1295 N/mm2
X-intercept = 1.79

	Ovariectomized	*Control Female*
Mean	1.75	1.65
Observations	7	8
df	13	
t Stat	2.402	
P(T<=t) two-tail	0.05	

	Castrated	*Control male*
Mean	1.76	1.61
Observations	9	9
df	16	
t Stat	4.858	
P(T<=t) two-tail	0.001	

	Control Female	*Control Male*
Mean	1.65	1.61
Observations	8	9
df	15	
t Stat	1.325	
P(T<=t) two-tail	NS	

	Ovariectomized	*Castrated*
Mean	1.75	1.76
Observations	7	9
df	14	
t Stat	-0.298	
P(T<=t) two-tail	NS	

	Operated	*Control Mice*
Mean	1.76	1.63
Observations	16	17
df	31	
t Stat	5.084	
P(T<=t) two-tail	0.001	

	Control Mice	*Young*
Mean	1.63	1.78
Observations	17	8
df	23	
t Stat	-3.874	
P(T<=t) two-tail	0.001	

	Young	*Operated*
Mean	1.78	1.76
Observations	8	16
df	22	
t Stat	0.527	
P(T<=t) two-tail	NS	

Table 4.6. Student's unpaired t-test was performed on the x-intercept data from the various categories of mice. The length of the toe region was determined to be the point at which the regression line of the linear region of the stress-strain curve intercepts the x-axis of the stress-strain curve.

NS = non-significant at the 0.05 level.

	Ovariectomized	*Control Female*
Mean	0.00510	0.00605
Observations	7	8
df	13	
t Stat	-1.637	
P(T<=t) two-tail	0.126	

	Castrated	*Control Male*
Mean	0.00499	0.00646
Observations	9	9
df	16	
t Stat	-2.975	
P(T<=t) two-tail	0.009	

	Control Female	*Control Male*
Mean	0.00605	0.00646
Observations	8	9
df	15	
t Stat	-0.772	
P(T<=t) two-tail	NS	

	Ovariectomized	*Castrated*
Mean	0.00510	0.00499
Observations	7	9
df	14	
t Stat	0.200	
P(T<=t) two-tail	NS	

	Operated	*Control Mice*
Mean	0.00504	0.00627
Observations	16	17
df	31	
t Stat	-3.335	
P(T<=t) two-tail	0.002	

	Control Mice	*Young*
Mean	0.00627	0.00491
Observations	17	8
df	23	
t Stat	3.274	
P(T<=t) two-tail	0.003	

	Young	*Operated*
Mean	0.00491	0.00504
Observations	8	16
df	22	
t Stat	-0.312	
P(T<=t) two-tail	NS	

Table 4.7. Student's unpaired t-test was performed on the weight (mg)/ length (mm) data from the various categories of mice.

NS = non-significant at the 0.05 level.

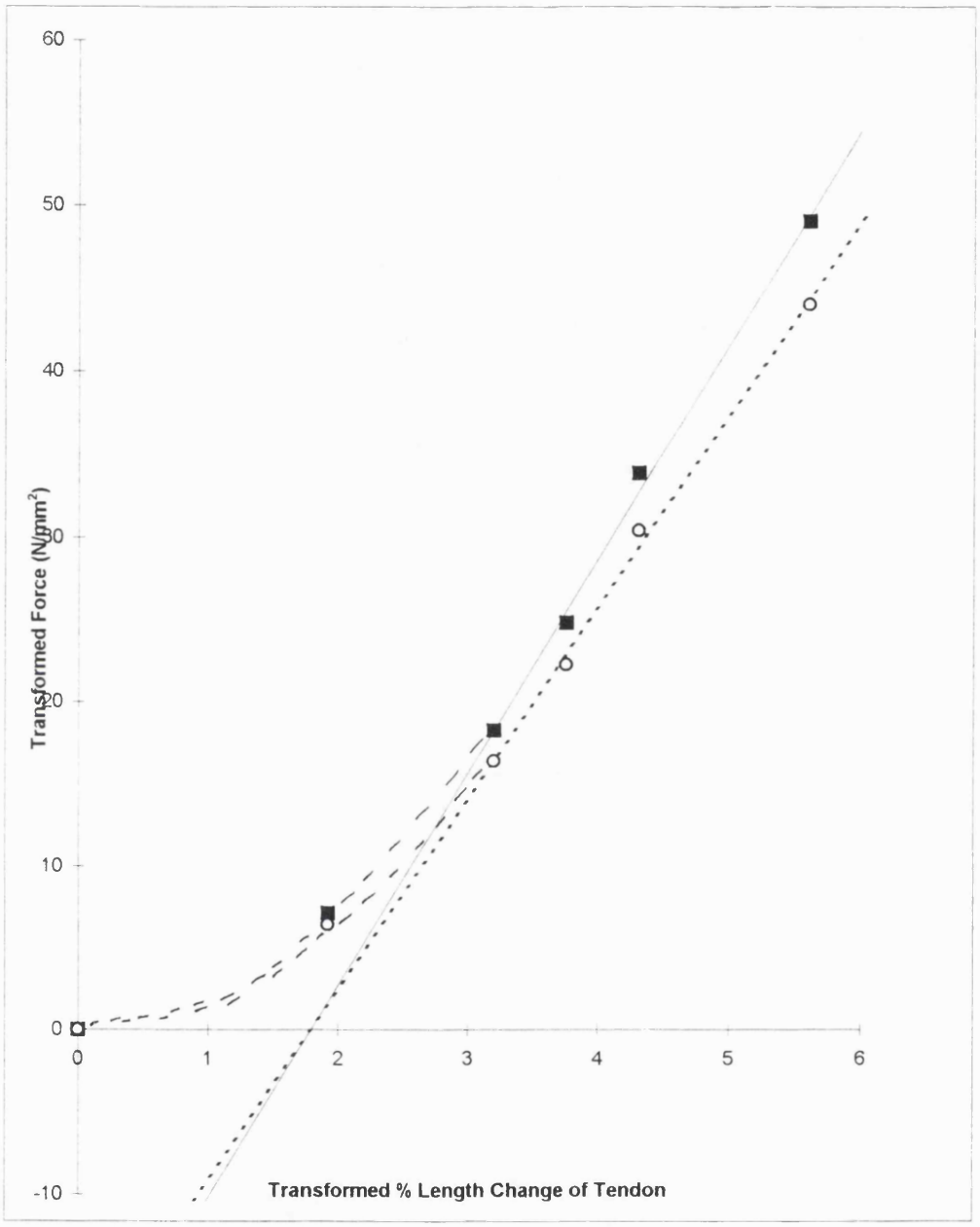

Figure 4.16. Force developed in the tendon plotted as a function of the % length change of the tendon subjected to two length change speeds, 2ms (■) and 100ms (○). Results from a typical experiment for a tendon from a young adult are shown. The length and force plotted are the transformed length and force (see page 204 for details). The regression line is fitted through the linear part of the trace. The tendon is stiffer at the faster step time.

Young's modulus (linear region):
2ms step time = 1295 N/mm^2

100ms step time = 1162 N/mm2

the stiffness of the tendon is greater at the faster length step compared to the slower length step. For all eight tendons tested at the two speeds this was found to be the case (average percentage increase 14.3 %), the paired t-test shows the significance at the 0.05 level (see table 4.8).

4.7.8. Markers

Markers were placed on the tendons from 4 young adult mice to divide it up into 3 sections, of around 2mm in length (see figure 4.10b). The tendon sections were normalized for size by dividing the length of the section by its starting length (3-4% stretched length). Similarly the tendon length was normalized, by dividing its length by its starting length (3-4% stretched length). The normalized section length was plotted as a function of the normalized whole tendon length (see figure 4.17). If the y-intercept obtained is zero then the section is stretching in proportion to the tendon length and the slope will be 1. If a section stretches to a greater proportion than its length the y-intercept is negative and if the section stretched to a lesser proportion than its length the y-intercept is positive. At dissection the tendon ends were identified: the end attached to the toe was identified as section A; the end attached to the EDL muscle was called section C. However no significant difference was found in the y-intercepts obtained between the two ends of the tendons (sections A & C) (see tables 4.9a & b). No significant difference was found between the y-intercepts from the end sections (sections A and C) and the middle section (section B). Thus it is concluded that the tendon is neither slipping in the clip nor damaged by it.

Figure 4.18, simulates a tendon with two sections, in which both sections stretch in proportion to its length. Section B was made to be initially twice as long as section A. It can be seen that the y-intercept for each section is zero. In the current experiments it was expected that the y-intercepts for the different sections of the tendon would add up to zero, if the length of the sections add up to the total length of the tendon. This was found to be the case with the un-normalized data, but not for the normalized data (see table 4.9). Figure 4.19, simulates a tendon with two sections of equal length, A and B: Section A was made to be 3 times as stiff as section B and therefore section A stretches three times less than section B. The data for each section was normalized, by dividing the section length by its starting length and plotted as a function of the

Young	Tendons	Age 3-5 months		
Tendon number	Young's Modulus fast release (2ms)	Young's Modulus slow release (100ms)	Difference fast-slow	% Increase in stiffness
A1	1482	1302	180.14	13.8
A2	1511	1348	162.67	12.1
B1	1012	926	85.95	9.3
B2	1226	1044	181.56	17.4
C1	1429	1240	188.41	15.2
C2	1295	1163	132.44	11.4
D1	984	834	150.01	18.0
D2	1007	844	163.24	19.3
Mean	1243.13	1087.58	155.55	14.6
sd	221.20	205.13	33.55	3.5
sem	78.20	72.52	11.86	1.3
n	8	8	8	8
Mean stiffness increase =		14.30%		

t	13.11
df	7
p	Significant at the 0.05 level of significance

Table 4.8. Student's paired t-test shows the Young's Modulus of the tendon at 2ms step speed is significantly faster than at 100ms step speed.

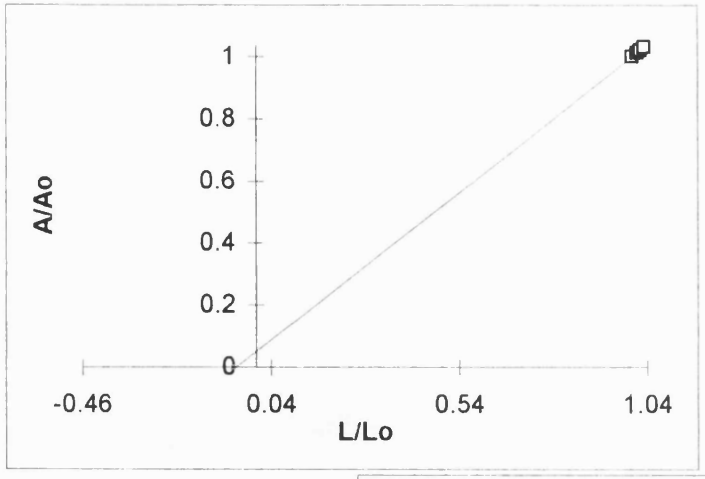

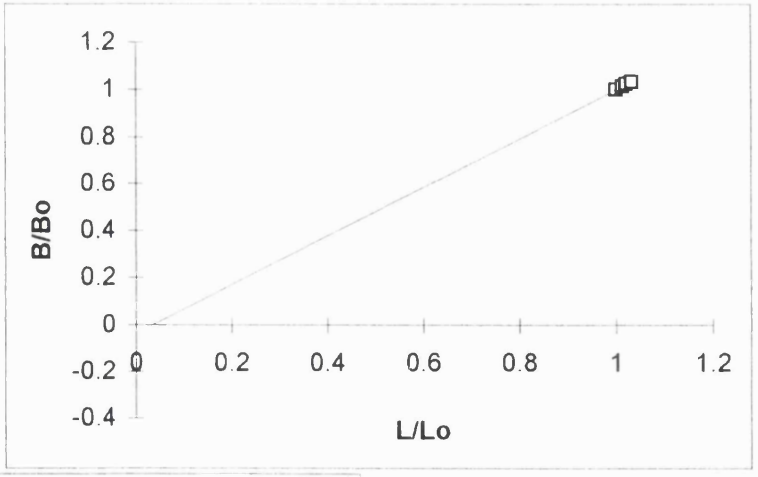

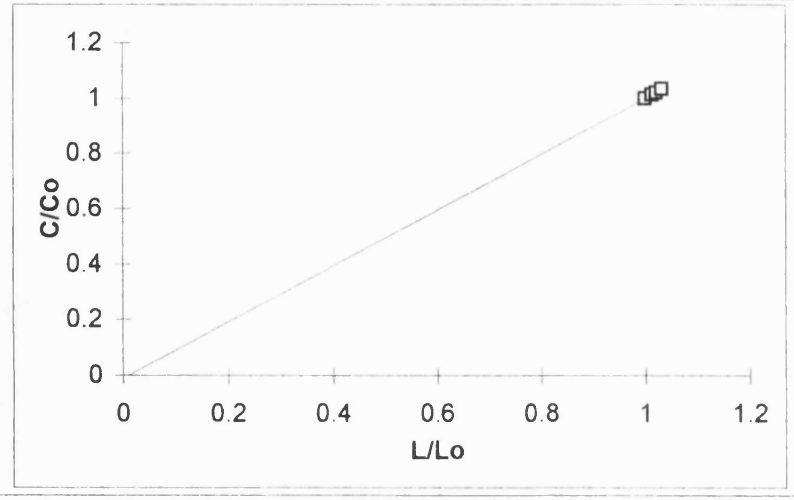

Figure 4.17. Shows the results from one marker experiment. The tendon was divided into 3 sections, called A, B, and C. The length of the section (e.g. A) was normlized for size by dividing by its 3% stretched starting length (e.g. A/Ao). The normalized section length was plotted as a function of the normalized tendon length (L/Lo). The regression line is constrained to go through the start point since it is known with certainty, if the tendon is not stretched there is no length change.
Tendon length (Lo) = Ao + Bo + Co

Tendon No. A1				
Section	Length (mm)	Slope	Normalized y-intercept	Unnormalized y-intercept
A	1.97	0.949	0.051	0.10
B	2.16	1.037	-0.037	-0.08
C	2.06	1.010	-0.010	-0.02
Sum	6.19		0.004	0.00

Tendon No. A2				
Section	Length (mm)	Slope	Normalized y-intercept	Unnormalized y-intercept
A	2.01	1.09	-0.090	-0.18
B	2.17	0.93	0.068	0.15
C	2.11	0.98	0.015	0.03
Sum	6.29		-0.007	0.00

Tendon No. B1				
Section	Length (mm)	Slope	Normalized y-intercept	Unnormalized y-intercept
A	2.21	0.98	0.023	0.05
B	2.29	1.09	-0.088	-0.20
C	2.23	0.93	0.069	0.15
Sum	6.73		0.003	0.00

Tendon No.B2				
Section	Length (mm)	Slope	Normalized y-intercept	Unnormalized y-intercept
A	2.49	1.03	-0.03	-0.08
B	2.31	0.94	0.06	0.14
C	2.62	1.02	-0.02	-0.06
Sum	7.42		0.006	0.00

Normalized y-intercept mean data				
Section	mean	sd	sem	n
A	-0.0117	0.062	0.031	4
B	0.0008	0.076	0.038	4
C	0.0123	0.041	0.020	4

B		
	Section A	*Section B*
Mean	-0.0117	0.0008
Observations	4	4
df	6	
t Stat	-0.255	
P(T<=t) two-tail	NS	

	Section A	*Section C*
Mean	-0.0117	0.0123
Observations	4	4
df	6	
t Stat	-0.646	
P(T<=t) two-tail	NS	

	Section B	*Section C*
Mean	0.0008	0.0123
Observations	4	4
df	6	
t Stat	-0.265	
P(T<=t) two-tail	NS	

Table 4.9a. Summarizes the data obtained in the marker experiments. The normalized y-intercepts do not add up to zero because the starting lengths were not the same. The unnormalized y-intercept is equal to the normalized y-intercept multiplied by the starting length of the section. The starting length of the tendon was taken as the 3% stretched length.
NS = non-significant at the 0.05 level of significance.
b) A Student's unpaired t-test was performed on the normalized y-intercepts from the marker experiments.
Length of tendon = Section A + Section B + Section C

Starting length of tendon (Lo)	Starting length of section A (Ao)	Starting length of section B (Bo)
1000	500	500

Section A y-intercept	0.5
Section B y-intercept	-0.5
Sum	0

Length of tendon (L)	Length of section A (A)	Length of section B (B)	L/Lo	A/Ao	B/Bo
1000	500	500	1.00	1.00	1.00
1100	525	575	1.10	1.05	1.15
1200	550	650	1.20	1.10	1.30
1300	575	725	1.30	1.15	1.45
1400	600	800	1.40	1.20	1.60

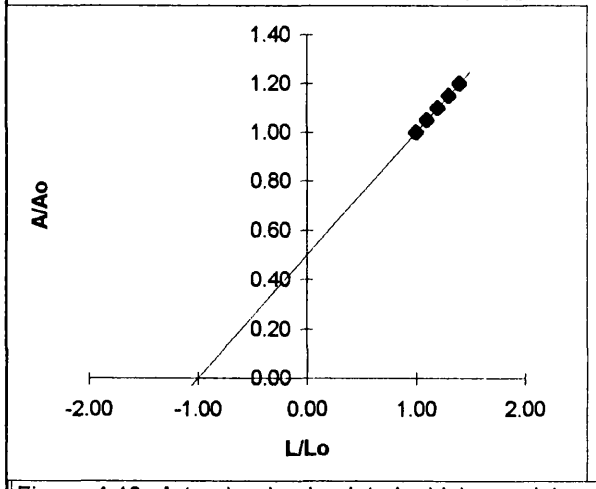

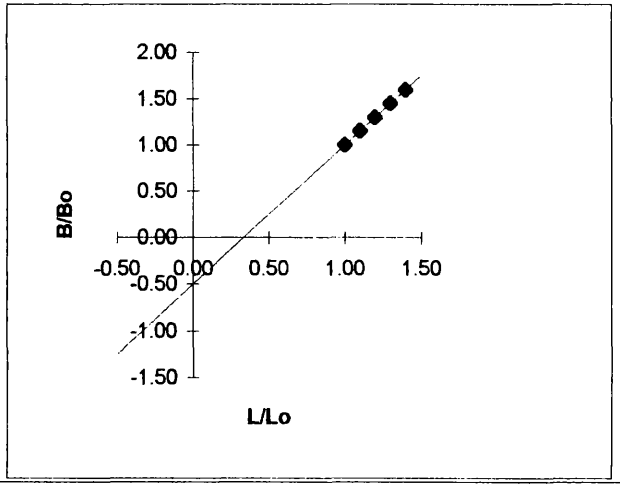

Figure 4.19. A tendon is simulated which consists of two section A and B, of initial equal length. Section A is three times as stiff as section B, and therefore section A stretches three times less than section B. The data for each section has been normalized by dividing the section length by its initial starting length. The y-intercepts of the regression line for the two sections add up to zero.

normalized tendon length. As was the case for the actual experimental results, a positive y-intercept was obtained for a section that stretched less and a negative y-intercept for a section that stretched more. The y-intercepts for the two sections added up to zero, because the section starting lengths were the same. The reason in the current experiment that the normalized y-intercepts do not add to zero, is because the starting lengths of the sections were not equal.

Thus to summarise the y-intercepts for the different sections of the tendon add to zero:
1) If the data is not normalized by dividing it by it's starting length.
2) If the data is normalized, but the starting lengths are the same for each section.

4.8. Discussion

The present series of experiments have shown that the measurements of tendon stiffness are variable, the coefficients of variation between tendons from different animals were found to be on average 15% for all groups. However previous workers have also found large variations in tendon stiffness. Ker (1981), found a coefficient of variation of 15% between the stiffness of plantaris tendon in sheep. The variation between tendons (4%) from the same mouse was found to be smaller than between mice. The results from the marker experiments, show the section of the tendons next to the clips and the middle section stretch in proportion to the tendon length. This shows that the tendon stretches uniformly and thus the whole tendon is not damaged by the clip, nor is the tendon slipping in the clip. It is possible that the large variation found in the stiffness values from different mice used in the current experiment, is due to the possibility that these animals might have different muscle strengths. The coefficient of the mean for the variation in muscle strength for mouse EDL muscle has been found to be 11.4% (Brooks & Faulkner, 1991). This is of a similar magnitude to the variation in tendon stiffness and thus supports this argument. This seems a likely proposition since it is known that muscle, tendon and bone strength are all interlinked. These points indicate that the variations in stiffness are due to physiological reasons rather than experimental errors.

4.8.1. Viscoelasticity

In accordance with previous workers findings (Herrick *et al.*, 1978) when the tendon

Original length of the tendon (Lo)	Original length of section A (Ao)
15	5

Length of the tendon (L)	Length of section A (A)	L/Lo	A/Ao
15	5	1	1
30	10	2	2
60	20	4	4
120	40	8	8

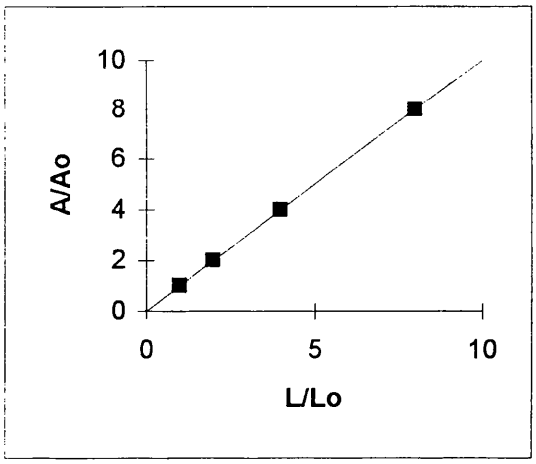

Original length of the tendon (Lo)	Original length of section B (Bo)
15	10

Length of the tendon (L)	Length of section B (B)	L/Lo	B/Bo
15	10	1	1
30	20	2	2
60	40	4	4
120	80	8	8

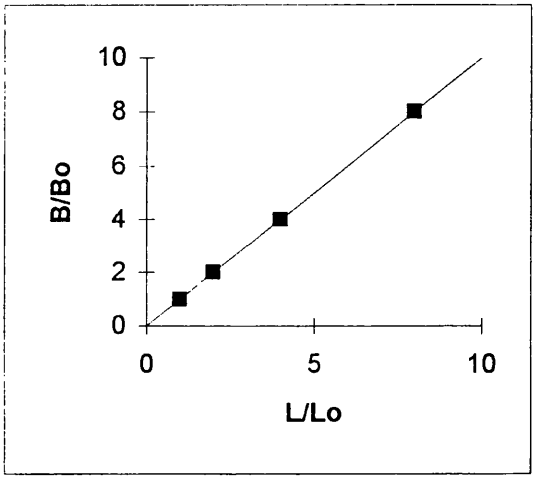

Figure 4.18. Simulation of a tendon with two sections. Both sections stretch in proportion to its length. Section B was made to be initially twice as long as section A. The y-intercept for each section is zero.

was subjected to a length change at a faster (2ms) speed the stiffness value of the tendon was greater (14%) than at a slower (100ms) speed.

4.8.2. Yield Point

It is unlikely that the stretches the tendons were subjected to damaged them, because the tendon were subjected to forces of around two times the isometric force, which is the maximum force they are subjected to in vivo. The isometric force of EDL muscle is about 0.36N (Brooks & Faulkner, 1991). The tendons in the current experiments were subjected to lengths changes of between 0-7%. The yield point was not determined so as not to damage the tendon. All tendons were stretched to approximately 7% strain without the yield point occurring. Although in some tendons at around 6% strain the force baseline after the stretch was found to be lowered (since the start point was 3% stretched), indicating damage had occurred to the tendon and thus this might be the beginning of the yield point. Indicating that the yield point in EDL tendon is higher than in RTT, in which it occurs at about 4% strain. RTT is known to break at strains of around 8-10%. It is likely that RTT is not subjected to high forces and thus it is not designed to deal with high forces, hence the low yield point of around 4% found for RTT by previous workers. It is thought that the RTT normally operate in the toe region (Rigby *et al.*, 1959).

Normal upper bound physiological strain in tendon has been estimated to be 18% in canine tendon, by Walker *et al.*, (1976). Based on studies of intact equine superficial flexor tendons, Herrick *et al.*, (1978) observed that strains in excess of 12% may be physiologically normal in the horse knee and in vivo strain rates may exceed 200%/s (Herrick *et al.*, 1978). There are two possible explanations for these observations: (1) the crimp angle and low modulus toe in the load bearing tendons are larger than that observed in RTT and (2) load bearing tendons can be reversibly cycled into the linear portion of the stress-strain curve, whereas RTT cannot and only operates in the toe region (Silver, 1987).

4.8.3. The Current Experiments Compared To Previous Results

The data on table 4.1 tabulating the results from tendon compliance studies obtained by previous workers, shows a wide range in Young's modulus (30 fold). The values

obtained by the other workers, in the table for Young's modulus are much lower, this is likely to be due to the much lower strain rates they used in stretching the tendons. For example Rigby *et al.*, (1959) used a strain rate of 1 to 20 % per minute. Whereas in the current experiments the strain rate was 1.8×10^4 to 1.7×10^5 % per minute. The value for Young's modulus obtained in the current experiment is similar to that obtained by Ker (1981), who used a strain rate considerably faster than the other workers. The strain rates used in the current experiments were considered more physiological, since when an animal lands from a jump the muscle-tendon complex is stretched very rapidly when the foot hits the floor. Thus the tendon will be fully stretched in a few milliseconds. Then the length change will go into the muscle. It will take about 10ms for the foot of a mouse to go down to the ground from a small jump of say 8cm. If the muscle is active when the foot touches down the tendon will be stretched in the first fraction of the 10ms. Therefore a stretch speed of 2ms is appropriate to represent a quick stretch. In the current experiments the tendon stretch was held for 100ms. From table 4.1, it can be seen that this is similar to the time used by Ker, (1981). The holding time will affect the next point above it, which becomes important as the tendon is stretches near its yield point. The greater the holding time the greater the stress the tendon is subjected to.

The present experiment was started with the tendon at 3-4% stretched length, because this defines the zero point better than if the measurements were made on a tendon at an unstretched length. Rigby *et al.*, (1959) commented that the very first stretch of a new tendon, which they termed a 'conditioning stretch', produces a slight permanent elongation of about 0.6% which is never recovered. After all subsequent stretches the tendon returns to this conditioned length, and so in their work they did not consider this stretch. Thus in the current series of experiments this problem has been over come by starting the tendon at a 3-4% stretched length. Tendons are not pure collagen so the first stretch may involve the rupture of other components of the tendon (tendon cells, blood vessels, nerves, ground substance, etc.) which takes no subsequent part in the mechanical behaviour.

4.8.4. Oestrogen And Testosterone

In the present study the tendons from the control mice were found to be approximately

15% stiffer than the tendons from the operated mice (15 months). No difference was found between the stiffness of young (3-5 months) and operated (15 months) mice. Which indicates that removing the gonads, can reverse the increase in tendon stiffness with age. Collagen content is known to increase with maturation and ageing of the tissue (Everitt & Delbridge, 1976). The dry weight / unit length of the tendons from the control mice were found to be 26% greater than from the operated or young adult mice. The dry weight fraction of tendon is known to be a good indicator of its collagen content (Shadwick, 1990). Thus the results indicate, that ovariectomy or castration inhibits the increase in collagen content of the tendon with age. Stiffness increases with age in the tendon primarily due to two reasons:

1) Collagen content increases, there is evidence in humans that a decreased breakdown in collagen occurs at about 65 years of age, as determined by decreased hydroxyproline excretions (Kivirikko, 1970).

2) Collagen becomes progressively more cross-linked with age (Naresh & Brodsky, 1992).

In women, ovarian secretions decrease greatly after the menopause, whereas in rodents, ovarian secretions continue several months after loss of oestrous cycles and causes the persistent vaginal cornification characteristic of acyclic aging rodents (Mobbs *et al.*, 1984). In female mice there are known to be three phases of the oestrogen cycle frequency according to age:

Phase 1: 3-4 months, infrequent, irregular cycling.

Phase 2: 3-14 months, maximal cycling frequency.

Phase 3: 19-20 months, steadily declining cycle frequency (Nelson et al., 1982). Ageing male mice show a decline in testosterone secretion and perhaps a decrease in spermatogenesis (Harman & Talbert, 1985).

Since young adult mice (3-5 months) and control mice (middle aged mice, 15 months) are known to have ovarian cycles (Mobbs *et al.*, 1984). It is likely that in the current study the oestrogen levels in the young adult female (3-5 months) mice and the control female mice (15 months), are similar. Whereas the ovariectomized and castrated mice will have low levels oestrogen and testosterone respectively following the operation. Indicating the removal of the gonads might prevent the increase in collagen content with

age.

The results for ovariectomy are in accordance for previous finding. Experiments by Arvay & Takacs (1965), showed that in female ovariectomized rats the absence of oestrogen delayed the ageing of collagen; i.e. the thermic contraction was found to be reduced in the absence of oestrogen than in normal female and control rats. Whereas castrated male rats in the absence of testosterone no significant difference was found (Arvay & Takacs, 1965). In addition it has been found that the administration of oestrogens to human subjects rapidly decreases the excretion of hydroxyproline in both men and women. The decreased hydroxyproline excretion following oestrogen administration is probably partly due to decreased collagen breakdown, but an anabolic action of these hormones may contribute to this effect. Testosterone administration has effects similar to, though less marked than oestrogens on urinary hydroxyproline (Kivirikko, 1970).

Further evidence is provided by the effect of oestrogen on the skin. Collagen in the skin changes both qualitatively and quantitatively throughout life. The dermis of the skin is composed predominantly of collagen and 5% of elastin (Kligman *et al.*, 1985). It has been shown the dermis thins in old age. From early adulthood onwards there is a gradual decrease in the absolute amount of collagen per unit area of skin (Kligman *et al.*, 1985). It is thought that changes in the collagen of the skin in post menopausal women are due to a decrease in the level of oestrogen. Women's skin has been shown to age faster than men's skin, especially after the menopause (Kligman *et al.*, 1985). Perhaps it is possible the effects of the lack of oestrogen on the collagen in the skin are greater than in the collagen in the tendon because the turnover rate of collagen is very low except in the uterus, cervix and skin (Tonna, 1977).

4.9. Conclusions

No large changes in tendon stiffness were found in the present experiments. However there are two small changes.

1) Age increases the stiffness of the EDL tendon in mice.

2) Removing the gonads inhibits the increase in the stiffness of the EDL tendon in mice with age.

4.10. Further Experiments

The time course of the stiffening of the tendon with age needs to be determined. Since this effect is contrary to the effect of the reduction in the oestrogen levels, which results in the tendon being less stiff. Therefore one might expect that the time course of the stiffening of the tendon with age to be different in men and women. It is possible that in women the time course of the stiffening of the tendons is slower than in men. A consequence of the dramatic loss of oestrogen which occurs in women at the menopause, whereas in men the reduction in testosterone levels is much slower. Thus experiments needed to be conducted in vivo to determine the time course of the stiffening of the tendon with age in both men and women

DISCUSSION

Summary of the Findings From Each Chapter

Chapter 1

The model has contributed to the knowledge on how tendon can be matched to muscle and shows (for the given muscle properties incorporated in the model) an optimum amount of tendon compliance is needed for efficient jumping. This can be described by a dimensionless number, which therefore suggests that the determinants of the optimum conditions might not depend on the geometry of the system. The actual tendon compliance in mouse and man is similar to what would be expected from this dimensionless number to be optimum. This suggests that meeting this optimum is one of the determinants of tendon compliance.

Chapter 2

The time course of the decline in F/CSA in men with age was determined. This study contributes to the knowledge of the hormone dependence of muscle strength. By suggesting that testosterone has a role analogous to that of oestrogen in women.

Chapter 3

The compliance of aponeurosis was determined in mouse soleus muscle, in order to asses the degree of compliance external to the muscle. The aponeurosis was found to contribute a large part of compliance to the MTC.

Chapter 4

Tendon stiffness is hormone dependent, like muscle force which is also hormone dependent. In ovariectomized and castrated mice it was found that the extensor digitorum longus tendons were approximately 15% more compliant than in aged matched control mice. Indicating that in the absence of oestrogen and testosterone the increase in stiffness of the tendon with age is inhibited.

Changes In The MTC With Age

1) With age the tendon stiffness increases (see chapter 4).

2) F/CSA of muscle decreases with age (see chapter 2).

Assuming the person cannot do anything to alter the tendon stiffness and that the same task has to be achieved, as before the increase in tendon stiffness, then the person can do either of two things to increase the muscle force:

1) Increase the charge time (i.e. increase the time the muscle is on for).
2) Increase the amount of muscle used.

The question that is being asked is:
Is more muscle on for less time more efficient than less muscle on for more time? The model has shown that there is an optimum muscle amount (for a given spring stiffness). An amount of muscle smaller than the optimum, means that the muscle is on for longer (to achieve the same jump height), which is less efficient. Thus the answer to the question, seems to be that it is more efficient for more muscle to be on for less time, up to the optimum level of muscle amount. Therefore it would seem sensible for the animal to choose to re-optimize its muscle amount. So that not much efficiency may be lost in all but maximum contractions.

Simulating an aged muscle (30% reduction in F/CSA, and a 18% increase in tendon stiffness), the model has shown, it would be more efficient for a person to utilize a greater muscle mass, than to keep the muscle on for longer, in order to achieve a set task (see table 1.3). This option is of course subject to there being more muscle available. People also suffer muscle atrophy (Essen-Gustavsson & Borges, 1986: Kallman *et al.*, 1990: Vandervoort & McComas, 1986) at the same time as the decrease in muscle F/CSA and increase in tendon stiffness. When this happens the person has no option but to keep the muscle on for longer, which as shown in figure 1.35b, results in a huge increase in energetic cost.

Tendon Stretching Experiments

The increase in tendon stiffness with age in mouse EDL tendon was found to be 18%. Increase in tendon stiffness is one factor in diminishing movement of old people, however it is not a major factor. The model has shown that increasing the spring stiffness by 100% from optimum only increases ATP use by 21%.

Model Simulation Of Ovariectomized / Castrated Mouse

The fact that the increase in spring stiffness is having a smaller effect on the energetic cost than the decrease in F/CSA can be seen by considering the situation of the ovariectomized / castrated mouse, where the F/CSA of the muscle decreases by 30%, but the stiffness of the tendon remains the same. In this case the animal has to produce a Pmaxf of 50N, a 43% increase, to achieve the same jump height as before the decrease in F/CSA.

The question whether everybody stores the same proportion of energy in their tendons, needs to be answered. In old age, the muscle produces less force due to the reduction in F/CSA and the tendon stiffness increases. The consequence will be the tendon is able to store less energy because the weaker muscle is not able to stretch the stiffer tendon to a sufficient degree. One might therefore expect to find that less energy could be stored in the tendons of elderly women (age 75 years, weak muscles, stiff tendons) as compared to non-HRT post menopausal women (age 50 years, weak muscles, compliant tendons).

Quick Release Experiments

The quick release experiments were performed on mouse muscle was to determine the proportion of total compliance due to crossbridges and aponeurosis. The degree of aponeurosis compliance was found to be a large proportion; 41% of the compliance of mouse soleus muscle is due to the crossbridges and 59% is due to aponeurosis compliance. Muscle and tendon work together, the amount of tendon determines how much spring is in the muscle. It is impossible to cut between the muscle and tendon as they interdigitate. In order to determine the proportion of the compliance in the whole muscle, the T1-T2 transition needs to be known. The muscle experiments have shown that in the mouse muscle the T1-T2 transition is faster than in frog muscle. This is not surprising since most other properties of mouse muscle are faster than in frog muscle. The speed of the T1-T2 transition helps the

muscle to develop power, and is one of the factors that tends to make mouse muscle more powerful than frog muscle. The T1-T2 transition is one of the features of muscle that gives the force velocity curve its shape.

Conclusions:

The hypothesis this thesis is investigating is: Are the changes that occur with age in muscle and tendon related and do they suffice to maintain relatively efficient locomotion, when combined with the appropriate change in motor control strategy?

The decrease in muscle F/CSA that occurs with age seems to be a consequence of reduced oestrogen or testosterone levels. The increase in tendon stiffness with age seems to be a consequence of increased cross-links derived from the process of non-enzymic glycosylation. Each of these changes individually increases the energetic cost of locomotion (see chapter 1). When they occur together their effects add together to further increase the cost of locomotion. The model has shown that in order to conserve efficiency (in achieving a set task) it is necessary to implement a change in motor control strategy, of utilizing a greater muscle amount rather than keeping a smaller mass of muscle on for a longer time.

REFERENCES

Alexander, R. McN. (1974). The mechanics of jumping by a dog *(Canis familiaris). J. Zool. (London)* **173**, 549-573.

Alexander, R. McN. (1988). Elastic Mechanisms in Animal Movement. Cambridge University Press.

Alexander, R. McN. (1989). Energy saving mechanisms in terrestrial locomotion. In "Energy Transformations in Cells and Organisms" pp 170-174 (W. Wieser and E. Gnaiger, Eds). Georg Thieme Verlag.

Alexander, R. McN. (1990). Animals, pp. 479-484. Cambridge University Press.

Alexander, R. McN. (1995). Leg design and jumping technique for humans, other vertebrates and insects. *Phil. Trans. R. Soc. Lond. B*, **347**, 235-248.

Alexander, R. McN., and Bennet-Clark, H.C. (1977). Storage of elastic strain energy in muscle and other tissues. *Nature (London)* **265**, 114-117.

Alexander, R. McN., Jayes, A.S., Maloiy, G.M.O., and Wathuta, E.M. (1981). Allometry of the legs muscles of mammals. *J. Zool. (Lond.)*, **194**, 539-552.

Alexander, R. McN., and Vernon, A. (1975). The dimensions of knee and ankle muscles and the forces they exert. *J. Human Movement Studies,* **1**, 115-123.

Alnaqeeb, M.A., Al Zaid, N.S., and Goldspink, G. (1984). Connective tissue changes and physical properties of developing and ageing skeletal muscle. *J. Anat.*, **139**, 677-689.

Amis, A., Prochazka, A., Short, D., Trend, P.St.J., and Ward, A. (1987). Relative displacements in muscle and tendon during human arm movements. *J. Physiol. (London)* **389**, 37-44.

Anderson, F.C., and Pandy, M. G. (1993). Storage and utilization of elastic strain energy during jumping. *J. Biomechanics*, **26**, 1413-1427.

Andreassen, T.T., Seyer-Hansen, K., and Bailey, A.J. (1981). Thermal stability, mechanical properties and reproducible cross-links of rat tail tendon in experimental diabetes. *Biochimica et Biophysica Acta* **677**, 313-317.

Aniansson, A., Hedberg, M., Henning, G.B., and Grimby, G. (1986). Muscle morphology, enzymic activity, and muscle strength in elderly men: a follow-up study. *Muscle and Nerve* **9**, 585-591.

Arvay, A. (1976). Reproduction and ageing. In "Hypothalamus, Pituitary and Ageing" (A.V. Everitt and J.A. Burgess, eds.). pp. 362-375. Charles C. Thomas, Springfield, Illinois.

Arvay, R., and Takacs, J. (1965). The influence of hormone changes during pregnancy on the velocity of collagen ageing. *Gerontologia* **11**, 188-197.

Barrett, B. (1962). The length and mode of termination of individual muscle fibres in the human sartorius and posterior femoral muscles. *Acta Anat.* **48**, 242-257.

Biewener, A.A., and Blickhan, R. (1988). Kangaroo rat locomotion: Design for elastic energy storage or acceleration. *J. exp. Biol.* **140**, 243-255.

Brenner, B. (1984). The rate of force redevelopment in single skinned rabbit psoas fibers. *Biophys. J.* **45**, 155a.

Brooks, S.V., and Faulkner, J.A., (1988). Contractile properties of skeletal muscle from young and aged mice. *J. Physiol. (London)* **404**, 71-82.

Brooks, S.V., and Faulkner, J.A., (1991). Forces and powers of slow and fast skeletal muscles in mice during repeated contractions. *J. Physiol. (London)* **436**, 701-710.

Bruce, S.A., Newton, D. and Woledge, R.C. (1989a). Effect of age on voluntary force and cross-sectional area of human adductor pollicis muscle. *Qtr. J. Exp. Physiol.*, **74**, 359-362.

Bruce, S.A., Newton, D. and Woledge, R.C. (1989b). Effect of subnutrition on normalized muscle force and relaxation rate in human subjects using voluntary contractions. *Clinical Science* **76**, 637-641.

Caccia, M.C., Harris, J.B., and Johnson, M.A. (1979) Morphology and physiology of skeletal muscle in ageing rodents. *Muscle and Nerve* **2**, 202-212.

Cavagna, G.A., and Citterio, G. (1974). Effect of stretching on the elastic characteristics and contractile component of frog striated muscle. *J. Physiol. (London)* **239**, 1-14.

Cavagna, G.A., Heglund, N.C., Harry, J.D., and Mantovani, M. (1994). Storage and release of mechanical energy by contracting frog muscle fibres. *J. Physiol. (London)* **481.3**, 689-708.

Cavagna, G.A., Saibene, F.P., and Margaria, R. (1964). Mechanical work in running. *J. Appl. Physiol.* **19(2)**, 249-256.

Cetta, G., Tenni, R., Zanaboni, G., De Luca, G., Ippolito, E., De Martino, C., and Castellani, A.A. (1982). Biomechanical and morphological modifications in rabbit Achilles tendon during maturation and ageing. *Biochem.* J., **204**, 61-67.

Cook, C.S. (1993). The dynamic properties of a human muscle-tendon complex. Ph. D. Thesis, University of Birmingham.

Cooke, R., and Pate, E. (1985). The effects of ADP and phosphate on the contraction of muscle fibres. *Biophys. J.*, **48**, 789-798.

Curtin, N.A. (1990). Force during stretch and shortening of frog sartorius muscle:

effects of intracellular acidification due to increased carbon dioxide. *J. Muscle Res. Cell Motil.* **11**, 251-257.

Curtin, N.A., and Woledge, R.C. (1981). Effect of muscle length on energy balance in frog skeletal muscle. *J. Physiol. (London).* **316**, 453-468.

Dahlberg, E. (1982). Characterization of cytosolic estrogen receptor in rat skeletal muscle. *Biochim. Biophys. Acta* **717**, 65-75.

Davison, P.F. (1982). Tendon. *In* "Collagen in Health and Disease", (J.B. Weiss & M.I.V. Jayson, eds). pp. 498-505. Churchill Livingstone, Edinburgh.

De Haan, A., Jones, D.A., and Sargeant, A.J. (1989). Changes in velocity of shortening, power output and relaxation rate during fatigue of rat medial gastrocnemius muscle. *Pflügers Archiv.* **413**, 422-428.

Deyl, Z., Rosmus, J., and Adam, M. (1976). Pituitary and Collagen In "Hypothalamus, Pituitary and Ageing" (A.V. Everitt and J.A. Burgess, eds.). pp. 171-192. Charles C. Thomas, Springfield, Illinois.

Diamant, J., Keller, A., Baer, E., Litt, M., and Arridge, R.G.C. (1972). Collagen, ultrastructure and its relation to mechanical properties as a function of ageing. *Proc. R. Soc. Lond. B.* **180**, 293-315.

Dimery, N.J., Alexander, R. McN., and Ker, R.F. (1986). Elastic extension of leg tendons in the locomotion of horses (*Equuss caballus*). *J. Zool. (London)* **210**, 415-425.

Dunn, M.G., and Silver, F.H. (1983). Viscoelastic behaviour of human connective tissues: relative contribution of viscous and elastic components. *Connect. Tiss. Res.*, **12**, 59-70.

Edman, K.A.P. (1979). The velocity of unloaded shortening and its relation to sarcomere length and isometric force in vertebrate muscle fibres. *J. Physiol. (Lond.)*

291, 143-159.

Elliott, D.H. (1965). Structure and Function of mammalian tendon. *Biol. Rev.*, **40**, 392-421.

Elzinga, G., Steinen, G.J.M. and Versteeg, P.G.A. (1989). Effect of inorganic phosphate on length responses to changes in load in skinned rabbit psoas muscle. *J. Physiol. (Lond.)* **415**, 132P.

Essen-Gustavsson, B., and Borges, O. (1986). Histochemical and metabolic characteristics of human skeletal muscle in relation to age. *Acta. Physiol. Scand.* **126**, 107-114.

Everitt, A.V. (1973). The hypothalamic-pituitary control of ageing and age-related pathology. *Exp. Geront.* **8**, 265-277.

Everitt, A.V., and Delbridge, L. (1976). The role of the pituitary and the thyroid in the ageing of collagen in rat tail tendon. In "Hypothalamus, Pituitary and Ageing" (A.V. Everitt and J.A. Burgess, eds.). pp. 193-208. Charles C. Thomas, Springfield, Illinois.

Everitt, A.V., Wyndham, J.R., and Barnard, D.L. (1983). The anti-ageing action of hypophysectomy in hypothalamic obese rats: effects on collagen ageing, age-associated proteinuria development and renal histopathology. *Mechanism of Ageing and Development* **22**, 233-251.

Farley, C.T., Blickhan, B., Saito, J., and Taylor, R. (1991). Hopping frequency in humans; a test of how springs set stride frequency in bouncing gaits. *J. Appl. Physiol.*, **71**, 2127-2132.

Florini, J.R. (1987). Hormonal control of muscle growth. *Muscle and Nerve* **10**, 577-598.

Ford, L. E., Huxley, A.F., and Simmons, R.M. (1977). Tension Responses To Sudden

Length Change In Stimulated Frog Muscle Fibres Near Slack Length. *J. Physiol. (London)* **269**, 441-515.

Franzblau, C., and Faris, B. (1981). Elastin. In "Cell biology of extracellular matrix". (E.D. Hay, ed.). pp. 65-93. Plenum Press, New York.

Galley, P.M., and Forster, A.L. (1990). Human Movement. Churchill Livingstone, Melbourne.

Garrow, J.S. (1983). Indices of adiposity. *Nutr. Abst. Rev.* **53**, 697-708.

Goslow, G.E., Reinking, R.M. and Stuart, D.G. (1973). The cat step cycle: Hindlimb joint angles and muscle lengths during unrestrained locomotion. *J. Morphology* **141**, 1-42.

Grant, M.E., and Prockop., D.J. (1972). The biosynthesis of collagen (first of three parts). *New Eng. J. Med.*, **286(4)**, 195-199.

Gray's Anatomy, (1989) 37th edition (P.L. Williams and R. Warwick, eds.). Churchill Livingstone, London.

Greene, E.C. (1935). Anatomy of the rat. The American Philosophical society, Philadelphia.

Griffiths, R.I. (1991). shortening of muscle fibres during stretch of the active cat medial gastrocnemius muscle: The role of tendon compliance. *J. Physiol.*, **436**, 219-236.

Griffiths, R.I. (1989). The mechanics of the medial gastrocnemius muscle in the freely hopping wallaby. *J. exp. Biol.*, **147**, 439-456.

Grindrod, S., Round, J.M. and Rutherford, O.M. (1987). Type 2 fibre composition and force per cross-sectional area in the human quadriceps. *J. Physiol. (London)* **390**, 154P.

Harkness, R.D. (1964). The physiology of the connective tissue of the reproductive tract. *Int. Rev. Connect. Tissue Res.*, **2**, 155-211.

Harkness, R.D., Marko, A.M., Muir, M.M., and Neuberger, A. (1954). The metabolism of collagen and other proteins of the skin of rabbits. *Biochem J*, **56**, 558-569.

Harman, S.M., and Talbert, G.B. (1985). Reproductive ageing. In "Handbook of the biology of ageing". 2nd ed. (C.E. Finch and E. L. Schneider, Eds.), pp. 457-510. Van Nostrand Reinhold, New York.

Herrick, W.C., Kingsbury, H.B., and Lou, D.Y.S. (1978). A study of the normal range of strain, strain rate and stiffness of tendon. *J. Biomed. Mater. Res.*, **12**, 877-894.

Heglund, N.C., and Cavagna, G.A. (1987). Mechanical work, oxygen consumption, and efficiency in isolated frog and rat muscle. *Am. J. Physiol.*, **253**, C22-C29.

Hill, A.V. (1938). The heat of shortening and the dynamic constants of muscle. *Proc. R. Soc. London Ser. B* **126**, 136-195.

Howarth, J.V. (1958). The behaviour of frog muscle in hypertonic solutions. *J. Physiol. (London)* **144**, 167-175.

Hukins, D.W.L. (1982). Biomechanical properties of collagen. In "Collagen in Health and Disease", (J.B. Weiss & M.I.V. Jayson, eds). pp. 49-72. Churchill Livingstone, Edinburgh.

Hukins, D.W.L. (1984). Tissue components. In "Connective Tissue Matrix". pp. 1-53. (D.W.L. Hukins, Ed.). The Macmillian Press Ltd, London.

Huxley, A.F. (1957). Muscle structure and theories of contraction. *Prog. Biophys. Biophys. Chem.* **7**, 255-318.

Huxley, A.F. (1974). Muscular Contraction. *J. Physiol. (London)* **243**, 1-43.

Huxley, A.F. (1980). Reflections on Muscle. Liverpool University Press, Liverpool.

Huxley, A.F., and Simmons, R.M. (1971). Proposed mechanism of force generation in striated muscle. *Nature (London)* **233**, 533-538.

Huxley, H.E., Stewart, A., Sosa, H., and Irving, T. (1994). X-ray diffraction measurements of the extensibility of actin and myosin filaments in contracting muscle. *Biophysical Journal,* **67**, 2411-2421.

Ippolito, E., Natali, P.G., Postacchini, F., Accinni, L., and De Martino, C. (1980). Morphological, immunochemical, and biomechanical study of rabbit Achilles tendon at various ages. *J. Bone and Joint surgery* **62A (4),** 583-598.

Jennekens, F.G.I., Tomlinson, B.E., and Walton, J.N. (1971). Histochemical aspects of five limb muscles in old age an autopsy study. *J. Neurol. Sci.* **14**, 259-276.

Jones, D.A., and Rutherford, O.M. (1990). Effect of ageing and osteoporosis on the force-generating capacity of the quadriceps muscle in women. *J. Physiol. (London).* **423**, 84P.

Kallman, D.A., Plato, C.C., and Tobin, J.D. (1990). The role of muscle loss in the age-related decline of grip strength: cross-sectional and longitudinal perspectives. *J. Gerontology* **45(3)**, M82-88.

Kao, K-Y.T., Boucek, J.R. and Nobel, N.L. (1957). Rate of collagen formation in biopsy-connective tissue of the rat. *Proc. Soc. Exp. Biol. Med.* , **95**, 535-538.

Kastelic, J., Galeski, A., and Baer, E. (1978). The multicomposite structure of tendon. *Connect. Tiss. Res.*, **6(1)**, 11-23.

Ker., R.F. (1981). Dynamic Tensile Properties of the plantaris tendon of sheep. *J. Exp.*

Biol., **93**, 283-302.

Ker, R.F., Alexander, R. McN., and Bennett, M.B. (1988). Why are mammalian tendons so thick? *J. Zool.(Lond.)*, **216**, 309-324.

Kivirikko, K.I. (1970). Urinary excretion of hydroxyproline in health and disease. *Int. Rev. Connect. Tissue Res.*, **5**, 93-163.

Kligman, A.M., Grove, G.L., and Balin, A.K. (1985). Ageing of human skin. In "Handbook of the biology of ageing". 2nd ed. (C.E. Finch and E. L. Schneider, eds.), pp. 821-841. Van Nostrand Reinhold, New York.

Kram, R. and Taylor, C.R. (1990). The energetics of running a new perspective. *Nature (Lond.)*, **346**, 265-267.

Larsson, L., and Moss, R.L. (1993). Maximum velocity of shortening in relation to myosin isoform composition in single fibres from human skeletal muscles. *J. Physiol.*, **472**, 595-614.

Lexell, J., Henriksson-Larsen, K., Winblad, B., and Sjöström, M. (1983). Distribution of different fibre types in human skeletal muscles. 3. Effects of ageing studied in whole muscle cross sections. *Muscle and Nerve* **6**, 588-595.

Lindstedt, S., and Prockop, D.J. (1961). Isotopic studies on urinary hydroxyproline as evidence for rapidly catabolized forms of collagen in the young rat. *J. Bio. Chem.*, **236**, 1399-1403.

Loeb, G.E., Pratt, C.M., Chanaud, C.M., and Richmond, F.J.R. (1987). Distribution and innervation of short, interdigitated muscle fibres in parallel-fibred muscles of the cat hindlimb. *J. Morphology* **191**, 1-15.

Lombardi, V., and Piazzesi, G. (1990). The contractile response during steady lengthening of stimulated frog muscle fibres. *J. Physiol. (London)* **431**, 141-171.

Marcus, D.S., Reicher, M.A., and Kellerhouse, L.E. (1989). Achilles tendon injuries: the role of MR imaging. *J. Com. Ass. Tom.*, **13 (3)**, 480-486.

Marcus, R. (1991). Skeletal ageing: understanding the functional and structural basis of osteoporosis. *Trends Endocrinol. Metab.* **2**, 53-8.

McCarter, R. (1981). Studies of sarcomere length by optical diffraction. *In* "Cell and Muscle Motility" (R.M. Dowben and J.W. Shay, Eds.), pp. 35-62. Plenum, New York.

McKinlay, J.B. (1989). In "Progress In Clinical Research" volume **320** pp.163-192. (C.B. Hammond, F. P. Haseltine,and I. Schiff, Eds.), Alan R. Liss, Inc., New York.

Mendez, J., and Keys, A. (1960). Density and composition of mammalian muscle. Metabolism **9**, 184-188.

Michna, H., and Hartmann, G. (1987). Extracellular tendon matrix and androgens. *Acta Anatomica* **130 (1)**, 62.

Mobbs, C.V., Gee, D.M., and Finch, C.E. (1984). Reproductive senescence in female C57BL/6J mice: Ovarian impairments and neuroendocrine impairments that are partially reversible and delayable by ovariectomy. Endocrinology **115(5)**, 1653-1662.

Monnier, V.M., Kohn, R.R., Cerami, A. (1984). Accelerated age-related browning of human collagen in diabetes mellitus. *Proc. Natl., acad. Sci. USA.* **81**, 583-587.

Morgan, D. L., Proske, U., and Warren, D. (1978). Measurements of muscle stiffness and the mechanism of elastic storage of energy in hopping kangaroos. *J. Physiol. (London)* **282**, 253-261.

Naresh, M.D., and Brodsky, B. (1992). X-ray diffraction studies on human tendon show age-related changes in collagen packing. *Biochimica et Biophysica Acta* **1122**, 161-166.

Nelson, J.F., Felicio, L.S., Randall, P.K., Sims, C., and Finch, C.E. (1982). A longitudinal study of estrous cyclicity in ageing C57BL/6J mice: I. Cycle frequency, length and vaginal cytology. *Biology of Reproduction* **27**, 327-339.

Olsen, G.G., and Everitt, A.V. (1965). Retardation of the ageing process in collagen fibres from the rat tail tendon of the old hypophysectomized rat. *Nature* **206**, 307-308.

Oxlund, H. (1984). Changes in connective tissue during corticotrophin and corticosteroid treatment. *Danish Medical Bulletin.* **31 (3)**, 187-206.

Pate, E. and Cooke, R. (1989). A model of crossbridge action: the effects of ATP, ADP and Pi. *J. Muscle Res. Cell Motil.* **10**, 181-196.

Phillips, S.K. (1988). A comparison of maximum power output with other measures of muscle function in mouse and human skeletal muscle. Ph. D. Thesis, University of London.

Phillips, S.K., Bruce, S.A., Newton, D., and Woledge, R.C. (1992). The weakness of old age is not due to failure of muscle activation. *J. Gerontology* **47(2)**, M45-49.

Phillips, S.K., Bruce, S.A., and Woledge, R.C. (1991). In mice, the muscle weakness due to age is absent during stretching. *J. Physiol.* **437**, 63-70.

Phillips, S.K., Gopinathan, J., Meehan, K., Bruce, S.A., and Woledge, R.C. (1993c). Muscle strength changes during the menstrual cycle in human adductor pollicis. *J. Physiol. (London)* **473**, 125P.

Phillips, S.K., Rook, K. M., Siddle, N.C., Bruce, S.A., and Woledge, R.C. (1993a). Muscle weakness in women occurs at an earlier age than in men, but strength is preserved by hormone replacement therapy. *Clinical Science* **84**, 95-98.

Phillips, S.K., Rowbury, J. L., Bruce, S.A., and Woledge, R.C. (1993d). Muscle force generation and age: The role of sex hormones. In "Sensorimotor Impairment in the

Elderly" (G.E. Stelmach and V. Hömberg, eds.), pp. 129-141. Kluwer Academic Publishers, Holland.

Phillips, S.K., Wiseman, R.W., Woledge, R.C., and Kushmerick, M.J. (1993b) Neither changes in phosphorus metabolite levels nor myosin isoforms can explain the weakness in aged mouse muscle. *J. Physiol.* **463**, 157-167.

Pollock, C. M., and Shadwick, R.F. (1994b). Alllometry of muscle, tendon, and elastic energy storage capacity in mammals. *Am. J. Physiol.* **266**, R1022-R1031.

Pollock, C. M., and Shadwick, R.F. (1994a). Relationship between body mass and biomechanical properties of limb tendons in adult mammals. *Am. J. Physiol.* **266**, R1016-R1021.

Powell, P.L., Roy, R.R., Kanim, P., Bello, M.A., and Edgerton, V.R. (1984). Predictability of skeletal muscle tension from architectural determinations in guinea pig hindlimbs. *J. Appl. Physiol.* **57(6)**, 1715-1721.

Prockop, D.J., and Guzman, N.A. (1977). Collagen diseases and the biosynthesis of collagen. Hospital Practise, **12 (12)**, 61-68.

Rack, P.M.H. (1985). Stretch reflexes in Man: the significance of tendon compliance. *In* "Feedback and Motor Control in Invertebrates and Vertebrates" (W.J.P. Barnes and M.H. Gladden, Eds.), pp 217-229. Croom Helm, London.

Rack, P.M.H., and Westbury, D.R. (1984). Elastic properties of the cat soleus tendon and their functional importance. *J. Physiol (London).* **347**, 479-495.

Ramachandran, G.N. (1967). Structure of collagen at the molecular level. In "Treatise on Collagen. Vol 1. Chemistry of Collagen". (G.N. Ramachandran, Ed.). pp. 103-183. Academic Press, New York.

Reinig, J.W., Dorwart., R.H., and Roden, W.C. (1985). MR imaging of a ruptured

Achilles tendon. *J. Com. Ass. Tom.*, **9 (6)**, 1131-1134.

Reiser, K.M., (1991). Nonenzymatic glycation of collagen in ageing and diabetes. *Proc. Soc. Exp. Biol. Med.*, **196**, 17-29.

Rigby, B.J. (1964). Effect of Cyclic Extension on the physical properties of tendon collagen and its possible relation to biological ageing of collagen. *Nature (London)* **202**, 1072-1075.

Rigby, B.J., Hirai, N., Spikes, J.D., and Eyring, H. (1959). The mechanical properties of rat tail tendon. *J. Gen. Physiol.*, **43**, 265-283.

Ritchie. J.M., and Wilkie, D.R. (1958). The dynamics of muscular contraction. *J. Physiol. (London).* **143**, 104-113.

Round, J.M., Jones, D.A. Chapman, S.J., Edwards, R.H.T, Ward, P.S., and Fodden, D.L. (1984) The anatomy and fibre type composition of the human adductor pollicis in relation to its contractile properties. *J. Neurol. Sci.* **66**, 263-272.

Schottelius, B.A., and Senay, L.C. (1956). Effect of stimulation-length sequence on shape of length-tension diagram. *Am. J. Physiol.* **186**, 127-130.

Shadwick, R.E. (1990). Elastic energy storage in tendons: mechanical differences related to function and age. J. Appl. Physiol., **68(3)**, 1033-1040.

Shoshan, S., Finkelstein, S., Kushner, W., and Weinreb, M.M. (1972). Studies on maturation and crosslinking of collagen implants in hypophysectomized rats in vivo. *Connect. Tiss. Res.*, 1, 47-53.

Silver, F.H. (1987). Biological Materials. New York University. New York.

Smith, Q.T., and Allison, D.J. (1965). Cutaneous collagen and hexosamine and femur collagen of testosterone propionate treated rats of various ages. *Biochem, Pharmacol,*

14, 709-720.

Snedecor, G.W. and Cochran, W.G. (1976). Statistical Methods. (6th Edition). The Iowa State university Press, Iowa, USA.

Squire, J.M. (1986). Muscle: Design, diversity, and Disease. Benjamin/Cummings Publishing C., Inc., California.

Stahlberg, E., and Fawcept, A. (1982). Macro EMG in muscles of healthy subjects of different ages. *J. Neurol. Neurosurg. Psychiat.* **45**, 870-878.

Sutton, D. (1994). Radiology and Imaging for Medical Students. (6th Ed). pp. 1-18. Churchill Livingstone, Edinburgh.

Taylor, D.J., Crowe, M., Bore, P.J., Styles, P., Arnold, D.L., and Radda, G. K. (1984). Examination of the energetics of ageing skeletal muscle using nuclear magnetic resonance. *Gerontology* **30**, 2-7.

Tonna, E.A. (1977). Ageing of skeletal-dental systems and supporting tissues. In "Handbook of the biology of ageing". 1st Ed. (C.E. Finch and Hayflick, eds.), pp. 470-481. Van Nostrand Reinhold, New York.

Torp, S., Arridge, R.G.C., Armeniades, C.D., and Baer, E. (1975a). Structure-property relationships in tendon as a function of age. *Colston Papers* **26**, 197-121.

Torp, S., Baer, E., and Friedman, B. (1975b). Effects of age and of mechanical deformation on the ultrastructure of tendon. *Colston Papers* **26**, 223-250.

Trelstad, R.L., and Silver, F.H. (1981). In "Cell biology of extracellular matrix". (E.D. Hay, ed.). Chapter 7. Plenum Press, New York.

Tzankoff, S.P., and Norris, A.H. (1977). Effect of muscle mass decrease on age-related BMR changes. *J. Appl. Physiol.* **43**, 1001-1006.

van Leeuwen, J.L. (1991). Muscle function in locomotion. In "Mechanics of Animal Locomotion" (R. McN. Alexander, Ed), pp 191-250. Springer-Verlag, New York.

Vandervoort, A.A., and McComas, A.J. (1986). Contractile changes in opposing muscles of the human ankle joint with ageing. *J. Appl. Physiol.* **61(1)**, 361-367.

Verzar, F. (1963). Ageing of collagen. *Scientific America* **208 (4)**, 104-117.

Wainwright, S.A., Biggs, W.D., Currey, J.D. and Gosline, J.M. (1976). Mechanical Design in Organisms. Edward Arnold, London.

Walker, P., Amstutz, H.C., and Rubinfeld, M. (1976). Canine Tendon Studies. II. Biomechanical evaluation of normal and regrown canine tendons. *J. Biomed. Mater. Res.* **10**, 61-76.

Wickham, C.A.C., Walsh, K., Cooper, C., Barker, D.J.P., Margetts, B.M., Morris, J., and Bruce, S.A. (1989). Dietary calcium, physical activity, and risk of hip fracture: a prospective study. *Br. Med. J.* **299**, 889-892.

Woledge, R.C., Curtin, N.A. and Homsher, E. (1985). Energetic Aspects of Muscular Contraction. Academic Press, London.

Woo, S.L-Y., T.M., Gomez, Woo, Y-K., and Akeson, W.H. (1982). Mechanical properties of tendons and ligaments. The relationships of immobilization and exercise on tissue remodelling. *Biorheology* **19**, 397-408.

Woo, S. L-Y., Ritter, M.A., Amiel, D., Sanders, T.M., Gomez, M.A., Kuei, S.C., Garfin, S.R., and Akeson, W.H. (1980). The biomechanical and biochemical properties of swine tendons - long term effects of exercise on the digital extensors. *Connect. Tiss. Res.*, **7**, 177-183.

Yin, C. (1990). A study of the efficiency of converting free energy into mechanical work in mouse soleus muscles. Ph. D. Thesis, University of London.

Young, A. (1984). The relative isometric strength of type I and type II muscle fibres in the human quadriceps. *Clin. Physiol.* **4**, 23-32.